NOVEL NANO-ENHANCED PHASE CHANGE MATERIALS FOR THERMAL ENERGY STORAGE APPLICATIONS

By

Muhammad Aamer Hayat

School of Physics, Engineering and Computer Science

Submitted to the University of Hertfordshire in partial fulfilment of the requirements of the degree of Doctor of Philosophy

July 2024

Author's Declaration

I declare that the work in this dissertation was carried out in accordance with the requirements of the University's Regulations and Code of Practice for Research Degree Programmes and that it has not been submitted for any other academic award. Except where indicated by the specific reference in the text, the work is the candidate's work. Any views expressed in the dissertation are those of the author.

Signed: Muhammad Hayat **Date:** 31-07-2024

*Dedicated to my father**, Muhammad Yousaf**, whose dream was for me to pursue a PhD, and to my mother, **Shamim Akhtar**, whose unwavering love and support have been my greatest sources of strength and inspiration.*

SYNOPSIS

The increasing demand for efficient and sustainable thermal energy storage (TES) systems has driven extensive research into phase change materials (PCMs). Despite their high energy storage capacity, the low thermal conductivity of PCMs limits their application. This thesis investigates the development and enhancement of nano-enhanced PCMs (nano-PCMs) through the incorporation of various nanoparticles, aiming to improve their thermophysical properties, stability, and cost-effectiveness for use in energy-efficient building applications.

This study introduces novel approaches to enhancing PCMs by integrating multi-walled carbon nanotubes (MWCNTs), graphene nanoplatelets (GNP), and titanium dioxide (TiO_2) as both single and hybrid nanoparticles. Paraffin, with a phase change temperature of 27-29 °C, was selected for this study due to its alignment with the nominal indoor comfort temperature of buildings and its versatility for various TES applications within this temperature range. Advanced characterisation techniques, including Fourier-Transform Infrared Spectroscopy (FT-IR), X-ray Diffraction (XRD), Differential Scanning Calorimetry (DSC), Thermogravimetric Analysis (TGA), and Thermal Conductivity Analyzer, were employed to evaluate the thermophysical properties and stability of the developed nano-PCMs.

The key findings reveal that the GNP+MWCNTs hybrid at 1.0 wt.% achieved a remarkable thermal conductivity enhancement of 170% at 25°C, significantly improving thermal performance. TiO_2-based PCMs showed minimal reductions in latent heat, with decreases of -3.7%, -5.2%, and -5.5% for TiO_2, TiO_2+GNP, and TiO_2+MWCNTs, respectively, at 1 wt.%. These results underscore the potential of TiO_2 as a cost-effective nanomaterial for enhancing PCM stability and performance.

The investigation into surface-functionalised MWCNTs demonstrated superior stability and thermal performance. Functionalised MWCNTs-based PCMs exhibited a 158% increase in thermal conductivity at 25°C and maintained their performance over time, unlike unfunctionalised MWCNTs. The hybrid configurations of functionalised MWCNTs with TiO_2 nanoparticles revealed minimal reductions in latent heat, with the F-MWCNTs+TiO_2 (25:75) hybrid showing only a -0.36% decrease during melting and -1.19% during crystallisation.

A comparative analysis highlights the overall improved performance of hybrid nanoparticles. The GNP+MWCNTs hybrid combination displayed the highest thermal conductivity, while

the TiO_2+functionalised MWCNTs hybrid at various concentrations (25:75, 50:50, 75:25) exhibited enhanced stability and cost-effectiveness, making them suitable for large-scale applications. Specific heat capacity (Cp) values of functionalised MWCNTs-based nano-PCMs were notably higher, with maximum values of 3.5 J/g°C and 2.5 J/g°C at 25°C and 45°C, respectively. The enhanced stability and thermal properties of nano-PCMs, particularly those with hybrid nanoparticles, position them as effective solutions for thermal energy storage in energy-efficient buildings and renewable energy systems.

Overall, this research demonstrates the novel potential of nano-enhanced PCMs to address thermal management challenges in modern building applications, contributing to sustainable and cost-effective energy management solutions.

ACKNOWLEDGEMENTS

The journey of completing this PhD has been a transformative and rewarding experience, and I owe a great debt of gratitude to many individuals and organisations who have supported and encouraged me along the way.

First and foremost, I wish to express my deepest gratitude to my principal supervisor, Professor Yong Chen, whose invaluable guidance, patience, and unwavering support have been pivotal throughout my research. His profound expertise and dedication have shaped my academic journey in countless ways.

I am also profoundly thankful to my supervisory team, Professor Liang Li, Dr. Mose Bevilacqua, and Professor Yang, for their insightful feedback and encouragement, which have significantly enriched my work. Additionally, I extend my heartfelt thanks to Professor Pandelis Kourtessis and the members of the Doctoral Training Alliance. Special thanks to Jennie, Heather, Ellie, Sarah, and Emma for their exceptional support in making this PhD program possible.

The technical assistance provided by the Technical Support Group of SPECS and LMS has been indispensable. I am particularly grateful to our technical managers, Alex and Giorgos, and all members of the team, including Arthur, James Stanley, Christine, Sufyan, Eugene, and Shannon, for their direct and indirect contributions to this work.

I would like to acknowledge my fellow PhD journey companions, who have now become esteemed colleagues and friends. A special mention goes to Mahmoud, Surya, Kumar, Hamza, Aqib, Moeez, and Dr. Paul for their camaraderie, support, and the fun times that have greatly benefited my research.

A very special acknowledgment goes to my wife, Sadia, whose unwavering support and encouragement have been my bedrock. The birth of our son, Zayan, during this journey brought immense joy and a renewed sense of purpose. Their love, patience, and sacrifices have been my strength and motivation.

I am deeply appreciative of my friends Dr. Kamran Gohar, Dr. Shoaib Sarfraz, and Professor Zaheer Nasar. Special thanks to Professor Nasar, whose culinary skills delighted us and whose delicious meals provided a much-needed respite; his taste is indeed exceptional. I would like

to express my heartfelt gratitude to Dr Hafiz Muhammad Ali, my mentor and master's supervisor, for his invaluable guidance, support, and encouragement throughout my academic journey.

I am forever grateful to my family for their boundless love and support. My parents, siblings Mudassar, Nouman, and Qurrat, have always been my pillars of strength. The memory of my late uncle Asghar and my grandparents, Haji Muhammad Hayat Naul and Gulam Fatima, who left us during my PhD journey, remains close to my heart. Their unwavering faith in me continues to inspire my endeavors.

Finally, I extend my appreciation to my lifelong friends Abdullah, Awais, Zain, Shehryar, Hassan Shah, and Khawar, whose friendships have stood the test of time and provided much-needed laughter and relief throughout this journey.

This thesis is a testament to the collective support, encouragement, and love of all these incredible individuals. Thank you for being an integral part of my PhD journey.

LIST OF PUBLICATIONS

Journal articles

1. **M.A. Hayat**, Y. Chen, M. Bevilacqua, L. Li, Y. Yang, Characteristics and potential applications of nano-enhanced phase change materials: A critical review on recent developments, Sustainable Energy Technologies and Assessments. 50 (2022) 101799.
2. **M.A. Hayat**, Y. Yang, L. Li, M. Bevilacqua, Y.K. Chen, Preparation and thermophysical characterisation analysis of potential nano-phase transition materials for thermal energy storage applications, J Mol Liq. (2023) 121464.
3. **M.A. Hayat**, Y. Chen, Y. Yang, L. Li, M. Bevilacqua, Enhancing Thermal Energy Storage in Buildings with Novel Functionalised MWCNTs-Enhanced Phase Change Materials: Towards Efficient and Stable Solutions, Thermal Science and Engineering Progress (2023) 102313.
4. Ravasio, L., **Hayat, M. A**., Calay, R. K., Riise, R., & Chen, Y. (2024). An experimental study on thermophysical properties of nano-TiO_2-enhanced phase change materials for cold climate applications. *Journal of Thermal Analysis and Calorimetry*, *149*(6), 2549–2560. **(*Author contribution to this paper included the experimental design, development of the methodology, and thorough review of the manuscript.*)**
5. Zahid, I., Qamar, A., Farooq, M., Riaz, F., Habib, M. S., Farhan, M., Sultan, M., Rehman, A. U., & **Hayat, M. A**. (2023). Experimental optimization of various heat sinks using passive thermal management system. *Case Studies in Thermal Engineering*, *49*, 103262. ***(Author primary contribution in this paper involved collaborating extensively on the drafting, reviewing, and revising of the manuscript.)***

Book chapters

1. **M.A. Hayat,** Y. Chen, A brief review on nano phase change material-based polymer encapsulation for thermal energy storage systems, Energy and Sustainable Futures. (2021) 19–26.

Conference papers

- **M.A. Hayat,** Y. Chen, A study of graphene nanoplatelets-based phase change material for low temperature thermal energy storage applications, Published in Proceedings of EUROTHERM SEMINAR #116 Innovative solutions for thermal energy storage deployment, 24-26 May 2023, University of Lleida, Lleida, Spain.

TABLE OF CONTENTS

LIST OF FIGURES

LIST OF TABLES

LIST OF ABBREVIATIONS

2D	Two dimensional
Ag	Silver
Al	Aluminium
Al2O3	Aluminium oxide
CB	Carbon black
CBNP	Carbon black nanoparticles
CNFs	Carbon nano fibers
CNS	Carbon nano fillers
CNTs	Carbon nanotubes
Conc.	Concentration
CoO	Diamond oxide
CTAB	Cetyltrimethylammonium bromide
Cu	Copper
CuO	Copper oxide
CuP	Copper powder
DSC	Differential scanning calorimetry
Dt	Diatomite
DTG	Derivative thermogravimetry
EG	Expanded graphite
EP	Expanded perlite
EP	Expanded perlite
Eq.	Equation
ESH	Eutectic salt hydrate
Fe	Iron

Fe3O4	Iron oxide
F-M+T	Functionalised MWCNTs+TiO2
F-MWCNTs	Functionalised-MWCNTs
FTIR	Fourier transform infrared spectroscopy
GA	Gum arabic
GNP	Graphene nanoplatelets
GNS	Graphene nanosheets
GO	Graphene oxide
LA	Lauric acid
LH	Latent heat
LHTESS	Latent heat thermal energy storage system
L-MWCNTs	Large-Multi wall carbon nanotubes
M+T	Pure MWCNTs+TiO2
MA	Myristic acid
MgO	Magnesium oxide
MWCNTs	Multi wall carbon nanotubes
Nano-PCM	Nanoparticles enhanced PCM
Ni	Nickel
NP	Nano particles
OD	Outer diameter
OD	Outer Diameter
PA	Palmitic acid
PAN	Polyacrylonitrile
PANI	Polyaniline
PAR	Paraffin
PCM	Phase change material

PCS	Phase change material slurry
PE	Pentaerythritol
PEG	Polyethylene glycol
PMMA	Poly (acrylamide-co acrylic acid) copolymer
P-MWCNTs	Pristine-MWCNTs
PV	Photovoltaic
PVP	Poly vinyl pyrrolidone
PW	Paraffin wax
SA	Stearic acid
SDBS	Sodium dodeecycl-benzene
SDS	Sodium dodecyl sulphate
SF	Silica fume
SiC	Silicon carbide
SiO2	Silicon dioxide
S-MWCNTs	Small-Multi wall carbon nanotubes
SSL	Stearoyl lactylate
TC	Thermal conductivity
TD	Tetradecanol
TEM	Transmission electron microscopy
Temp.	Temperature
TES	Thermal energy storage
TGA	Thermogravimetric analysis
TiO2	Titanium oxide
xGnP	Exfoliated Graphite Nanoplatelets

CHAPTER 1: INTRODUCTION

1.1 Introduction

Owing to enormous population growth and a high rise in energy consumption, the energy crisis is still a major issue in modern world [1]. Though researchers have considered and established renewable energy sources such as wind, solar, etc. to replace traditional fossil fuel energy resources, optimising the present use of energy should not be ignored. It is essential to understand how to preserve and maximise energy use before incorporating renewable energy. One strategy to conserve an excess energy is the use of thermal energy storage materials. Instead of releasing it into the atmosphere, the key concept of employing thermal energy storage systems is to preserve thermal energy for subsequent use. Three types of thermal energy storages are available, including latent heat, sensible heat and thermochemical heat storage systems [2,3].

Many researchers have extensively investigated and explored the latent heat storage mechanism using phase change materials (PCMs). PCMs provide impressive thermal storage characteristics and then during the phase transition process, they can accumulate and discharge significant quantities of latent heat. However, PCMs suffer from low thermal conductivity (TC) which results in poor heat transfer performance. A lot of TC enhancement techniques were investigated by different researchers to improve their TC values, such as metal foams [4], fins [5], heat pipes [6] and nanofillers[7]. Nanoparticles reinforced PCMs have the potential to improve the TC values of PCMs significantly because nanoparticles retain high thermal conductivity, low density, high specific surface area and they also have good compatibility with PCMs [8]. In this aspect, this thesis presents a significant effort on the use novel hybrid nanoparticles with PCMs in order to seek a high performance and economical nano-PCMs.

1.2 Background

The planet is facing a lack of natural resources since the 1970's oil crisis [9]. The scientific world is deeply concerned about the rise in world energy use. Global demand for energy is increasing steadily and increased utilisation of fossil fuels results in higher greenhouse gas emissions, particularly carbon dioxide (CO_2), which leads to heavy environmental problems such as ozone depletion, climate change and global warming [10]. According to the

International Energy Agency (IEA), Figures.1.1a and 1.1b show the statistics of major energy consuming sectors and their contribution to CO_2 emissions [11]. The primary reason for the increased energy consumption is the actual increase in standard of living and convenience requirements for heating in cold areas and cooling in hot areas [12]. Air-conditioning growth suggests billions of tons of increases in CO_2 emissions. Rise in air conditioner saturation has significant consequences, not just for total production of electricity and emissions of carbon dioxide, as well as for load managing [13]. Environmental researchers have projected that these CO_2 emissions would lead to an increase in global temperature by 1–3.5°C and a 15–95 cm rise in the sea level by 2050. Global temperature changes are contributing to change in climate. Climate change would contribute a major part in the growing competition of air conditioner purchases [14].

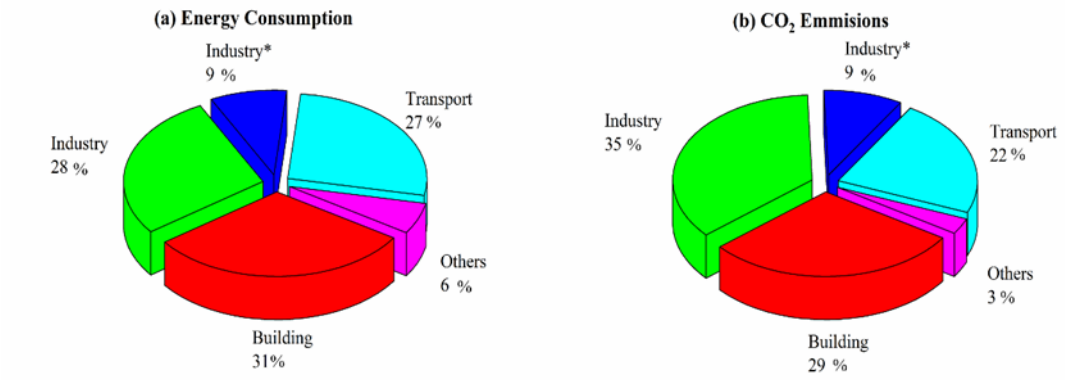

Figure 1.1 (a) Energy consumption sectors (b) Consequently, CO_2 emission [11].

Nature possesses many types of energy. Thermal energy is widely distributed between these types of geothermal energy, solar radiation, etc. Thermal based energy is considered as low-grade class of energy and generally treated as unused in industrial plants [15]. Furthermore, during the daytime the solar radiation tends to provide ample solar energy. But significant extent of energy is still squandered. If this waste energy was not consumed, it simply dissipates in the environment as wastage and results in an emission of poisonous gases as CO_2. If significant quantities of thermal based energy can be preserved and discharged when supplied and demanded, the consumption of conventional fossil fuels could be lowered, which plays a key role in resolving the energy crisis and the issue of environmental pollution. Therefore, storage of thermal energy has gained considerable interest and experience rapid growth [16]. Dorgan and Ellison [17] set forward comprehensive design strategies aimed at ice-cooling cold thermal energy storage systems in 1994. Through comprehensive modelling and simulation

approaches, performance enhancement of cool TES systems for energy efficient buildings has been developed. A few of these systems in buildings situated in arid and hot climate environments have also been field-tested and installed. As a consequence, such systems have contributed to a decrease in on-peak energy and power consumption of around 31% in such buildings. [18,19].

Thermal energy storage (TES) is among the main technologies for energy conversion and is therefore of great practical significance. One of its key benefits is that it is ideally suited for cooling and heating applications. There are different thermal energy storage methods i.e., a) sensible heat storage, b) latent heat storage and c) thermochemical heat storage, which are also shown in Figure 1.2.

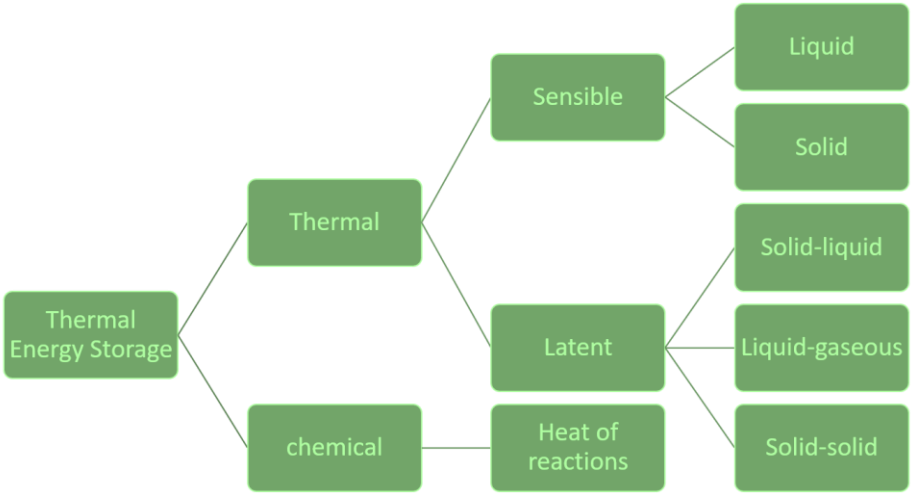

Figure 1.2 Thermal energy storage methods.

Thermochemical energy storage systems are less advanced compared to the sensible and latent heat storage systems and possesses greater technological complexity and higher capital cost [20,21]. Among these TES systems, latent heat thermal energy storage systems (LHTESS) have potential to store energy without an increase in the temperature, while sensible heat storage system increases their temperature during an energy storage process. That is the reason that from last two decades the scientific community is focused on the LHTESS in buildings to reduce the overall energy consumption, as building sector is the major energy consuming sector.

The LHTESS comprises of organic, inorganic, and eutectic phase change materials (PCMs). Furthermore, LHTESS have more energy storage capacity compared to sensible heat storage; that is why it entails comparatively trivial storage volume, which lowers the volume of required storage material. Another benefit is that, due to the nature of the phase transformation process, at almost constant temperatures the thermal energy retained can be recovered. The use of PCM for thermal energy storage (TES) offers an excellent and realistic solution in many domestic and industrial sectors to increase the efficiency of storage and energy utilisation [22–24]. The deployment of PCM for energy storage eliminates the gap between supply and demand, increases energy delivery networks efficiency and reliability, and plays an important general role in energy conservation [22,25]. Phase transition TES technologies have great fusion enthalpy and heat efficiency with the ability to absorb and release large quantities of thermal energy during phase change. Phase-changing thermal efficiency of a specific type of PCM depends solely on its properties. Phase change materials are divided into two main categories based on chemical composition: inorganic PCMs and organic PCMs. Figure 1.3 shows the classification of PCMs based on chemical structures, phase change temperature and phase change process.

High energy storage capacity, high stability, self-nucleation, no segregation, nontoxic, non-reactive, and non-corrosive are the strengths of PCMs and particularly organic PCMs, which include non-paraffins (n-alkenes) and paraffins (n-alkanes) materials [26]. Contrary to this, inorganic PCMs have high latent heat, flame retardance, and comparatively good TC. Nonetheless, inorganic PCMs have phase separation and subcooling, minimising their immediate discharge and utilisation of thermal energy for TES applications. For higher temperature applications inorganic PCMs are more suitable than organic PCMs, while for low temperature applications organic PCMs exhibits better performance [27]. Anyhow, PCMs usually suffers from low thermal conductivity which hinders its heat transfer rate[6]. In addition, lower thermal conductivity (TC), and leakage of PCMs through phase change hinders the performance of TES system. Due to lower thermal conductivity of PCMs, they have less heat transfer rate and leakage of PCMs results in the reduction of latent heat of fusion as its volume decreases during leakage.

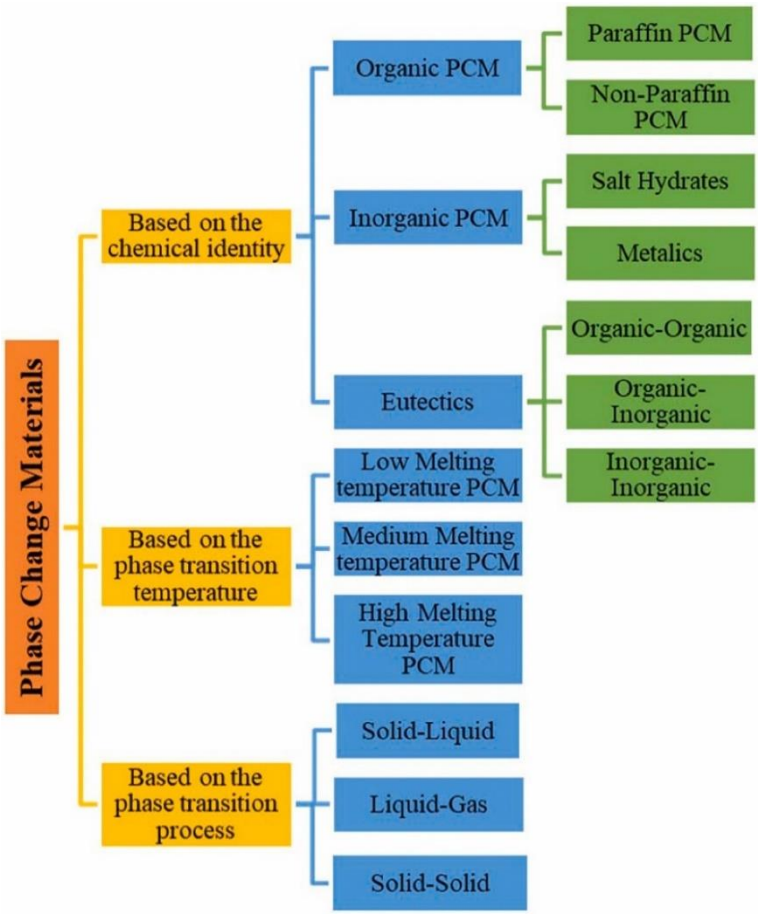

Figure 1.3 Phase change material Classifications [28].

1.3 Research Motivation

From the aforementioned discussion on TES systems and their potential features of minimising the gap between the supply and demand of energy, it has been seen that PCMs have potential to store thermal energy. As the building sector is the major energy consuming area and generates large amount of CO_2 emissions. Indeed, enhancing building insulation and the use of renewable energies are becoming advantageous areas of action for energy consumption reduction and the development of improved energy performance. From the past two decades, researchers have taken a significant and keen interest in the PCMs for thermal energy storage purposes, as the energy storage though PCMs is a passive cooling technique, it requires no external medium for flow and heat transfer characteristic. Moreover, the energy storage though PCMs is gaining popularity because of its inherent properties such as the high latent of fusion per unit volume and slight change in volume during the phase transformation.

However, PCMs suffer from low thermal conductivity, which affects their heat transfer performance during a charging and discharging process. Many research investigations have

conducted on mono nanoparticles for the enhancement in the TC of PCMs, but there are very few investigations on hybrid nanoparticles for an enhancement. So, it is desired to investigate an effect of hybrid nanofillers on the thermal characteristics of PCMs. The developed nano-enhanced PCMs (nano-PCMs) would be extremely useful for the building industry, bringing them a step forward in the race of competition.

1.4 Research Innovation

Recent research on nano-enhanced phase change materials is only focused on the effects of the concentration of mono nanofillers on the thermophysical characteristics of PCM. However, not the same effort has done on investigating the effect of hybrid and modified hybrid nanofillers on the nano-PCM properties. There is a significant research gap in the stability and thermal characteristics of hybrid nano-PCMs [29]. In addition, the novelty of this research lies in its targeted investigation into hybrid nano-PCMs. These materials represent a new frontier in PCM technology, where the synergy between different types of nanofillers could lead to unprecedented improvements in thermal conductivity and energy storage efficiency. Hybrid nanofillers, incorporating a combination of different nanoparticles, could overcome the limitations of mono nanofillers, offering enhanced thermal properties and greater stability during a phase change process.

1.5 Research Aim & Objectives

The primary aim of this study was to develop and evaluate the characteristics of novel, hybrid nano-enhanced Phase Change Materials (PCMs), for application in building energy storage systems. To fulfill this aim, the study is structured around several detailed and scientifically rigorous objectives:

- **Comprehensive literature review:** Conduct an in-depth literature review focusing on phase change materials and nano-enhanced phase change material energy storage systems to identify existing knowledge gaps and establish a theoretical foundation for the research.
- **Investigation of phase change materials with nanofillers:** Systematically examine different categories of PCMs in combination with various nanofillers to select the most appropriate PCM that synergistically works with nanofillers to enhance thermal performance.

- **Over-look an effect of nanofiller concentration:** Determine the detailed effects of concentration of nanofillers on latent heat storage and thermal conductivity, and superior dispersion within the PCM matrix.
- **Examination of mono and hybrid nanofillers effects:** Explore how both mono and hybrid nanofillers influence the thermal characteristics of nano-PCMs. This includes assessing how different combinations and formulations of nanofillers affect the heat storage and release capabilities of the PCM.
- **Study of modified nanoparticles impact:** Investigate the effects of modified nanoparticles on the overall thermophysical characteristics of nano-PCMs. To understanding how surface modifications of nanoparticles influence the thermal behavior of the nano-PCM.

This thesis gives a thorough investigation of nano-enhanced Phase Change Materials (PCMs), with the goal of further understanding in thermal energy storage. The present thesis consists of eight chapters, with the introductory chapter as the first. Chapter 1 presents a general overview of the background, significance, and objectives of this research. Furthermore, it outlines the motivation behind the selected topic. An extensive literature analysis provides the existing knowledge base in Chapter 2. Chapter 3 focuses into the detailed preparation processes of nano-enhanced PCMs, including synthesis methods, base PCM selection, nanoparticle integration, and detailing several characterisation methodologies used in the experimental setting. Chapters 4, 5, and 6 cover the thermophysical characterisation of single nanoparticles, hybrid nanoparticles, and surface-modified nanoparticles based PCMs. Chapter 7 presents a comparative study based on the findings from these chapters. The final chapter, Chapter 8, is a detailed summary that provides insights into significant findings, discusses consequences, and outlines future directions.

CHAPTER 2: LITERATURE REVIEW

A comprehensive critical review on the latest experimental and numerical studies published on nanoparticles enhanced phase change materials (nano-PCMs) has been conducted. Especially, this chapter is focused on the incorporation effects of nanoparticles on PCM thermal properties, specifically thermal conductivity, and energy storage capacity. All categories of nanofillers i.e., Graphene, CNTs, metals, metals oxides, metal carbides and nitrides and hybrid nanofillers are reported separately and a comparison between them has been presented. Figure 2.1 presents a comprehensive overview of the literature review on nano-enhanced PCMs. Central to the graphic is the phase change mechanism, depicting how PCMs store and release thermal energy during melting and solidification, with nanoparticles enhancing this process. Surrounding this core are segments illustrating the key research areas focused on in this chapter: thermophysical properties, preparation methods, characterisation analysis, stability enhancement, and applications. A journal paper based upon this critical literature review has been published [29].

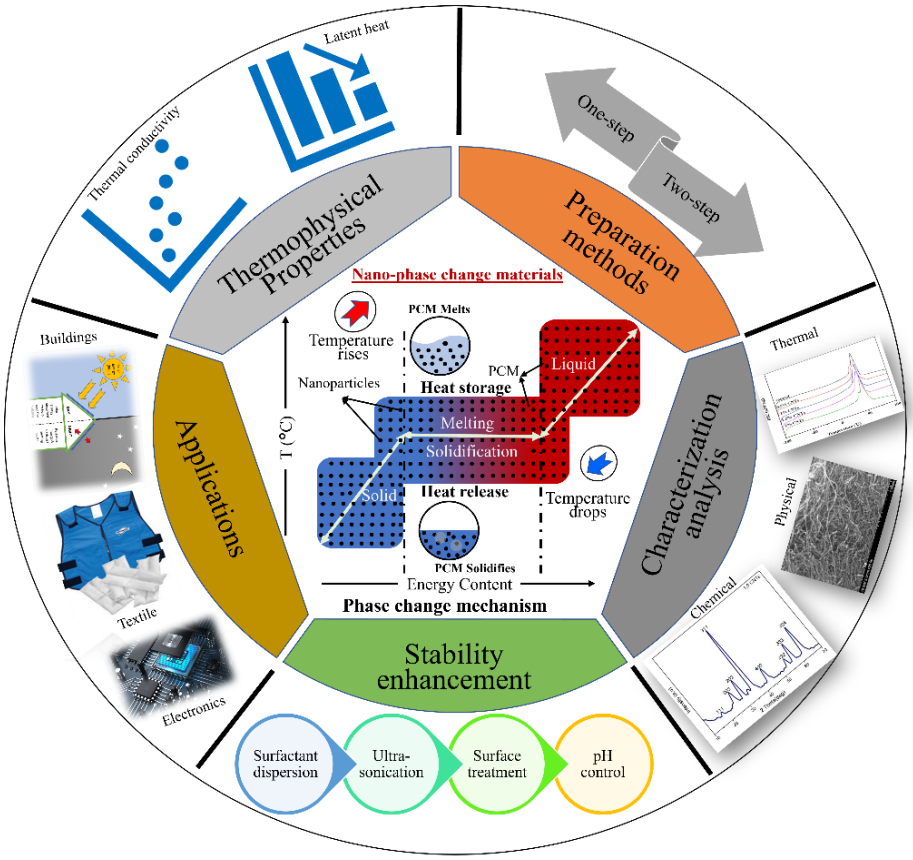

Figure 2.1 Overview of key research areas in nano-enhanced Phase Change Materials (PCMs).

2.1 Unitary nanoparticles based PCMs

There are various types of dispersants as shown in Figure 2.2, such as metal, metal oxides, carbon nanotubes, etc. This section critically examines the impact of all these nanoparticles on the thermophysical properties of PCM. Among all of these, carbon based nanofillers have high thermal conductivity (TC) and a list of the thermal conductivity of different particles is shown in Table 2.1.

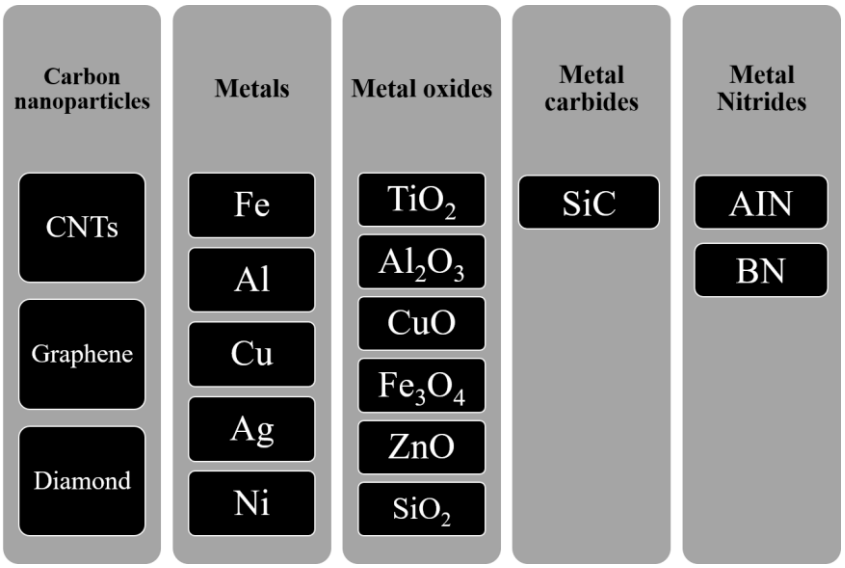

Figure 2.2 Graphical representation of the different type of nanoparticles.

Table 2.1 Thermal conductivity of different types of nanoparticles.

Nanoparticles	Thermal conductivity (W/m. K)
Titanium	21.9
Aluminum	237
Copper	401
Boron	27
TiO_2	8.4
Al_2O_3	36
CNTs	2000-6000
GNP	3500-5000
Diamond	2300
SiC	490

2.1.1 Graphene nanoparticle based PCMs

Graphene, “the mother of all graphitic forms of carbon”, has been widely used with PCMs because of its following advantages [30–32]:

i. little need of heat transfer fluid,
ii. reduced corrosion, clogging and erosion,
iii. larger surface area to volume ratio–enhanced the heat transfer ability,
iv. less requirement of pumping power and energy saver,
v. high thermal conductivity,

Researchers have conducted numerous studies to investigate the effects of thermal properties on PCMs with graphene based nanofillers. For instance, Kim and Drzal [33] prepared paraffin (T_m = 42–44°C) and xGNP based composite using melt and mixing method. They varied the concentration of xGNP by 1%, 2%, 3%, 5% and 7% to study their effects on the thermophysical characteristics of the PCM and they noted that a little rise in the thermal conductivity and latent heat was observed by increasing the volume fraction of xGNP. Similarly, Jeon et al. [34] prepared xGNP and paraffin (T_m = 53–57°C) based composites by identical preparation method as utilized by Kim and Drzal for thermal energy storage applications in buildings. The size of xGNP particles was also similar, but the values of melting temperature of both paraffins were different. Both thermal conductivity and latent heat results of two types of paraffins with different temperature ranges were compared with the similar 3% xGNP concentration and DSC results showed that paraffin with higher melting temperature had higher values of thermal conductivity and latent heat in comparison to paraffin with lower melting temperature.

The graphene oxide particles were investigated experimentally to stabilise the shape of polyethylene glycol (PEG) PCM for TES [35]. It was noted that due to the hydrogen bonding interaction between graphene oxide (GO) and PEG, PEG formed a strong network with 4% GO and showed better stability and no leakage above its melting temperature. In addition, the composite PCM enthalpy decreased with an increase in the graphene oxide (GO) concentration. Furthermore, melting temperature remained almost identical at all concentrations of GO. However, the solidification temperature increased with particle concentrations, but decreased at a higher concentration of GO. In their other study [36], they used graphene and graphene oxide nanofiller for thermal conductivity enhancement and stabilization of PEG respectively. The results showed that the incorporation of GO and GNP was effectively supporting materials

and conductive materials, respectively. Moreover, the latent heat was also enhanced slightly with the incorporation of hybrid nanofillers.

Various PEG and GNP based composites were also developed in which they varied the concentration of GNP from 0.5% to 2% with an interval of 0.5% [37]. Nano-PCMs were prepared by solution blending method which is different from the physical blending method used [6]in their both studies by Qi et al. [35]. The DSC analysis showed that the nano-PCMs prepared by this method depicted higher values of latent heat and thermal conductivity that was increased by 146% with only 2% of GNP. In addition, pure PEG and PEG/GNP composites were tested to investigate the photothermal performance and results revealed that PEG/GNP composites exhibit better heat storage performance than pure PCMs.

The influence of GNPs on the crystallization kinetics of pentaglycerine (PG) (T_m = 81°C) was investigated [38]. Both PCM and GNP were mixed for one hour at 400 rpm by a planetary ball mill. Activation energy which is a crucial factor in describing the complexity in the kinetics of crystallization was studied by a multiple scanning method. The results have indicated that the GNP content increases the activation energy throughout the analysis and the macroscopic thermal conductivity enhancement has a greater impact on the phase transition of PCMs compared with the microscopic activation energy. Thus, improving the thermal conductivity enables the crystallization of the PG/GNPs composites, which helps to increase the crystallization rate. Cui et al. [39] dispersed GNPs into the $Ba(OH)_2 \cdot 8H_2O$ inorganic PCM (T_m = 78°C) to study the supercooling, TC and heat storage performance of composite PCM. It has been reported that adding graphene nanoplatelets effectively reduces the supercooling degree and heat release time of $Ba(OH)_2 \cdot 8H_2O$. In addition, Zhang et al. and Cui et al. investigated GNPs with organic and inorganic PCMs respectively although their melting temperatures were almost identical. In the comparison of their results, DSC results showed that pure organic PCM exhibited greater energy storage value than virgin inorganic PCM. On the other hand, inorganic nanocomposite PCMs demonstrated higher thermal conductivity value than organic nanocomposite when they are compared at the similar concentrations of nano particles.

Graphene nano platelets with bee wax (T_m = 62°C) composite PCM were developed by sonication and ultra-sonication method for the improvement in the thermophysical characteristics of PCM [40]. The mass concentrations of GNP for the preparation of nano-PCMs were 0.05. 0.15 and 0.3 %. The results showed significant improvement in the latent

heat (22.32%) when the mass concentration of graphene nano platelets was increased. The reason behind the increase in the latent heat was explained by Brownian motion and nanoparticles clustering mechanism [41]. The graphene nanoplatelet random motion increased the likelihood of agglomeration within the base fluid of the beeswax. In addition, the Van der wall forces attracted each other between the graphene nanoplatelets and produced particle clusters [41]. Nevertheless, lower nanoplatelet concentrations allowed thermal storage to be more efficient per unit volume. The PCM with almost similar melting temperature (T_m = 66°C) as used by Amin et al. was investigated with graphene particles (1, 2, 3 and 4%) in the study conducted by Yavari et al. [42]. The method used for the preparation of nano-PCMs was also similar to the Amin et al. [40]. The results showed a decrease in the latent heat was noted with the rise in the particle concentration and at 4% of graphene the maximum reduction in the latent heat was 15.4%. They gave the reason behind the reduction in the latent heat that by the addition of graphene some PCM volume is replaced by graphene sheets which are not subject to the phase transition. A similar reason for the reduction of latent heat of PCM by the addition of nanoparticles was given by Putra et al. [43]. Furthermore, the results also showed that nano composite with a lower concentration of nanoparticles showed improvement in the latent heat value in contrast to the nano composites with the higher concentration [13, 32].

An experimental investigation on xGNP and graphene-based PCM composites was conducted to investigate the thermal performance and stability of PCM by solution mixing method [44]. Due to the larger surface area of graphene than that of xGNP, 2% graphene showed better stability because PCM absorbed completely in graphene. However, xGNP showed noticeable enhancement in the thermal conductivity compared to the graphene particles. Putra et al. [43] experimentally studied the Graphene/RT-22 (T_m = 22–24°C) based nano-PCM for the cold storage application. The width and thickness of graphene nanoparticles were less than 2μm and 2 nm, respectively. The result showed that with the addition of nanoparticles latent heat decreases, while the thermal conductivity of particles increases by 89.6% with the increase in the concentration of graphene nanoparticles.

Silver based graphene nanosheets (GNS) were developed and integrated with PEG PCM [45]. The multi-folded layered structure provides Ag–GNS a large surface area to support PEG for achieving the shape stability. Moreover, the results showed that the freezing and melting temperatures remained almost unchanged and latent heat was decreased when a concentration

of Ag–GNS particles was increased. However, the developed Ag–GNS/PEG composites showed high thermal energy storage properties and efficient photothermal conversion. The hybrid nanofillers (Ag-GNS) increased the composite photothermal conversion efficiency (88.7–92.0%) and materials thermal conductivity (49.5–95.3%). Like Zhang et al., Yang et al. [46] tested PEG PCM with boron nitride and GNP composite by solution mixing method. The synergistic effect between GNP and BN results in the improvement in TC and stability of PCM even at a small concentration of GNP (1%). What is more, the DSC results showed no significant change in their melting and solidification temperatures of the composite. Similarly, Zhou et al. [47] conducted an investigation on PEG PCM but in this study PCM was impregnated into the cellulose nanocrystal (CNC) hydrogel by a novel solvent exchange method. At the 97% mass concentration of PEG, PEG/CNC exhibited good latent heat value 151.8 J/g which was slightly lower than pure PEG 155 J/g. In addition, the PEG/CNC composite slowed down the crystallization rate indicating the extremely high specific area of the CNC nanofiber network and the heavy hydrogen bonding between CNC and PEG. In the meantime, the crystalline phase change temperature of PEG decreased from 40.1°C pure PEG to 33.5°C of PEG/CNC hybrid PCM. From these studies [45–47] in which PEG was used as PCM, Zhou et al. [47] showed good thermal performance in comparison to other studies. This may be because of the strong bonding between PCM and nanofiller which results in higher thermal efficiency. Furthermore, the size of nanoparticles may also be a factor because nanoparticles used in the study [47] were smaller than other ones and large size particles usually results agglomeration.

2.1.2 CNTs and nanoparticles based PCMs

Carbon nanotubes (CNTs) are commonly used as dispersants because of their high thermal conductivity. Therefore, in recent years the use of novel carbon allotropes has continued to increase. CNTs are lightweight materials and have great surface areas and small particle size, that improves the intermolecular attractiveness among the molecules in nano-PCM. Recent studies on the effect of CNTs on PCM thermal characteristics are critically explored in the following paragraphs.

The effects of applying different carbon nanofillers (CNs) over the energy storage capacity and TC of nanocomposite PCMs based on paraffin were examined [48]. The tested CNs included long and short MWCNTs, carbon nano fibers, and GNPs. Nanocomposite PCM samples with

CNs mass concentrations of (1–5) wt. % were prepared for each form of CNs with an increase of 1 wt.%. The results reported that the existence of carbon nanofillers improved nanocomposite TC, but the improvement depended on both the shape and size of the carbon nanofillers. Because of their 2D planar structure, which resulted in decreased filler/PCM thermal interface resistance, an increase of up to 164 % in the TC value was achieved at the concentration of 5 wt.% of GNPs. The small multi-wall carbon nanotubes (S-MWCNTs) showed the best dispersion among the three wire-shaped fillers and consequently the most pronounced enhancement. The existence of CNs, however, contributed to the diminution of latent heat ability with the increasing concentration of all CNTs. The PCM and carbon nano fillers (CNF) composite offered the highest latent heat potential at constant loading, which could be due to the size and shape of the particle (the larger shape and the size of the filler improves the heat conductive connections). Like carbon nano fibers (CNFs) as discussed earlier in [48], it was found that similar results in their experimental and numerical study in which they examined the effect of particles size on the latent heat diminution of MWCNTs based paraffin composite [41]. All volume fractions MWCNTs with larger diameters in the PCM resulted in good latent heat compared to CNTs with smaller diameters. Correspondingly, its numerical results reported that even though microscale particle adding improves performance the of thermal storage, nanoscale particles will degrade storage performance compared to pure paraffin.

The processing methods have also been explored. Zhang et al. [49] prepared nano-PCM emulsion using sonication method in which n-octadecane, octadecanol and MWCNT were used as PCM, nucleating agent and nanoparticles, respectively. The results showed that with 10% nano-PCM emulsion the thermal conductivity was increased linearly by the addition of MWCNTs, but with a little decrease in the latent heat. However, at 20% nano-PCM emulsion, the composite with 0.1% MWCNT and 0.5% octadecanol doubled the values of latent heat as compared to 10% nano-PCM emulsion. Meng et al. [50] prepared an eutectic mixture of three fatty acids the melting temperature of this eutectic mixture was nearly similar to the PCM used by Zhang et al. and the nanomaterial in both of these studies were also identical. Moreover, the infiltration method was used to prepare MWCNTs and fatty acids-based nano-PCM. They figured that latent heat values of mixed PCMs were lower than their individual values and by incorporation of different concentrations of MWCNTs (10%, 20%, 30%, 40%, 50%) latent heat of melting and solidification further decreased. Furthermore, this composite nano-PCM

showed higher heat storage capacity than the nano emulsion-based composite used by Zhang et al. However, nano emulsion-based composite decreased the supercooling up to a greater extent.

A study of a comparison between pristine and modified MWCNTs based nano enhanced PCM for thermal energy storage usages was reported [51]. The organo-silane-modified CNT based PCM demonstrated better stability dispersion compared to the pristine CNTs based PCM. What is more, with the incorporation of pristine CNTs electrical surface resistivity decreases. At lower concentration (0.1 %) of pristine CNTs the nano-PCM showed little increase in latent heat values. This could be because the larger surface area, greater dispersion capability of CNTs and great intermolecular interaction between the molecules had resulted in an increases in the latent heat [52]. On the other hand, silanised CNTs were found to be nonconductive because the functional groups attached to the surfaces significantly modified the surface properties of the Si-MWCNTs.

The other approaches of particle treatments have been studied. Qian et al. [53] have tried to develop the PEG and diatomite coated MWCNTs based stable composite PCM which showed good stability at PCM concentration of 60%, but with a significant decrease in the latent heat. In another study, [54] they compared two different carbon based nanofillers (GNPs and SWCNTs) with PEG as PCM. The small volume concentrations of 4% GNPs and 8% SWCNT were added into the PEG to form shape-stable composites. It was found that GNPs/PEG and SWCNTs/PEG held 96% and 92% heat storage density of pristine PCM and enhanced thermal conductivity by 1096% and 950% respectively as compared with the virgin PCM.

The concentration effects of CNTs and CNFs on the thermal conductivities of CNT and CNF based PCMs have been studied [55]. It was observed that the thermal conductivity increased with an increase in the content of (S-MWCNTs and L-MWCNTs) CNTs or CNFs. But CNFs exhibited higher thermal conductivity values compared to CNTs. Because CNTs easily entangle and form clusters which limits their efficiency in the PCM matrix. Moreover, CNFs having a higher diameter and have weak Van der Waals forces between the fibers results in the uniform dispersion of the PCMs matrix. That is why CNFs performed better than CNTs for thermal conductivity enhancement. Likewise, similar behaviour was observed [55] when CNFs and CNTs were compared. It was found that thermal conductivity increased with the addition of CNFs and CNTs, but CNFs showed higher thermal conductivity than CNTs for all

concentrations. On the other side, when Fan et al. [48] compared S-MWCNTs and L-MWCNTs (CNTs) with CNFs they found CNTs showed higher thermal conductivity than CNFs. This might be because of the difference in their sizes, as in both studies the sizes of nanofillers were different and this needs further investigation to identify the effect of the size of nanoparticles on thermal conductivity. However, PCM/CNFs composite offered the highest latent heat potential at constant loading. This could be due to the size and shape of the filler (the larger size and the shape of the form improves the heat conductive connections).

There are a few more reports of CNF effects on thermal properties of phase change materials. Like, Elgafy and Lafdi [56] compared experimental and numerical results of the paraffin based raw CNFs and surface treated CNFs composites. A good relationship between both experimental and analytical models was observed. By increasing the concentration of CNFs, the output power from the composites increased. Furthermore, surface treated 4% CNFs indicated better performance compared with untreated 4% CNFs based composite. Darzi et al. [57] combined electrospinning and electro spraying concurrently to develop PCMs based nanofibers. The spraying of graphene and carbon fibre powder significantly reduced the melting temperature of PCMs, whilst a decrease in the latent heat by large amount.

Chinnasamy and Cho [58] incorporated MWCNTs into lauryl alcohol as PCM at different concentrations ranging from 1 wt. to 5 wt. %. The results showed that the degree of supercooling was reduced by the addition of MWCNTs, and the TC was increased by 82.6% at 5 wt.% of CNTs. He et al. [59] investigated the effects of P-MWCNTs on PCM at three different particle concentrations ranging from 1 wt.% to 3 wt.%. They found that at 3 wt.% of MWCNTs, the TC of nano-PCM in solid was raised by 47.30%, with the reduced supercooling. However, the stability of the nanoparticles, which is a significant aspect of the overall performance of nano-PCMs [60], has been neglected in many previously published studies and needs more investigations.

The major drawback of using MWCNTs is their stability since their hydrophobic nature makes it difficult to disperse in any aqueous solution to obtain a homogeneous mixture [61,62]. The dispersibility of MWCNTs can be improved by functionalising MWCNTs and there are various ways to functionalise MWCNTs with additional groups to improve their dispersibility within enhanced PCMs, including acids [63], amines [64], polymers [65], and other groups. MWCNTs

thermal conductivity, stability, and compatibility with PCMs have all been proven to improve by functionalisation [66,67]. Recent studies have shown that acid (H_2SO_4+HNO_3) functionalisation of MWCNTs improves their thermal conductivity and stability, making them suitable for nano-phase change materials (nano-PCMs). The acid treatment not only increases the surface areas of the MWCNTs but also creates functional groups on their surfaces, which improves their dispersion and interaction with the PCM matrix. These functionalised MWCNTs have been shown to augment the heat transfer properties of PCMs and increase their thermal reliability [68]. Kumar et al. [69] explored pristine multi-walled carbon nanotubes (MWCNTs) and acid functionalised multi-walled carbon nanotubes (F-MWCNTs) as nanoparticles to enhance the thermophysical properties of inorganic salt hydrate PCM. The results showed that the addition of 0.5 wt. % MWCNTs improved the thermal conductivity by 50% compared to pure salt hydrate PCM. Furthermore, the inclusion of 0.5 wt. % F-MWCNTs increased TC by 84.78% compared to pure salt hydrate PCM. In their other investigation [70], they employed varied concentrations of functionalised and un-functionalised MWCNTs with salt hydrate PCM. The incorporation of 0.7 wt.% MWCNTs improved the thermal conductivity of PCM to 0.78 W/mK, while 0.7 wt.% F-MWCNTs improved the TC of PCM to 0.92 W/m.K, compared to pure salt hydrate PCM, and lowered the light transmittance to 92% and 93.49%, respectively. Fikri et al. [71] examined the TC enhancement of organic PCM (A70) by incorporating various mass fractions (0.1 wt.–1.0 wt. %) of F-MWCNTs. The results found that the thermal conductivity of the composite was enhanced by the addition of 1.0 wt. % of F-MWCNTs compared to the pristine PCM. Additionally, it was observed that the nano-PCM was thermally stable up to 200 °C and did not undergo any chemical reactions with the base PCM.

Despite the potential benefits demonstrated by functionalised MWCNTs as nano-enhanced phase change materials (PCMs), a crucial aspect that has received limited consideration is the stability of the MWCNT-enhanced PCM. It is well established that the stability of nanoparticles is a crucial factor in determining the overall performance of nano-PCMs [72,73]. Several methods have been investigated by researchers including pH adjustment, and surfactant addition [74]. However, among these techniques, acid functionalisation was proven as an effective method with better long-term stability of MWCNTs within PCM [75]. In recent literature [66,69–71,76,77], studies on functionalised MWCNTs have emerged, however, the stability of such functionalised MWCNTs has not been fully addressed. Although MWCNTs

are not low-cost particles, their exceptional properties such as their high aspect ratio, high TC, and efficient heat transmission properties as compared to other existing nanofillers have the potential to justify their applications in highly efficient nano-PCMs for TES [78]. An innovative approach is needed to evaluate the stability and sustainability of the modified and un-modified MWCNTs-based PCM, which has been previously neglected in the current available literatures.

2.1.3 Metal and metal oxides nanoparticles based PCMs

Nanoparticles based on metals are produced through metals to nano size materials by constructive or destructive processes. The metal nanoparticles have unusual characteristics, for example small size around 10-100 nm and cylindrical and spherical structures. On the other hand, metal oxide type nanofillers are produced to change the characteristics of their corresponding metal nanomaterials. In contrast with their metal counterparts, these nanoparticles have excellent properties.

The effects of TiO_2 nanoparticles on the thermal properties of paraffin wax PCM have been studied. Wang et al. [79] tested TiO_2 nanoparticles (20nm) with paraffin wax to enhance the thermophysical characteristics of PCM. The increase in thermal conductivity and latent heat was spotted by the inclusion of 0.7% TiO_2, while latent heat started decreasing when TiO_2 concentration exceeded 0.7%. In another study [80] Teng and Yu also used paraffin as PCM and tested with different concentrations of TiO_2 nano additives. The nanoparticles size and nano-PCM preparation method were similar to the study performed by Wang et al. [51]. Moreover, they also found an increase in the latent heat of melting with the addition of up to 2% of TiO_2 in the paraffin. However, the thermal conductivity of nano-PCM composite increased linearly with TiO_2 nano fillers but TiO_2 base nano-PCM was found to be more thermally and chemically stable.

A two-step method was employed to prepare TiO_2/paraffin composites for the improvement of thermal properties of energy storage materials [81]. TiO_2/paraffin composites with and without stearoyl lactylate sodium (SSL) as a surfactant were tested for thermal characteristics and stability. Several volume concentrations of TiO_2 (0.5%, 0.7%, 1%, 2%, 3% and 4%) were investigated and the results showed that paraffin samples with 1 wt.% and 3 wt.% of TiO_2 had higher latent heat values of 165.1 and 167 J/g for without and with SSL respectively. Haghighi et al. [82] investigated SDS surfactant with TiO_2 and paraffin based nanofillers to study the

thermal performance of nano-PCM, except surfactant remaining materials (PCM and nanoparticles) was almost identical to the material used by Sami and Etesami [81]. The results showed that SDS-based TiO_2/paraffin composites exhibited highest (179.8846 J/g) enthalpies compared with the pristine PCM having an enthalpy of 142.3565 J/g. By comparing these two studies [81] and [82], it was observed that latent heat value was increased compared to pristine PCM, however SDS surfactant-based nano-PCM showed higher energy storage capacity with greater latent heat value as compared to the SSL surfactant-based nano-PCM composite. Haghighi et al. [82] also performed a comparative analysis by employing different nanofillers (i.e. CuO, TiO_2, Al_2O_3 and graphene) with paraffin and the latent heat values of these composites are shown in Figure 2.3. It was found that at 2 wt.% TiO_2/paraffin composite revealed higher heat storage capacity than other composites, while graphene/paraffin composite depicts higher thermal conductivity because of the higher thermal conductivity value of graphene. Correspondingly, when examining the energy storage capacity of various nanofillers (Al_2O_3, TiO_2, SiO_2, and ZnO) Teng and Yu [80] uncovered that the TiO_2/paraffin combination exhibited high heat storage capacity at all concentrations in comparison to other nanofillers.

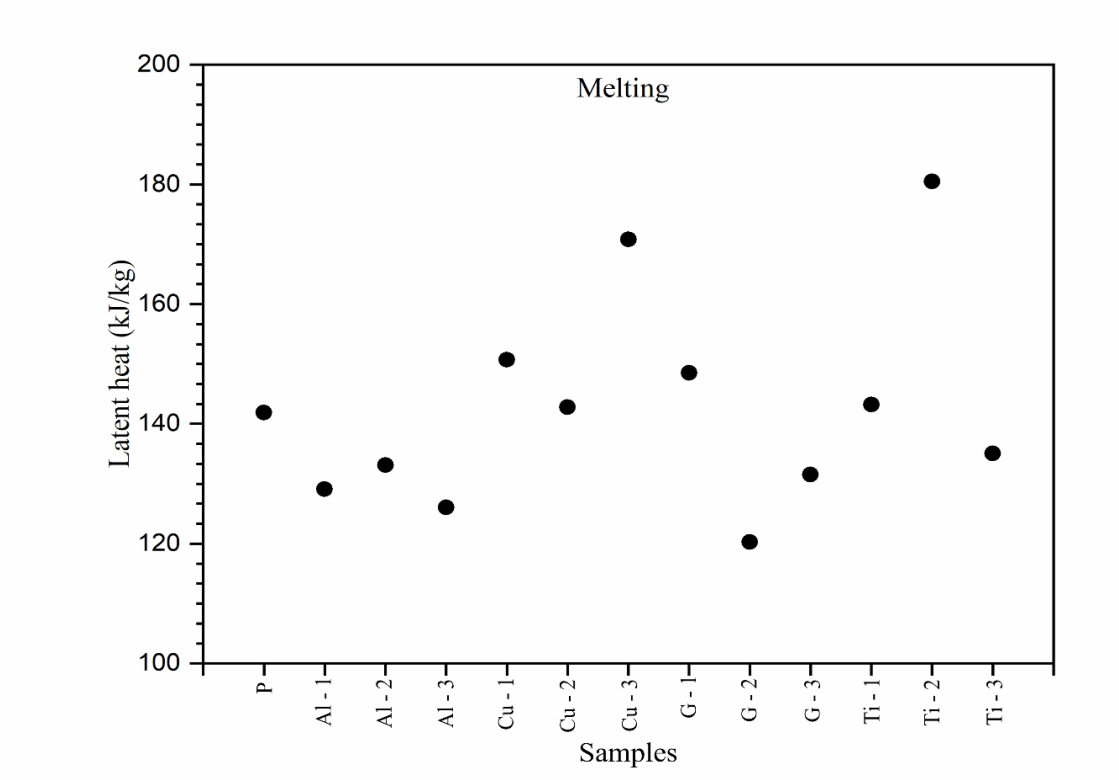

Figure 2.3 Latent heat comparison between paraffin based different composites [82].

The two step method has also been employed to prepare nano enhanced PCM in which stearic acid (T_m = 57 -59 °C) was used as PCM and TiO_2 as nanoparticles [83]. The results showed an inverse relationship between latent heat and TC as shown in Figure 2.4, which was due to the interaction between the nanoparticles and PCM. Moreover, both decline in latent heat and increase in TC of the PCM strongly depend on the type (i.e., grapheme, CNTs, metal, and metal oxide nanoparticles), shape, size, and volume fraction of the nanoparticles. Similarly, a slight decrease in the latent heat of fusion was noticed with an upsurge in the particle concentration in another experimental study investigated by Sharma et al. [84]. This may be because of changes in physicochemical characteristics caused by the TiO_2 nanoparticles dispersal. Both palmitic acid PCM and TiO_2 (0.5%,1%, 3% and 5%) nanoparticles were employed to develop nano-PCM for solar thermal energy storage energy applications [84]. The nano composite has shown that the TiO_2 nanoparticles do not affect PCM chemical structure but do improve the chemical stability [84].

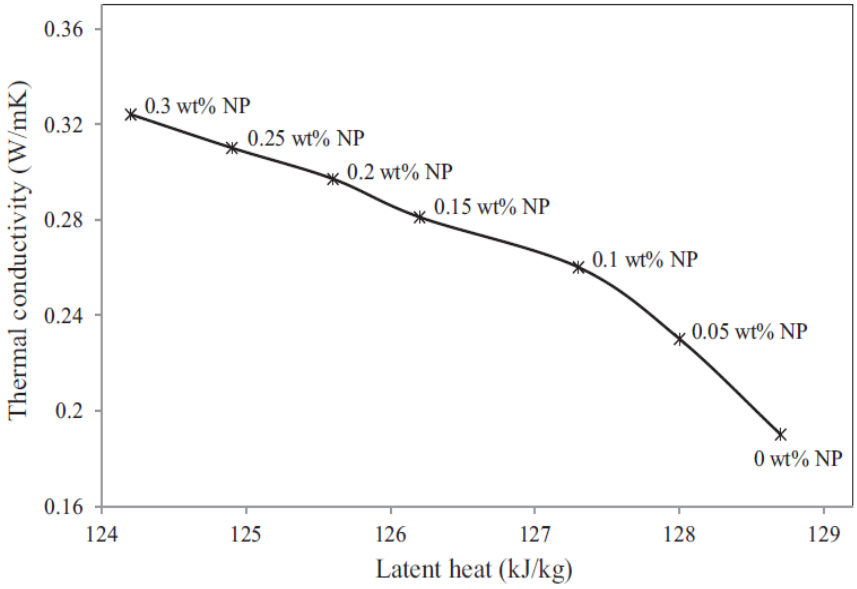

Figure 2.4 Effects of nanoparticle concentration on the thermal conductivity and latent heat of composite PCMs [83].

An effect of the size of TiO_2 nanoparticles on the eutectic salt hydrate inorganic PCM was reported [85]. The results demonstrated that TiO_2 nanoparticles with a smaller size (25nm) exhibited greater stability when integrated with the PCM, compared to larger particles (100nm). Moreover, it was noticed that surface adsorption capacity was improved with a reduction in the size of nanoparticles, which increased the nucleation and growth rate of nano-PCM while producing improved crystalline content.

Many studies were carried out on PCMs with Al_2O_3 particles. Mohamed et al. [86] developed α-Al_2O_3 (1.4–2 nm) nanoparticle paraffin wax based PCM in which an upsurge in thermal conductivity and latent heat was observed with the increase in nanoparticles concentration, while Babapoor and Karimi [87] found the decrease in the latent heat value for Al_2O_3 (20nm) based paraffin composite even at the same concentration of nano alumina used by Mohamed et al. This may be because of different particle size utilised by Mohamed et al. and Babapoor and Karimi. Furthermore, different metal oxide nanoparticles having particle size of 11 and 20 nm (SiO_2, Al_2O_3, ZnO, and Fe_2O_3) were compared with paraffin. The results showed that 8% SiO_2 (11nm)/paraffin composite indicated better stability compared to other composites. However, Al_2O_3/PCM composite demonstrated highest thermal conductivity value and overall and it performed better than other composites.

Two types of organic PCMs (RT-20 and RT-25) with carbon black (CB) and Al_2O_3 nanoparticles were studied and tested [88]. The results showed that an addition of only 1% of carbon black and Al_2O_3 particles resulted in the enhancement of latent heat value for all composites, except for RT25/CB composite. Furthermore, the nano-PCMs based on Al_2O_3 were considered unstable and a certain deposition of nanoparticles was identified. However, the nano-PCMs based on CB were highly stable and showed higher thermal conductivity than Al_2O_3 based nano composite[88]. Coated Al_2O_3 nanoparticles with ionic surfactant were also investigated to improve the stability of based nano-PCM [89]. It was found that emulsion density fit excellently with the prediction based on the theory of mixtures. Further, a decrease in the latent heat was observed in the nano-PCMs as compared with pure PCM. In theory (equation (2.1)), the latent fusion heat of composite materials is supposed to decrease linearly with the addition of particles [41].

$$h_{sl,nPCM} = \frac{\partial_{pcm,s}\ h_{sl,bPCM}\,(1-\emptyset_p)}{\partial_{nPCM}} \tag{2.1}$$

where, $\partial_{pcm,s}$ represents the PCM density in the solid phase, ∂_{nPCM} is the theoretical density of nano-PCM, $\emptyset_p$ is particle volume fraction, and $h_{sl,bPCM}$ is the solid-liquid latent heat of the base fluid.

Similarly, inorganic salt hydrates PCM and nano-α-Al_2O_3 have also been investigated with surfactants [90]. It was reported that the latent heat was decreased from 280 J/g to and 256.9 J/g for with and without nano-α-Al_2O_3 particles, correspondingly. The results also showed that the impregnation of 4.5% of nano-α-Al_2O_3 particles decreased the supercooling degree from

7.8°C to 1.6°C and their melting temperature was also reduced from 33.7°C to 31.6°C. Moreover, it was observed that nano-α-Al_2O_3 particles had a small influence on phase transition behaviour. As the nano-α-Al_2O_3 mixing ratio increased from 3.0 to 4.5 wt. %, the latent heat of modified ESH decreased further slightly.

The numerical studies have also been performed by various researchers on the nano-PCMs to investigate their thermal characteristics. Akhmetov et al. [91] numerically scrutinized the impact of doping of Al_2O_3 nanofillers on paraffin wax. The simulation results showed that the incorporation of Al_2O_3 improved the heat transfer of PCMs, but no significant change was observed in latent heat and specific heat capacity. Furthermore, composite PCMs reduce the melting and solidification time compared to pristine PCMs, these reductions in charging and discharging time led to greater charging and discharging efficiency of the system. Bayat et al. [92] numerically investigated the two different nanoparticles (CuO and Al_2O_3) with paraffin as PCM to observe a melting process of this PCM. They found that by adding a small percentage of nanoparticles (2 %) thermal performance was enhanced. Arasu et al. [93] in their numerical investigation also found that lower volumetric alumina content in paraffin wax had lower cost and high energy storage capability compared to higher concentrations. Furthermore, raising the percentage of nanoparticles not only stopped the thermal enhancement but also decreased it and Al_2O_3 nanoparticles showed better performance than CuO at the same concentration. Despite the higher thermal conductivity of CuO, due to the high viscosity, heat transfer decreased [92]. Chen et al. [94] used PCM slurry with three different nanoparticles (i.e., Cu, TiO_2 and Al_2O_3) to enhance the performance of solar thermal energy storage systems. The results demonstrated that TiO_2 with 0.1% concentration in PCM showed better stability and thermal performance compared to Al_2O_3 nanoparticles. Similar to the study [94] it was reported in a current study that Cu nanoparticles exhibited poor stability they precipitated completely at the bottom after 72 hours.

In an empirical investigation on the melting of nano enhanced PCM (i.e. Al_2O_3/paraffin) in a squared enclosure heated horizontally and vertically, it was reported that with an increase in the volumetric concentration of alumina the melting rate of PCM was decreased [93]. This was because of the increased viscosity at higher concentrations of alumina which hindered the natural convection. Furthermore, vertical wall heating depicts a better melting rate and energy stored than horizontal wall heating in a square enclosure due to the increased natural convection

effect. In the subsequent study [95], a numerical investigation on PCM embedded nano-Al_2O_3 (2%, 5% and 10%) was also performed and the results were compared with those from pure PCM in a concentric double pipe heat exchanger. In comparison to simple paraffin wax, nano-Al_2O_3 based paraffin wax greatly enhanced the charging and discharging performance. Table 2.2 demonstrates the influence of nanofillers on the charging and discharging rate of different PCMs.

PCMs with metal nanoparticles have also been studied. Ma et al. [96] investigated metal nanoparticles and expanded graphite (EG) as a supporting material based nano-PCM. It was observed that 11% EG and 1.9% Cu nanoparticles with paraffin were an optimal composition for nano-PCM at which no leakage was found during the phase change of PCM. Moreover, with this composite PCM thermal conductivity was enhanced by nine times, while a little decrease in the latent heat value was noted. Cui et al. [97] also examined Cu nanoparticles but they used an inorganic PCM. In their study, they synthesised nano enhanced PCM to study the effect of supercooling. It was concluded that 0.5% of Cu nanoparticles in the salt hydrate ($CH_3COONa.3H_2O$) PCM showed a minimum supercooling effect on the composite system.

What is more, that the inclusion of Cu nanofillers improves the heat storage efficiency by storing heat in a short time as compared to virgin PCM. Subsequently, Gupta et al. [98] examined magnesium nitrate hexahydrate (MNH) an inorganic PCM with two different metallic nanoparticles (Cu and Fe) for the solar thermal energy systems. The results have shown that 0.5% of Cu and Fe nanoparticles enhance the melting and solidification rate of nano-PCMs by (5.6% and 7.8%) and (30% and 35%) respectively compared to pristine PCM. Moreover, like the study [97] Gupta et al. also examined 0.5% Cu nanoparticles which displayed higher thermal conductivity compared to 0.5% of Fe nanofillers.

Due to their high thermal conductivity copper oxide was also used as a nanofiller with PCMs for the improvement in the thermal properties of PCMs. CuO nanoparticles with the RT-42 PCM were studied for the enhancement of thermal performance of Building-Integrated Concentrated Photovoltaics (BICPV) and were compared with the different configurations [99]. Only 0.5% of nano enhanced PCM showed an increase in the thermal conductivity and depicted better heat transfer performance than pure PCM. In another study [100] a comparative analysis between two different nano enhanced PCMs (i.e. PANI/paraffin wax (PWP) and

CuO/paraffin wax (PWC)) was performed. It was found that 1% PANI/PCM and 0.1% CuO/PCM based nano enhanced composites increased the latent heat of nanocomposite by 8.20% and 7.81% respectively. The latent heat improvement maybe because of the strong interaction between the paraffin wax and the PANI nanofillers. Further, the large surface areas of PANI nanofillers might also be the reason, which leads to the greater intermolecular interaction between the PCM and nanoparticles. Therefore, for the nanocomposite to shift its phase from solid to liquid, more energy needs to be supplied. The nano-PCM showed visual signs of agglomeration and deposition of nano-CuO composite due to the difference in their densities. In future work, other forms of TCE of nanoparticles with a density of the similar order as the base PCM could be used to overcome agglomeration problem.

Table 2.2 Influence on the charging and discharging time with nanoparticles incorporation.

Reference	Nano-enhanced PCM		Charging/discharging effect
	PCM	Nanofiller	
Ebrahimi and Dadvand [101]	Paraffin wax	Al_2O_3	By the addition of the 2wt.% of Al_2O_3 nanoparticles the melting time was reduced at all heating modes.
Singh et al. [102]	Sugar alcohol (d-mannitol)	GNP	The melting time was reduced by 11%, 39% and 55% with the 1, 3 and 5 wt.% of GNP nanoparticles in the PCM.
Ebadi et al. [103]	Coconut oil	CuO	With only 0.0218 wt.% of CuO nanofillers the overall melting time was reduced by 15%.
Farzanehnia et al. [104]	Paraffin wax	MWCNTs	Compared to pristine PCM, applying MWCNTs to PW decreased the discharging period by 6 %. In addition, the PCM and nano PCM presence reduced the temperature rise and improved the electronic components working time.
Abdulateef et al. [105]	RT-82	Al_2O_3	In paraffin, the existence of nanoparticles enhances the overall performance, particularly in the discharging phase.
Khan and Ahmad Khan [106]	Paraffin	GnP, Al_2O_3 and aluminium nitride (AlN)	Introducing AIN, Al_2O_3 and GNP to pristine PW raises the melting rate by 36.47%, 28.01% and 44.57%, and the solidification rate by 34.95%, 14.63% and 41 %, respectively.
Kalaiselvam et al. [107]	Eutectic PCM	Al and Al_2O_3	In comparison with pure PCM, the addition of Al and Al_2O_3 nanofillers decreased the discharging process by 4.97 % and 12.97 %, respectively.
Ma et al. [108]	RT-24	Cu	At a specific time, Cu/RT-24 based nano PCM charged and discharged 8.3 and 25.2 times more energy respectively, as compared to the neat PCM.
Xiao et al. [109]	Binary nitrate	EG	The dispersion of 20% EG into the PCM decreased charging and discharging time by 26.9% and 68.8%, correspondingly.

Nano magnetite (Fe_3O_4) based PCM needs to be prepared by sol-gel method and dispersed these particles in the paraffin PCM for energy storage purposes [110]. In this study, the particles having different concentration (1%, 5%, 10% and 15%) was added to melted PCM, then this mixture was stirred for two hours with an ultrasonic water bath to get a homogenous mixture. In the DSC analysis, it was discovered that latent heat of the nano composite PCM was increased by 20% by the addition of 10% of Fe_3O_4 and with almost negligible change in melting temperature. Later, in the other study [111] a higher concentration of Fe_3O_4 (10% and 20%) was employed. For 10% and 20% Fe_3O_4 the thermal conductivity was enhanced by 48% and 67% respectively. Besides, when latent heat value was compared with that from their previous study for 10 % of Fe_3O_4 [110] both studies showed an increase in the latent heat compared to virgin PCM, but their previous study showed higher latent heat than the current study [110]. This may be because of little difference in the preparation method of nano-PCM from the same team, however, this needs a further investigation for future work to identify the reason.

Silicon nanoparticles based PCM has also been explored to observe their thermal characteristics. From the literature silicon-based nanoparticles were found to be stable. Although thermal conductivity increased with the addition of Si based particles, latent heat was found to be decreased with these particles. Recently, Ranjbar et al. [112] have reported excellent thermal stability, good phase change behavior, and enhanced thermal conductivity for n-heptadecane by the loading of SiO_2 nanoparticles. The melting and solidification enthalpies for nanocomposites were 123.8 and 120.9 J/g respectively. Furthermore, gypsum was added into the nanocomposites to observe its performance for building performance and they found that nanocomposites integrated gypsum maintains the room temperature at a comfortable range. Babapoor and Karimi [87] also found good stability of SiO_2 based nano-PCM when they compared it with other nanoparticles. They dispersed different metal oxide nanoparticles (SiO_2, Al_2O_3, ZnO, and Fe_2O_3) in paraffin PCM and it was noted that 8% SiO_2/paraffin composite showed better stability compared to other composites.

In some studies, authors investigated a combined effect of silicon-based nanoparticles with other supporting materials. For example, Zhang et al. [113] experimentally studied the effect of silica nano particles and EG on n-Eicosane phase change material. It was noted that silica nano particles prevent leakage during melting due to their strong adsorption capability and the leakage test showed that the maximum adsorption mass fraction of n-eicosane in CPCM

occurred at 70% wt.%. Moreover, the addition of 3% EG into n-Eicosane/silica nano-PCM increases the thermal conductivity and latent heat of nano-PCM, but a decrease in the latent heat was also observed when EG concentration exceeds by 3%. Tony and Mansour [114] investigated paraffin with silica treated ZnO nanofillers and compared the results with un-treated ZnO. The results illustrated that treated ZnO/PCM showed better stability than untreated ZnO due to the synergistic effect between PW and SiO_2. This may be explained by the presence of the coated layer of SiO_2 on ZnO enabling a good dispersion throughout the host paraffin wax. This provides more sites for inorganic nanoparticle materials, which enhances the probability of absorbing heat leading to an increase in the latent heat of fusion of paraffin wax.

2.1.4 Metal carbides and metal nitrides nanoparticles based PCMs

Different forms of nano boron nitrides (BN) have been studied for better performance of composite PCMs. Fang et al. [115] integrated hexagonal boron nitride nanosheets (h-BN 100nm) with PEG for the preparation of nanocomposites. As a result of improved thermal conductivity by the incorporation of h-BN, the melting and crystallization rates were also reported to be accelerated by up to 25%. Moreover, 10% of h-BN improved its TC of the composite by 60% and reduced the latent heat by 12%. Huang et al. [116] prepared anisotropic reduced graphene oxide/boron nitride (rGO/BN) composite aerogel to form CPCM. The addition of BN enhances anisotropic aerogel rigidity to lessen its contraction during the thermal cycle, and also increases its thermal conductivity. The axial thermal conductivity was 1.68 W/m K, which was 504 % greater than that of pure paraffin, while the mass ratio of GO to BN was 1:20. At the identical BN concentration, latent heat was decreased at a higher rate for rGO/BN composite than h-BN/PEG composite in the previous study [115]. This is because of rGO does not contribute towards the latent although rGO contributes towards the enhancement in the thermal conductivity.

It has been reported that an introduction of metallic carbides (MXene) to PCM may have significant effects on PCM properties. Aslfattahi et al. [117] integrated metallic carbides (MXene) with paraffin PCM for the development of energy storage materials. They investigated nanocomposite at different concentrations of MXene (0.1, 0.2 and 0.3%) and found an increase in the thermal conductivity and specific heat capacity of nanocomposites by 29.5% and 43% for 0.2 and 0.3 wt. % of MXene particles. In comparison to pure PCM, the

latent heat of nanocomposite decreased with the addition of particles, however, a larger concentration of particles showed greater latent heat compared to particles with lower concentration. In the other study, Krishna et al. [118] used (Ti_3C_2) MXene nanofiller with palmitic acid as PCM (T_m=60-62°C) for solar thermal power plants. In this study, thermal conductivity enhancement at 0.1% of MXene was greater than that in their previous study because the DSC results showed that no shift in melting temperatures for MXene/PA composites was noted. However, with 0.1% MXene concentration an increase of 4.36% in the palmitic acid enthalpy was observed probably because of strong interactions between PA and MXene.

A variety of nanofillers were investigated to examine the performance of the nano-PCM composite. Typically, Rao et al. [119] prepared nano aluminum nitride (AIN) and paraffin based nano PCM for energy storage purposes. The DSC results indicated that with 3% of AIN latent heat of the nano PCM was decreased from 171.13 J/g to 165.32 J/g. However, AIN/paraffin composite PCMs exhibited good structural and thermal stability. Selvaraj et al. [120] used beryllium oxide nanomaterials (0.5%, 1%, 1.5% and 2%) with deionized water and PEG PCMs. It was found that latent heat efficiency and thermal diffusivity of 2% BeO nano-enhanced PCM was improved by up to 23% and 30%, respectively, compared with those of the base material (PEG). Wu et al. [121] prepared two dimensional montmorillonite nanosheets (2DMts) using the ultrasonic method. A phase-change energy storage composite material (2DMt/SA) was prepared using a self-assembly technique, with 2DMts as the host and energy storage molecule stearic acid (SA) as the guest. The composite 2DMt/SA had a high latent heat storage potential (192.4 J/g), almost similar to that of the pristine PCM. Moreover, the thermal stability of 2DMt/SA was significantly improved as compared with SA PCM.

2.1.5 Overview of the effects of single type of nanoparticles in PCM thermal properties

Overall, the dispersion of different nanofillers in the PCM matrix could result in an increase in the thermal conductivity and a decrease in the latent heat value. In comparison to other nanoparticles, carbon-based particles have showed good thermal stability which results in the greater enhancement of thermal conductivity and moderate decrement in the energy storage capacity of PCM because carbon based nanofillers are highly conductive and their greater surface area contributes towards the greater intermolecular interaction with PCM molecules.

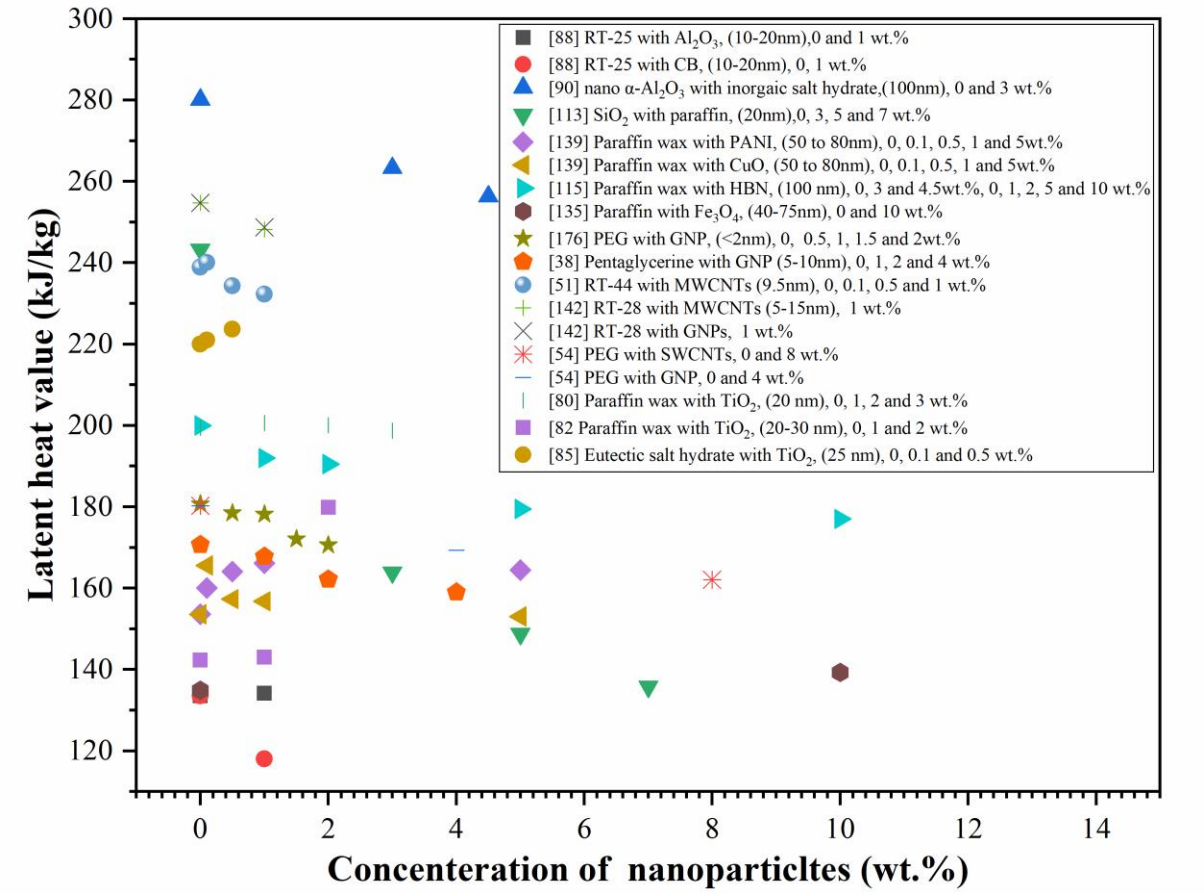

Figure 2.5 Effects of nanoparticle concentration on latent heat.

Important parameters of nano-PCMs from useful studies on single and hybrid nano-PCMs have been summarised in Table 2.3 and 2.4, respectively. Figure 2.5 and Figure 2.6 show the latent heat and thermal conductivity comparison of some important studies, when different nanoparticles were used with PCMs.

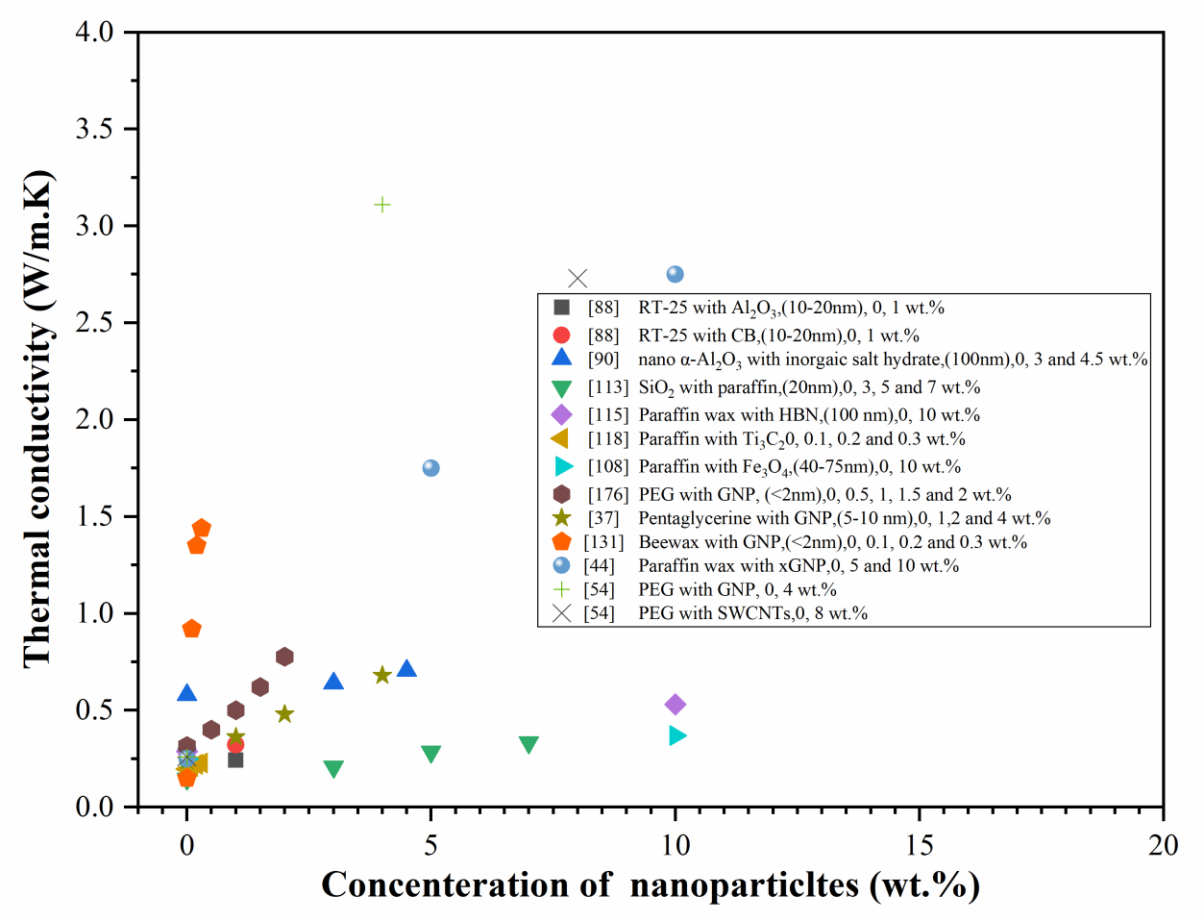

Figure 2.6 Effects of nanoparticle concentration on thermal conductivity.

The latent heat and thermal conductivity data from different studies were collected to compare the results of latent heat and TC when the PCM was pristine and when different types of nanofillers were dispersed into it. Although the difference in the various parameters (thickness, size, and PCM) make the comparison between references complicated, the best composite by keeping an eye on all aspects could be identified. As shown in Figure 2.5, almost in all studies latent heat value reduces with a rise in the nanoparticles concentration as compared with pristine PCM. Several justifications for the decrease in the latent heat have been reported by different scholars, as given below.

- This might be due to the increased thermal conductivity on PCM based composites, which accelerates the evaporation of pure PCM [122].
- The weak intermolecular forces between PCM and nanoparticles [122].
- The non-melting enthalpies of nanoparticles, that would reduce the composites melting enthalpy [122].

- The realignment of the PCM molecules in the existence of severely charged nanoparticles is difficult, which is also a significant explanation for the reduction of the composites latent heat [123].
- Latent heat may also decrease due to the reduction of mass fraction of PCM in PCM based nano composites [43].
- The leakage of PCM during phase change also contributes to the reduction of latent heat [124].
- Since the distributed filler inhibits the local molecular bonding condition and impedes the PCM melting cycle [125].

However, polyaniline (PANI) and CuO based paraffin wax composites showed little enhancement in energy storage capacity compared with the virgin PCM this may be because of the large surface areas of nanoparticles and strongest intermolecular interactions between PCM and nanofillers. On the other hand, SiO_2/paraffin combination showed highest decrement in the latent in contrast to the pure paraffin wax. Furthermore, among all the nano composites CNTs and TiO_2 based PCM composites showed excellent stability for the thermal energy storage capacity. PCM incorporated with TiO_2 nanoparticles either showed an increase in the latent heat or demonstrated little decline in the value compared to the pure PCM.

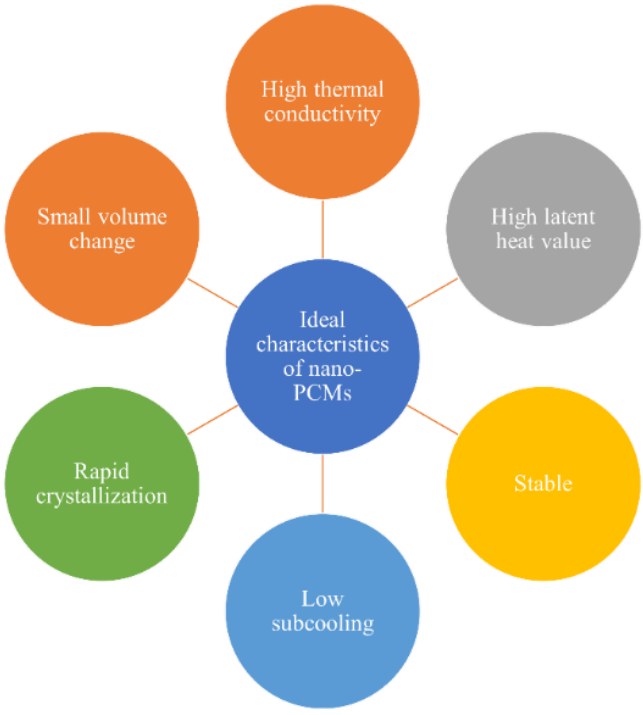

Figure 2.7 Ideal characteristics of nano-PCMs.

Figure 2.6 shows the relationship between particles concentration and thermal conductivity, and it appears that they have a direct relation between them. As the weight percentage of the nanoparticles increases, the thermal conductivity value surges. It can be suggested that the nanofillers with high thermal conductivity values have shown greater enhancement when they are impregnated with PCM. For instance, a small concentration of GNP particles has shown magnificent improvement in the TC due to their high TC values. Moreover, Figure 2.7 shows some ideal characteristics of nano-enhanced PCMs identified from the literature.

2.2 Hybrid nanoparticles based PCMs

The studies have been reported by different investigators in which they examined the thermo physical properties of more than one nanoparticle (hybrid nanoparticles) with different PCMs. Qi et al. [36] used graphene and graphene oxide nanofiller for thermal conductivity enhancement and stabilization of PEG respectively. The nanocomposite samples were prepared by physical blending method with 2 wt. % of graphene oxide (GO) and 0.5 wt. %, 1 wt. %, 2 wt. % and 4 wt. % of GNPs. The results showed that the incorporation of GO and GNP was shown to be effective supporting materials and conductive materials, respectively. Moreover, the latent heat was also enhanced slightly with the incorporation of hybrid nanofillers. In the other study [126], again they investigated hybrid graphene nanoplatelets (GNP) and GO with PEG but used a different preparation method (Vacuum impregnation). Further, in this study the content of nanoparticles was lesser than in their previous study [36]. The comparison results of the two experiments showed that the low nanofiller content displayed more latent heat than the higher particulate content. For thermal conductivity, it was the opposite that a high concentration of particles led to higher thermal conductivity compared. Because graphene-based particles have greater thermal conductivity so a higher concentration of graphene nanoparticles in the PCM further boosts their TC value. However, further investigation is needed by using both methods for similar particle concentration to identify the efficient method.

Table 2.3 Thermal properties of single type nanoparticle-based nano-PCMs.

References	PCM			Nanoparticles		Thermal conductivity (W/m. K)		Latent heat of melting (kJ/kg)		Latent heat of crystallization (kJ/kg)		Nanoparticles	
	PCM	**T_m (°C)**	**T_c (°C)**	**Material**	**Wt. (%)**	**Pure**	**Nano-PCM**	**Pure**	**Nano-PCM**	**Pure**	**Nano-PCM**	**Shape**	**Size**
[127]	RT-22	22	-	GNP	0.05	0.15	0.46	163.31	161.43	169.02	68.68		
			-		0.1		0.92		160.95		165.56	Rolled thin	w 2μm thick 2 nm
			-		0.15		1.1		155.47		164.53		
[128]	PEG	55.8		GNP	2	0.316	0.776	180.7	170.6	161.3	151.3	-	T < 2 nm, W< 2nm
[129]	RT-64	61		GNP	3	0.295	0.605	230.4	225.38	-	-	-	
					5		0.830		210.18				130 nm
					7		1.040		194.53				
[130]	n-octadecane	28	-	xGNP	3	0.28	0.98	256.5	245.8	-	-	-	-
[131]	Hexadecane	18-20		xGNP	3	0.66	0.992	232.41	217.33	-	-	-	
	Octadecane	26-30				0.49	0.873	241.97	240.92				T <10 nm
	Paraffin wax	53-57				0.35	0.454	142.72	140.99				

Continued...

References	PCM			Nanoparticles		Thermal conductivity (W/m. K)		Latent heat of melting (kJ/kg)		Latent heat of crystallization (kJ/kg)		Nanoparticles	
	PCM	**T_m (°C)**	**T_c (°C)**	**Material**	**Wt. (%)**	**Pure**	**Nano-PCM**	**Pure**	**Nano-PCM**	**Pure**	**Nano-PCM**	**Shape**	**Size**
[132]	Salt hydrate	30	-	GO	2	0.68	1..05	220	200.3	147	160	Hexagonal	thick 1.318nm Size 500nm
[133]	Paraffin wax	59	-	S-MWCNTs	5	0.263	0.324	207	178.2	-	-	-	815 nm
				L-MWCNTs	5		0.309		177.3				3050nm
				CNFs	5		0.305		185				150200 nm
				GNP	5		0.7		186.5				420 nm
[134]	Paraffin	60	54	TiO_2	1	-	-	199.4	200.6	194.5	193.9	-	20-30nm
					3	-	-		198.7		193.6	-	
[135]	Paraffin wax	42	-	Fe_2O_3	10	0.25	0.37	134.9	139.3	-	-	-	40-75nm
[136]	Paraffin wax	30	-	α Al_2O_3	2	-	-	159.46	210.99	26.143	34.591	-	1.4-2nm

Continued…

References	PCM			Nanoparticles		Thermal conductivity (W/m. K)		Latent heat of melting (kJ/kg)		Latent heat of crystallization (kJ/kg)		Nanoparticles	
	PCM	**T_m (°C)**	**T_c (°C)**	**Material**	**Wt. (%)**	**Pure**	**Nano-PCM**	**Pure**	**Nano-PCM**	**Pure**	**Nano-PCM**	**Shape**	**Size**
[137]	Paraffin wax	26.5		Al_2O_3	5	0.13	-	243.1	225.6	-	-	-	-
					10				212.3				
[138]	Inorganic SH	59		Cu	0.5	0.921	1.155	242.4	234.5	-	-	-	10-30 nm
	Paraffin wax	58	-	PANI	0.1	0.203	0.203	153.6	160.03				
					1		0.298		166.2				
					5		0.247		164.43				
[139]				CuO	0.1	0.203	0.246	153.6	165.62	-	-	-	50-80 nm
					1		0.332		156.76				
					5		0.268		153.04				

Table 2.4 Thermal properties of hybrid nano-PCMs.

References	PCM			Nanoparticles		Thermal conductivity (W/m. K)		Latent heat of melting (kJ/kg)		Latent heat of crystallization (kJ/kg)		Nanoparticles	
	PCM	T_m (°C)	T_c (°C)	Material	Wt. (%)	Pure	Nano-PCM	Pure	Nano-PCM	Pure	Nano-PCM	Shape	Size
[140]	PEG	60	-	GO/GNP	2/0.5			170.5	174.6	0.29	-	-	-
					2/1				174.7		-		
					2/2				175.9		-		
					2/4				178.1		1.72		
[141]	Paraffin wax	60	-	SiC/CuO	0.5/0.5	0.172	0.226	166.7	160.3	-	-	-	15 nm
[142]	RT-28	28	-	CuO/Al_2O_3	0.75/0.25	0.22	0.328	254.73	248.51	-	-	-	CuO <50 nm, Al_2O_3 13 nm
				GNP/MWCNTs			0.430		245.18	-	-	-	MWCNTs 5-15nm
[143]	n-octadecanol	61	-	GO/SiO_2	0.05/0.05	-	-	237.8	136.2	-	-	-	15 nm
					0.5/0.5				145.6				
					2/2				129.6				

A few of studies were found on hybrid nanoparticles in which researchers combined different nanoparticles to improve the thermal properties of PCM. Zhang et al. [144] used GO/SiO_2 hybrid aerogel as the matrix supported for the preparation of composite PCMs for insulation. The hybrid aerogel was synthesised with the addition of 0.5 wt.% of GO in silica gel with a high surface area (948 m^2/g) and low thermal conductivity (0.0277 W/m k). The latent heat and thermal conductivity of the composite PCM reached maximum values of 145.6 J/g and 0.0808 (W/m K) respectively when the mass percentage of graphene oxide was 0.5 %. Moreover, the GO/SiO_2 hybrid aerogel-supported composite PCM was found to be beneficial for conversion from light to heat. Arshad et al. [145] experimentally investigated carbon and metal oxides based single and hybrid nanoparticles for the thermal management of electronic devices. The experimental results showed a little decrease in the latent heat capacity of hybrid nanoparticles based PCM as compared with pristine PCM. However, hybrid metal oxides (Al_2O_3/CuO) based nano-PCM showed a higher latent heat value than that of carbon-based hybrid nanoparticles (GNPs/MWCNTs), while for thermal conductivity (GNPs/MWCNTs) hybrid composite exhibited better performance than hybrid metal oxides. So, further research may be needed on the metal oxide and carbon-based hybrid nanofillers to investigate their performance. Manirathnam et al. [146] conducted an energy analysis for a solar water heater and compared the results with three cases, PCM, nano-PCM and without both. The nano-PCM was prepared by using the two-step method in which paraffin wax was combined with SiC and CuO (1 wt.%) nanoparticles. The results showed that the values of energy efficiency were 33.8%, 38.3% and 41.7% for all three cases i.e., without PCM, with PCM and with nano-PCM, respectively. Parameshwaran et al. [147] developed hybrid nanofillers (Cu and TiO_2) and dispersed these fillers into the PCM for enhancement in the thermal properties of composite PCMs. They found that Cu nanoparticles were adsorbed on the TiO_2, which helped to achieve better heat transfer across pure PCM layers. The addition of these fillers into PCM also minimised the supercooling effect and enhanced the latent heat values contrast to pure PCM. Moreover, nano enhanced PCM remained thermally stable up to 100.4 °C.

A comparison between hybrid nano-PCM and mono nano-PCM regarding the latent heat and thermal conductivity is shown in Figure 2.8 and Figure 2.9, respectively. Both figures show the enhancement or deterioration in the percentage of latent heat and thermal conductivity when nanoparticles were incorporated into the PCM.

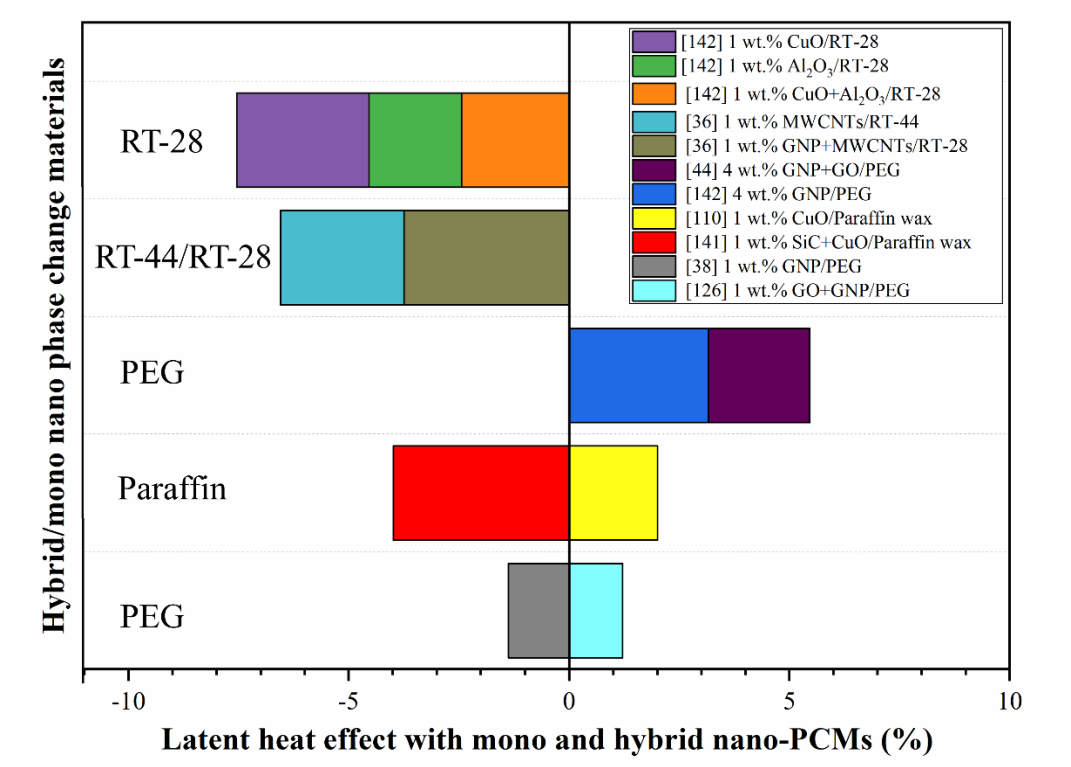

Figure 2.8 Hybrid and mono nanofiller effects on PCM latent heat.

As shown in Figure 2.8, the increment or decrement in a percentage of latent heat has been taken with reference to the latent heat of pure PCM. Figure 2.8 demonstrates that latent heat percentage declines with the addition of either mono or hybrid particles and the possible reasons for this decline in energy storage capacity have been discussed in Section 2.1.5. Among all composites, PCM dispersed with SiC/CuO nanoparticles shows a greater decrease in the latent heat. GO/GNP based PEG PCM composite shows little increase in the energy storage capacity due to the strong physical interactions between GO and PEG in PEG/GNP/GO composite, which has also prevented the leakage of PCM during a phase change. In addition, CuO/paraffin composite also reveals an intensification in the latent heat, and it might be attributable to the large surface areas of CuO nanofillers which leads to an intermolecular contact between the PCM and CuO, while due to the poor physical interaction between SiC and paraffin the decrement in the latent heat has been reported. Although in most cases latent heat diminishes with impregnation of mono or hybrid nanofillers, mono nanoparticles have shown more decline than hybrid nano-PCM composites.

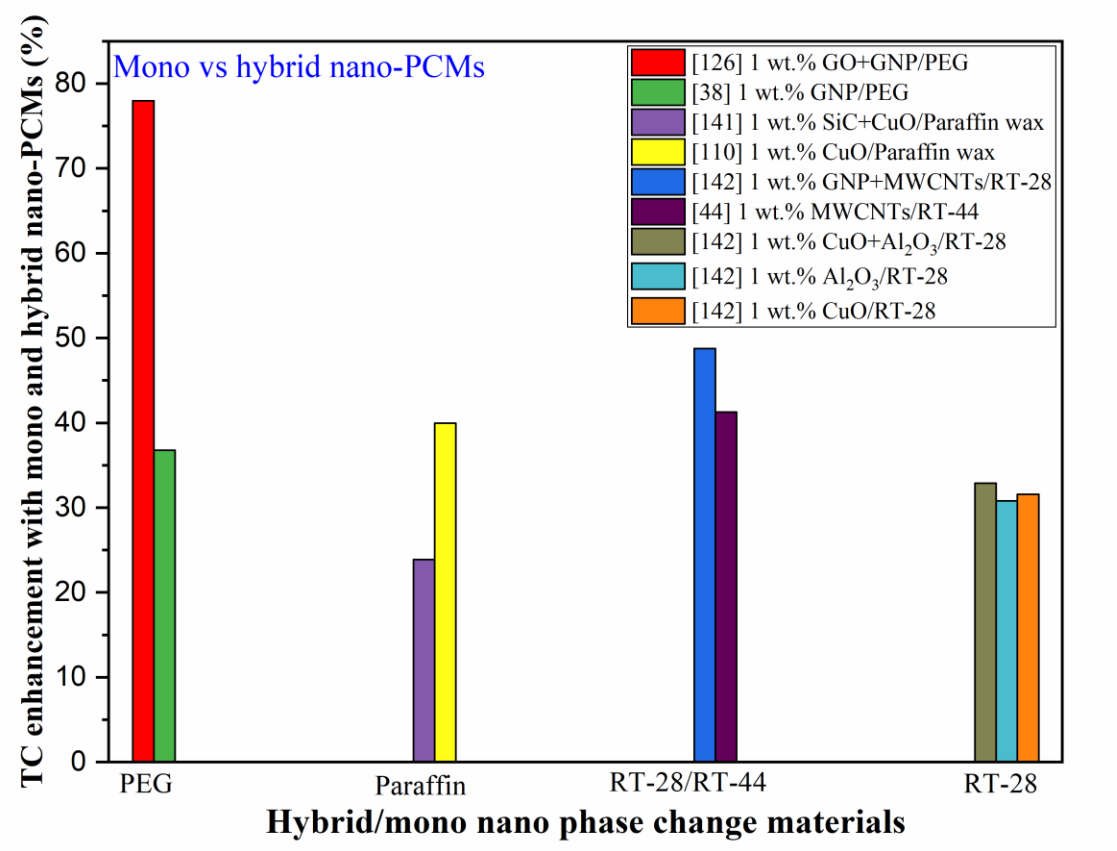

Figure 2.9 Hybrid and mono nanofiller effects on PCM thermal conductivity.

Similarly, a thermal conductivity comparison of mono and hybrid particles shown in Figure 2.9 has been conducted to get an idea about the potential nanofillers. From Figure 2.9 it can be seen that the hybrid nanofillers based PCM composites have shown a higher increase in thermal conductivity than mono nanofillers based PCMs, but due to the poor interaction and thermal resistance between SiC and paraffin wax it has shown a decrease in thermal conductivity, while CuO/paraffin has depicted excellent TC. What is more, due to the higher TC value of GNPs it demonstrated a great enhancement in TC than other nanoparticles. Table 2.4 has summarised the thermal properties of different studies on hybrid nanofiller based PCM composites.

Overall, the inclusion of all nanomaterials into the PCM results in an increase in thermal conductivity and a decline in latent heat. The carbon-based nanofillers showed greater enhancement in the thermal conductivity than other particles because of their high conductivity values. In addition, carbon-based nanoparticles have good stability because of their lower density

and large surface area. In addition, carbon-based nanoparticles have good stability because of their lower density and large surface area. However, CNTs do not disperse into PCMs properly and lead to agglomeration because of their hydrophobic nature. This issue can be overcome by the surface treatment of CNTs. On the other side, metal oxide particles, such as, TiO_2 particles have showed little change in the latent heat because of their greater intermolecular interactions with PCMs, but they depict only small increase in the thermal conductivity, as metal and metal oxide particles have low thermal conductivities. That is the reason that carbon-based particles are usually preferable by researchers since a significant improvement in thermal conductivity with carbon-based fillers is appropriate for a small reduction in the energy storage capacity of PCMs. However, one main disadvantage of the carbon-based particles is that they are expensive compared to the metal and metal oxide particles. Hybrid nanoparticles (i.e., carbon and metal or metal oxide particles) with a small proportion of carbon particles and a large concentration of metal or metal oxide particles could minimise the overall cost of particles, while also improving the thermophysical characteristics of the nano-PCM.

2.3 Preparation methods for nano-PCMs

Two main techniques are commonly followed for the preparation of nano phase change materials to conduct an experimental investigation and are termed as single-step method and two-step method [72]. Figure 2.10 shows the preparation methods for nano enhanced PCM composites. Simultaneous dispersion of individual nanoparticles or the dispersion of nanocomposites in the base fluid are the approaches listed in the literature for the preparation of nano-PCM. This section has presented a brief overview of nano phase change material preparation techniques.

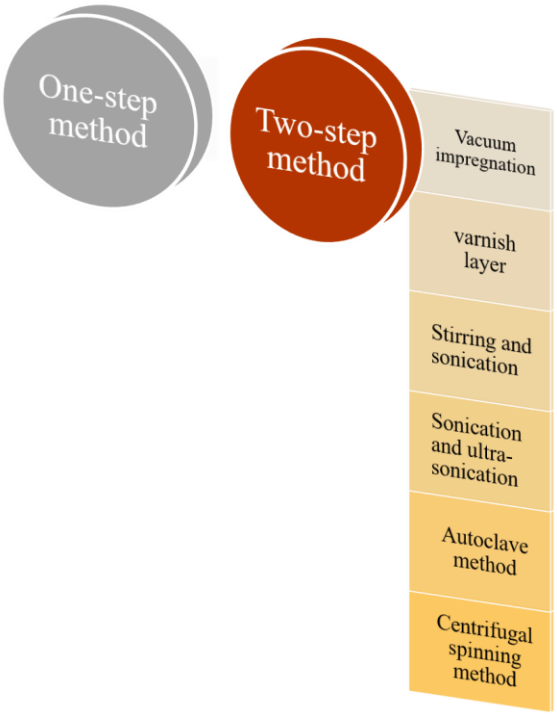

Figure 2.10 Preparation methods for nano enhanced PCMs.

2.3.1 One-step method

As shown in Figure 2.11, nanoparticles are synthesised and dispersed at the same time in one-step process, in simple words, all the processes are carried out in a single phase, that is the reason why this method is called the one step method. In order to achieve better stability and to avoid the formation of clusters this approach is considered the most successful. Moreover, the transporting, storage, drying, and mixing of nanofillers in the PCM are not required in this process, thus optimizing the dispersion of nanoparticles in the corresponding PCM and decreasing the conundrum of particle accumulation [148]. This technique is only utilized on a limited scale since it is more expensive than the two-step method.

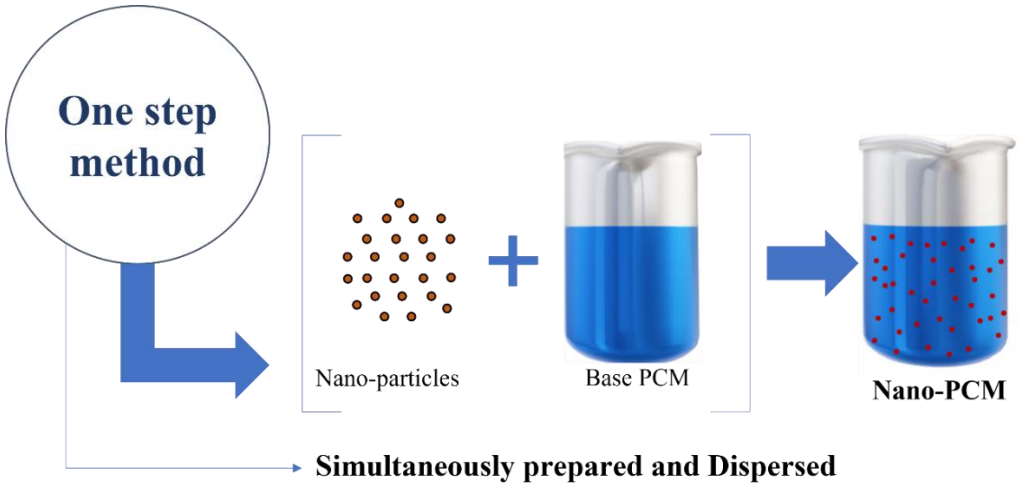

Figure 2.11 One step method for a PCM preparation [149].

Typically, Mohamed et al. [86] blended urea and $Al(NO_3)_3 \cdot 9H_2O$ into purified water and microwaved this mixture for 3-5 minutes. The petroleum wax was then applied to this solution and the mixture was sonicated for half an hour to obtain the petroleum wax/alpha-nano alumina composite. By direct synthesis technique, Teng and Yu [80] prepared nano-PCM in which TiO_2, Al_2O_3, ZnO and SiO_2 nanoparticles were mixed with paraffin wax with 1.0 wt.%, 2.0 wt.%, and 3.0 wt.% concentration, and the concoction were stirred for 0.66 hours to attain smooth dispersion.

2.3.2 Two-step method

In two step technique, nanofillers are primarily collected in dry powder form utilizing various mechanical and chemical methods such as, ball milling, chemical reduction, and sol-gel methods. The nanofiller powder obtained is then combined with the base PCM and for homogeneous particle dispersion. Distinct methods were used including ultrasonication and magnetic stirring. The two-step schematic diagram is shown in Figure 2.12. The greatest advantage of this method is the processing of nanocomposites on a commercial scale; however, this technique has the problem of agglomeration of particles and thus enhances the use of a single-phase preparation process [148,150]. To prevent filler agglomeration, surfactants are used by forming a barricade and reducing the surface tension among the PCM and the suspended fillers. Furthermore, surfactants help to stabilise the nanofluid by generating zeta potential and repulsive forces [151].

By two-step method, prominent researchers prepared various nano-PCMs under distinct stirring and sonication times. Sharma et al. [99] developed nano-PCM by mixing CuO with a mass fraction of 0.5% in RT-24 PCM at 60°C and then the blend was ultrasonicated for 1440 minutes in an ultrasonicator apparatus. Latibari et al. [152] investigated SiO_2 nanofiller with palmitic acid as PCM and SDS dispersant using the two-step method. Firstly, dispersant was dissolved into the distilled water and then PCM was incorporated, and the mixture was stirred at 1000 RPMs for two hours. The solution was added to the palmitic acid emulsion drop by drop, and the mixture was stirred for four hours at 500 rpm. The emulsion was then cooled to room temperature and rinsed with centrifuged and distilled water. The white powder produced by the process was collected and dried for 10 hours before being washed with toluene to extract any unencapsulated palmitic acid. The solvent was centrifuged once more, and the white powder was collected and dried for an entire day.

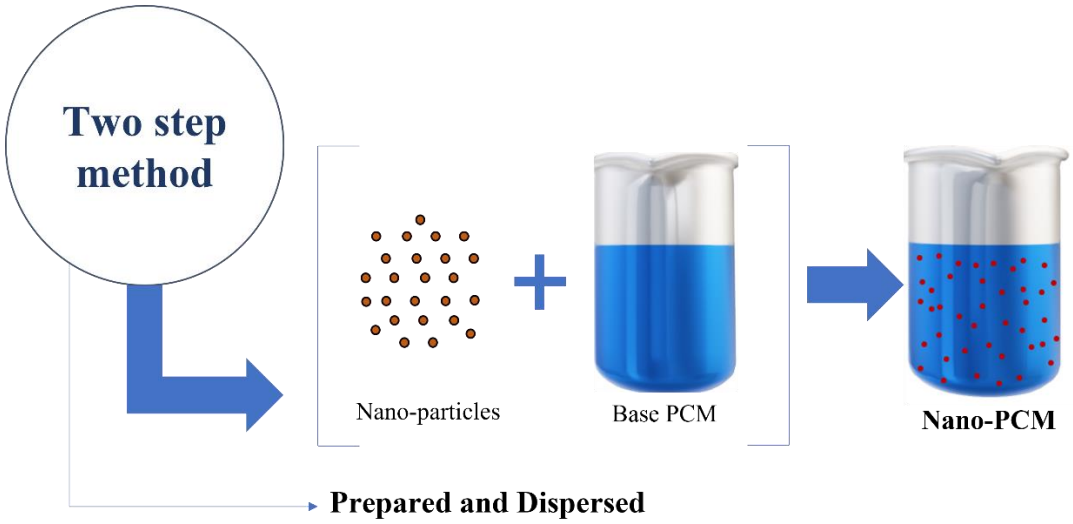

Figure 2.12 Two-step method for a PCM preparation [149].

2.3.2.1 Vacuum impregnation method

Figure 2.13 shows a vacuum impregnation process. Typically, Sari et al. [153] prepared the expanded graphite (EG) and fatty acid (PCM) composite using the vacuum impregnation method. There are three stages. Firstly, porous expanded graphite was placed into the flask which was connected with water tromp apparatus for the removal of air from porous EG, for a 30-minute evacuation process continued at vacuum. After the removal of air from EG, the valve between the PCM container and flask was opened to permit melted PCM into the container to cover up all

porous EG. Lastly, the vacuum procedure was completed, and the air was permitted into the container which forces the melted PCM to penetrate completely into the pores of EG. The EG/fatty acid was instantaneously heated through the infiltration procedure at a steady temperature beyond the melting point of PCM to check the leakage from the pores.

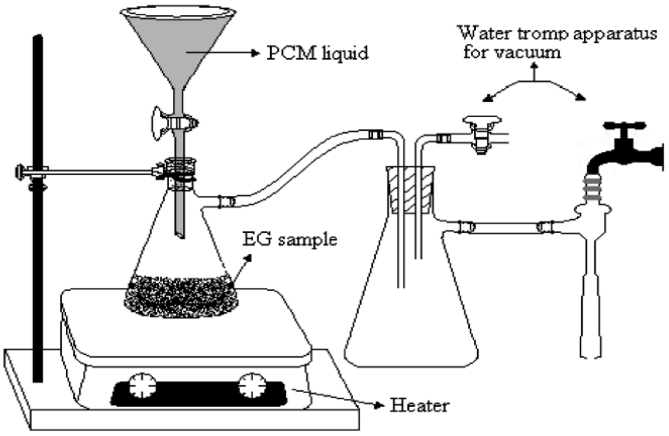

Figure 2.13 Vacuum impregnation process [153].

2.3.2.2 Varnish layer method

Varnish is a hard, transparent, protective film that is mainly employed in wood finishing but can also be implemented to other materials. The varnish layer method is used to prevent PCM leakage during solid-liquid phase change by film formulation utilising varnish [154]. Wi et al. [155] used the varnish layer technique for the preparation of PCM/xGNP composites. In this method, n-octadecane melted PCM was directly mixed with xGNP. Then this mixture was impregnated into the hollow to form a cylindrical sheet, and the cylindrical sheet was enclosed with varnish to prevent the seepage of PCM during melting. Finally, the composite was allowed to be dried for two complete days at 50% relative humidity and a constant temperature of 25°C. The cylinder-shaped hollow was formed by blending 1:0.45 water and plaster, creating a cuboid using a cylindrical mould.

2.3.2.3 Stirring and sonication

In the stirring and sonication method mixtures are first stirred using magnetic stirrer for certain time and rotational speeds, and then the stirred mixture is subjected to sonication at a particular frequency to get uniform dispersal of nanofillers in the base PCM. Jeon et al. [34] followed a stirring and sonication method for the preparation of PCM/xGNP composite. In this method, PCM

was melted beyond its melting point and in the next step liquid PCM was mixed with xGNP using a stirrer for 20 minutes at the stirring speed of 1000 rpm. Then this mixture was sonicated in a sonicator for 20 minutes and left for cooling.

2.3.2.4 Sonication and ultra-sonication

Figure 2.14 shows the schematic of this process. Typically, Putra et al. [43] prepared their nano-PCM using sonication and ultra-sonication method. In this method, the graphene and melted PCM were mixed with a stirrer and left for sonication at the frequency of 40 Hz. Then the obtained nano-PCM was subjected to ultra-sonication in the ultra-sonicator bath at 45°C for three hours till the full dispersion of graphene with RT-22.

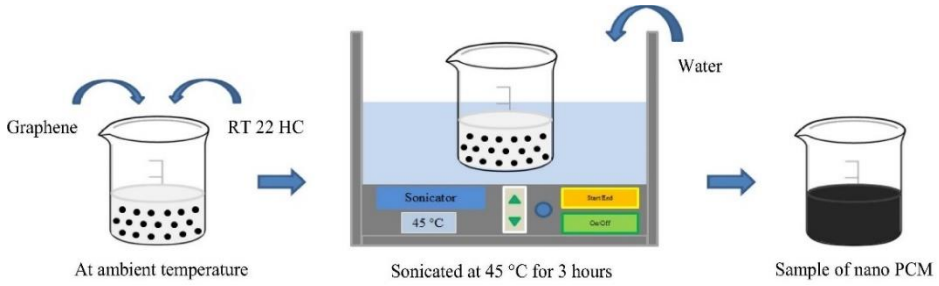

Figure 2.14 Schematic of sonication and ultra-sonication method [43].

2.3.2.5 Autoclave method

Autoclave processing is among the oldest and most commonly used methods of processing high-performance composite materials. Zeng et al. [156] prepared nano-PCM using the autoclave method, which to enhance the absorptivity of PCM. In their approach, PCM (TD) was mixed with ethanol. After mixing, PCM was melted and infiltrated directly into the EG then TD/EG composite was heated up to 70°C to evaporate the ethanol from the composite.

2.3.2.6 Centrifugal spinning method

Centrifugal spinning is a better and effective way to quickly produce nanofibers. It uses centrifugal force rather than high voltage to generate nano-PCM. Figure 2.15 shows the schematic and actual illustration of centrifugal spinning method. Chen et al. [157] prepared shape-stable nano-PCM using the centrifugal spinning method. Firstly, PAN/PEG/SiC were mixed in the N-dimethylformamide solvent. Then for the homogenous dispersion of PAN, PEG and SiC in the N-

dimethylformamide solution, the mixture was stirred in a magnetic stirrer at 25°C for 24 hours. After stirring the prepared solution was allowed into the spinning vessel and PCMs fibres were obtained by ejecting the solution at 4300rpm.

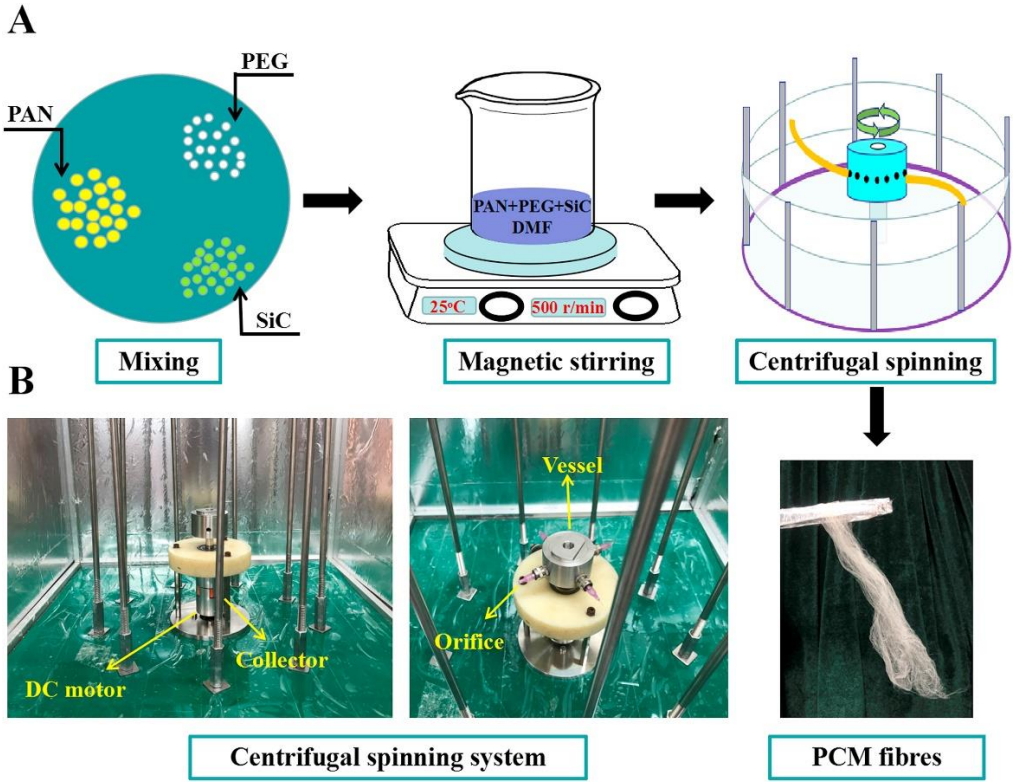

Figure 2.15 Centrifugal spinning method [157].

2.3.3 Discussion

Even though the one-step method improves the stability duration and provides better dispersion of nanoparticles, its disadvantages, such as high costs, complex process, and the limitation of small-scale production of nano-PCMs limit its application. In addition, one step nano-PCM preparation technique can help to achieve long-term stability, but it still awaits the attention of the investigators to make it a more cost-effective and smart process by eliminating the production quantity constraint. On the other hand, the two-step technique is the most employed method for the preparation of nano phase change materials at a larger scale, but this method suffers from stability issues. To deal with the stability issue investigators used different techniques these techniques are discussed in the next section.

2.4 Stability improvement methods

The biggest problem is the stability of nano particle enhanced PCMs, which not only disturbs the efficiency of the system but also swaps the tremendous results into disturbing ones. The justification for the increased thermal conductivity of nanofluids is the proper dispersion of nanoparticles in base fluids. As the particles form clusters, they begin to settle at the base of the in-service unit, which increases the thermal resistance. As phase change does not occur in the thermal resistance layer in the experimental temperature range, this interface layer does not contribute to the phase-change heat, but it can reduce the unit volume of the thermal storage. In addition, the thicker thermal resistance layer also decreases the efficiency of the nano-PCMs heat conduction. The reason for starting with stability is that it is the issue that invites the researchers to consider the various particles and their combinations, the testing of multiple PCMs, the use of magnetic stirrers and ultrasonic mixers, and their effects on thermo-physical properties. Therefore, it is the stability that has created many problems or, in other words, a great challenge for researchers. The various strategies for enhancing the stability of nano-PCMs are shown in Figure 2.16 and detailed discussion will be followed.

2.4.1 Surfactants Addition

In these studies, [49,81–84,87,94,97,125,158–161] dispersants have been used to make the nano particle/tube enhanced PCMs more stable. The dispersants are organic molecules that prevents cluster formation and modifies the nanoparticles surface properties[162]. Dispersants are categorized into four categories and each type either carries negative, positive or no charge heads as shown in Figure 2.17. The types of dispersants chosen for various nanoparticles vary because of the different characteristics of the different nanoparticles in suspension. If the type of dispersants is not correct, the dispersants will not be adsorbed stably on the surfaces of nanoparticles, and the particle coating will be incomplete, thereby weakening the nanoparticles' dispersive effects [94].

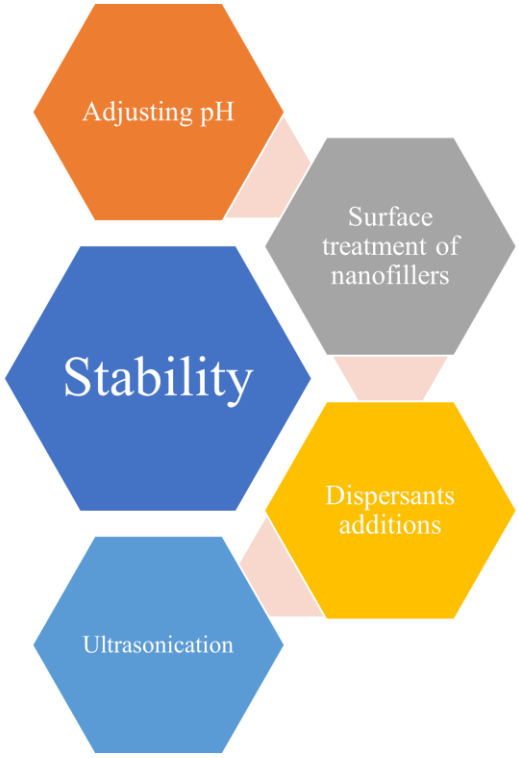

Figure 2.16 Nano-PCM Stability improvement techniques.

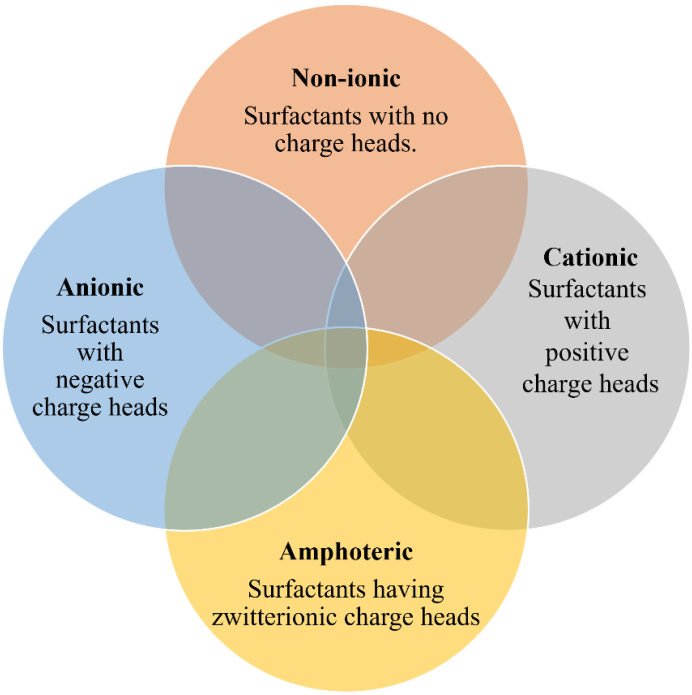

Figure 2.17 Classification of surfactants based on the composition of the head.

Chen et al. [94] used dispersants (i.e. GA and SDBS) in their preparation of TiO_2 based nano-PCM and observed the stability of nano-PC. SDBS showed better stability than GA even after six months. Tao et al. [160] investigated the effects of two different surfactants (SDS and SDBS) on nano-PCMs (i.e. carbonate salt/MWCNTs). They concluded that without surfactants nano-PCMs nanomaterials would aggregate which weakened the thermal performance of nano enhanced PCMs and especially when nanoparticles had large surface areas (SWCNTs, graphene). The nano-PCM dispersion could be improved with the addition of surfactants. However, these surfactants decompose at higher temperatures that result in a reduction of thermal performance. So that is the reason that an optimum concentration of surfactants is important. It is worth to note that SDS decomposes less mass (18%) compared with SDBS (89%). Table 2.5 shows the incorporation effects of different surfactants on the thermophysical characteristics of nano-PCM.

Table 2.5 Surfactants used with different nano-PCM composites.

Reference	Surfactant	PCM	Nanoparticles	Surfactant %
[94]	SDBS, arab gum (GA)	Alkyl hydrocarbon PCS	TiO_2	0.1
[158]	SDBS	Paraffin wax	GO	0.3
[49]	Sodium dodecyl sulphate (SDS)	n-octadecane	MWCNT	2
[81]	SSL	Paraffin	TiO_2	1
[163]	SSL	Paraffin	Al_2O_3	1
[97]	Sodium dodecyl sulfonate	Salt hydrate ($CH_3COONa.3H_2O$)	Cu	0.25
[81]	SSL	Paraffin	TiO_2	1

Zeng et al. [164] used cetyltrimethylammonium bromide (CTAB) for the better dispersion of MWCNTs in the tetradecanol PCM. Similarly, Wu et al. [121] used CTAB as supporting material with 2DMt/SA composite and it was observed that CTAB based nano-PCM showed higher stability compared to pure nano-PCM. Asadi et al. [165] investigated the effect of three different surfactant forms (SDS, CTAB, Oleic acid) on the stability of water-based nanofluid $Mg(OH)_2$. The supplementation of CTAB surfactant has shown a great impact on stability according to the results. Figure 2.18 shows the samples which were prepared after 30 days with different surfactants and it can be seen that without dispersant particles settled down at the bottom of the surface, among all

surfactants CTAB based nanofluid showed better stability. Wu et al. [166] examined five different surfactants (GA, Span-80, cetyl trimethyl ammonium bromide (CTAB), Hitenol BC-10 and SDBS) with various nanoparticles based PCM. The Cu/paraffin composite PCM with Hitenol BC-10 shows strong dispersed properties after 12 hours, due to large steric hindrance.

Figure 2.18 Impact of surfactants on stability of nanofluid $Mg(OH)_2$/water (after 30 days) [165].

Table 2.6 shows the surfactant used with different nanoparticles. It appears that sodium stearoyl lactylate (SSL) surfactant is attractive to paraffin matrix PCMs [81,163] to improve the stability of nano-enhanced Paraffin PCMs. Sami and Etesami [81] also investigated the effect of the sodium stearoyl lactylate (SSL) surfactant on the stability of paraffin/TiO_2 composites. They found that the addition of SSL induced delays in instability and enhanced sample properties. The nanocomposite's thermal conductivity with SSL, after thermal cycles, was more than that of the nanocomposite without SSL. Liu et al. [90] used mixed surfactants (MS) for the preparation of ESH/α-$Al2O_3$ nano composite, where MS consists of hydroxyethyl cellulose (HEC) and sodium alginate (SA) in mass at a rate of 1:1. To achieve a more uniform solution, HEC plays the role of stabiliser, and SA acts as an emulsifier. In addition, SA as anionic surfactant and HEC as a non-ionic surfactant were mixed to produce a synergistic effect of the non-ideal mixed surfactant system, which had a better performance in the EHS high-concentration salt solution.

2.4.2 Surface treatment of nano particles/tubes

The surface treatment of CNFs/CNTs with acid, oxidation and alkali could minimise the impurities on the surface and result in better stability with PCMs. The shape alteration of nanoparticles was usually observed in CNTs. In this method, nitric and sulphuric acids are used to wash the surfaces of CNTs [162]. Meng et al. [50] prepared shape stable PCM by using the combination of three inorganic fatty acids as a PCM (Palmitic acid, Lauric acid and Capric acid). CNTs were used not just as thermal conductivity enhancers but as well as supporting material. The MWCNTs were treated with acid and the morphologies of untreated and treated MWCNTs can be seen in Figure 2.18. Through Figures 2.19 (a) & (b), it is shown that the morphologies of pristine MCNTs and modified MCNTs are very different. The presence of certain particles adherences on the surfaces of the pristine CNTs leading to CNT's size enlargement. This means the pure CNT's multi-porous structure had consumed those impurities which leads to the agglomeration phenomenon. Fortunately, its size became smaller when CNTs were processed and dispersed which showed the reduced impurity content. In addition, CNTs may be used as suitable supporting materials for PCM shape stabilisation due to the multi-porous structure and greater physical absorption ability in PCM. The pore structure and better adsorption characteristics of the CNTs make the fatty acids firmly attached to the CNTs channel and reduce the liquid of internal fatty acids to guarantee fatty acid stability. Likewise, Harish et al. [167] treated GNP with nitric acid before dispersion in to PCM, modified GNP showed high thermal boundary conductance compared to other nano fillers (CNTs) reported in the literature [168,169]. Furthermore, exfoliated GNP based PCM composite exhibit almost no change in the latent heat and melting temperature compared to pristine PCM. Elgafy and Lafdi [56] also treated CNTs with acid which results in better stability and reduction in cooling time of PCM.

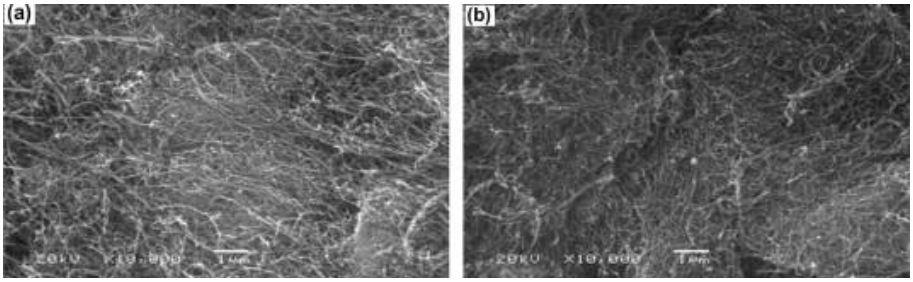

Figure 2.19 (a) untreated MWCNTs, and (b) treated MWCNTs [50].

Table 2.6 Effects of surfactants on thermophysical properties of nano-PCMs.

Reference	Nano-PCM/Surfactants		Findings
	Nano-PCM	Surfactants	
Harikrishnan et al. [170] (2017)	Myristic acid Silicon dioxide (0.2 to 1.0 wt.%)	SDBS	• TC increases with the increase in the concentration of the nanofillers. • 1.0 % of SiO_2 nanoparticles enhanced the TC by 87.27% and slightly decreased the latent heat of melting by -1.09%, which is almost negligible.
Rufuss et al. [171] (2018)	Paraffin CuO, TiO_2, GO (0.3 wt.%),	SDBS	• TC improves with the inclusion of nanomaterials. Pristine PCM (0.26 W/m.K), CuO (0.335 W/m.K), GO (0.523 W/m.K) and TiO_2 (0.325 W/m.K). • The increase or decrease of energy storage capacity varies with nanoparticles. Pristine palmitic acid (102 kJ/kg), CuO (168 kJ/kg), TiO_2 (118 kJ/kg) and graphene oxide (64.7 kJ/kg) respectively.
Zeng et al. [164] (2009)	Palmitic acid with long and short MWCNTs (0- 5 wt.%),	CTAB and SDBS	• CTAB composites showed greater TC than SDBS samples. Further, CTAB samples also have higher thermal conductivity relative to surfactant-free composites at low nanoparticle concentrations. • At small concentration of pure MWCNT latent heat decreases, then slightly improves and decreases with more increases in concentration value. The phase transition enthalpy of pristine MWCNT enhanced PCM was influenced by surfactants.
Parameshwaran et al. [172] (2013)	Organic ester Ag (0.1, to 5.0 wt.%)	PVP	• The TC of PCM with the incorporation of silver nanoparticles increases linearly. At 5.0 wt.% of Ag nanofillers TC value was increased from 0.257 to 0.765 W/m.K). • Incorporation of 5 wt.% nanomaterials decreased the latent heat of solidification and melting by 7.3 % and 8.2 %, receptively.
Bahiraei et al. [173] (2017)	Paraffin wax CNF, graphene, and graphite (2.5 to 10 wt.%)	PVP	• The TC of composites increases with the inclusion of nanofillers in the solid state. This situation is not, however, valid in a liquid state. Thermal conductivity is not dependent on temperature in both solid and liquid states.

Lin et al. [125] (2018)	PW, stearic acid, octadecanol, rGO fillers (0.5 to 10 wt.%),	SDBS	• At low particles concentrations the addition of nanoparticles found advantageous. However, the latent heat of fusion deteriorates at a higher particle volume in comparison to that of pristine paraffin wax. • PCM TC enhances with the increase in particle concentration. • With the incorporation of fillers, PCM latent heat of fusion declines.
Zhang et al. [49] (2020)	n-octadecane MWCNT (0.1, 0.25, 0.5 and 1.0%)	SDS	• It was noted that with SDS surfactants MWCNTs displayed excellent dispersion and stability even after three months. • TC increased linearly with fillers concentration, but with a little decrease in the latent heat.
Kabeel et al. [158] (2020)	Paraffin wax GO (0.3 wt.%),	SDBS	• Comparison to PCM without nanomaterials as an additive element, the TC of Nano-PCM was enhanced by 52%.

Wang et al. [174] applied a mechano-chemical treatment to customize CF surfaces to increase CF's dispersibility. The results depicted that treated CF based PCM composite showed better enhancement in thermal conductivity and latent heat values in comparison with untreated CF/PCM composite. Because treated CFs have strong interactions with PCM than untreated CFs. Consequently, treated CF/PCM absorbed more heat during melting compared with untreated CF/PCM with identical mass. Avid et al. [175] treated MWCNTs by a salinization process and it was found that silane modified MWCNTs exhibited better stability than pristine MWCNTs. It is suggested that **s**urface treatment of nano particles/tubes plays a key role in stability of nano enhanced PCMs. Table 2.7 shows the effect of surface modification of nanofillers on the thermal properties of nano-PCM especially on TC and latent heat. It appears that acid treated particles showed enhancement in both TC and latent heat. Further, small size particles exhibit greater thermal properties due to their better dispersion in the PCM matrix.

2.4.3 Ultrasonication treatment of nano PCM solution

Ultrasonication is a process by which the suspended nanoparticles are disturbed by using high-frequency waves. Researchers used this technique most frequently because of its ease. The other advantage of this technique over others is that it does not affect on nanoparticles surface properties. The instruments used in the ultrasonication procedure are the ultrasonic vibrator, ultrasonic bath and homogenizer, nevertheless magnetic stirrer also allows the process to increase stability. The stability of the different nano-PCMs prepared using a two-step method has been summarised in Figure 2.20. In most cases, after using dispersion methods such as ultrasonication and/or magnetic stirring the thermal cycles do not exceed 1000. The maximum thermal cycles achieved with nano-PCM was 5000 utilising TiO_2 nanoparticles.

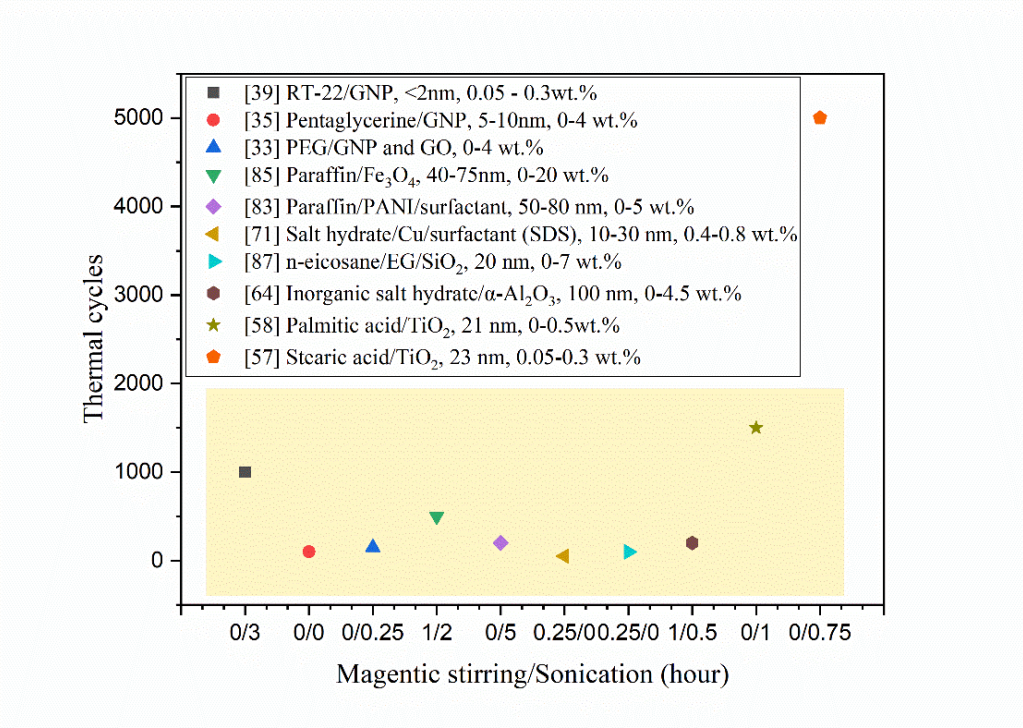

Figure 2.20 Nano-PCMs thermal cycle stability with different magnetic stirring and sonication time.

He et al. [176] dispersed GNPs in the ethanol and ultrasonicated for one hour to obtain homogeneous suspension, and then these GNPs were impregnated into the PEG PCM. Manirathnam et al. [146] ultrasonicated SiC and CuO nanoparticles and paraffin wax based PCM at 36 kHz for two hours to obtain the homogenous solution. Similarly, Arshad et al. [145] performed ultrasonication at 40 kHz for one hour and at temperature of 50°C during the preparation of different hybrid nano-PCMs. Afrand et al. [177] performed seven hours of ultrasonication and two hours of magnetic stirring for the ethylene-glycol based hybrid nanofluid to obtain the stabilized nanofluid. Asadi et al. [165] disclosed that sonication was significant on the stability, but up to a certain limit after that antithesis effect had been exerted. Moreover, they investigated the stability of $Mg(OH)_2$ nanofluid over different sonication periods of time (i.e. 10, 30, 50, 80, and 160 minutes) and better stability of nanofluid was observed at sonication duration of 30 minutes. Besides, there are many studies in which either ultrasonication duration, frequency or temperature was missed. Due to lack of information, it is difficult to compare the results from these studies. For instance, Salyan and Suresh [178] investigated the effect of various concentrations (0.1%, 0.2% and 0.5%) of CuO nanoparticles on the D-Mannitol. A low-energy ball mill was used for 2.5 hours at 250 rpm to properly disperse the nanoparticles in the PCM. Subsequently, at a frequency of 40 kHz, an ultrasonic

vibrator was used, but not specifying the time duration and temperature. Motahar et al. [179] performed an experimental analysis on n-octadecane PCM solidification enhanced with titanium oxide (TiO_2) nanoparticles with mass fractions of 1%, 2% and 4%. The blend was first mechanically stirred and then used in an ultrasonic bath for 15 minutes, 40°C. The mixing conditions in the study were not specified. It appears that ultrasonication treatment of nano PCM solution is an efficient way to improve the stability of nano enhanced PCMs.

2.4.4 Particle size

Stokes presented an expression as shown in equation (2.2) according to which the speed of particles sedimentation (V) depends upon the viscosity of the base fluid μ_{bf}, size of nanoparticles (r), the gradient between the suspended nanoparticles and the base fluid ($\rho_{np} - \rho_{bf}$).

$$V = \frac{2r^2}{9\mu} (\rho_{np} - \rho_{bf}) \quad (2.2)$$

From the above equation it is clear that the velocity of particle sedimentation reduces with a reduction of the particle size. The Brownian motion theory about nanoparticles states that when the particle size is reduced to the critical particle size determined from Eq. (2.2), the sedimentation shall then be zero [180].

Liu et al. [85] inspected an effect of the size of TiO_2 nanoparticles on the eutectic salt hydrate inorganic PCM. The results revealed that the smaller size of TiO_2 nanoparticles (25nm) had greater stability with PCM than particles with greater size (100nm). Esfe et al. [181] stated that the fluid's thermal conductivity was improved when particle size decreased as a result of better dispersion of nanoparticles in a base fluid as shown in Figure 2.21. From the aforementioned studies, it can be concluded that the smaller size nanofillers depicts better stability than the large size particles.

Table 2.7 Thermophysical characteristics of nano-PCMs with surface treatment of nanoparticles.

References	PCM		Nanofillers			Thermal conductivity		Latent heat		Morphology	
	PCM	T_m (°C)	Modification	Material	Wt. (%)	Pure	Nano-PCM	Pure	Nano-PCM	Shape	Size
[33]	Paraffin	51	Sulfuric acid	xGnP	1	0.28	0.35	128.8	134	-	< 10nm
					3		0.55		132.4		
					5		0.7		131.5		
[34]	Hexadecane	18-20	Sulfuric acid	xGnP	3	0.66	0.992	232.41	217.33	-	
	Octadecane	26-30				0.49	0.873	241.97	240.92		< 10 nm
	Paraffin	53-57				0.35	0.454	142.72	140.99		
[50]	Fatty acids	16.8	Nitric acid	MWCNTs	10	0.15	0.40	140.5	122.3	-	8–15nm
					20		0.63		101.6		
					30		0.64		87.1		
					40		0.65		76.4		
					50		0.66		57.3		
[51]	Paraffin	44	Saline treated	MWCNTs	0.1	0.15	0.232	238.9	236.3	-	9.5 nm
					0.5		0.241		236		
					1		0.261		239		
[122]	Paraffin	40	Microwave	xGnP	0.2	0.29	0.31	135.65	141.61	-	-
					0.5		0.32		163.28		
					1		0.34		169.02		
					2		0.41		143.83		

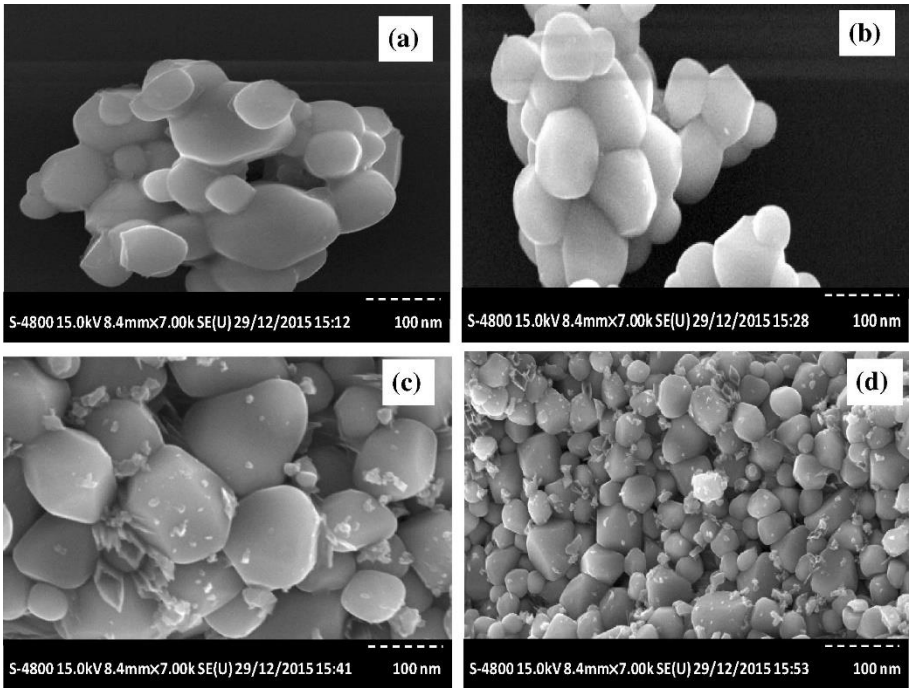

Figure 2.21 SEM images of TiO_2 nanoparticles: (a) 15, (b) 30, (c) 45, (d) 60 min after execution of sonication [182].

2.4.5 pH maintaining method

The similar pH value of the nanofluid and the pH of the base fluid (PCM) will result in stable suspension. Second, to get a sustainable suspension, the nanofluid's pH should be far from the isoelectric point [183,184]. The Al_2O_3-Cu hybrid nanofluid exhibited well-dispersed nanoparticles with a pH value of 5.5 according to Suresh et al. [183]. Xian-Ju et al. [184] proposed optimum pH values of 8 and 9.5 for alumina (0.1 wt. %) and copper (0.2 wt. %) water-based nanofluids, respectively. Qing et al. [185] analysed the impact of pH on transformer oil stability SiO_2-graphene hybrid nanofluid and observed that pH samples 9 and 12 exhibited low stability of compared with pH fluids 10 and 11. Toghraie et al. [186] examined the effect of pH on TiO_2 nanofluid stability when preparing MWCNT-TiO_2/EG-W hybrid nanofluid. The samples were prepared using specific pH values of 3, 6, 9 and 12. After 48 hours, the samples were analysed and revealed that the pH-value 9 fluid supported the particles better dispersed than others. Askari et al. [187] tested the stability of the nanofluid iron oxide and Graphene at various pH values (3, 5, 7, 8, and 10). The tests were analysed after 10 min, two weeks, and one month after sonication and showed that the sample with pH values of 8 and 10 was stable even after one month as shown in Figure 2.22. Qing et al. [188] tested SiO_2-graphene stability at four different pH values, ranging from 9 to 12. The results showed that

the sample became more stable at a pH value of 11, while at a pH value of 12 the stability was disrupted. It is observed that the optimal pH value is important factor for the better stability of the nanofluid, and the studies showed that preparation of the nanofluid with the pH value identical to the pH value of base fluid results in good stability.

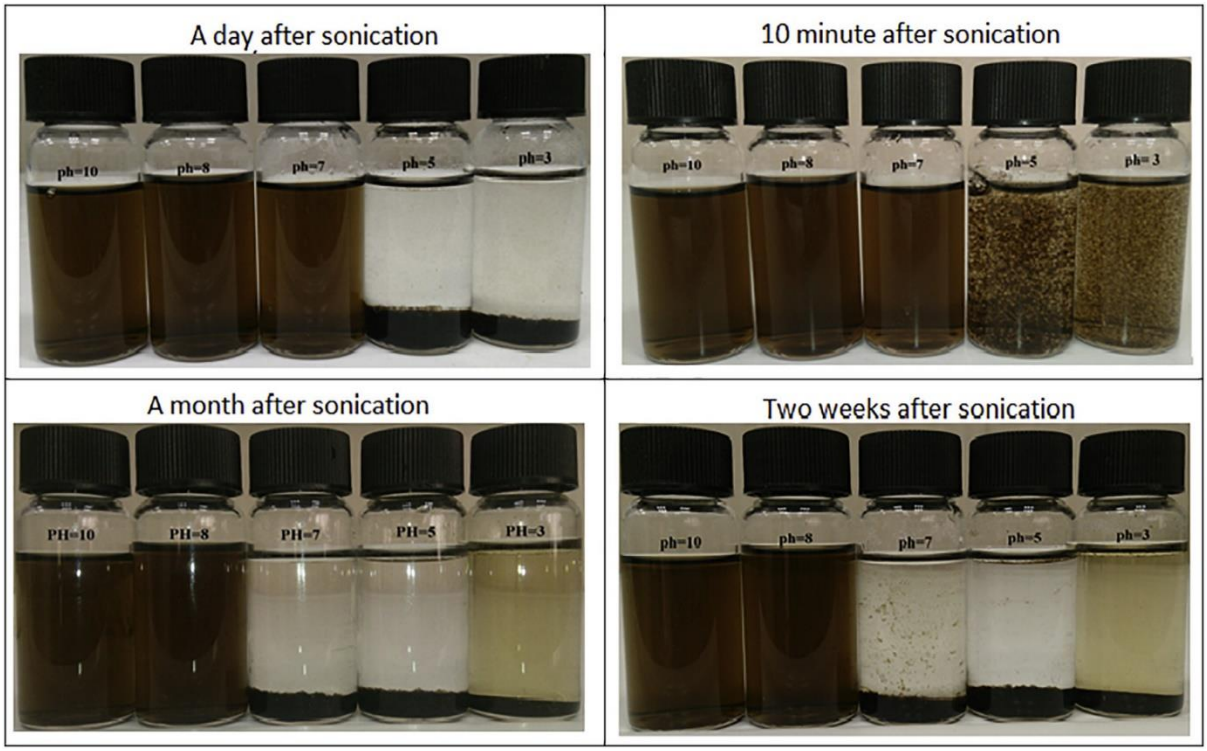

Figure 2.22 pH-value effects on stability of Fe_3O_4/graphene nanofluid [187].

2.4.6 Discussion

Following the above stability study it has been found that the stability of nano-PCM can be influenced by variables such as surfactant addition, surface treatment, ultrasonication, particle shape and size, pH value, stirring time and particle concentration. Researchers need to concentrate on the above-mentioned considerations for their future studies in order to achieve better dispersion of nanoparticles in PCMs. The stability study ends by stating that the use of nanofluids in real life applications is not feasible without achieving long-term stability. However, the following points are concluded from the aforementioned stability improvement methods.

- The stability of nano-PCMs can be improved by the addition of surfactants, but they decompose at higher temperatures when they are added in a large amount which results

in the reduction of thermal performance. That is the reason that a concentration of the surfactant in the nano-PCMs is an important factor.

- The surface-treated nanoparticles with acids showed good dispersion in PCMs as compared with the pristine nanoparticles.
- Ultrasonication of the nano-PCM enhances the stability of particles, however in some studies mixing parameters are missing. The stability of nano-PCM can be further analysed by varying the different parameters, such as an ultrasonication frequency, temperature and time.
- It was found that smaller size with larger surface area particles show better stability because the small size particles increased the Brownian motion which leads to greater particles to particles interaction.
- The pH value adjustment provides better stability results because the ideal pH value increased the electrostatic repulsive forces that decreased the agglomeration effect of particles and improved the nanofluid stability time. Many research have been done on the impact of pH on nanofluids pH, but a gap is open for researchers to work in the case of mono nano-PCMs and hybrid nano-PCMs.
- The stability of the nano-PCMs depends on the different factors as discussed above but as shown in the Figure 2.20, TiO_2 based nano-PCM remain stable for higher thermal cycles than carbon nanomaterial based nano-PCM.

2.5 Applications of nano-PCMS

The new renewable energy sources, such as wind energy & solar energy, have been developed and used to protect the environment and conserve energy. Nevertheless, these renewable energy resources are fluctuating and intermittent. PCMs can fill the gap between energy demand and supply, and thereby address the limitations of renewable energy. In phase change materials, energy is stored as latent heat which can be used for industrial and domestic purposes beyond peak hours. Because of the higher energy storage capability of PCMs they could be employed in buildings, electronics management, solar, refrigeration, excess heat recovery, textiles, food preservation, underfloor heating systems, etc.

2.5.1 Buildings

As an energy storage material, the available or extra energy could be stored in the PCM during a charging cycle. The retained energy can then be recovered and distributed to the end-user

through the discharging cycle. As a result, stored energy helps to reduce the peak demand on the national electricity grid and to use power during off-peak time. The use of thermal energy storage (TES) systems will help the consumer by a reduction in energy rates, technologically advanced load factor, enhancing space temperature regulation plus slower capital expenditure in modern generation equipment [189]. PCMs are widely used in construction in numerous ways of such as cement mortar, concrete mixing, sandwich panels, gypsum plaster, wall panels, and blocks to fulfil the energy utilization of buildings for cooling, warming, ventilation and air conditioning and lighting [190]. But very few studies are available in which nano enhanced phase change materials were used as energy storage materials in buildings for heating and cooling purpose PCMs.

Table 2.8 summarises the application of nano-PCM in buildings. Parameshwaran and Kalaiselvam [191] used silver nanoparticles with PCM for air conditioning purposes in buildings. PCM incorporated with nanofillers showed enhancement in the heat transfer process during charging and discharging cycles. Furthermore, the results depicted that the developed air conditioning system with nano-PCM showed 24-51% and 58%, per day and an on-peak energy saving potential, correspondingly for a yearly operation comparison to the traditional air conditioning unit. Similarly, Ke et al. [192] investigated fatty acids eutectics/silver nanoparticle composite for thermal energy storage applications. The developed composite showed low phase change temperatures, high phase change enthalpies and good thermal stability, which indicates that the composite has the potential to be used in buildings for energy storage purposes. Hussain et al. [193] developed activated carbon and eutectic PCM based nano-PCM for cold storage applications. The synthesized material showed excellent enhancement in the heat transfer with little thermal expandability and could be used for low thermal energy storage applications in buildings. Sayyar et al. [194] incorporated graphene nanosheet based PCM into the gypsum wallboard and its thermal performance was evaluated.

The use of nano-PCM in the wallboard delayed the time at which peak temperature was reached and reduced the interior temperature fluctuations. The findings of the numerical studies showed that substantial improvements in the energy efficacy of buildings can be achieved by integrating nano-PCM with building materials. Moreover, the findings suggested that by applying nano-PCM a reduction of 79% in energy consumption to maintain the internal temperature within the thermal comfort range was observed. Zhang et al. [195] dispersed

modified MWCNTs with the organic n-hexadecane PCM. The significant effect of MWCNT particles on the reduction of n-hexadecane supercooling allows a compelling way to increase system energy efficiency in building heating and cooling applications. Jeon et al. [34] impregnated xGnP particles with three different PCMs having distinct melting temperatures. They found that xGnP based nano-PCMs maintained the latent heat and the melting temperature of the PCM and developed composite can be classified as energy-saving materials for domestic buildings utilizing the radiant heating method.

Ma et al. [108] integrated solar photovoltaic thermal (PVT) collectors and nano-PCM with a ceiling ventilation system to examine the effect of copper nanoparticles in the PCM. Comparison with the use of pure PCM, 25.1 % more heat was discharged, and 8.3 % more heat was charged from nano-PCM during the three winter test days. Sharma et al. [99] reported passive cooling approach for the BICPV by integrating micro-fins, PCM and nano-PCM. They also carried out this work with the goal of implementing the advantages of this method in order to improve the efficacy of BICPV. The experimental findings revealed that when micro fins were integrated with PCM, the temperature at the centre of the system decreased by 10.7°C and 12.5°C when nano-PCM was integrated micro fins. Correspondingly, a temperature drops of 9.6°C and 11.2°C was found when PCMs and nano-PCM were used for unfinished surfaces relative to natural convection. In addition, the effective TC has been increased by 0.35%. Therefore, these findings have shown that a combination of these passive technologies can be considered for the thermal improvement of BICPV.

As the building sector is the largest energy consuming sector and the integration of nano-PCMs with buildings were found to be very useful in terms of reduction in overall energy consumption, but no significant attention is utilized in this area. Moreover, that stability of nano-PCMs also needs an attention of the researchers because poor stability of nano-PCM limits its application in building sector. Therefore, there is a need to critically explore the further aspects of the application nano-PCMs in buildings.

2.5.2 Electronics thermal management

PCMs have been used for the thermal control of electronic components. To boost the thermal efficiency, many researchers have integrated nanofillers with the pristine PCM since they have superior thermal characteristics so in electronic devices, they can be used as coolants. Tariq et al. [196] narrated graphene nanoparticles with two different organic PCMs for the thermal

controlling of electronic components. The results reported that with only 0.008% of graphene nanoparticle RT-44/GNPs composite reduced the base temperature of the heat sink by 25% and 16% with RT-64HC/GNPs combination. Figure 2.23 shows the schematic of their experimental setup. In another study, Fan et al. [197] examined GNP and CNTs/PCM based heat sinks using different heat loads. Results demonstrated that GNP/PCM composite based heat sink exhibited better performance than CNTs. However, CNTs were shown to be beneficial for the enhanced heat transfer of the TES-based heat sink. Kumar et al. [198] carried out an experimental investigation to verify the thermal efficiency of nano-PCM heat sinks together with heat pipes for electronic cooling purposes. It was noted that heat storage capacity was improved by the addition of nano-PCM due to which a decline in sensible temperature increase occurred, further preserving the central temperature of the heat sink at ambient temperature for a prolonged period. Bahiraei et al. [173] inspected the thermal control of electronics using paraffin-based carbon nanostructures. Prepared nano-PCM samples were perceived to regulate the system temperature adequately by using 18% of the system's latent heat capacity compared to pure paraffin. Moreover, the results also showed that with 7.5% and 10% graphite-based nano-PCM improved the thermal efficiency of latent heat management systems. Having analysed the phenomenon of thermal characteristics of RT65 PCM and CNTs Alshaer et al. [199] found that along with the introduction of even a small quantity of CNTs, TC was substantially improved compared with numerical models. Further, there was also a remarkable improvement in the latent heat of the composite relative to the pure PCM (RT65). Another study, done by Alimohammadi et al. [200] presented an impact of nano-PCM on the electronic chipset cooling by considering both natural and forced convection conditions. For the distinct values of the heat flux, six different heat sink configurations were carried out. In both forced and free convection, these cooling-combinations were investigated i.e., simple heat sink, heat sink with PCM, and heat sink with nano-PCM. Further, only 1% of Fe_3O_4 nanoparticles was used with Mn $(NO_3)_2$ PCM. Results depicted that the nano-PCM and PCM heat sinks, reduced the temperature of the electronic chipset to 10.5°C and 14°C for both forced and free convection as compared with an empty heat sink. Wang et al. [201] examined paraffin based nano SiO_2 composite for the thermal management of electronic devices. Three paraffin/SiO_2 composites were prepared with 60%, 70% and 75% of PCM in nano-SiO_2. The results indicated that with 75% PCM and 25% nano-SiO_2 nanoparticle based nano-PCM showed enhancement in the thermal performance of electronic components was around 21.8%. Colla et al. [202] discovered the effects of different concentrations (0.5 wt.% to 1 wt.%) of Al_2O_3 in the RT-55

and RT-44 organic PCMs with melting temperature of 55°C and 45°C respectively. The results showed that the nano-PCM were able to delay the melting process relative to the reference temperature. As a result, these findings of thermal characteristics indicated that nano-PCM could be used in electronics for passive cooling and energy storage purposes. The aforementioned studies show that for electronic components nano-PCM performed better than pristine PCM because of the presence of high conductive particles. Further, type of nanofiller play a significant role in the stability of nano-PCM and it is found that carbon based nanofillers showed good thermal stability than other nanoparticles.

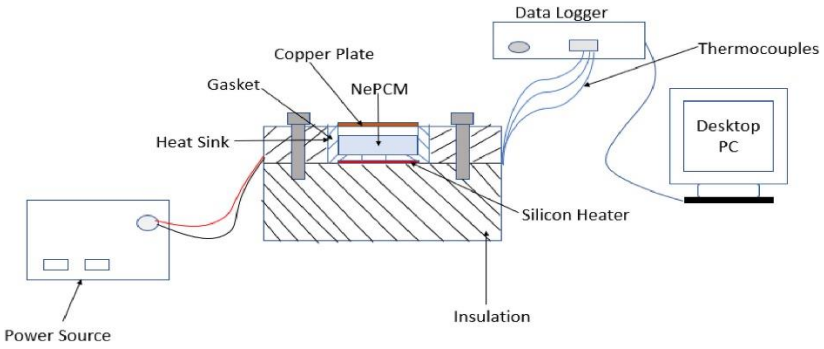

Figure 2.23 Schematic of the experimental setup used by Tariq et al. [196].

2.5.3 Textile

PCMs have been used in textiles for safety or durable finishing of cotton or wool, softeners of the skin and durable fragrances [203]. Furthermore, textiles must be designed and processed in such a manner that they have the potential to control dynamic heat besides the skin [204]. Such thermo-modulated textiles require the usage of PCMs which provide thermal comfort to the human body by maintaining the body hot or cold depending on the immediate climate. A great deal of attention has been paid to the evolution of usable textiles with PCMs, which can retain and emit excess heat during their phase transition.

The pre-treated polyamide and polyester fabrics with silver nanofillers showed improvement in the anti-fungal efficiency [205]. Due to the anti-bacterial properties of silver nano-crystals Potiyaraj et al. [206] synthesised silver nano-crystals on silk fibers. The resulting silk fibres can be utilised as an antibacterial agent and photo-catalyst in water splitting applications. Hebeish et al. [207] processed silver nanofillers utilising hydroxypropyl starch for the preparation of highly efficient anti-bacterial textiles. The solution of silver nanofillers was applied with and without binders to cotton fabrics. The authors found that after 20 washing

cycles, the binder maintained its anti-bacterial properties and that silver nanoparticles stayed static on the surface of the fabric material. Li et al. [208] examined the resilience of nano-ZnO antibacterial properties for the functionalization of cotton fabric to sweat.

The fabrics treated with Ag/TiO_2 showed a color change, hence Dastjerdi et al. [209] conducted an investigation to resolve this problem. Both nanoparticles were treated with different concentrations of the cross-linked polysiloxane. The findings showed that treatment with polysiloxane could help to increase the bioactivity of TiO_2 together with its photo-catalytic function. The production of smart textiles with good thermal stability and added durability is currently a hot research subject.

2.5.4 Medical

The antiseptic usefulness of PCMs is a substantial and evolving area for the advancement of hybrid functionality materials. Silver-based nanocomposites are widely utilised materials with PCMs due to their inherent antibacterial activity in medical uses. Tobaldi et al. [210] prepared Ag-modified TiO_2 nanoparticles using the sol-gel method to analyse the photocatalytic and antibacterial properties of both ultraviolet and visible light displays. Under ultraviolet light, Ag nanoparticles demonstrated strong antibacterial activity against Escherichia coli (Gram-negative bacteria) relative to methicillin-resistant Staphylococcus aureus (Gram-positive bacteria). Hirst et al. [211] shown the high-tech applications of self-assembled supramolecular nanostructured phase change materials whilst progressing to regenerative medicine electronic devices. Previous molecular gels have been used for low cost operations, but then several changes have been made to nanoscale assembly processes. Besides that, in the future, this technique would have to cope with a better understanding of the connections that would promote nanomanufacturing between molecular building blocks. For enhancement beyond the skin-depth limit, a metallic nano slit was used by Seo et al. [212]. They proposed that a wide range of applications will be provided for nanostructures for these operations to improve skin-depth treatments, in concentrating systems and as an enabling mechanism for applications in sub-nano-optics. Further, nano-PCMs can also be used with certain vaccines/medicines to keep them at their desired temperature.

Table 2.8 Summary of literature on energy preservation by integration of nano-PCMs in buildings.

Reference	Nano-PCM		Findings
	Nanofiller	**PCM**	
Xie et al. [213]	Cesium tungsten bronze	Salt hydrate	Nano-PCM was incorporated into a double-walled glass to preserve solar energy and minimize heat transfer. The findings showed that the amount of heat transfer from an atmosphere reduced with the dispersion of nano-PCM.
Zhao et al. [214]	Bentonite	n-octadecane + n-eicosane	Authors utilized two distinct nano-PCMs in bentonite to conserve thermal energy that can be sufficient to adjust indoor temperatures in both summers and winters. The analysis indicates that the developed nano-PCM could be used to control indoor temperature.
Li et al. [215]	Al_2O_3	Paraffin wax	To boost the thermal efficiency, nano-PCM was filled in double glazed windows. The numerical and experimental findings showed that the minimal energy consumption was achieved with a 1 % Al_2O_3 nanoparticles and at a 100 nm nanoparticle diameter.
Sayyar et al. [194]	xGnP	Palmitic and capric acid	The eutectic fatty acid/graphite nanofiller based composite was integrated with a panel wall to improve the thermal performance. It was observed that the room with the nano-PCM wall could minimize the heat transfer by 79%.
Venkitaraj et al. [216]	CuO 0.1 wt.%	Neopentyl glycol	The experimental study was conducted to develop nano-enhanced PCM for the cooling purposes of buildings. The results indicate that the nano-PCM reduced the melting and solidification rate with 0.1 wt.% nanoparticles. Further, the decline in the room temperature by 3°C was observed.

Continued…

Biswas et al. [217]	EG	n-heptadecane, paraffin	The investigation was conducted to examine the cooling and heating effect by the integration of nano-PCM in the building wall. The wall comprising nanoparticles was found to reduce the maximum temperature and reduce the interior heat transfer, allowing air-conditioning devices to work more effectively in order to cool the interior.
Parameshwaran and Kalaiselvam [191]	Ag 1wt.%	Paraffin	The experimental examination was conducted to enhance the thermal efficiency of the air-conditioning system. The outcomes showed that, due to the enhancement of TC and heat transfer rate, nano-PCM enhance heat transfer mechanisms and improves the charging and discharging by about 10 %.
Huang et al. [218]	MWCNT 0.0625 to 0.5 wt.%	Ethylene glycol	The nano-PCM was developed for the cold energy storage applications. It was noted that the MWCNT enhanced the TC up to great extent without effecting the latent heat.

2.5.5 Overview

Due to the global increase in energy demand, nano-PCMs are used in buildings by different incorporation methods. In addition, because of their better thermal conductivity and high latent heat of the nano-PCM researchers have employed nano-PCM composites in many other applications such as smart textiles, thermal cooling of electronics and the medical industry. Apart from these applications, nano-PCMs have also been used for PV panels cooling, food packaging and cold storage applications. A detailed review on the applications of nano enhanced phase change materials has recently been reported by Tariq et al. [149]. The important elements that researchers should need consider are the choice of PCM and the concentration of nanoparticles. PCM phase transition temperature should be in the range of application temperature and an appropriate concentration is also essential because higher concentration leads to higher viscosity, which hinders the natural convection. Furthermore, the proper selection of PCM and nanofillers lead to the long-term thermal stability which is an important factor and results in greater performance of nano-PCMs in all applications. This is the reason that it is important to select an appropriate material and different stability improvement methods can also be employed for better efficiency of nano-PCMs. Figure 2.24 shows some of the applications of the nano-enhanced phase change materials.

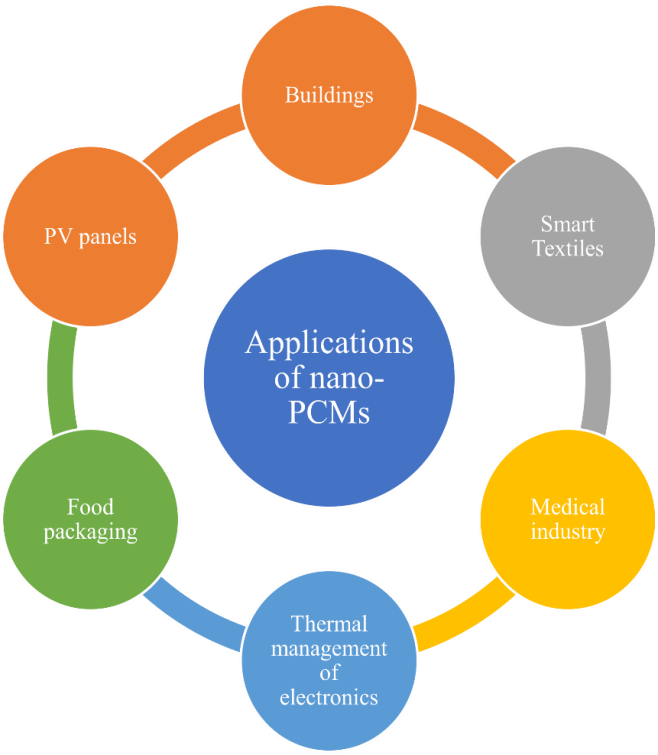

Figure 2.24 Applications of nano enhanced PCMs.

2.6 Summary

Previous studies [62,219,220] have examined the impact of incorporating various nanoparticles into PCMs and have highlighted challenges associated with their use. Significant drawbacks identified include stability issues and reductions in latent heat when nanomaterials are added. A comprehensive study is needed where nanoparticles with better stability and minimal impact on energy storage capacity are meticulously selected and tested, as informed by a thorough literature review. Additionally, there is a lack of research investigating the modification of nanoparticles and its effects on the stability and thermophysical properties of nano-PCMs. Furthermore, in-depth research is required to understand how the shape and size of nanomaterials influence thermal and physical stability of nano-PCMs.

This literature review on nano-enhanced PCMs reveals several gaps, particularly in the study of hybrid and modified hybrid nanofillers, which are less explored compared to mono nanofillers. A significant challenge lies in enhancing the thermal conductivity of PCMs to boost heat transfer efficiency. This challenge is compounded by the fact that increasing nanoparticle concentration often leads to a decrease in latent heat. Moreover, more research is needed to determine the effect of nanofiller concentration on latent heat storage and thermal conductivity, while ensuring stability and cost-effectiveness. The effects of modified nanoparticles on the thermophysical characteristics of nano-PCMs also require more detailed investigation.

Overall, the review identifies critical areas where further research is necessary: selecting stable nanoparticles with a minimal impact on energy storage, understanding the influence of nanoparticle shape and size, investigating hybrid and modified nanofillers, enhancing thermal conductivity without compromising latent heat, and exploring the effects of nanoparticle modification on the stability and thermophysical properties of nano-PCMs. Addressing these gaps will significantly advance the application of nano-enhanced PCMs in thermal energy storage systems.

CHAPTER 3: METHODLOGY

This chapter outlines the comprehensive methodology employed in the study of nanoparticles enhanced phase change materials (Nano-PCMs). The aim is to provide a clear and replicable framework for the research, ensuring that the results obtained are reliable and can contribute significantly to the field. Given the complexity and novelty of Nano-PCMs, an appropriate and well-structured methodology is crucial for the success of this research.

3.1 Materials

In this study, two primary types of materials were utilised. The first type includes Phase Change Materials (PCMs) for thermal energy storage, and the second type comprises nanofillers, which enhance the PCMs' thermal conductivity, thereby improving heat transfer.

3.1.1 Phase change material (PCM)

The selection of the appropriate PCM is very important for the good thermal performance of a thermal energy storage system. There are some important thermal and chemical properties that must be considered before selecting the PCM. Figure 3.1 shows the selection criteria that have been employed to choose the appropriate PCM. Paraffin (PAR), a typical type of PCM, with a nominal melting temperature of 27-29 °C was utilised in this study and was provided by Rubitherm GmbH, Germany. This specific PCM with a melting temperature range of 27-29°C was selected for its proximity to the nominal indoor temperature of buildings and its versatility for use in other thermal energy storage applications within that temperature range. Additionally, PCMs, particularly paraffin, offer several strengths, including high energy storage capacity, enhanced stability, self-nucleation, absence of segregation, non-toxicity, non-reactivity, and non-corrosiveness [221]. Paraffin's compatibility with various additives, including nanoparticles, contributes to its thermal stability. Moreover, its availability, cost-effectiveness, and eco-friendliness make it a favourable option for thermal energy storage applications. The thermophysical characteristics of paraffin (RT-28HC), a typical type of PCM, are presented in Table 3.1.

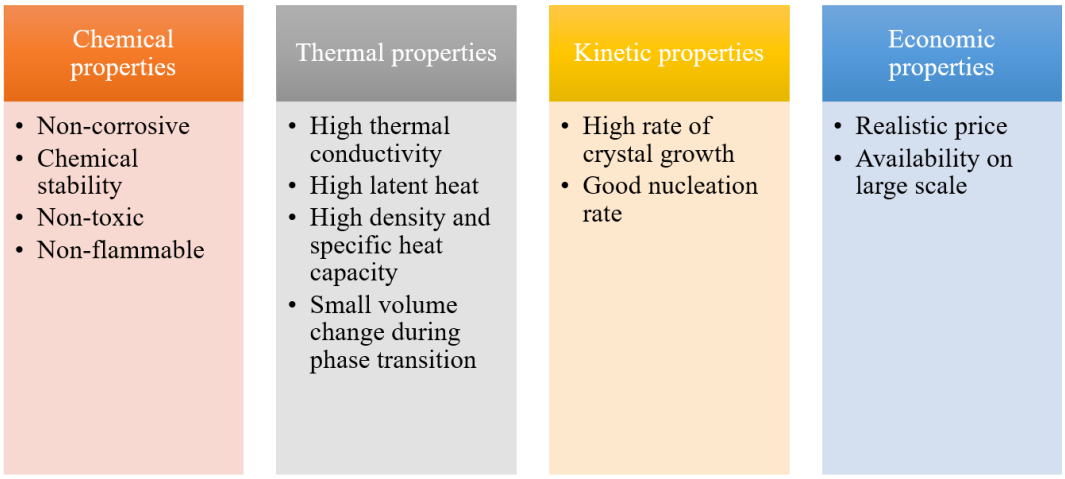

Figure 3.1 Selection criteria for the PCMs.

Table 3.1 Thermal properties of RT-28HC, a typical type of PCM [222].

PCM	Melting temperature (°C)	Heat storage capacity (kJ/Kg)	Specific heat capacity (kJ/Kg)	Thermal conductivity (W/m. K)	Density (kg/m^3)
RT-28HC	27-29	250	2	0.2	880 at 15°C 770 at 40°C

3.1.2 Nanoparticles

The nanoparticles should have good intermolecular interactions with the PCM for better stability and good thermal performance. Researchers found that the nanofillers with high TC, greater surface area, low density, high aspect ratio and significant van der Waals forces could enhance the thermal properties of the nano-enhanced PCMs. Because the high surface area of the nanofillers results in the greater intermolecular interactions between the nanoparticles and the PCM molecule in the matrix of nano-PCMs [58].

After a critical literature review shown in Chapter 2, three different nanomaterials were selected as the thermal conductivity enhancers, including metal oxide nanoparticles i.e., titanium (IV) dioxide (TiO_2), carbon-based nanomaterials, i.e., graphene nanoplatelet (GNP) and multiwall carbon nanotubes (MWCNTs), to improve PCM thermal conductivity. Sigma-Aldrich, UK, provided anatase TiO_2 nano powder with 99.7% trace metals basis, particle size < 25 nm, density of3.9 g/mL, and surface areas of 45−55 m^2/g at 25 °C; GNP with particle size <2 µm and surface areas of 750 m^2/g and MWCNTs with outer diameter of 6-13 nm, length of 2.5-20 µm, surface areas of 220 m^2/g, 98% trace metals basis, and density of 2.1 g/mL at 25 °C. As shown in Tables 2.3-2.4 in Chapter 2, the reason for selecting these nanomaterials is due to

their better thermal and chemical properties which make them compatible with PCM molecule. For instance, they can be easily synthesised, have higher surface areas, good thermal conductivity and have a less effect on the latent heat of the PCM.

3.1.3 Surfactants

The dispersants are organic particles comprises of lipophilic and hydrophilic groups that prevent cluster formation and modify the nanoparticles surface properties[162]. The types of dispersants chosen for various nanoparticles vary because of the different characteristics of the different nanoparticles in suspension. If the type of dispersants is not correct, the dispersants will not be adsorbed stably on the surface of the nanoparticles, and the particle coating will be incomplete, thereby weakening the nanoparticles' dispersive effect [94]. The dispersants serve as a buffer and minimizes interfacial tension among the particles suspended and the PCM [151]. It allows the suspension relatively stable through escalating the repulsive forces and also provides the suitable means of chemically transforming the suspension from hydrophobic to hydrophilic [223]. Surfactants are categorised as non-ionic, anionic, cationic, and amphoteric as shown in Figure 3.2.

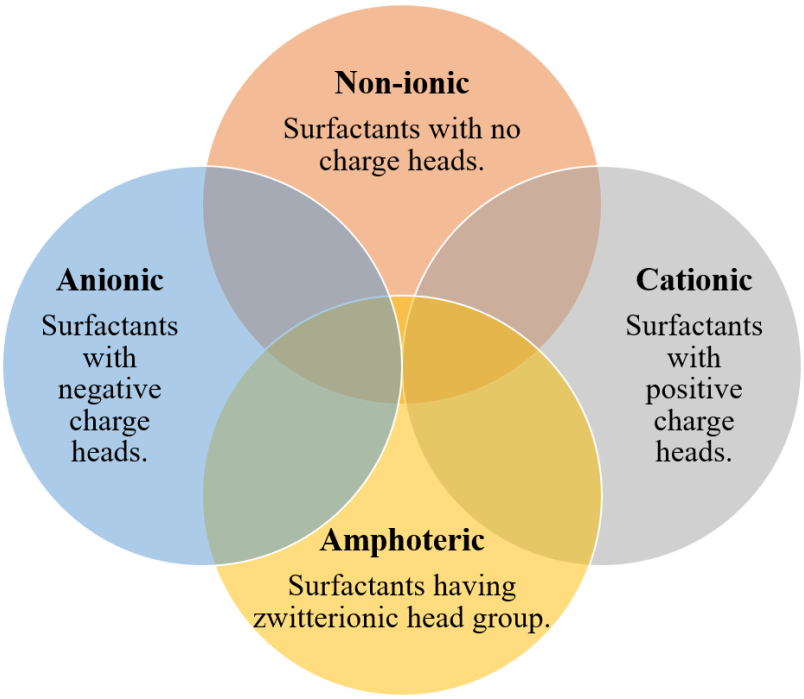

Figure 3.2 Classification of surfactants based on the composition of their head groups.

To minimise clustering and enhance dispersion by reducing the agglomeration effect, a range of dispersants was evaluated. Among them, three surfactants sodium dodecyl sulfate (SDS), cetyltrimethylammonium bromide (CTAB), and sodium dodecylbenzene sulfonate (SDBS) were tested for their efficacy in physically modifying nanoparticles. Initially, nano-PCM samples incorporating

each of these surfactants were prepared, followed by a phase of physical observations. These assessments revealed that samples modified with SDBS exhibited greater stability compared to those treated with SDS or CTAB [29]. Consequently, SDBS was selected for use in all subsequent samples.

In addition, two fundamental mechanisms underlie the stabilisation of nanoparticles in suspensions, namely electrostatic repulsion and steric hindrance, as illustrated in Figures 3.3 (a) and (b). Electrostatic repulsion occurs when ionic polymers adsorbed onto the nanoparticles create a charged layer, enhancing the repulsive forces between them. Steric hindrance, on the other hand, relies on the volume restriction and the mixing or osmotic component, which involves the compression of the adsorbed layer. This phenomenon is influenced by two key factors: the physical limitation imposed by the adsorbed polymers and the effects of polymer layer compression. Notably, certain dispersants, such as Sodium Dodecylbenzene Sulfonate (SDBS) depicted in Figure 3.3 (d), can offer both electrostatic repulsion and steric hindrance, providing a dual mechanism of stabilisation. This dual stabilisation mechanism, offered by SDBS, is pivotal in ensuring uniform dispersion, thereby effectively preventing the aggregation of nanoparticles and guaranteeing stable suspensions. The preference for SDBS over alternative surfactants is credited to its proven effectiveness in leveraging these stabilisation mechanisms. The mechanisms facilitating the effective dispersion of nano-titania in molten erythritol through triethanolamine (TEA) can be seen in Figures 3.3 (c) and 3.3 (e).

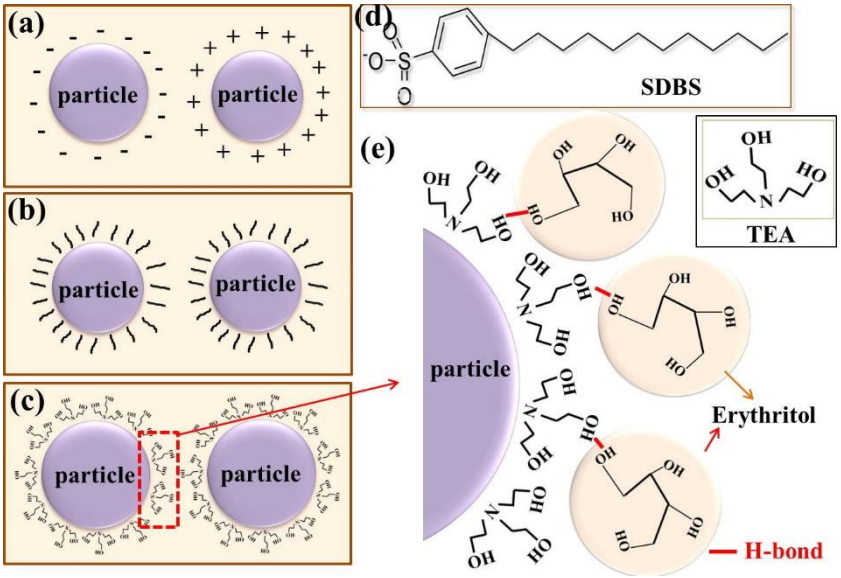

Figure 3.3 Schematic of the stabilising mechanisms, (a) electrostatic repulsion, (b) steric hindrance, (c) and (e) stabilizing mechanism of TEA as dispersant for the TiO_2–erythritol system, (d) the structure of SDBS [224].

3.1.4 Acids

It is well established that the stability of nanoparticles is a crucial factor in determining the overall performance of nano-PCMs [72,73]. Several methods have been investigated by researchers including pH adjustment, and surfactant addition [74]. However, among these

techniques, acid functionalisation was proven as an effective method with better long-term stability of MWCNTs within PCM [75]. For the surface treatment of multi-walled carbon nanotubes (MWCNTs), two acids, namely nitric acid with a concentration of >= 70 - < 90% and sulfuric acid with a purity of 99.99%, were employed. The use of acids in the surface treatment of multi-walled carbon nanotubes (MWCNTs) serves several purposes.

For instance, to remove impurities and functionalise the surface of MWCNTs, thereby enhancing their dispersibility and compatibility with other materials. Additionally, acid treatment can introduce functional groups (such as carboxylic acid groups) onto the surfaces of MWCNTs, which can improve their interaction with surrounding matrices and enhance the overall properties of composites.

3.2 Experimental Methodology

As shown in Fig.3.4, specific experimental research methods were employed to synthesise and characterise nano-PCMs, as well as to assess their thermophysical characteristics, ensuring the achievement of the research goals and objectives. The keys to effective heat storage and transfer in PCMs are the latent heat and thermal conductivity; hence, a PCM that exhibits both high latent heat and enhanced thermal conductivity, alongside a stable chemical structure, is deemed most suitable. In this study, an organic PCM known for its high latent heat was examined. To increase the PCM's thermal conductivity, three distinct nanoparticles were integrated, either singly or in a hybrid mixture, at varying concentrations ranging from 0 wt.% to 1 wt.% for mono nano-PCMs. The optimal mass concentration ratio for hybrid mono nano-PCMs was maintained at 70%/30% of the total mass or a loading content of 1.0 wt.% of nanomaterials. For the TiO_2 based hybrid particles (i.e., TiO_2/MWCNTs and TiO_2/GNP), 70% of the TiO_2 particles were used since they have better stability, and less impact on latent heat because of their good intermolecular interactions with the base PCM, and they are also economical [225]. Studies have shown that TiO_2 contributes to the stability of the composite material, whereas incorporating carbon-based nanoparticles ensures enhanced thermal conductivity without significantly compromising the material's structural integrity [60,226]. The 70%/30% ratio thus optimises the combination of these features to meet the specific requirements of energy storage systems, aiming to enhance both stability and thermal performance. Comprehensive experimentation was undertaken to investigate the physical, chemical, and thermal characteristics of the materials, employing various characterisation techniques. Initially, PCM-based mono and hybrid nanoparticles, without any modifications,

were prepared. Subsequently, the optimum concentration was determined through statistical analysis. Then functionalised multi-walled carbon nanotubes (MWCNTs) based single and hybrid nano-PCMs were developed at this identified optimal concentration. An overview of these approaches is shown in Figure 3.4. The functionalised MWCNTs were subsequently utilised in combination with TiO_2 nanoparticles to explore the impact of hybrid particles on the thermophysical properties of nano-enhanced PCMs. Furthermore, the performance of these functionalised MWCNTs and TiO_2-based hybrid nano-PCMs was compared with that of pristine MWCNTs and TiO_2-based hybrid nano-PCMs.

3.3 Synthesis of Nanoparticles Enhanced Phase Change Materials

Two main techniques are commonly followed for the preparation of nano phase change materials to conduct an experimental investigation and are termed as single-step method and two-step method. Simultaneous dispersion of individual nanoparticles or the dispersion of nanocomposites in the base fluid is the approaches reported in the literature for the preparation of nano-PCM. This section has presented a brief overview of nano phase change material preparation techniques which are useful for this project.

3.3.1 One step method

As shown in Figure 3.5, nanoparticles are synthesised and dispersed at the same time in one-step process, in simple words, all the processes are carried out in a single phase, that is the reason why this method is called the one step method. In order to achieve better stability and to avoid the formation of clusters this approach is considered the most successful. Moreover, single-step method does not require storage, drying, transportation, and dispersion processes, resulting in improved nanoparticle dispersion within the base fluid and reduced agglomeration [148]. This technique is only utilised on a limited scale since it is more expensive than the two-step method.

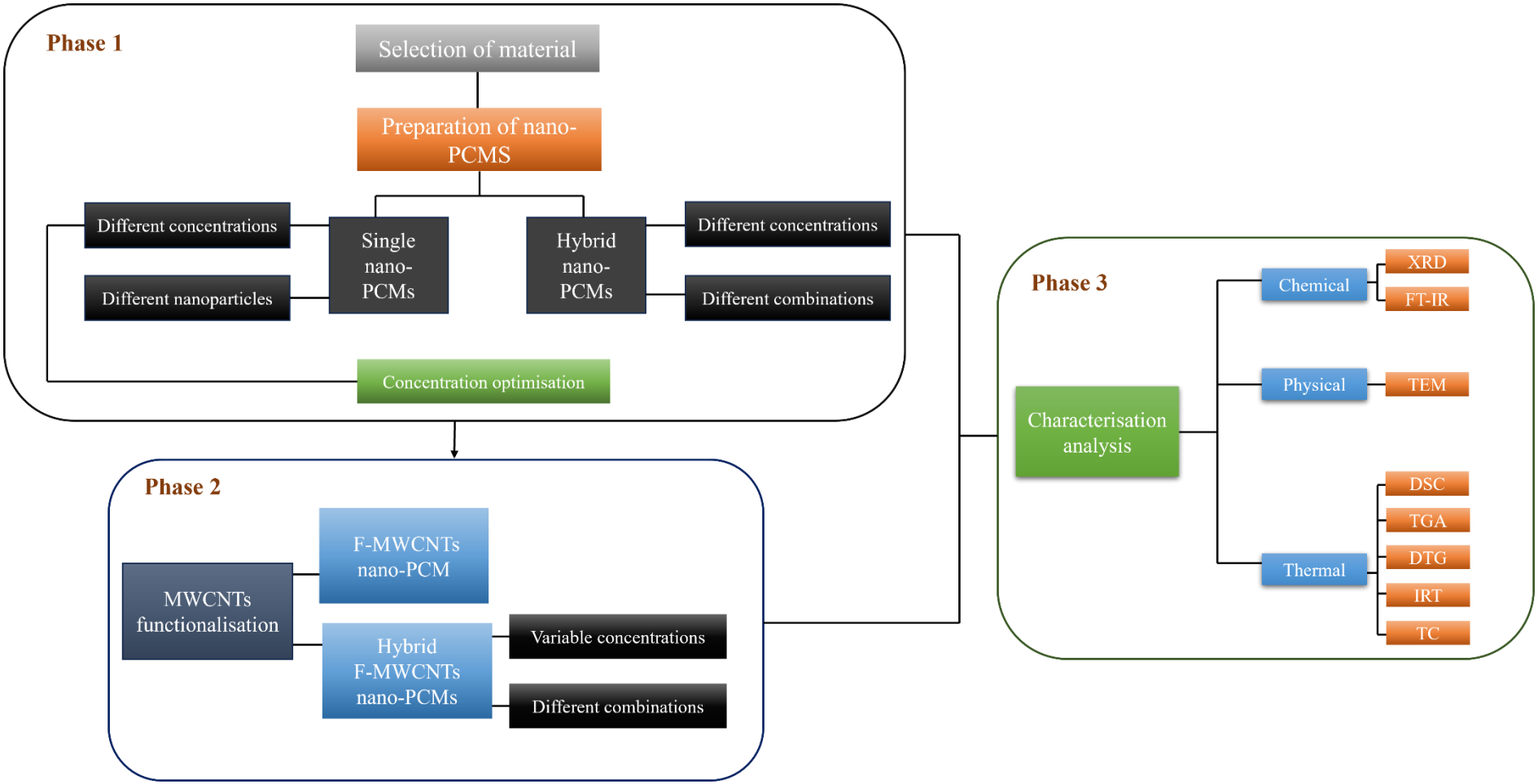

Figure 3.4 Methodology of research adopted in current study.

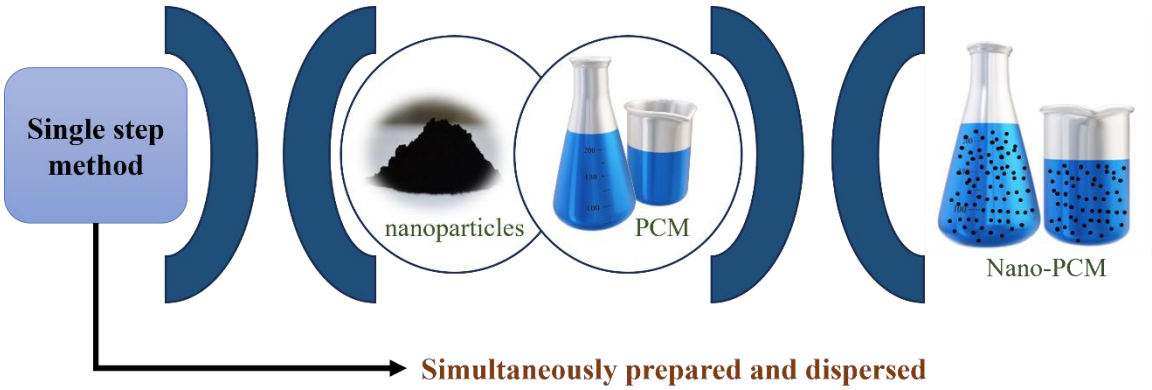

Figure 3.5 One step method for a PCM preparation [149].

3.3.2 Two-step method

In the two-step technique, nanofillers are primarily collected in dry powder form utilizing various mechanical and chemical methods such as, ball milling, chemical reduction, and sol-gel methods. The nanofiller powder obtained is then combined with the base PCM and for homogeneous particle dispersion. Distinct methods were used including ultrasonication and magnetic stirring. The two-step schematic diagram is shown in Figure 3.6. The greatest advantage of this method is the processing of nanocomposites on a commercial scale; however, this technique has the problem of agglomeration of particles and thus enhances the use of a single-phase preparation process [148,150].

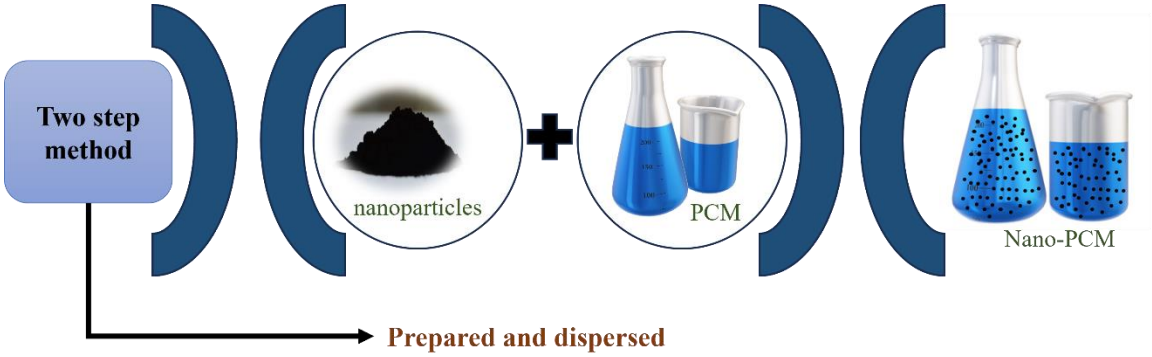

Figure 3.6 Two-step method for a PCM preparation [149].

In this study, the synthesis of nanoparticles enhanced phase change materials (nano-PCMs) was approached through the implementation of the two-step method. This methodology was meticulously chosen for its economic feasibility and scalability in producing large quantities. This method has been significantly employed in the fabrication of nanofluids [227]. The schematic diagram of the two-step method used for the preparation of mono and hybrid nano enhanced PCMs is shown in Figure 3.7. Furthermore, 25 % sodium dodecylbenzene sulfonate

(SDBS) was incorporated for each concentration of TiO_2, GNP, and MWCNT nanofillers. The mass concentration ratio of hybrid nano-PCMs (TiO_2/MWCNT, TiO_2/GNP and GNP/MWCNT) was held at 70%/30%. The 70%/30% ratio establishes a balance between the characteristics given by each type of nanoparticle. Titanium dioxide (TiO_2) nanoparticles, for example, have better stability, but multi-walled carbon nanotubes (MWCNTs) or graphene nanoplatelets (GNPs) provide better thermal conductivity. The goal of altering the ratio is to optimise the combination of these features to fulfil the needs of the intended application, such as energy storage systems.

First, RT-28 PCM was melted in a thermal bath at a constant temperature of 60 °C and then a fixed amount of nanofillers were added into a certain quantity of PCM. To obtain a homogeneous solution and to break up the particle clusters, a magnetic stirrer was used for two and half hours at 500 rpm at 60 °C to stir and homogenise the mixture. After that, SDBS was added separately into the mixture and continued further stirring for half-hour to get better dispersion of nanoparticles in the PCM since SDBS has good hydrophilicity which significantly decreases the tension of PCM surface during nano-PCMs preparation. Secondly, to enhance the dispersion and homogeneity of nanofillers while minimising aggregation and sedimentation, all samples were sonicated for 45 minutes utilising a probe sonicator at a 40% amplitude and 20 kHz frequency. High-frequency sound waves were applied during sonication, which causes the fluid to form cavitation bubbles. These bubbles collapse violently, causing localised high temperatures and pressures. This process ensures that nanoparticle agglomerates are broken up and distributed uniformly throughout the base fluid. Furthermore, sonication encourages the release of trapped air bubbles, which improves the nano-PCM samples homogeneity even more. Lastly, all the nano-PCM samples were cooled to room temperature.

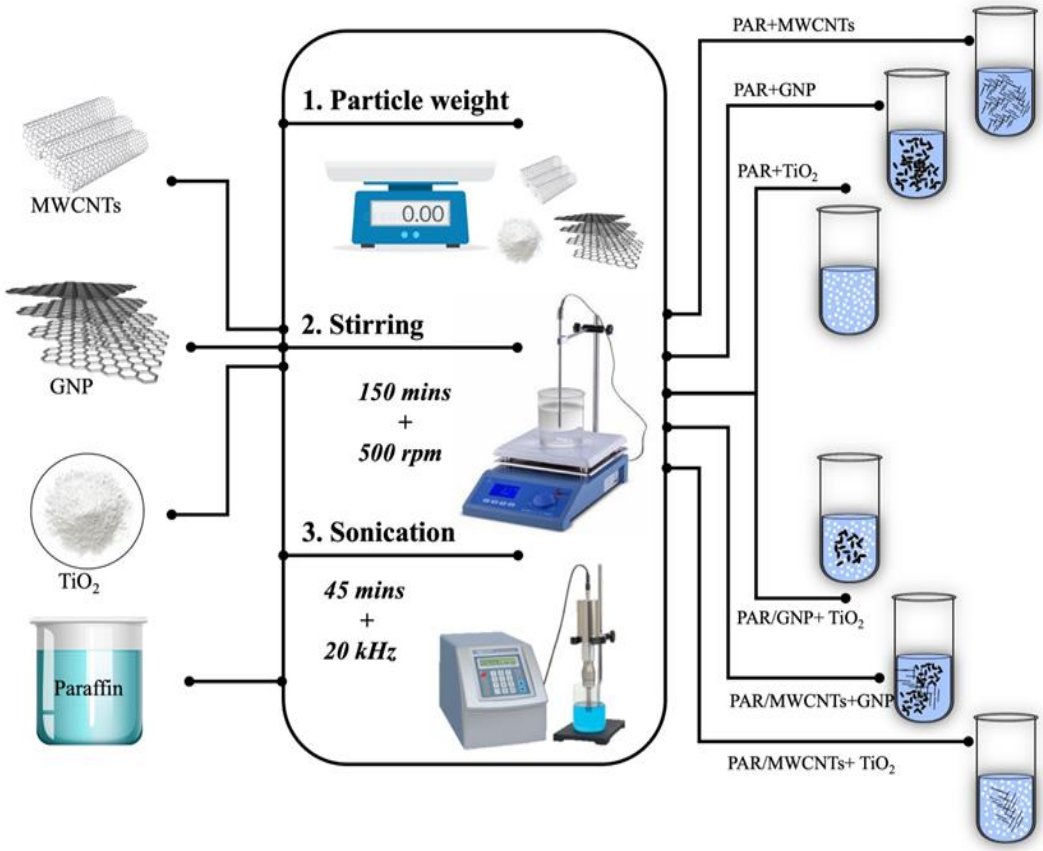

Figure 3.7 Schematic illustration of two-step method.

The similar two-step method was adopted for the preparation of the acid functionalised MWCNTs based nano-phase change material, as shown in Figure 3.8.

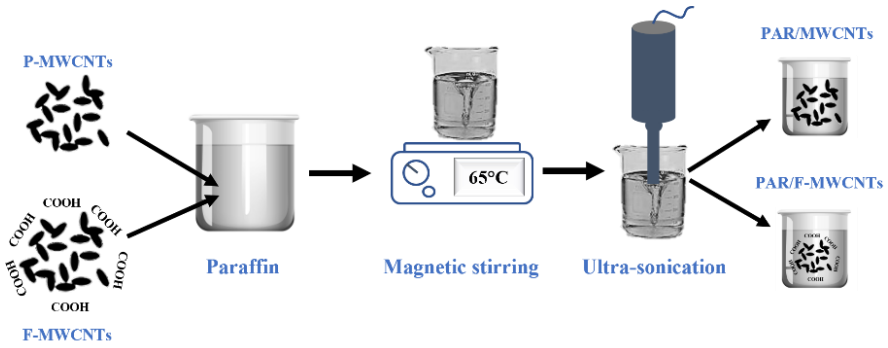

Figure 3.8 Schematic of a F-MWCNTs based PCM.

3.4 Functionalisation of MWCNTs

Figure 3.9 shows the schematic of a typical functionalisation process for MWCNTs. An acidic treatment of MWCNTs by strong acids was employed, which could effectively introduce oxygen-containing functional groups, such as –COOH on the surfaces of MWCNTs, as shown

in Figure 3.10. These functional groups can react with the other functional groups which can improve the dispersion of MWCNTs themselves or in a PCM matrix [228]. Three grams of MWCNTs were sonicated for two hours at 60 °C while suspended in a solution of H_2SO_4 and HNO_3 (3:1, v/v). After removing the resulting supernatant, the sediment was neutralised by deionized water washing. The product was then dried for 24 hours at 80 °C in a vacuum oven, as shown in Figure 3.9, and then ready to be employed.

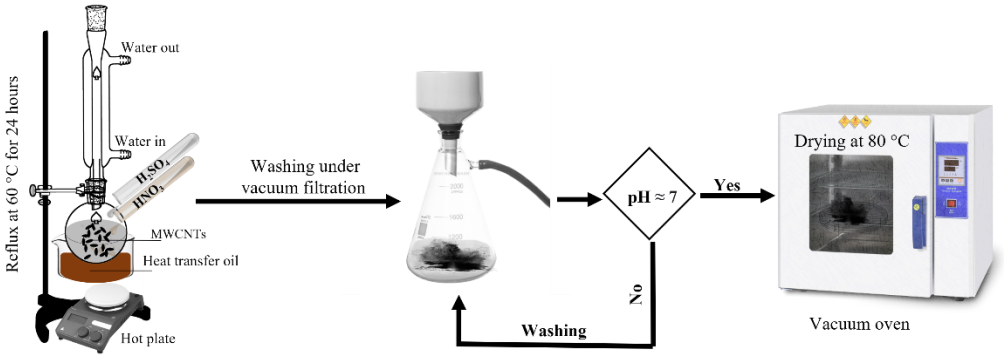

Figure 3.9 A typical schematic of functionalisation process of MWCNTs.

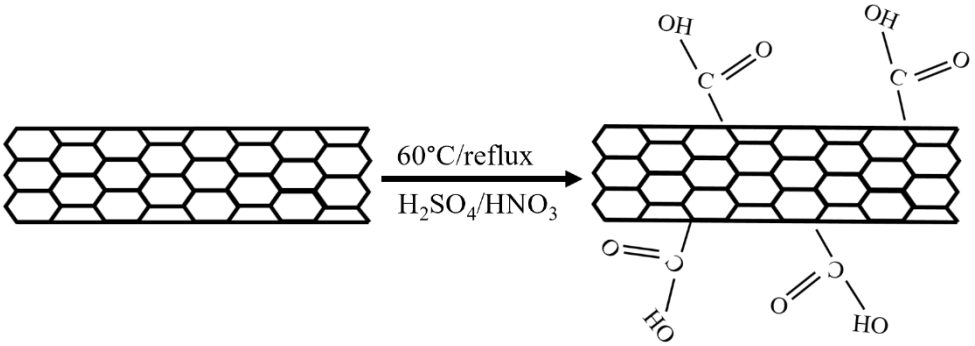

Figure 3.10 Schematic grafting of COOH bond after reflux.

3.5 Characterisation Techniques

Numerous characterisation techniques were employed to examine the chemical and structural attributes of the base PCM and the PCM augmented with nanofillers, to gain a deeper understanding of their structures and properties. These methods included Fourier transform infrared spectroscopy (FTIR), X-ray diffraction (XRD), Differential scanning calorimetry (DSC), Transmission electron microscopy (TEM), Thermogravimetric analysis (TGA) and Derivative thermogravimetry (DTG), and Thermal conductivity measurement (TC) apparatus.

3.5.1 Fourier transform infrared spectroscopy

A Fourier transform infrared spectroscope (FTIR, Perkin Elmer Frontier) was employed to investigate the absorption spectra and chemical structure of the pure nanoparticles, functionalised nanoparticles, pure PCM and nano-PCMs at the room temperature. The molecular bonds absorb specific resonant frequencies that are indicative of vibration and rotation energies, thus providing insights into the molecular structure [229]. Fourier Transform Infrared Spectroscopy (FTIR) analyses were conducted to detect the structural modifications in the chemical bonds of the Phase Change Material (PCM) following the incorporation of nanoparticles. These studies also verified the formation of chemical bonds for the functionalised multi-walled carbon nanotubes. The FTIR experiments were carried out at wavelengths ranging from 600 to 4000 cm^{-1}, with a spectral resolution and accuracy of 4 cm^{-1} and 0.01 cm^{-1}, respectively. Figure 3.11 shows the Fourier transform infrared spectroscope setup that this project has employed.

Figure 3.11 FT-IR setup.

3.5.2 X-ray diffraction (XRD)

In the technique of X-ray diffraction, the surface of the sample is exposed to a monochromatic X-ray beam at an angle θ. The X-rays experience constructive interference after diffraction by the crystalline phases within the sample, and are then detected by a goniometer at an angle θ.

The Bragg's law illustrates this principle (Equation 3.1). Scanning over a range of angles of X ray incidence produces a pattern characteristic for the analysed crystalline phase. This can be used to determine the crystalline phases present in the material such as spacing between the lattice planes which can then be used to identify the crystalline phases.

$$n\lambda = 2d \times \sin\theta \tag{3.1}$$

where,

n is the order of interference band

λ is the wavelength of X rays

d is the spacing between crystal planes

θ is the angle of incidence.

X-ray diffractometer with Cu-Kα radiation was provided by Bruker, UK and employed to study the crystalline structures of the base PCM and composite PCMs within the 2θ range of 5° - 60°. Figure 3.12 illustrates the configuration of the X-ray diffractometer apparatus.

Figure 3.12 XRD setup.

3.5.3 Differential scanning calorimetry

The thermal stability, thermal conductivity, and latent heat of melting and solidification were among the measured thermal parameters of the composite PCMs. Differential scanning calorimetry (DSC-Q200, TA Instrument Inc., UK) was utilised to investigate the melting,

crystallisation temperature and latent heat of pure paraffin and composite paraffin enhanced with nanofillers over the temperature range of 5 – 55 °C at a heating and cooling rate of 1°C min^{-1} under an N_2 atmosphere. The temperature range (5–55°C) is chosen to cover the expected phase transition temperatures of the material under investigation. A heating/cooling rate of 1°C min^{-1} is commonly used in DSC analysis for PCM and nano-PCM samples. This rate allows for sufficient time for the sample to equilibrate at each temperature interval, ensuring accurate measurement of heat flow associated with phase changes. Before the experiments, the DSC was calibrated by measuring the ΔH_{fusion} and T_{onset} of high purity standard indium (ΔH_{fusion}=28.7 Jg^{-1} and T_{onset}=156.6 °C) samples. Figure 3.13 a and b shows the DSC setup the cell containing samples.

A modulated differential scanning calorimeter was used to determine the specific heat capacity of samples (MDSC; Q200, TA Instruments, Inc.). The MDSC generated Cp data with an accuracy of up to ± 2%. The samples were placed in a DSC apparatus using a Tzero hermetic pan and lid (TA Instruments). The sample mass ranged between 10 and 15 mg. To perform the heat capacity measurements with the MDSC, a standard automated procedure was applied. The samples were heated between 10°C and 55°C at a heating rating rate of 2 °C.min^{-1}.

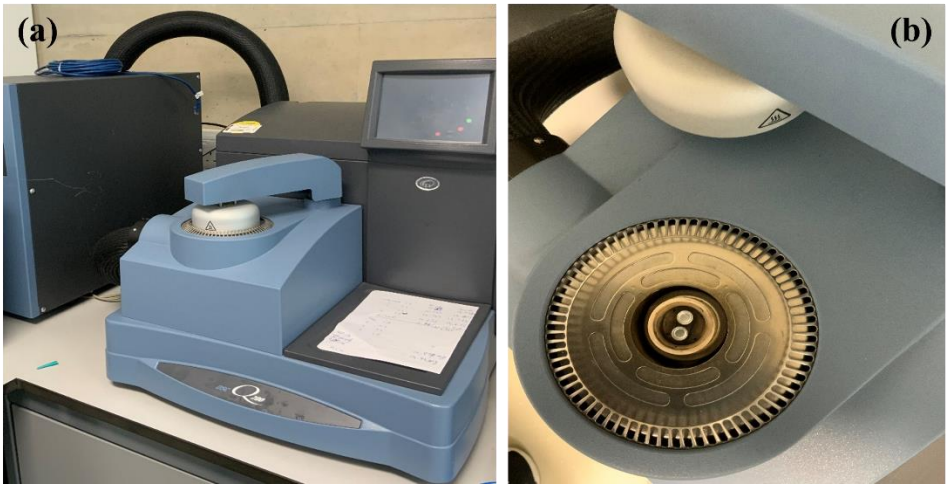

Figure 3.13 (a) DCS machine (b) loading cell containing samples.

3.5.4 Thermogravimetric analysis and Derivative thermogravimetry

Thermogravimetric analysis (TGA) and derivative thermogravimetry (DTG) are two important analytical techniques used to assess the thermal stability of both the pure phase change materials (PCMs) and the nanoparticle-enhanced phase change materials (nano-PCMs). TGA quantifies a material sample's weight loss as a function of temperature, employing a precise

mass balance to determine the difference between a pan containing the material and an empty pan. Platinum pans were utilised for these tests. A TGA Q-50 instrument from TA Instruments Inc., UK shown in Figure 3.14 was used for these tests. The materials underwent a regulated heating rate of 10 °C min^{-1} within a temperature range of 40°C to 400°C for the analysis. A nitrogen gas purge was kept going throughout the experiment at a flow rate of 100 mL min^{-1} in order to ensure an inert analytical environment and to stop oxidation or other processes that might have an impact on the measurement accuracy [230].

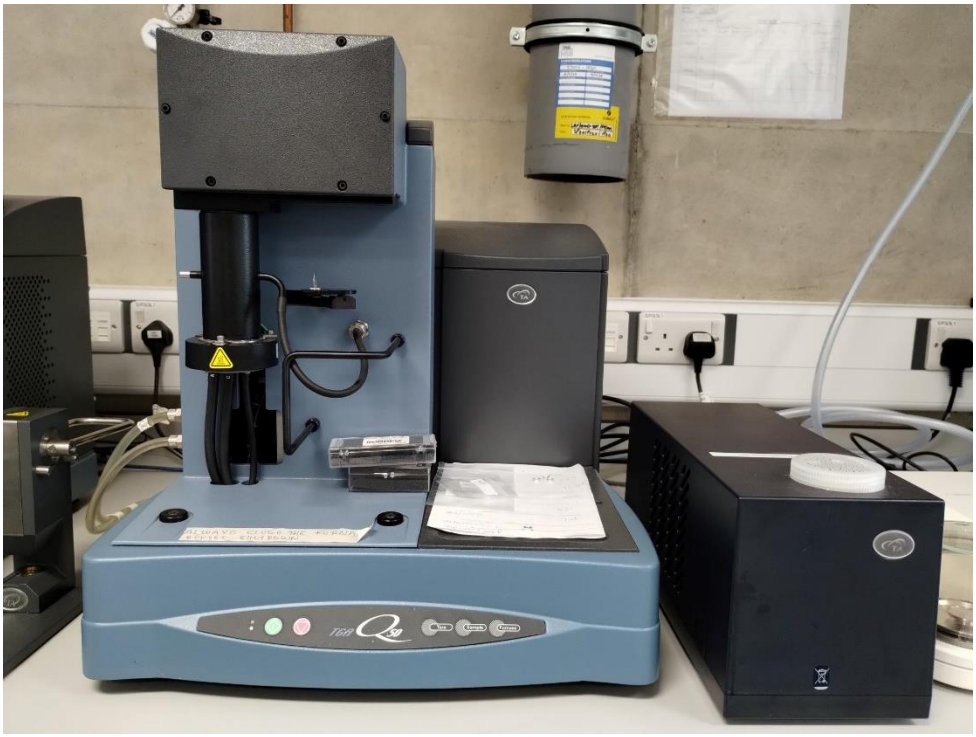

Figure 3.14 Thermogravimetric analysis (TGA) instrument.

3.5.5 Thermal conductivity

A Hot Disk Thermal Constant Analyzer (TPS-2500S) was employed to determine the thermal conductivity of the PCM and nano-PCM samples. The technique is standardised in ISO 22007-2. Figure 3.15 depicts the thermal conductivity setup with the sample holder's design, which includes six channels at the bottom for effective heat transmission. A new aluminium sample holder as shown in Figure 3.16 was fabricated and placed inside the heat immersion circulator to evaluate thermal conductivity at different temperatures. Since the manufacturer's testing holder is confined to room temperature measurements, this sample holder was developed according to the TPS 2500S manufacturer's recommendations to test PCMs at various temperatures other than a room temperature. To raise the temperature of the sample, the Hot Disk sensor 5465 (3.089 mm radius) was used, which consisted of a double spiral thin metal

foil sandwiched between two thin sheets of insulating Teflon material. In addition, hot disk equipment was calibrated with the stainless-steel samples provided by the supplier, and the difference between the obtained experimental results and those provided in the manual was less than 0.5%, which is much less than the instrument measurement error (i.e., ± 5%). Each sample reading was repeated three times to ensure measurement accuracy and reliability.

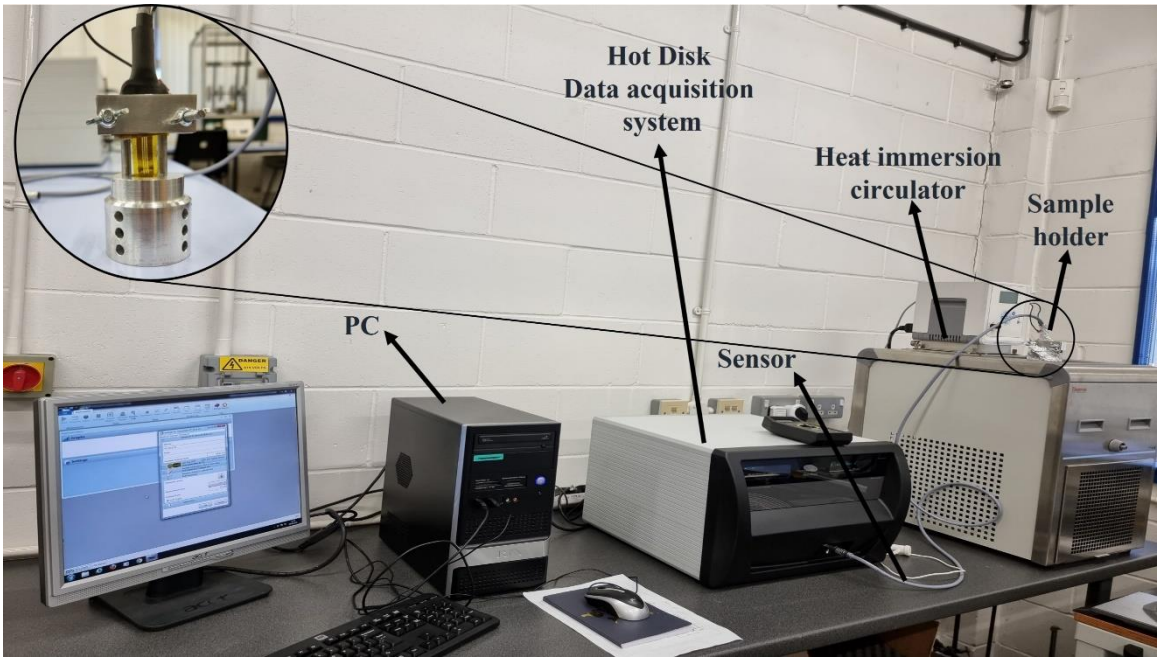

Figure 3.15 Thermal conductivity testing setup with sample holder.

Figure 3.16 Sample holder in thermal bath.

3.5.6 Transmission electron microscopy

Transmission electron microscopy (TEM) was used to examine the surface structures of nanoparticles used in this study (i.e. titanium dioxide (TiO_2), multi-walled carbon nanotubes (MWCNTs), graphene nanoplatelets (GNPs), and chemically functionalized MWCNTs) using a JEOL JEM-1400F operating at an accelerating voltage of 120 kV. For sample preparation, isopropyl alcohol was added to 0.2g of nanoparticles in a test tube to form a suspension. This suspension was subjected to ultrasonication for one minute at a frequency of 20 kHz. A drop of this dispersed sample was mounted on a holey carbon film on 300 mesh copper grids (from Agar scientific) using a micro pipette. The grid was allowed to dry at a drying chamber at 27 °C for three hours allowing the isopropyl alcohol to evaporate completely. Following this, the grids were placed in the TEM chamber for an analysis.

3.6 Summary

This chapter highlights the importance of the materials used, describes the experimental methods employed including sample preparation and discusses how the results pertain to the study's objectives. The two-step synthesis method was employed, involving the dispersion of nanofillers in the PCM followed by sonication to ensure uniform distribution. Characterisation techniques used include FTIR, XRD, DSC, TGA, and thermal conductivity measurement to analyse the thermal, chemical and structural properties of the Nano-PCMs. Essentially, this chapter lays the groundwork for the following sections, in which the specific experiments conducted and their outcomes in depth will be explored. The content herein offers the necessary background for the comprehensive analysis that ensues.

CHAPTER 4: THERMOPHYSICAL CHARACTERISATION OF SINGLE AND HYBRID NANO-PHASE TRANSITION MATERIALS

This chapter reports the main results from a thorough investigation of an organic PCM incorporated with carbon and metal oxide-based single and hybrid nanofillers (GNP, MWCNTs, TiO_2, GNP+MWCNTs, GNP+TiO_2 and MWCNTs+TiO_2) at five different concentrations (0.2 wt.%, 0.4 wt.%, 0.6 wt.%, 0.8 and 1.0 wt.%) to determine the influence of nanoparticles on the thermophysical properties of nano-PCMs. Thermal conductivity, FT-IR, XRD, DSC, and TGA are characterisation methods that have been utilised to look into the characteristics of nano-enhanced phase change materials, and some interesting outcomes are reported. The results reported in this chapter, exploring the characterisation of single and hybrid nano-phase change materials, have been published by author in a scholarly article in 2023 [231].

4.1 Microstructure characterisation of nano particles with TEM

Transmission electron microscopy (TEM) was used to examine the surface structures of TiO_2, GNP and MWCNTs nanoparticles, as shown in Figure 4.1. The analysis revealed distinctive morphological characteristics for each nanoparticle type. The MWCNTs exhibit a one-dimensional tubular structure with diameters ranging from 6 to 10 nm, reflecting their elongated and narrow form. GNPs display a two-dimensional planar configuration with lateral dimensions typically between 800 and 1200 nm, highlighting their broad, flat profiles. Lastly, the TiO_2 nanoparticles were characterised by a well-defined cubic nanocrystalline structure with particle sizes from 20 to 22 nm, indicating their compact and symmetrical geometry. These dimensions underscore the unique structural attributes of each type of nanoparticles, which contribute to their distinct physical and chemical behaviours when these particles are integrated into composite materials.

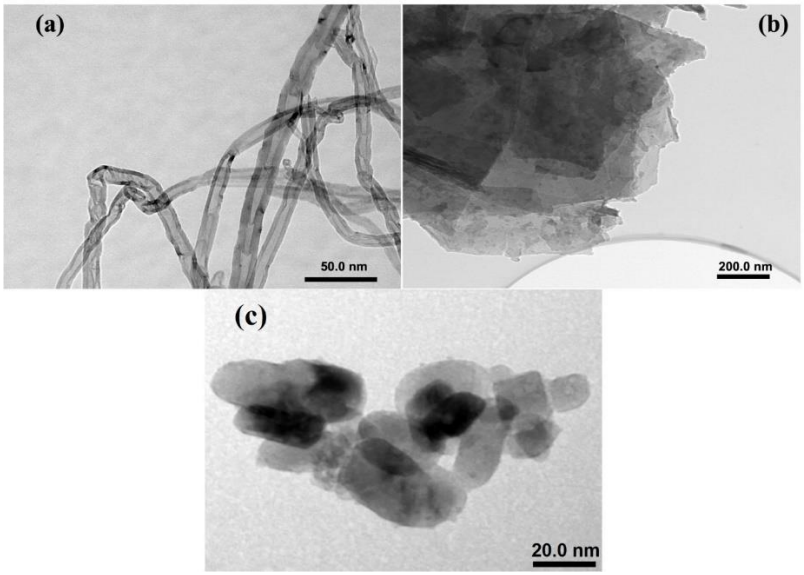

Figure 4.1 Typical TEM images of (a) MWCNTs, (b) GNP, and (c) TiO_2.

4.2 Analysis of FT-IR spectra

FT-IR spectroscopy was used to investigate the chemical interactions and functional groups of base PCM, nanofillers, and composite PCMs impregnated with mono and hybrid nanofillers. For mono and hybrid nano-PCMs, samples with 1 wt.% of nanoparticles were used to observe chemical interactions between the PCM and nanomaterials. FT-IR spectrum transmittance bands of GNP, MWCNTs, TiO_2, pure paraffin, PAR+GNP, PAR +MWCNTs, PAR +TiO_2, PAR/GNP+MWCNTs, PAR/GNP+TiO_2, PAR/MWCNTs+TiO_2 between the wavenumbers of 600 and 4000 cm^{-1} are shown in Figure 4.2. No major stretching or bending peaks from MWCNTs and GNPs were observed in their infrared spectra since they lacked functional groups. The TiO_2 stretching vibrations are associated with the peaks at 635 and 643 cm^{-1}. Three transmittance peaks at 2945, 2905, and 2842 in the pristine paraffin spectrum showed moderate anti-symmetrical stretching vibrations of the -CH_3 and -CH_2- groups. In paraffin, the peak at 1490 indicated moderate C-H scissoring of the alkane (-CH2- and -CH3) groups. The modest rocking vibration of C-H in the long-chain methyl group can be seen in the peak at 750. Similar patterns of FT-IR spectra for nano-PCMs have been reported in different studies [232,233]. The FT-IR spectra of PAR+GNP, PAR+MWCNTs, PAR+TiO_2, PAR/GNP+MWCNTs, PAR/GNP+TiO_2, and PAR/MWCNTs+TiO_2 showed no substantial new peaks or significant peak shifts in the nano-PCMs, confirming that paraffin, GNP, MWCNTs, and SDBS only have physical interactions between them, and it is suggested that there is no chemical interaction between the PCM and nanoparticles.

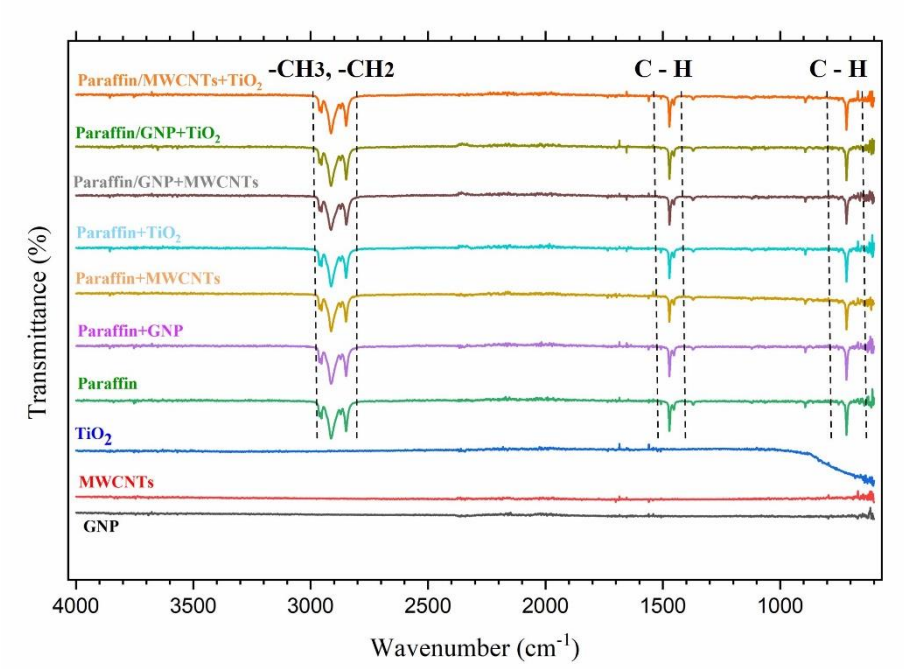

Figure 4.2 FT-IR spectra of different samples.

4.3 XRD analysis

The crystallinity and unit cell dimensions of nanoparticles, paraffin, and paraffin embedded with single and hybrid particles were investigated utilising XRD. The XRD peaks obtained for the MWCNTs, GNP, TiO_2, paraffin, PAR/MWCNTs, PAR/GNP, PAR/TiO_2, PAR/MWCNTs+GNP, PAR/MWCNTs+TiO_2, and PAR/GNP+TiO_2 are shown in Figure 4.3. For both the mono and hybrid nano-PCMs, the samples with 1.0 wt.% of nanoparticles were used to see the crystal planes of the nano-PCMs. The diffraction peaks at 24.34° (002) and 41.12° (100) with PDF No. 00-058-1638 [142] indicate the presence of MWCNTs [234]. The primary peaks in the XRD curve of GNP at 26.32°,43.30° and 54.48° may belong to the (002), (100) and (004) crystal planes of carbon from the GNP, correspondingly. The TiO_2 nanoparticle peaks at 2θ = 25°, 37.4°, 47.3°, and 53.8° correspond to the (101), (004), (200), respectively, and (105) lattice planes, confirming the anatase form of TiO_2 nanofillers with PDF No. 03-065-5714. The XRD sharp spectrum peaks of paraffin were obtained at 7.92°, 11.7°, 15.5°, 19.4°, 19.8°, 22.19°, 23.4°, 24.64°, 27.1°, 31.0°, 34.08°, 39.4°, and 44.3° with Miller indices (002), (003), (004), (010), (011), (401), (102), (111), (007), (008), (009), (122), and (0010), assigned to the crystal structure of n-octadecane identified in the crystallography open database. As the presence of nanofillers in a PCM is a small amount, fewer physical changes were observed, as shown in Figure 4.4. Because of the anatase crystal structure of TiO_2, the paraffin+TiO_2 composite has shown sharp intensities compared with the other nano-enhanced PCMs. Despite

the high intensity of the paraffin+TiO_2 composite, no new peaks were identified, indicating that the pristine paraffin crystal structure was not altered by the addition of TiO_2 nanofillers. Hence, it is suggested that the paraffin crystal structure has not been changed, and the single and hybrid nano-PCMs hold the MWCNTs, GNP and TiO_2 peaks.

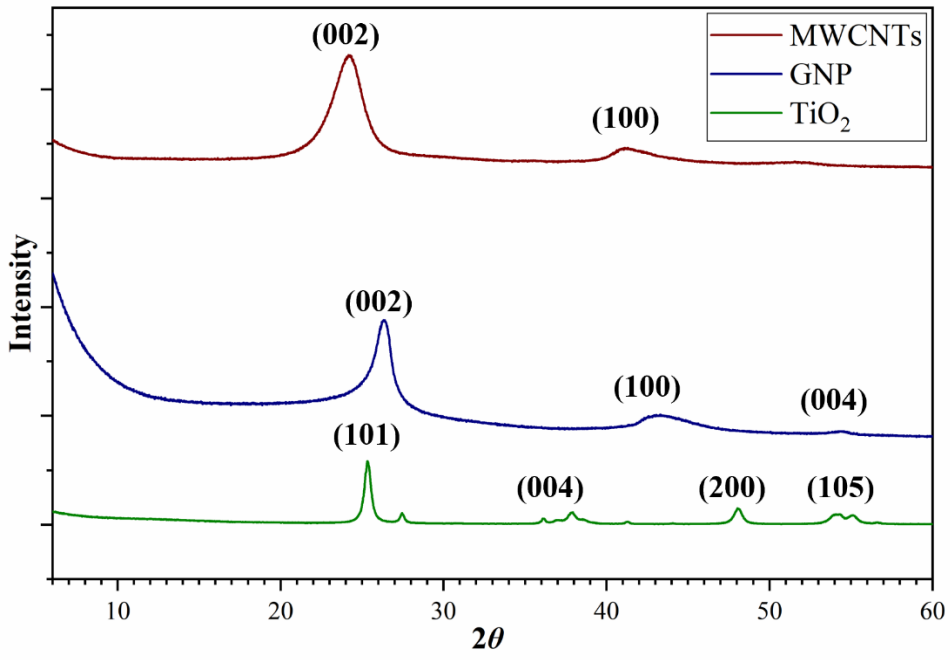

Figure 4.3 XRD patterns of nanoparticles.

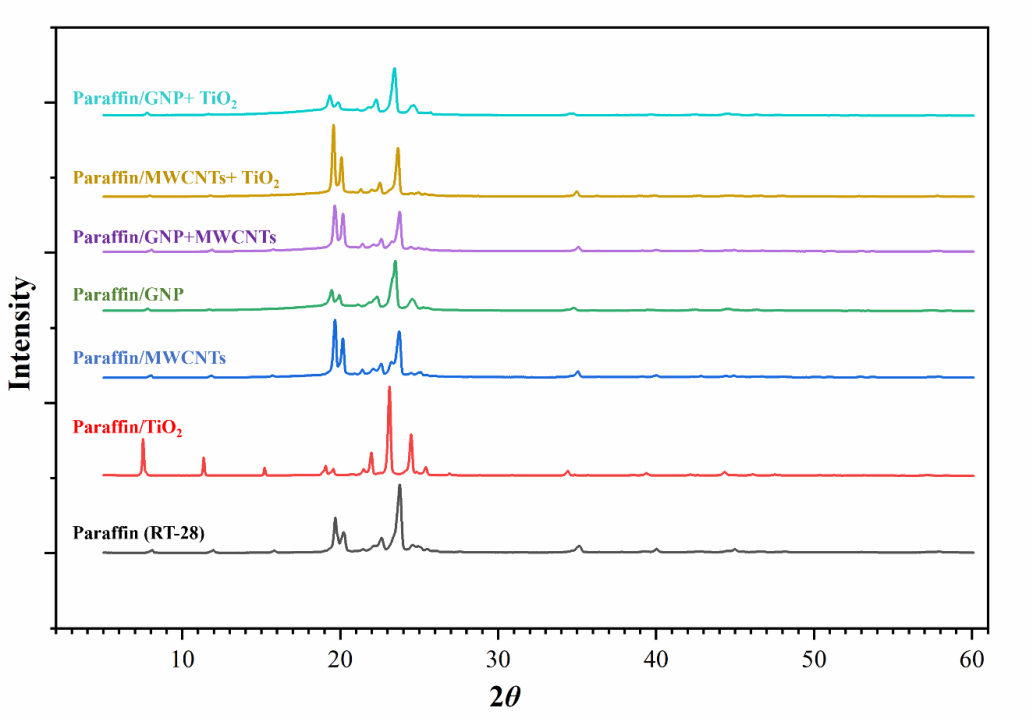

Figure 4.4 XRD patterns of distinct single and hybrid nano-PCMs.

4.4 Phase-transition properties

Phase transition temperature and enthalpies of the pristine PCM and nano-PCMs with single and hybrid nanofillers during melting and solidification were examined using DSC. Figures 4.5 (a - c) depict the melting and crystallisation processes of single type nanoparticles based PCM and Figures 4.6 (a – c) show typical DSC curves of hybrid nanomaterial based PCMs at five different concentrations. The values of phase transition temperatures, enthalpies, and supercooling degrees for both mono and hybrid nano-enhanced PCMs are listed in Tables 4.1 and 4.2, respectively. It can be seen that the incorporation of single and hybrid nanomaterials results in a very minor effect on the melting and solidification temperatures of the PCM. Similarly, a slight reduction in latent heat was observed with the inclusion of nano additives. During melting, a single endothermic peak is noticed for both pure paraffin and composites, which indicates isomorphous crystalline structures of both pure paraffin and paraffin composites [235]. On the other hand, two exothermic peaks were identified in all samples during the solidification process. This bimodal crystallisation phenomenon refers to the metastable rotator phase that occurs before final crystallisation because of heterogeneous nucleation [236,237].

Supercooling occurs when a PCM remains in its liquid state at a temperature below its solidification point. In the realm of thermal energy storage systems, the phenomenon of entering a supercooled state is often regarded as a drawback as it hinders the release of latent heat [238]. The supercooling degrees (ΔT) of single and hybrid nano-enhanced PCMs are reported in Tables 4.1 and 4.2, respectively. It can be seen that the degree of supercooling of the PCM was reduced after the incorporation of nanofillers. However, slight variations in TiO_2 based nano-PCMs are observed with a maximum increase of 42% in ΔT, which are attributed to the crystallisation confinement of titanium dioxide particles within the paraffin [232]. Overall, the decrease in ΔT demonstrates the increased importance of nanoparticles as nucleating agents in terms of effective homogenous nucleation and surface adsorption.

As shown in Tables 4.1-4.2, the latent heat of melting (ΔHm) and solidification (ΔHs) for the pristine paraffin were found to be 248.4 J/g and 251.7 J/g, correspondingly. It was observed that with an increase in the concentration of nanoparticles, the latent heat slightly decreased and the maximum reductions of -3.7%, -6.8%, -6.4%, -5.07%, -5.5%, and -5.2% and -4.12%, -7.31%, -7.2%, -6.9%, -6.4%, and -5.9% were seen at the highest concentration (i.e., 1.0 wt.% of nanomaterials) for PAR+TiO_2, PAR+MWCNTS, PAR+GNP, PAR/MWCNTs+GNP,

PAR/MWCNTs+TiO_2 and PAR/GNP+TiO_2 during melting and solidification, respectively. Such a reduction in latent heat could be due to the non-melting enthalpies of the nanofillers. In addition, single and hybrid titanium oxide particle based PCMs showed a smaller reduction in the latent heat of melting and crystallisation compared to carbon-based nano-PCMs. It has been reported [225] that the incorporation of TiO_2 nanofillers into the PCMs gives a negligible reduction in the latent heat. In some studies, an increase in the enthalpies was observed with the addition of TiO_2 nanomaterials, which could be due to the better stability and interactions between the TiO_2 particles and PCM molecules [225,239]. Conversely, the high thermal conductive carbon-based particles (i.e., MWCNTs, and GNP) have stability issues and due to their high thermal conductivities, as they accelerate the evaporation of paraffin, which affects the heat storage capability [8,32]. The theoretical value of the latent heat was also determined for all composites using equation 4.1 [240].

$$\Delta \boldsymbol{H_{nanoPCM}} = \Delta \boldsymbol{H_{PCM}}(\mathbf{1} - \boldsymbol{wt}.\%) \tag{4.1}$$

where $\Delta H_{nanoPCM}$ signified the latent heat of nano-enhanced PCMs, ΔH_{PCM} signifies the latent heat of pristine paraffin, $wt.\%$ corresponds to the mass percentage of nanomaterials.

It is evident that the calculated latent heat of each PCM composite is greater than the latent heat measured in the laboratory with DSC. This could be due to the dispersion stability, surface morphology, and structure of the nanomaterials in the base PCM [241]. Overall, for all the PCM composites, no significant reduction in latent heat was observed; therefore, they may be used for thermal storage applications. Especially, TiO_2 based novel hybrid particle (MWCNTs+TiO_2 and GNP+TiO_2) based PCMs have the potential to be employed in buildings as energy storage materials since they have better stability, are economical, and have minimum effect on phase change enthalpies compared to carbon-based single and hybrid nanocomposites.

Figure 4.7 shows how the specific heat capacity (the amount of heat needed to raise the temperature of a substance by a certain amount) of paraffin and nano-PCMs changes as the temperature increases from 10 °C to 55 °C in both solid and liquid states. The specific heat capacity has a relatively minimal effect on the overall amount of thermal energy that can be stored using these materials because of the low thermal energy density in the sensible heat storage phase. However, the specific heat capacity still affects other factors that affect the total amount of heat that can be stored within a certain temperature range by using these materials [235].

As shown in Figure 4.7(a), the specific heat capacity of the nano-PCMs increased gradually as the temperature increased from 10 °C to 25 °C in the solid phase. In contrast, the specific heat capacity remained constant in the liquid phase, as shown in Figure 4.7(b). The results of the specific heat capacity analysis for both phases demonstrated concurrence with prior research findings[242–244]. The specific heat capacity of paraffin was 1.928 J/g °C in the solid phase and 1.887 J/g °C in the liquid phase. It is evident that the addition of nanoparticles to the PCMs increased the specific heat capacity in both the solid and liquid phases. At 25 °C and 55 °C, the specific heat capacities of the nano-PCMs were 4.011 J/g °C and 2.556 J/g °C, respectively.

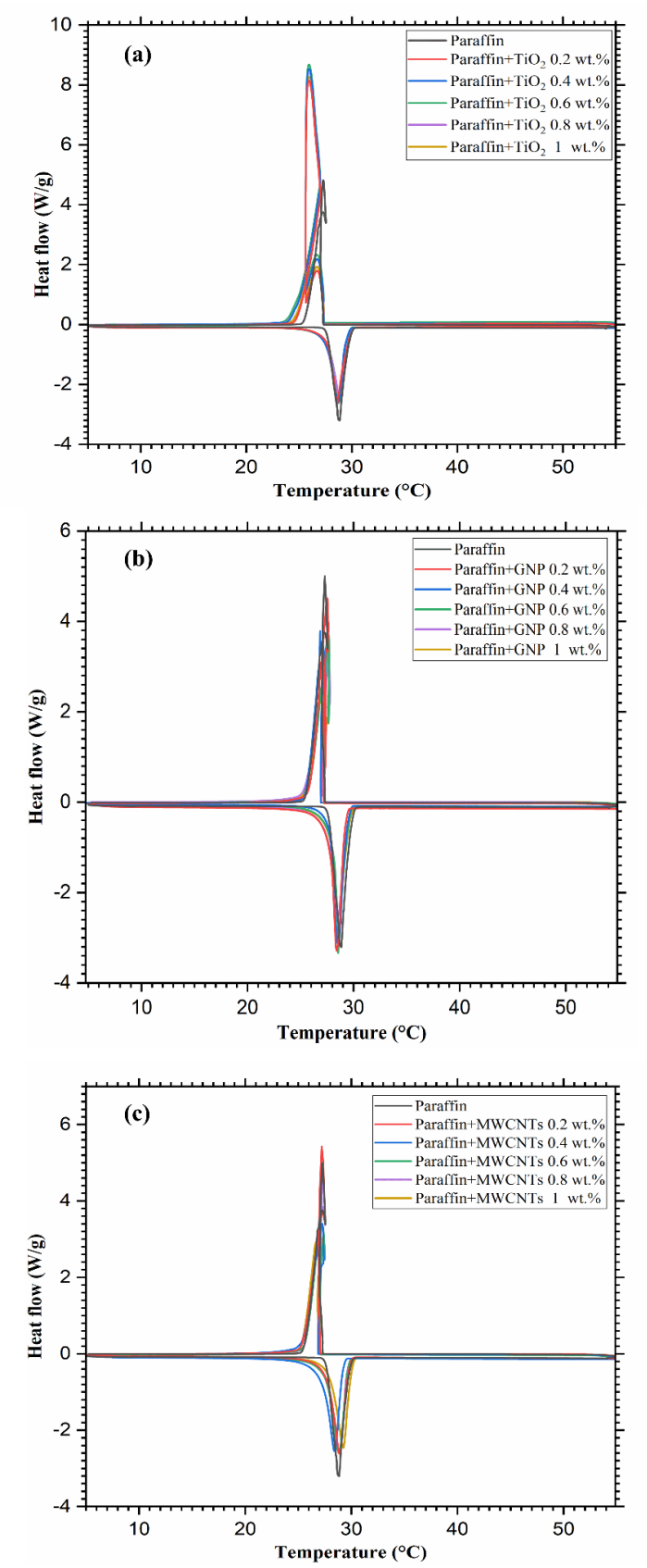

Figure 4.5 DSC curves of pure PCM and single nano-enhanced PCMs (a) PAR+TiO_2, (b) PAR+GNP, (c) PAR+MWCNTs.

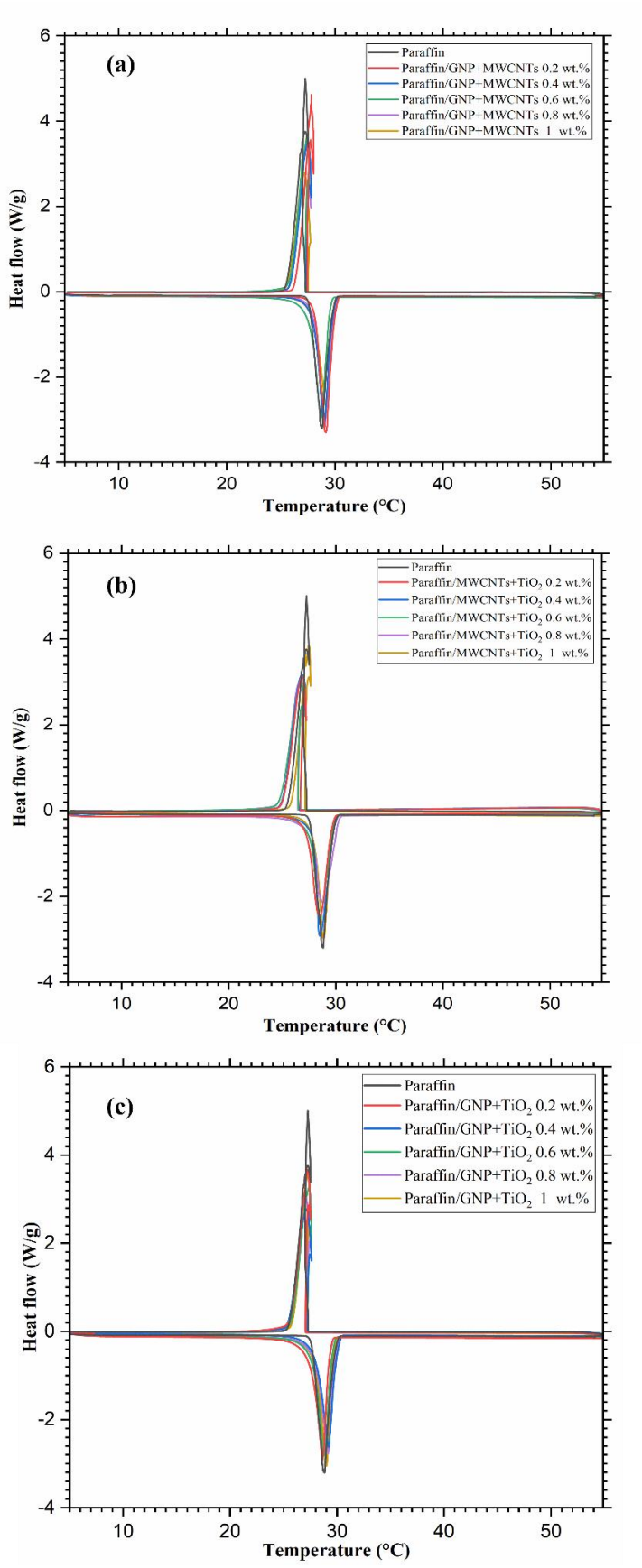

Figure 4.6 DSC curves of pure PCM and hybrid nano-enhanced PCMs (a) PAR/MWCNTs+GNP, (b) PAR/MWCNTs+TiO_2, and (c) PAR/GNP+TiO_2.

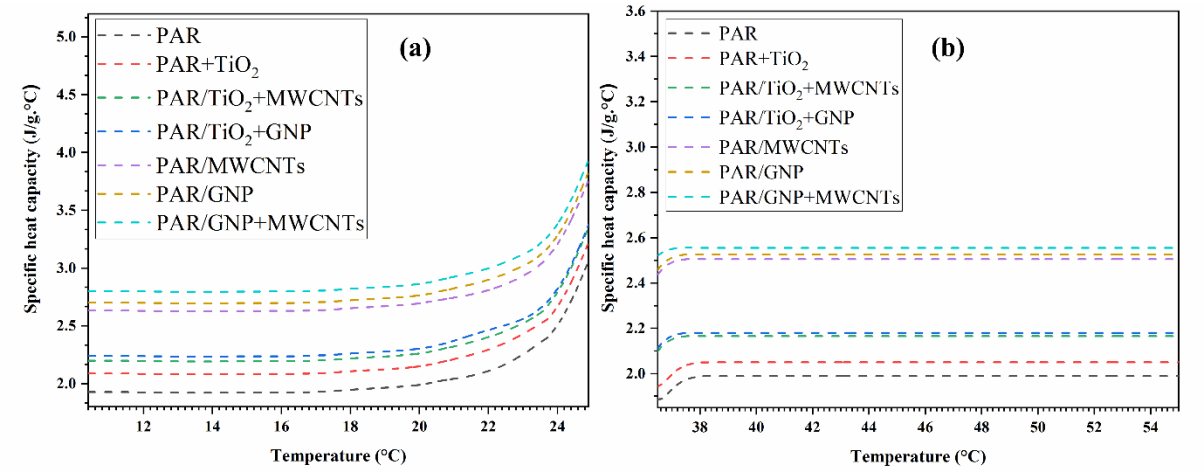

Figure 4.7 Specific heat capacity of paraffin and nano-PCMs versus temperature (a) in a solid phase and (b) in a liquid phase.

4.5 Thermal reliability

The thermal stability of PCM and PCM composites was examined using TGA and DTG (derivative thermogravimetric analysis). The TGA curves of the pristine and nano-PCMs are displayed in Figures 4.8 (a – f). It can be seen from the TGA peaks that there is no discernable mass loss up to ~130 °C for either paraffin or its composites. As the temperature increased, the weight loss became more pronounced, reaching its maximum degradation temperature while leaving a constant residue behind. For pure paraffin, the maximum degradation temperature observed was 211.34 °C with 0.8272% residue. The evaporation of paraffin causes such decomposition, wherein hydrocarbon chains disintegrate into monomers. Furthermore, it was discovered that with the inclusion of nanoparticles, the maximum degradation temperature increased because highly thermally conductive nanoparticles improved the thermal conductivity of the nano-PCMs, which resulted in faster and more uniform heat transfer. With an increase in the weight percentage of nanoparticles, the final, residual, initial, and onset temperatures increased. Basically, the nanomaterials form a shielding layer on the surface of paraffin which impedes vaporisation during thermal deprivation. The DTG peaks of the samples shown in Figures 4.9 (a – f) demonstrate that all the mono and hybrid nano-PCMs have similar thermal decompositions. As no weight loss was observed until ~130 °C for all samples, therefore the developed nano-PCMs have the potential to be employed in buildings and other thermal energy storage applications.

Table 4.1 Thermal properties of PCM composites with a single type of nanoparticles.

Sample	Melting				Crystallisation				
	T_{peak}	ΔHm_{exp}	ΔHm_{cal}	Relative error %	T_{peak}	ΔHm_{exp}	ΔHm_{cal}	Relative error %	ΔT
Paraffin (PAR)	28.92	248.4			27.26	251.7			1.66
PAR+TiO_2 0.2 wt.%	28.67	247.1	247.90	0.32	26.46	249.3	251.19	0.75	2.21
PAR+TiO_2 0.4 wt.%	28.68	246.7	247.40	0.28	26.32	247.2	250.69	1.39	2.36
PAR+TiO_2 0.6 wt.%	28.79	244.1	246.90	1.13	26.54	246.02	250.18	1.66	2.25
PAR+TiO_2 0.8 wt.%	28.84	243.8	246.41	1.06	26.86	244.73	249.68	1.98	1.98
PAR+TiO_2 1 wt.%	28.83	239.2	245.4	2.52	26.67	241.32	249.18	3.15	2.16
PAR+MWCNTS 0.2 wt.%	28.88	244.1	247.90	1.53	27.2	246.2	251.19	1.98	1.68
PAR+MWCNTS 0.4 wt.%	28.4	239.7	247.40	3.11	27.24	241.1	250.69	3.82	1.16
PAR+MWCNTS 0.6 wt.%	28.78	237.2	246.90	3.93	27.23	239.4	250.18	4.31	1.55
PAR+MWCNTS 0.8 wt.%	28.8	235.5	246.41	4.42	27.08	236.7	249.68	5.20	1.72
PAR+MWCNTS 1 wt.%	28.96	231.3	245.4	5.74	27.35	233.3	249.18	6.37	1.61
PAR+GNP 0.2 wt.%	28.37	244.7	247.90	1.29	27.52	246.8	251.19	1.75	0.85
PAR+GNP 0.4 wt.%	28.91	240.3	247.40	2.87	27.29	243.5	250.69	2.86	1.62
PAR+GNP 0.6 wt.%	28.53	238.2	246.90	3.52	27.6	240.2	250.18	3.99	0.93
PAR+GNP 0.8 wt.%	28.43	236.7	246.41	3.94	27.64	238.6	249.68	4.03	0.79
PAR+GNP 1 wt.%	28.59	232.4	245.4	5.29	27.67	233.5	249.18	4.96	0.92

T_{peak}: peak temperature (°C), **ΔHm_{exp}**: latent heat of melting experimental (J/g), **ΔHm_{cal}**: latent–heat of melting calculated (J/g), **RE**: relative error, **ΔT**: super–cooling degree (°C).

Table 4.2 Thermal properties of PCMs composites with hybrid types of nanoparticles.

Sample	Melting				Crystallisation				
	T_{peak}	ΔHm_{exp}	ΔHm_{cal}	Relative error %	T_{peak}	ΔHm_{exp}	ΔHm_{cal}	Relative error %	ΔT
Paraffin (PAR)	28.92	248.4			27.26	251.7			1.66
PAR/MWCNTs+GNP 0.2 wt.%	28.95	242.8	247.90	2.05	27.82	245.1	251.19	2.42	1.13
PAR/MWCNTs+GNP 0.4 wt.%	28.89	239.6	247.40	3.15	27.41	241.5	250.69	3.66	1.48
PAR/MWCNTs+GNP 0.6 wt.%	28.71	237.76	246.90	3.70	27.46	239.3	250.18	4.35	1.25
PAR/MWCNTs+GNP 0.8 wt.%	28.94	235.8	246.41	4.30	27.42	236.2	249.68	5.40	1.52
PAR/MWCNTs+GNP 1 wt.%	28.96	230.9	245.4	5.90	27.19	234.1	249.18	6.05	1.77
PAR/MWCNTs+TiO_2 0.2 wt.%	28.49	245.7	247.90	0.88	26.84	247.5	251.19	1.47	1.65
PAR/MWCNTs+TiO_2 0.4 wt.%	28.5	243.3	247.40	1.65	26.85	245.7	250.69	1.99	1.65
PAR/MWCNTs+TiO_2 0.6 wt.%	28.53	239.5	246.90	3.00	26.72	241.8	250.18	3.35	1.81
PAR/MWCNTs+TiO_2 0.8 wt.%	28.78	236.5	246.41	4.02	26.69	239.7	249.68	3.99	2.09
PAR/MWCNTs+TiO_2 1 wt.%	28.86	234.6	245.4	4.40	27.48	235.5	249.18	5.49	1.38
PAR/GNP+TiO_2 0.2 wt.%	28.62	246.5	247.90	0.56	27.26	248.1	251.19	1.23	1.36
PAR/GNP+TiO_2 0.4 wt.%	28.98	243.8	247.40	1.45	27.16	246.3	250.69	1.75	1.82
PAR/GNP+TiO_2 0.6 wt.%	28.78	240.2	246.90	2.71	27.36	241.9	250.18	3.31	1.42
PAR/GNP+TiO_2 0.8 wt.%	28.93	237.1	246.41	3.77	27.09	240.2	249.68	3.79	1.84
PAR/GNP+TiO_2 1 wt.%	28.88	235.4	245.4	4.07	27.2	236.8	249.183	4.68	1.68

T_{peak}: peak temperature (°C), **ΔHm_{exp}**: latent heat of melting experimental (J/g), **ΔHm_{cal}**: latent–heat of melting calculated (J/g), **RE**: relative error, **ΔT**: super–cooling degree (°C).

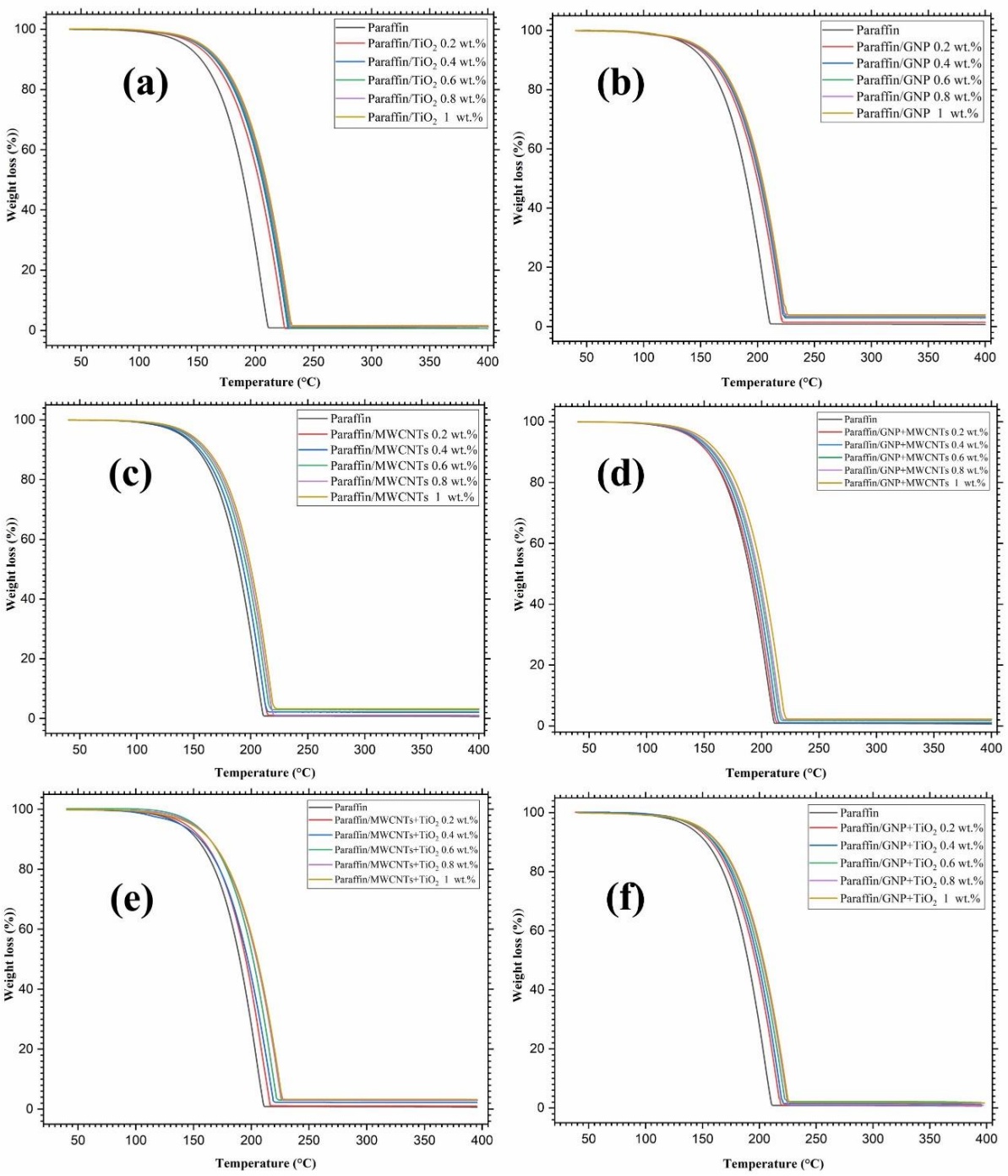

Figure 4.8 TGA curves of single and hybrid nano enhanced PCMs (a) PAR+TiO_2, (b) PAR+GNP, (c) PAR+MWCNTs, (d) PAR/MWCNTs+GNP, (e) PAR/MWCNTs+TiO_2, and (f) PAR/GNP+TiO_2.

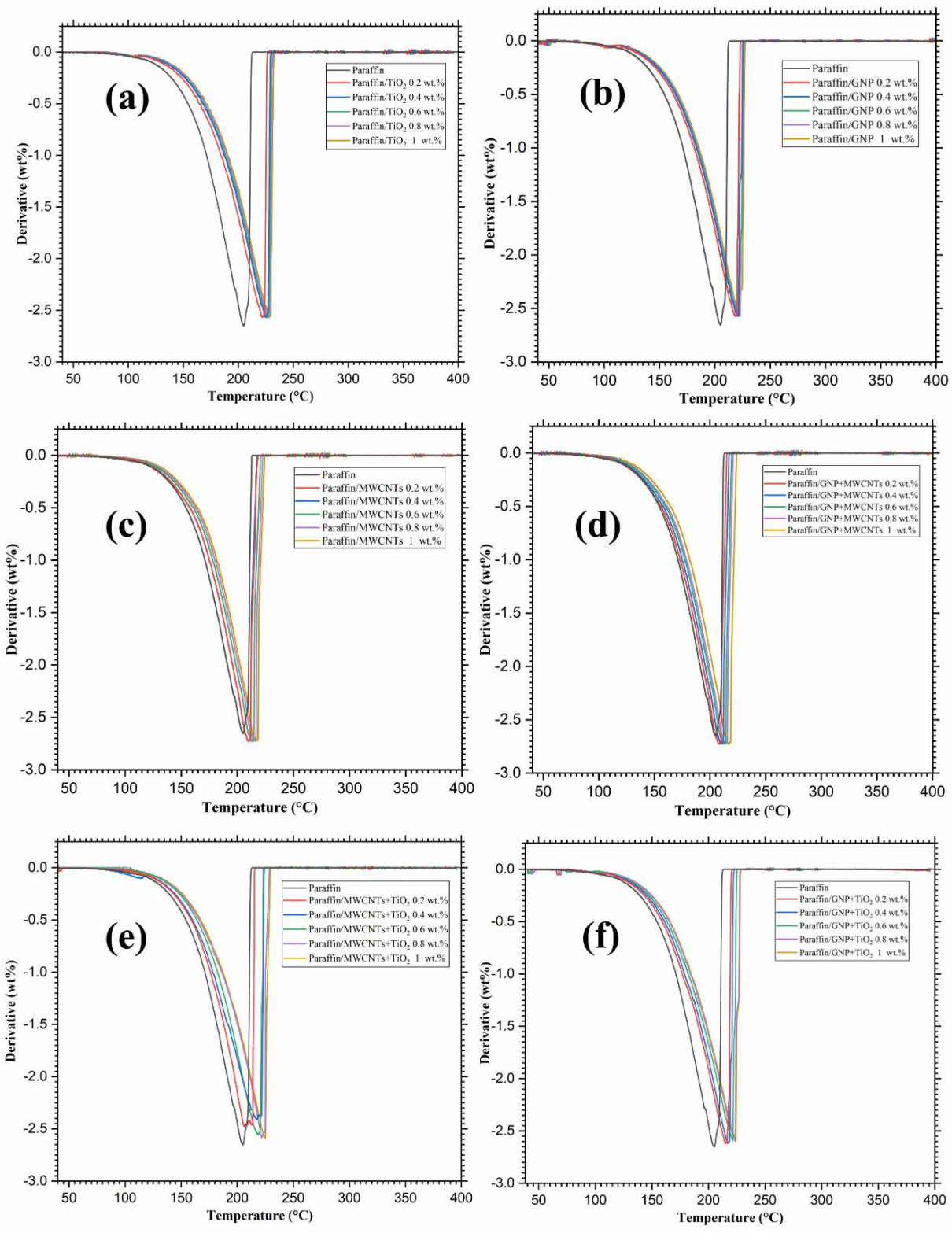

Figure 4.9 DTG curves of single and hybrid nano enhanced PCMs (a) PAR+TiO_2, (b) PAR+GNP, (c) PAR+MWCNTs, (d) PAR/MWCNTs+GNP, (e) PAR/MWCNTs+TiO_2, and (f) PAR/GNP+TiO_2.

4.6 Nanoparticles dispersion stability

Images of the freshly prepared samples and the samples left in a hot water bath at 60 °C for 48 hours are shown in Figures 4.10 (a – d). Apart from the single MWCNT nanoparticles based PCM a uniform dispersion after 48 hours of sonication of mono and hybrid nano-PCMs was observed. As shown in Figure 4.10(b), MWCNTs settled down after 48 hours when they were incorporated in the PCM, since the hydrophobic nature of MWCNTs prevents them from dispersing uniformly in the PCM. MWCNTs-based hybrid composites, on the other hand, demonstrated a uniform dispersion after 48 hours due to the small amount (i.e., 30%) of MWCNTs used in the hybrid composites and their good interactions with TiO_2 and GNP particles.

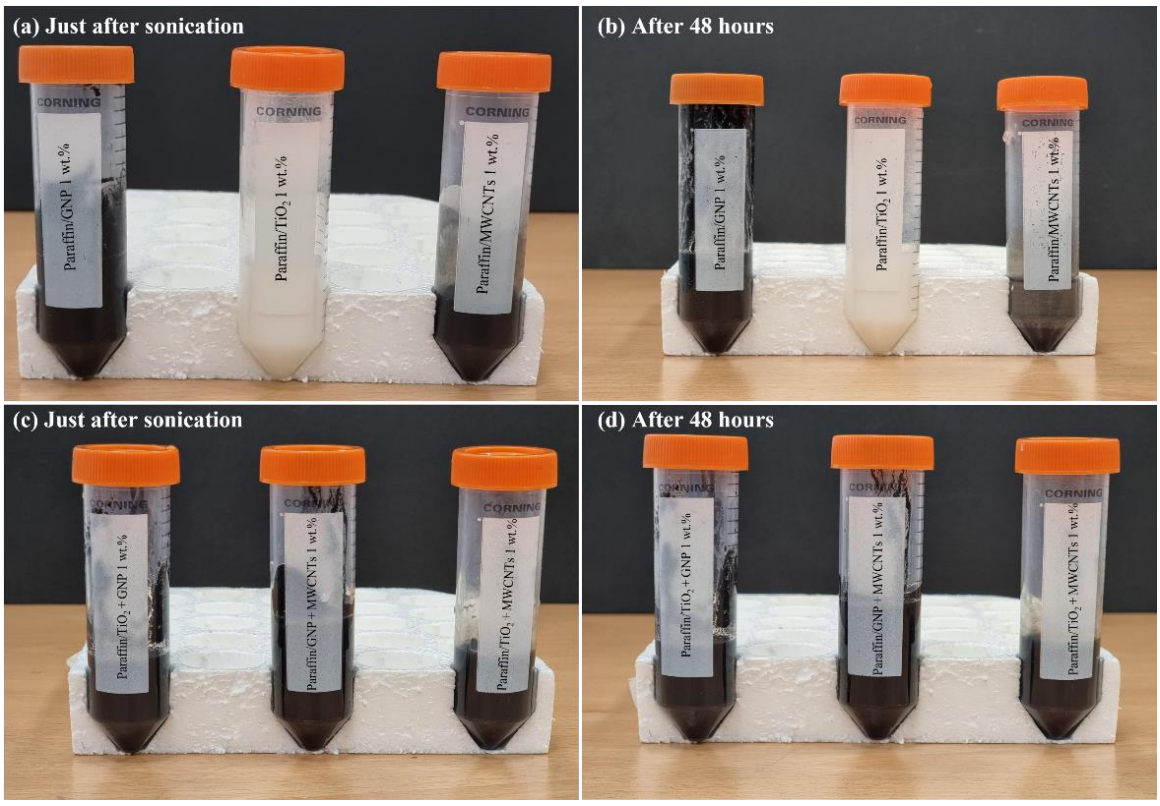

Figure 4.10 Status of samples with a time duration,

(a) Single type particles-based nanocomposites just after sonication, (b) single type particles-based nanocomposites after 48 hours (c) hybrid type particles-based nanocomposites just after sonication, (d) hybrid particles-based nanocomposites after 48 hours.

4.7 Thermal conductivity

The major purpose of PCMs is to properly capture and discharge thermal energy during melting and solidification. Thermal conductivity determines how fast the thermal energy is stored and released during the melting and crystallisation of the PCM. Pure PCMs have poor thermal conductivity, which limits the rate of heat storage and release and restricts their applications. A PCM with greater thermal conductivity decreases the melting and solidification time and accelerates the heat transfer during these processes [29]. Thermal conductivity of the pure PCM, single, and hybrid PCM samples (PAR+GNP, PAR+MWCNTs, PAR+TiO_2, PAR/GNP+MWCNTs, PAR/GNP+TiO_2, and PAR/MWCNTs+TiO_2) were measured at six different temperatures ranging from 5 °C to 25 °C for solids and 30 °C to 55 °C for liquids, as illustrated in Figures 4.11 (a – f).

As shown in Figure 4.11 (a) and (b), at 5 °C and 15 °C, nano-PCMs were solid, and as the nanoparticle loading concentration increased, MWCNTs and GNP-based mono and hybrid nanoparticle based PCMs demonstrated higher thermal conductivity than TiO_2 and TiO_2-based hybrid particle based PCMs. It can be seen that the mono and hybrid carbon-based nano-PCMs have shown greater enhancement because of the superior thermal conductivities of GNP and MWCNTs nanofillers. Overall, GNP+MWCNTs hybrid nanoparticles-based nano-PCMs showed higher thermal conductivity in comparison to TiO_2+MWCNTs and TiO_2+GNP since they have a higher concentration (70 wt.%) of TiO_2 and lower concentration of GNP and MWCNTs (30 wt.%). Therefore, due to lower thermal conductivity, titanium oxide TiO_2+MWCNTs and TiO_2+GNP type hybrid nano-PCMs have shown lower conductivity but they performed better than mono TiO_2 nanoparticles based PCM.

Similar thermal conductivity trends were observed at 25 °C but a significant increase in the thermal conductivity was detected at 25 °C as can be seen in Figure 4.11 (c). As the melting temperature of the PCM is 28 °C, and near melting temperature nano-PCMs are in a metastable state, the crystalline arrangement of the PCM becomes unstable and a surge in temperature quickens the molecular vibration in the lattice, therefore the thermal conductivity of pristine PCM and nano-PCMs rises abruptly near the melting temperature (i.e., 25 °C) [245]. The thermal conductivities of 0.29, 0.759, 0.719, 0.4, 0.785, 0.51 and

0.484 W/m.k were obtained for paraffin, PAR+GNP, PAR+MWCNTs, PAR+TiO_2, PAR/GNP+MWCNTs, PAR/GNP+TiO_2, and PAR/MWCNTs+TiO_2 at 1 wt.%, respectively.

In the liquid phase at 35°C, 45°C and 55 °C, the thermal conductivity values obtained for mono and hybrid nano-PCMs were below 0.2 W/m.K. Although as in the solid state a constant trend was observed in the liquid state, in that the thermal conductivity decreased significantly as shown in Figures 4.11 (d–f). The cause for exceptionally low TC at 35°C, 45°C, and 55 °C is that at these temperatures, the PCM is completely melted, and the arranged microstructure of the PCM in the solid state has been changed to a disorganised microstructure in the liquid state. In addition, heat is conducted by lattice vibrations in solids as molecules move within their lattice structures. Solids are more effective than liquids in terms of their lattice vibration and free-electron motion. Thus, solid PCMs have a greater thermal conductivity value than those of the liquid PCMs.

The percentage enhancement in the thermal conductivities after the dispersion of nanofillers was also measured at temperatures ranging from 5°C to 55 °C, as shown in Figures 4.12 (a – f). The thermal conductivity enhancement factor was calculated using equation (4.2):

$$\boldsymbol{\eta = \frac{K_{nano-PCM} - K_{PCM}}{K_{PCM}} * 100} \qquad (4.2)$$

where, $K_{nano-PCM}$ and K_{PCM} are the thermal conductivities of nano-enhanced PCMs and pristine PCM, respectively.

As demonstrated in Figures 4.12 (a) and (b), the carbon-based (GNP+MWCNTs) hybrid nanofillers attained higher enhancements in effective thermal conductivities with maximum enhancements of 101.53% and 97.98% observed at 1 wt.% of PAR/GNP+MWCNTs at temperatures of 5 °C and 15 °C, respectively. On the other hand, TiO_2 based nano-PCM depicted the lowest enhancement because of its low thermal conductivity. In addition, with an increase in the percentage concentration of the nanoparticles, the thermal conductivity enhancement increased.

The significant relative enhancement in the thermal conductivity with carbon-based nanoparticles can be seen in Figure 4.12(c). The hybrid nanoparticles showed substantial

improvements of 170%, 75.8%, and 66.89% for GNP/MWCNTs, GNP+ TiO_2, and MWCNTs+TiO_2 at 1 wt.%, respectively. As mentioned earlier, the large improvement of PCM composites in the thermal conductivity at 25 °C is because vibrations within the molecule lattice structures of the PCM and PCM composites increase near the melting temperature (i.e., 28 °C), which results in a sudden increase in thermal conductivity of nano-PCMs.

However, when nano-PCMs were changed to complete liquid form at 35°C, 45°C and 55 °C, the comparative enhancement in thermal conductivity was lower than with solids. As illustrated in Figures 4.12 (d-f), the maximum enhancement in thermal conductivity was no more than 45% for all the PCM composites. As with solids, GNP+MWCNTs based PCM showed maximum enhancement compared to the other nano-PCMs at 35°C, 45°C and 55 °C.

Overall, TC results have shown that with the addition of the particles, the thermal conductivities of single and hybrid nano-PCMs were increased because the employed nanomaterials have greater thermal conductivities in comparison to the base PCM. In addition, higher values of thermal conductivities were observed in the temperature range of 5 °C to 25 °C, when the PCM is in solid form. In contrast, the thermal conductivity values significantly decreased at higher temperatures (35 °C to 55 °C) when the PCM was in liquid form. This shows that the temperature influenced on the thermal conductivity of PCMs. In comparison to the other nano-PCMs, it can be suggested that the GNP+MWCNTs based PCM demonstrated the greatest improvement at all temperatures. This is because carbon-based nano additives are known to have superior physical properties such as hydrogen bonding, capillarity, and surface tension, which enable the adsorption of fresh samples on their pores and surfaces during phase transition without leakage [246].

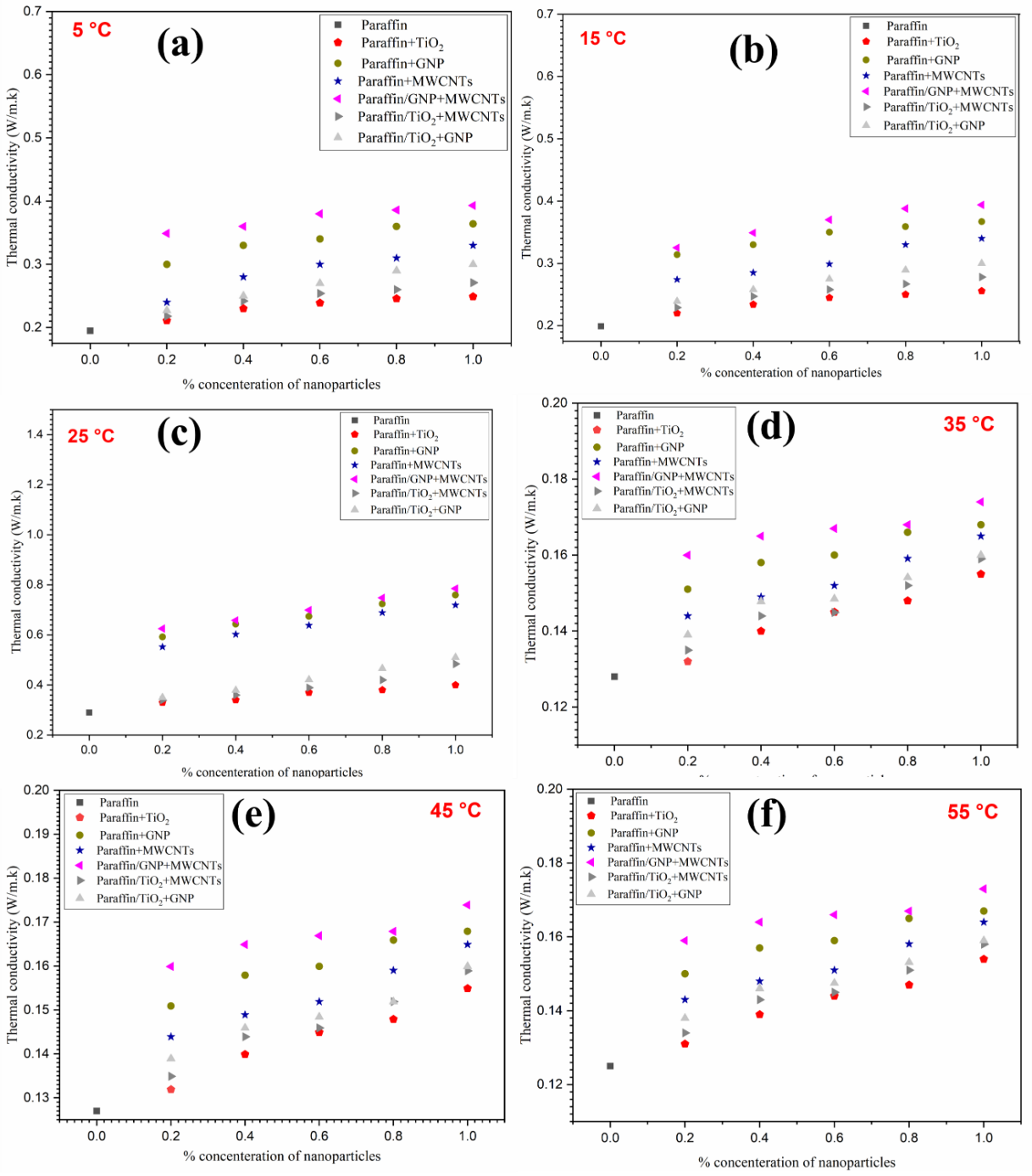

Figure 4.11 Influence of nanofillers concentration on thermal conductivity at various temperatures.

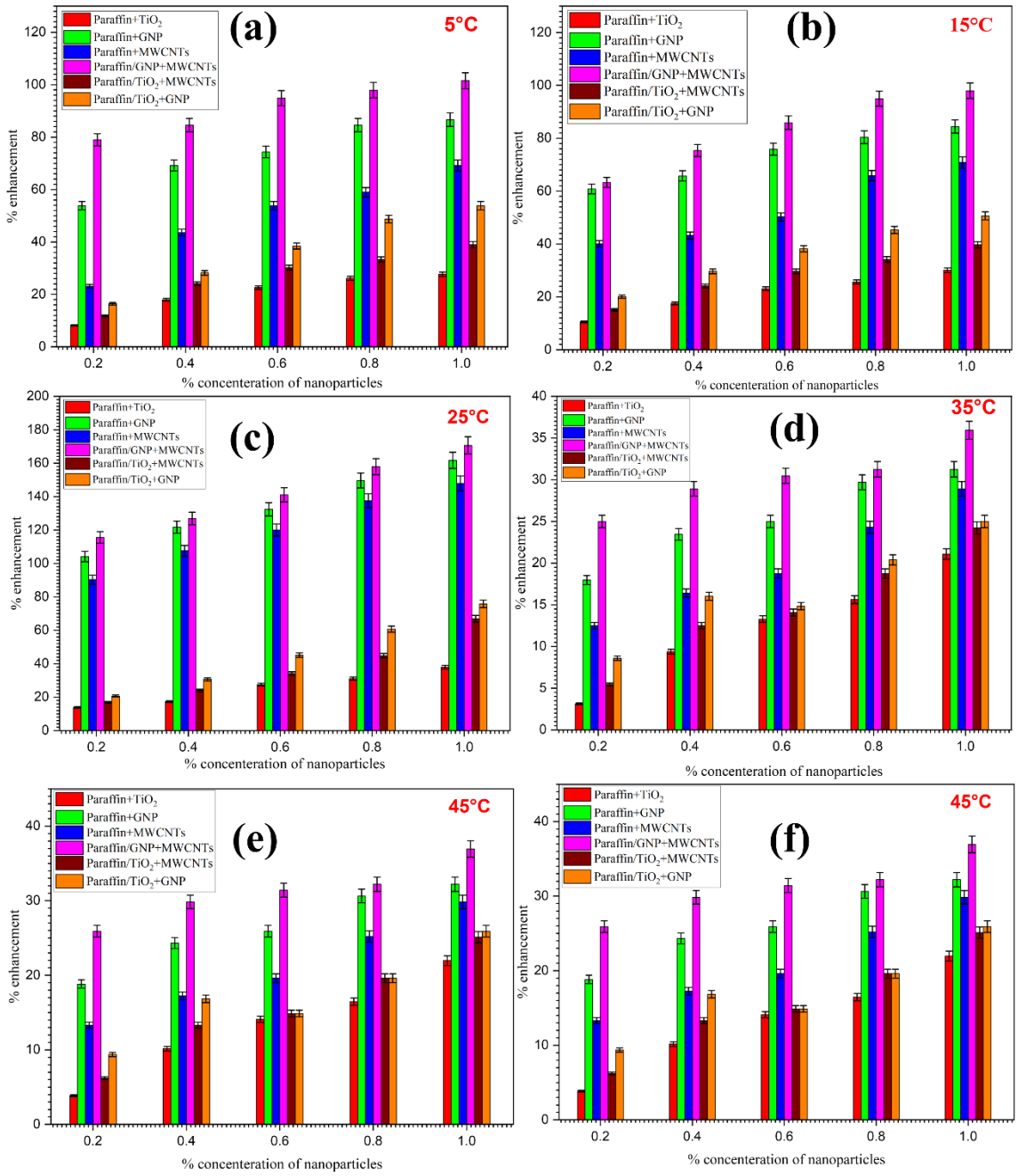

Figure 4.12 Impact of particles concentration on TC enhancement at different temperatures.

4.8 Repeatability and thermal stability

The repeatability of experimental work is critical, especially in the case of nanofluids, such as liquid nano-PCMs. The characteristics repeatability of the nanofluids ensured their stability during a period of time. Therefore, after 48 hours, the thermal conductivity of prepared mono and hybrid nano-PCMs were tested; the results are presented in Figure 4.13. It can be seen that good repeatability has been achieved. As shown in Figure 4.13, a maximum deviation of ± 5% was observed for hybrid nano-PCMs, and ±8 % for single nano-PCMs excluding MWCNTs based nano-PCMs. The thermal conductivity of single type MWCNTs decreased significantly after 48 hours, potentially due to their hydrophobic nature, and the MWCNTs settled down after 48 hours, as shown in Figure 4.13 (a). However, all other single and hybrid nano-PCMs were found to be very stable. The thermal stability of the phase change material (PCM) and the nanoparticle-modified PCMs (nano-PCMs) was also evaluated by subjecting them to 100 heating and cooling cycles. As shown in Figure 4.14, the phase-change properties of the materials were not significantly affected by the thermal cycles since there are no additional secondary curves in the differential scanning calorimetry (DSC) graphs. The variations in the phase change temperatures and enthalpies for the nano-PCMs were less than 1%, indicating a promising level of stability to be employed in an application. The thermal stability above 100 thermal cycles was also tested where two samples of pure paraffin and paraffin enhanced hybrid nanoparticle based PCM (i.e., GNP+MWCNTs), were subjected to 200 cycles of heating and cooling. As shown in Figures 4.14 (h and i), both samples were found to have remained stable after 200 thermal cycles without experiencing any notable changes, demonstrating the high stability of both pure PCM and nano-enhanced PCMs. This suggests their capability to be used in thermal energy storage applications.

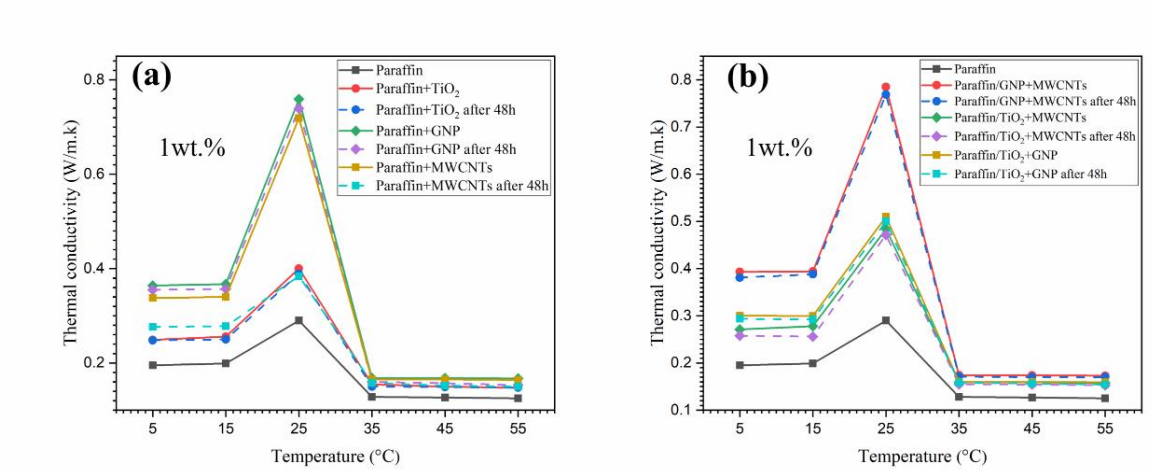

Figure 4.13 Thermal conductivities versus temperature of nano phase PCMs after 48 hours (a) single, and (b) hybrid nano-enhanced phase change materials for thermal conductivity after 48 hours.

To investigate the chemical interactions of the samples after 100 thermal cycles, FTIR analysis was performed. For both the mono-and hybrid nano-PCMs, the samples with 1 wt. % of nanoparticles were used to observe chemical interactions between the PCM and nanomaterials. As shown in Figure 4.15, the FT-IR spectra of the samples treated 100 times (i.e., PAR, PAR+GNP, PAR+MWCNTs, PAR+TiO_2, PAR/GNP+MWCNTs, PAR/GNP+TiO_2, and PAR/MWCNTs+TiO_2) showed no substantial new peaks or significant peak shifts in the nano-PCMs. This is to confirm that paraffin, GNP, TiO_2, MWCNTs, and SDBS have only physical interactions between them, and they do not have any chemical interaction between the PCM and nanoparticles even after 100 thermal cycles.

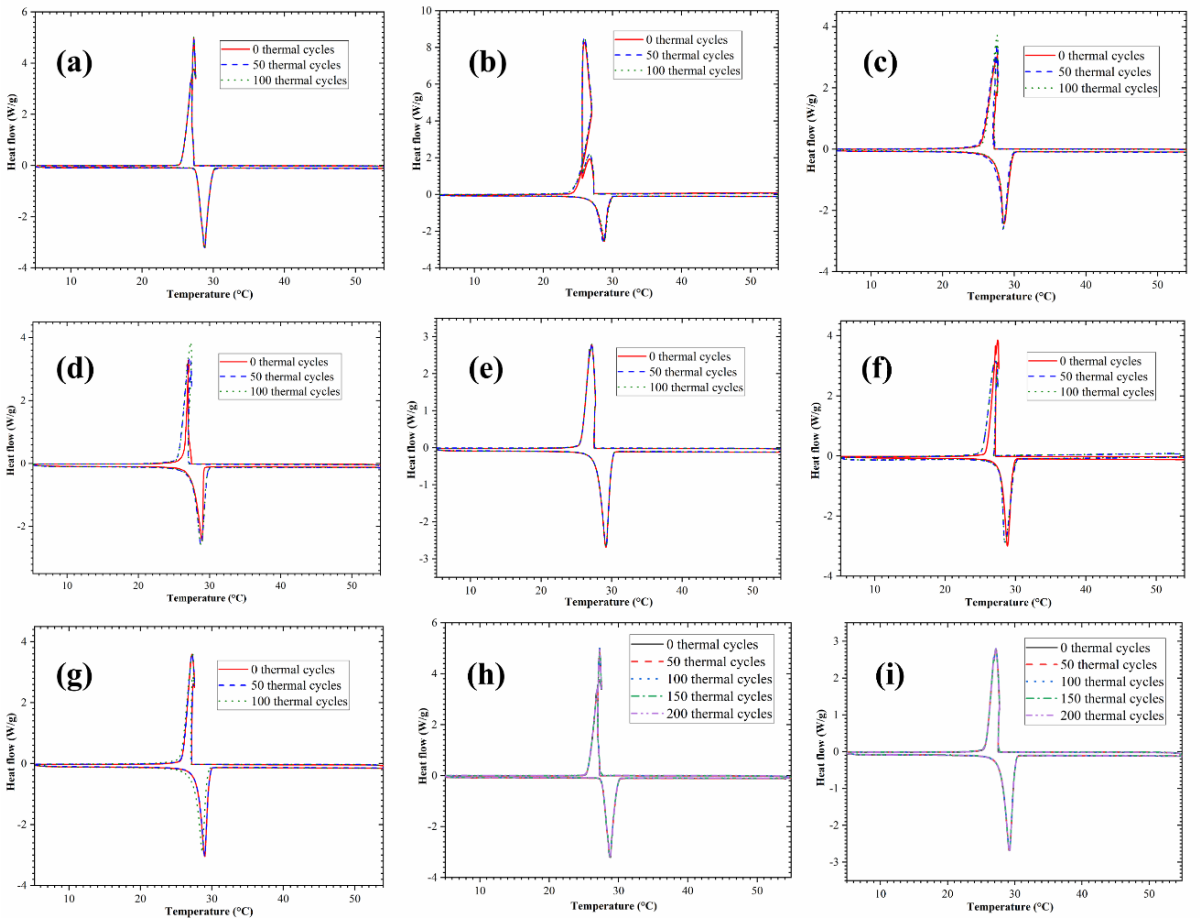

Figure 4.14 DSC thermal cycle curves of single and hybrid nano enhanced PCMs (a, h) PAR (b) PAR+TiO_2, (c) PAR+GNP, (d) PAR+MWCNTs, (e, i) PAR/MWCNTs+GNP, (f) PAR/MWCNTs+TiO_2, and (g) PAR/GNP+TiO_2.

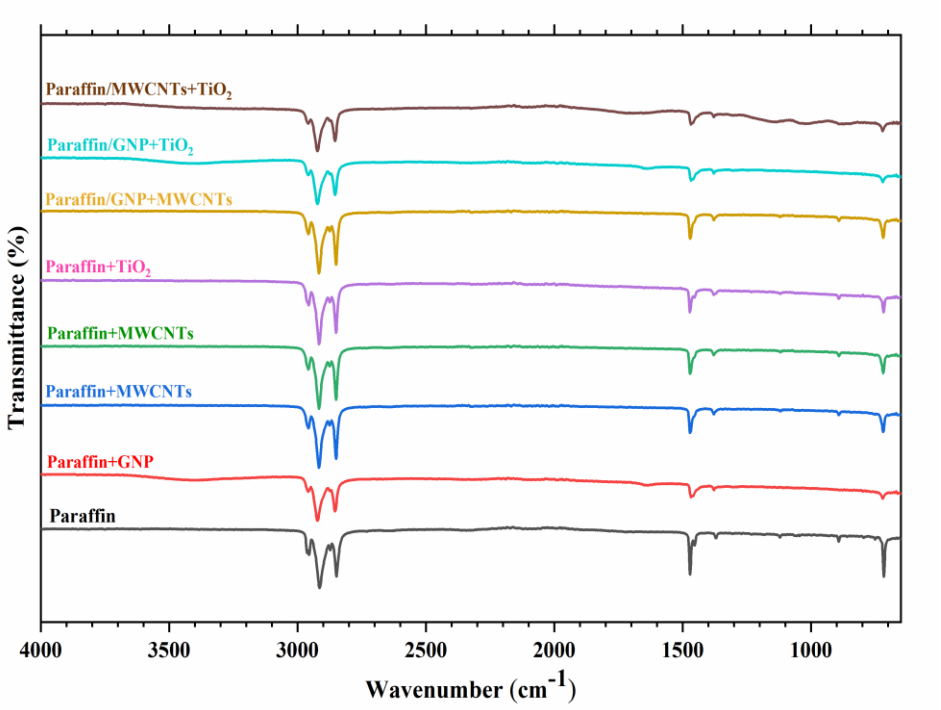

Figure 4.15 FT-IR spectra of thermally treated samples.

4.9 Summary

The effects of both single and hybrid nanoparticles on the phase change materials (PCMs) thermophysical properties have been examined. This study showed that the inclusion of both types of nanoparticles slightly altered the melting and solidification temperatures but with minimal impact on the overall phase transition properties. For instance, single-type nanoparticles (PAR+TiO_2 at 1 wt.%) exhibited a melting temperature of 28.83°C and a latent heat of melting (ΔHm) of 239.2 J/g, compared to the hybrid type (PAR/MWCNTs+TiO_2 at 1 wt.%) with a melting temperature of 28.86°C and ΔHm of 234.6 J/g, , and the pure PCM which had a melting temperature of 28.92°C and a ΔHm of 248.4 J/g. The introduction of nanoparticles, both single and hybrid, slightly reduced the latent heat compared to the pure PCM, with a maximum reduction of 6.8% for PAR+MWCNTs in latent heat of fusion, suggesting a minor impact on the energy storage capacity. The hybrid nanoparticles, however, demonstrated a greater increase in thermal conductivity, a crucial factor for the rapid storage and release of thermal energy. Specifically, the hybrid nano-PCM (PAR/GNP+MWCNTs at 1 wt.%) recorded a thermal conductivity of 0.864 W/m.K, slightly higher than the single type (PAR+GNP at 1 wt.%)

which was 0.82 W/m.K. Additionally, hybrid nano-PCMs showed superior thermal stability and dispersibility over time compared to single carbon-based nanoparticles. This suggests that hybrid nanoparticles form more stable composites, potentially leading to more reliable PCM applications, particularly in scenarios requiring efficient thermal energy management.

CHAPTER 5: EFFECTS OF SURFACE MODIFICATION OF MWCNTS ON NANO-PCM PROPERTIES

The chapter presents and discusses the impact of acid functionalised and un-functionalised MWCNTs nanofillers on the thermophysical characteristics and stability of nano-phase change materials. Results from advanced analytical techniques have confirmed that functionalisation significantly improves the dispersion and stability of MWCNTs within the PCM matrix. The findings from this study on the thermophysical properties of functionalised MWCNTs in nano-phase change materials have been documented in a peer-reviewed article published in 2024 [247].

5.1 Concentration optimisation

Initially, the pure MWCNTs-based PAR samples were prepared with MWCNT's concentration ranging between 0.2 to 1.0 wt.% and then the latent heat (LH) and thermal conductivity (TC) of the prepared samples were measured at 15 °C and 25 °C respectively. An Analysis of Variance (ANOVA) was used to identify the suitable concentration at which TC could be the maximum while an LH reduction was the least. Two responses were analysed in this model; thermal conductivity and latent heat, and both responses were given the same importance. In the analysis, particle concentration (i.e., 0.2 wt.% to 1.0 wt.%) and temperature (15 °C and 25 °C) have been considered as factors.

Equations (5.1) and (5.2) demonstrate the mathematical model utilised to establish the relationship between input variables and dependent responses implemented in regression models.

$$\mathrm{TC} = -43 - 5.5 * (\mathrm{Conc.}) + 4.8 * (\mathrm{temp.}) + 3.1 * (\mathrm{Conc.}) * (\mathrm{temp.}) \quad (5.1)$$

$$\mathrm{LH} = \text{-}0.739 - 6.025*(\mathrm{Conc.}) + 7.02164\mathrm{E}\text{-}18*(\mathrm{temp.}) \quad (5.2)$$

Table 5.1 demonstrates the fit statistics for the initial response, calculated with ANOVA, a Design-Expert software. The regression analysis indicates coefficients of determination

(R^2) greater than 0.95 for both responses, with only a small number of data points separating the regression line from the response points. The adjusted R^2 values are also over 0.96, signifying that only a small portion of the variance occurred. To evaluate the model's ability to predict new observations, the predicted R^2 was examined. The results indicate a correlation of good quality, with a difference of 0.2 between the adjusted and predicted R^2 values. This implies that sufficient signals with satisfactory precision ratios of 61.2354 and 27.6835 for the first and second responses, respectively, could be obtained.

Table 5.1 The fit statistics for the obtained initial response.

First Response	**Std. Dev.**	**2.89**	**R^2**	**0.9964**
	Mean	86.90	**Adjusted R^2**	0.9964
	C.V. %	3.32	**Predicted R^2**	0.9889
			Adequate Precision	61.2354
Second Response	**Std. Dev.**	0.319	**R^2**	0.9762
	Mean	-4.35	**Adjusted R^2**	0.9694
	C.V. %	7.30	**Predicted R^2**	0.9531
			Adequate Precision	27.6835

The 3D plot of particle concentration and temperature as a function of TC and LH is shown in Figure 5.1. It can be seen that an increase in MWCNT's concentration results in an increase in TC while inducing a slight reduction in LH at both investigated temperatures of 15 °C and 25 °C. It was also observed that the optimal MWCNT concentration for achieving the highest overall TC was 0.984 wt.%, which corresponded with a modest decrease in LH by -6.6%, as shown in Figure 5.2. This reduction in LH was deemed acceptable given the significant enhancement in TC of 147.2% at this concentration. However, since there was no significant difference observed between 0.984 and 1 wt.% of MWCNTs, the concentration of 1.0 wt.% was chosen for all experiments in this study.

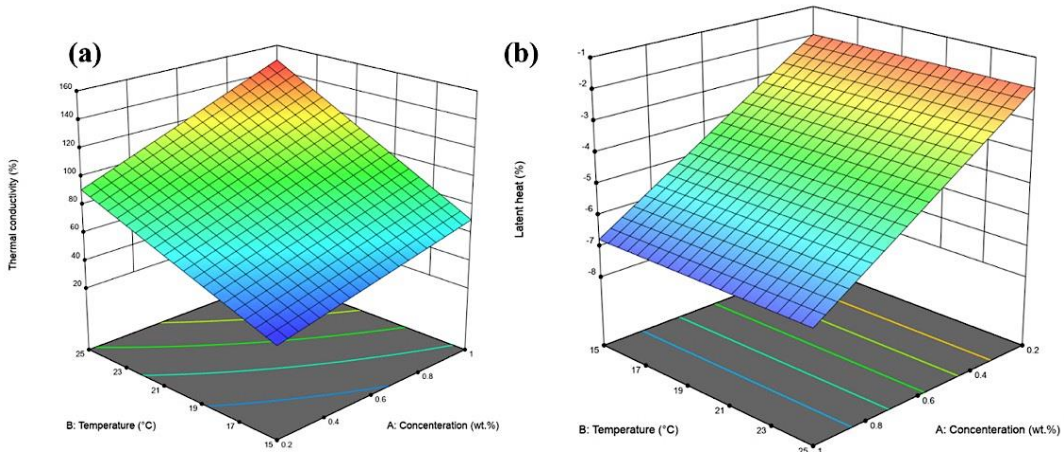

Figure 5.1 3D plot of particle concentration and temperature as a function of (a) TC, (b) LH.

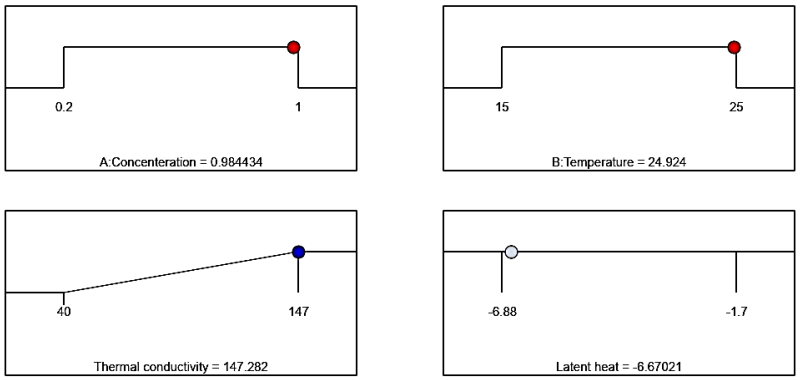

Figure 5.2 Typical optimised response predicted by ANOVA.

5.2 Stability of the prepared samples

To evaluate the efficacy of the method, visual depictions of the samples were taken before and after they were subjected to a thermal bath for 48 hours at 65 °C. As shown in Figures 5.3 (a–b) the untreated MWCNTs have been sedimented after 48 hours of sonication, while the functionalised MWCNTs still remained well dispersed, which indicates that the surface modification of MWCNTs may play an important role in the anti-glomeration of MWCNTs themselves and in producing stable and well-dispersed nano-PCMs.

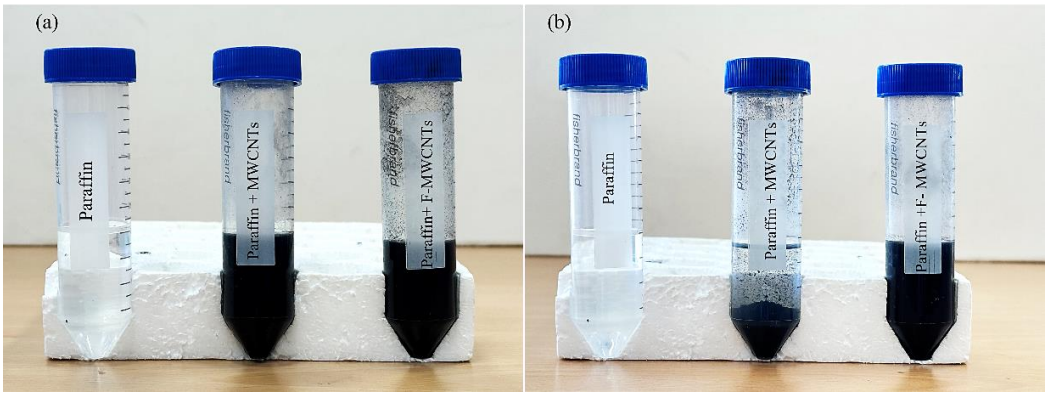

Figure 5.3 Samples just after sonication (a), and after 48 hours of sonication (b).

5.3 Micro-structure analysis

Both the structures and particle size of functionalised and un-functionalised MWCNTs were examined with a TEM. The results revealed that the untreated MWCNTs had a size range of 6-9 nm as shown in Figure 5.4 (a), while the functionalised MWCNTs had an increased size range of 12-15 nm as shown in Figure 5.4 (b). This increase in size indicates the successful attachment of the –COOH group to the MWCNTs. Similar observations reported in numerous studies [69,71] confirmed that the surface modification process has crafted the COOH group to the MWCNTs. In addition, the F-MWCNTs appear straighter and have smoother surfaces than pure MWCNTs, implying that the COOH attachment to the MWCNT's surface.

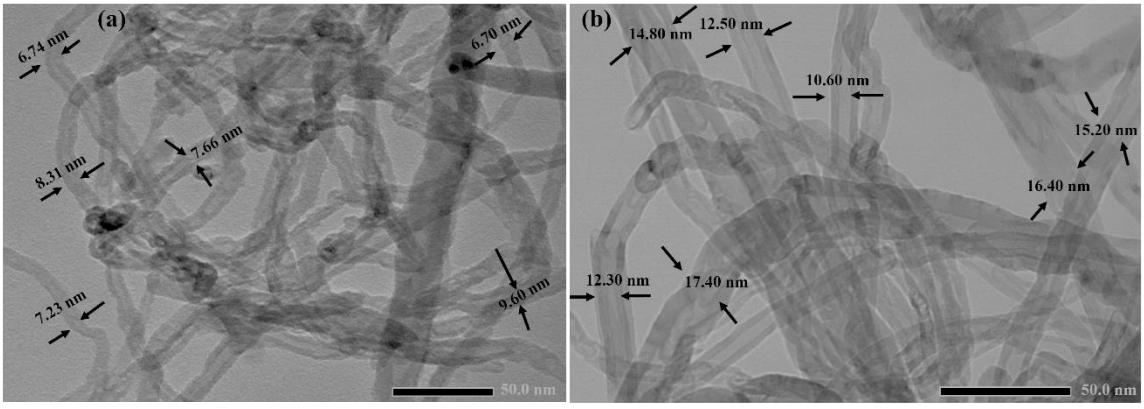

Figure 5.4 TEM images of (a) P-MWCNTs, (b) F-MWCNTs.

5.4 Infrared spectroscopy analysis

The sample's chemical interactions and functional groups were studied using FT-IR spectroscopy, as shown in Figure 4.2, between 600 and 4000 cm^{-1} spectra transmittance. Figure 5.5 depicts the FT-IR bands of MWCNTs, F-MWCNTs, pure paraffin, PAR/MWCNTs, and PAR/F-MWWCNTs, respectively. It can be seen that no stretching or bending peaks appeared in the MWCNTs infrared spectra due to the absence of functional groups. However, F-MWCNTs depict a broad absorption band around 3400 cm^{-1} owing to O–H stretching of the carboxylic group, and a band around 1635 cm^{-1} corresponds to the C=O stretching vibration, and the band around 1410 cm^{-1} is ascribed to C–H bending, which confirms the acid functionalisation of the P-MWCNTs [63]. The pristine paraffin spectra contained three transmittance peaks between 2800 and 3000 cm^{-1}, which demonstrated mild asymmetrical stretching vibrations of $–CH_2-$ and $–CH_3$ groups. The peak at 1490 cm^{-1} in PAR revealed a substantial amount of C–H scissoring of the alkane groups. The peak at 750 cm^{-1} was attributed to the rocking vibration of C–H in the long-chain methyl group [231,233]. FT-IR spectra for nanocomposites have been confirmed in recent research with similar patterns [69–71]**.** The paraffin incorporated with un-functionalised and functionalised MWCNTs did not show any new peak confirming only physical interactions between paraffin and MWCNTs without chemical interactions. Moreover, the PAR/F-MWCNTs showed no peak from F-MWCNTs, which could be due to the very low concentration of F-MWCNTs within the paraffin.

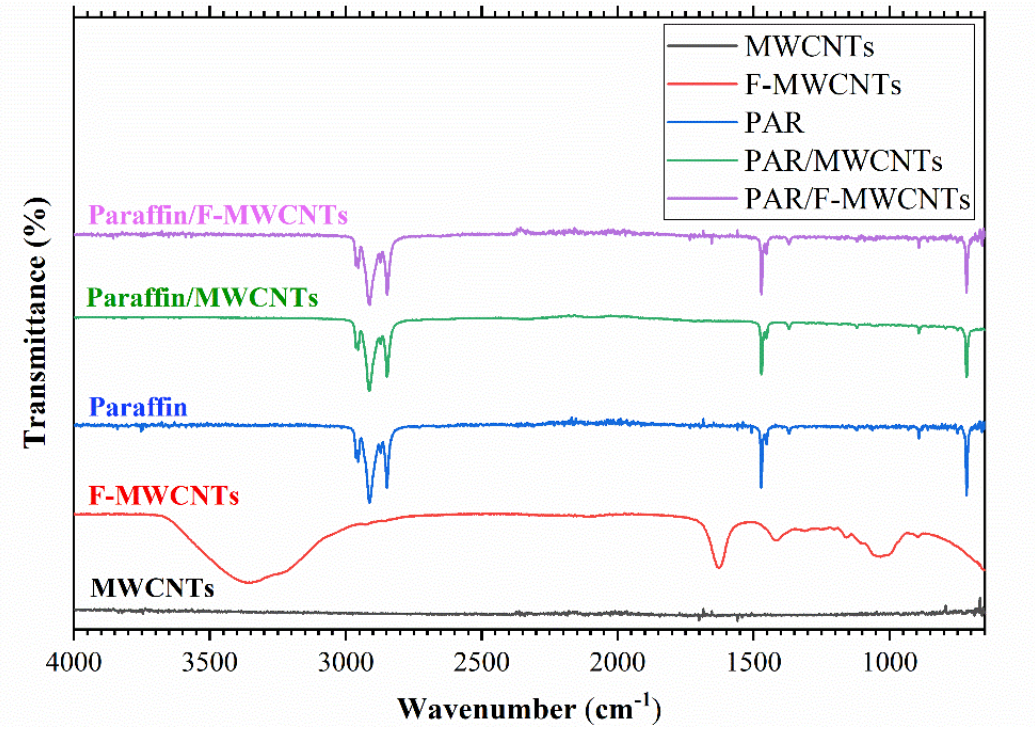

Figure 5.5 FT-IR spectra of functionalised and untreated samples.

5.5 Crystal structures

XRD analysis with the device shown in Figure 3.12 was performed on the pure MWCNTs, F-MWCNTs and with paraffin incorporated both type of nanotubes. It was mainly used to investigate the efficacy of functionalisation of MWCNTs using a 3:1 mixture of H_2SO_4-HNO_3. In Figures 5.6, the XRD profiles of pristine and acid-functionalised MWCNTs are illustrated. It is evident that both the pristine and oxidised samples exhibit a diffraction peak at 24.34° (002), 41.12° (100) and 25.58° (002), 43.30° (100), respectively, resembling the graphite crystal structure. This observation suggests that the functionalisation process does not alter the bulk structure of the MWCNTs. The right-shift of the (002) peak for F-MWCNTs can be attributed to a reduction in the lattice parameter, which is often caused by the removal of impurities during the acid functionalisation process [248,249]. The acid treatment (H2SO4-HNO3) helps eliminate carbon-related impurities, leading to a slight compression of the crystal lattice. This shift suggests a structural change due to the improved purity and reduction of defects in the MWCNTs, contributing to the decrease in lattice spacing and overall reflection intensity at (002). Additionally, the disappearance of impurity peaks further supports the accomplishment of acid functionalisation.

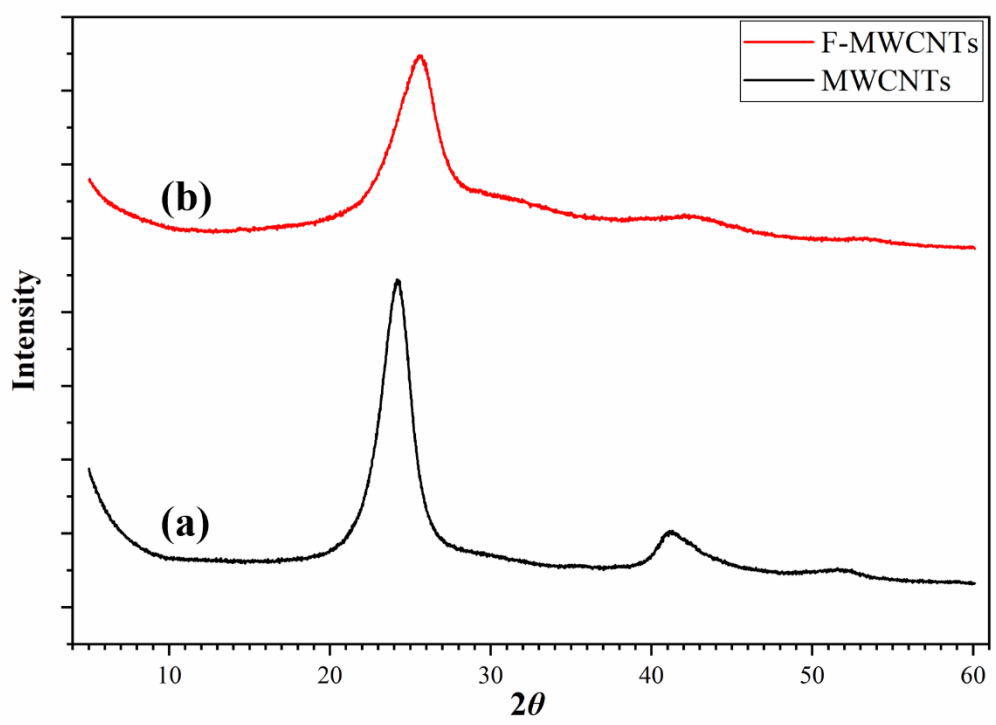

Figure 5.6 XRD curves of (a) MWCNTs, (b) F-MWCNTs.

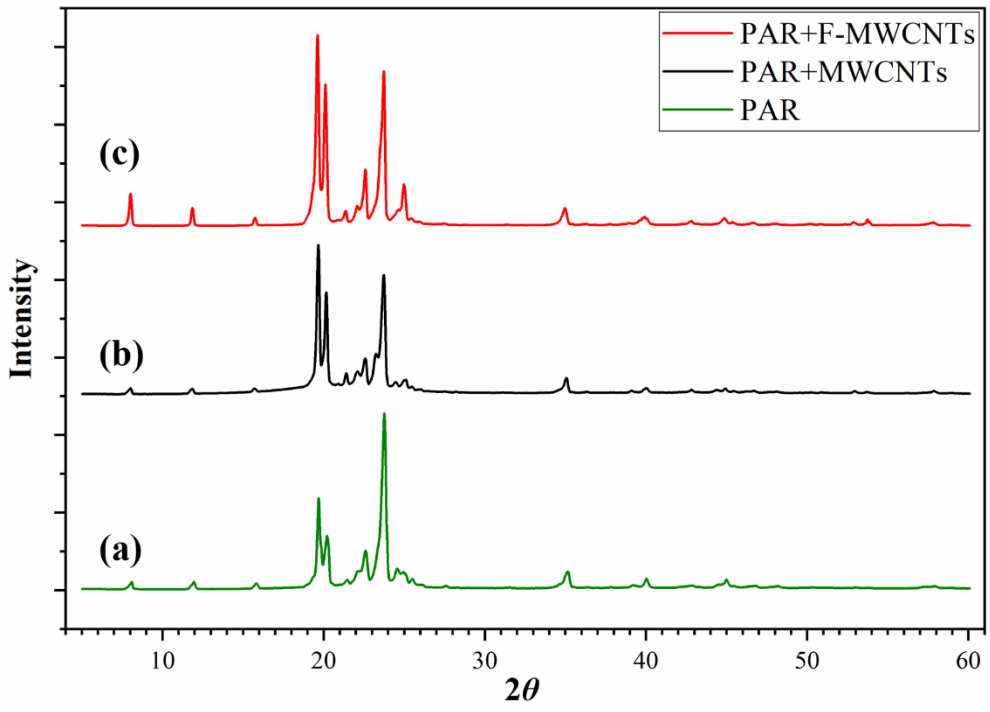

Figure 5.7 XRD patterns of (a) PAR+MWCNTs, (b) PAR+F-MWCNTs.

Figure 5.7 depicts the XRD spectrum peaks of paraffin, recorded at 7.92°, 11.7°, 15.5°, 19.4°, 19.8°, 22.19°, 23.4°, 24.64°, 27.1°, 31.0°, 34.08°, 39.4°, and 44.3°, corresponding to Miller indices (002), (003), (004), (010), (011), (401), (102), (111), (007), (008), (009), (122), and (0010). These indices are attributed to the crystal structure of n-octadecane, as identified in the crystallography open database. Given the minimal concenteration of nanofillers in the PCM, the introduction of functionalised and pristine MWCNTs into paraffin does not alter the crystal structure of the nano-enhanced PCM.

5.6 Thermodynamic properties

Thermal properties during melting and crystallisation of pristine PCM and CNTs-enhanced PCM were investigated between the temperature range of 15 °C to 45 °C with a DSC. The solidification and melting phenomena of the pure PAR and the PAR impregnated with the modified and the unmodified MWCNTs are shown in Figure 5.8. Moreover, the melting and crystallisation values of latent heat, temperatures, and degree of supercooling for all samples are provided in Table 5.2. It was observed that the inclusion of functionalised and un-functionalised MWCNTs into the PCM has only a minute impact on melting and crystallisation temperatures. However, because of the non-melting enthalpies of the CNTs a small decline in the melting and solidification enthalpies was noticed with the incorporation of treated and untreated CNTs [250]. In the melting process, only one endothermic peak was observed for all the samples, which shows the isomorphous crystalline structure of the pristine PCM and the CNTs-enhanced PCM. Similarly, one exothermic peak can be seen during the cooling of treated and untreated CNTs based PCM, which confirms that the addition of both additives does not vary the solidification process significantly . Two peaks were noted for pure PCM during the solidification process, and this could be due to the metastable rotator phase, which appears prior to final crystallisation due to heterogeneous nucleation [236,237]. To further verify the thermal stability of all the samples they were exposed to 200 thermal cycles with a DSC. There was no significant change which was reflected in the thermal properties of the pure PCM and nano-PCMs, as shown in Figures 5.8 (a-c). Overall, less than 1% variation in the phase transition temperatures and enthalpies was observed after 200 cycles, suggesting a promising thermal stability level for TES applications in buildings.

The supercooling degree (ΔT) of pure paraffin and composites is stated in Table 5.2. ΔT was reduced slightly by the incorporation of pristine MWCNTs into the PCM and for modified MWCNTs-based PCM a minor increase in ΔT, which is almost negligible [251]. The overall decline in ΔT shows the significance of nanomaterials as nucleating agents for efficient surface adsorption and homogenous nucleation.

The specific heat capacity (Cp) was measured in the liquid and solid forms when the temperature rises from 15 °C to 45 °C as shown in Figures 5.9 (a-b). The Cp is usually ignored by researchers since it has a low thermal energy density during a sensible heat storage process and a comparatively little effect on the total amount of thermal energy that can be retained using these materials. However, the Cp still influences other variables that influence the total amount of stored heat in a given temperature range when such materials are used [231]. It can be seen from Figure 5.9 that in the solid phase, from 15 °C to 25 °C the Cp of the pure PAR and nano-PAR improved steadily with an increase in temperature. On the other hand, it remained constant during the liquid state from 35 °C to 45 °C. Furthermore, the results showed that the nano-enhanced PCM depicts higher Cp compared to the pure PCM. The *C*p values of the pure PAR and PAR with treated and untreated MWCNTs at 25 °C and 45 °C were 3.132 J/g °C, 3.838 J/g °C, 3.858 J/g °C and 1.89 J/g °C, 2.505 J/g °C, 2.525 J/g °C, respectively.

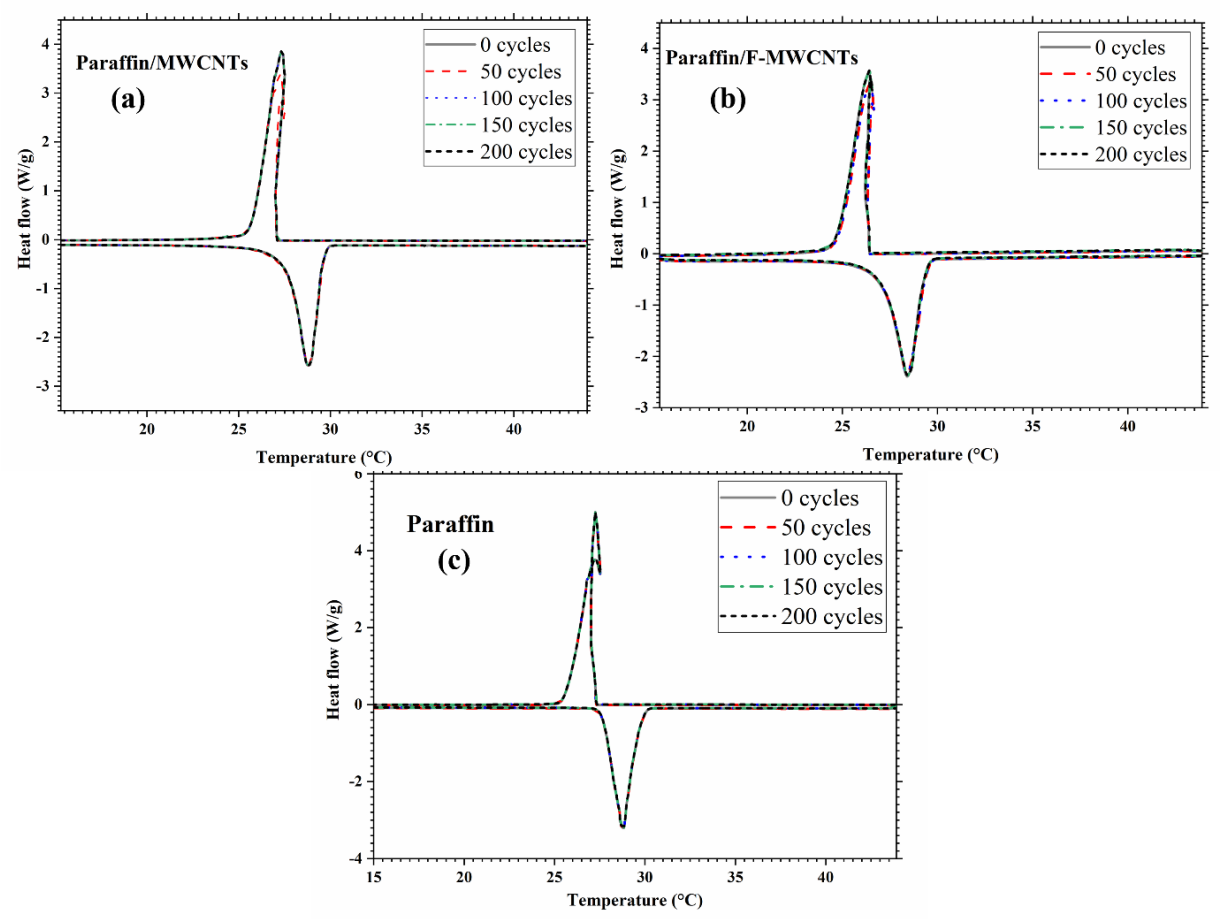

Figure 5.8 DSC curves of (a) PAR/MWCNTs, (b) PAR/F-MWCNTs and (c) pure PAR.

Table 5.2 Thermal properties of samples.

Sample	**Melting**		**Crystallisation**		
	T_{peak}	ΔHm	T_{peak}	ΔHc	ΔT
PAR	28.92	248.4	27.26	251.7	1.66
PAR/MWCNTS	28.96	231.3	27.35	233.3	1.61
PAR/F-MWCNTS	28.46	229.7	26.78	232.2	1.68

$T_{\mathbf{peak}}$: peak temperature (°C), ΔHm: latent heat of melting (J/g), ΔHc: latent heat of crystallisation (J/g), ΔT: super–cooling degree (°C).

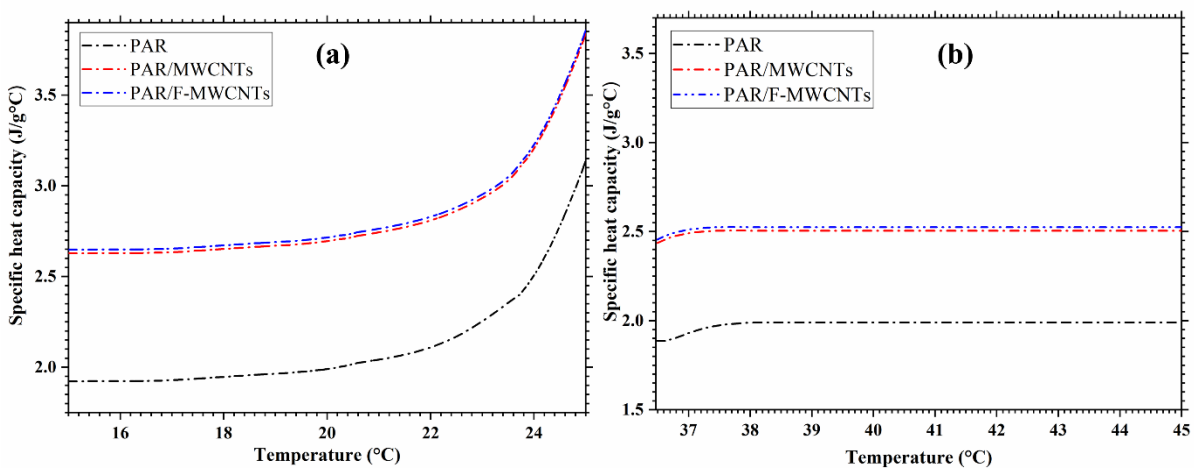

Figure 5.9 The specific heat capacity (*C*p) of PAR and nano-PAR (a) solid, and (b) liquid.

5.7 Thermal durability

The thermal stability of pristine PCM and nano-PCMs was analysed with TGA and DTG. Figures 5.10 (a-b) show typical TGA and DTG curves of the PAR and nano-PAR. It can be seen from the TGA analysis in Figure 5.10 (a) that neither the PAR nor its composites exhibit any noticeable reduction in mass up to ~130 °C. Then the weight loss became more prominent as the temperature continuously increased, achieving its highest degradation temperature while having left a fixed residue behind. The degradation temperature for PAR impregnated with MWCNTs and F-MWCNTs was 228.46 with 1.438% residue and 230.39 °C with 1.861% residue, respectively. The decomposition occurred as a result of paraffin evaporation, in which hydrocarbon chains disintegrated into monomers. In addition, the incorporation of pure and modified MWCNTs increased the maximum degradation temperature of the nano-PAR because the highly thermally conductive nanoparticles had fastened and uniformed the heat transfer. In essence, the nanoparticles formed a shielding layer on the surface of the PAR preventing vaporisation during thermal deprivation. The DTG analysis in Figure 5.10 (b) shows that pure PAR and nano-PAR have almost analogous thermal decompositions. TGA and DTG tests revealed that the functionalised nano-PCMs remained stable and did not lose weight until 130 °C, confirming that the produced new materials have the potential to be used for TES. For their application in buildings, they could be encapsulated in a suitable material or supporting structure that ensures the confinement of leakage problems while allowing controlled charging and discharging of thermal energy as needed.

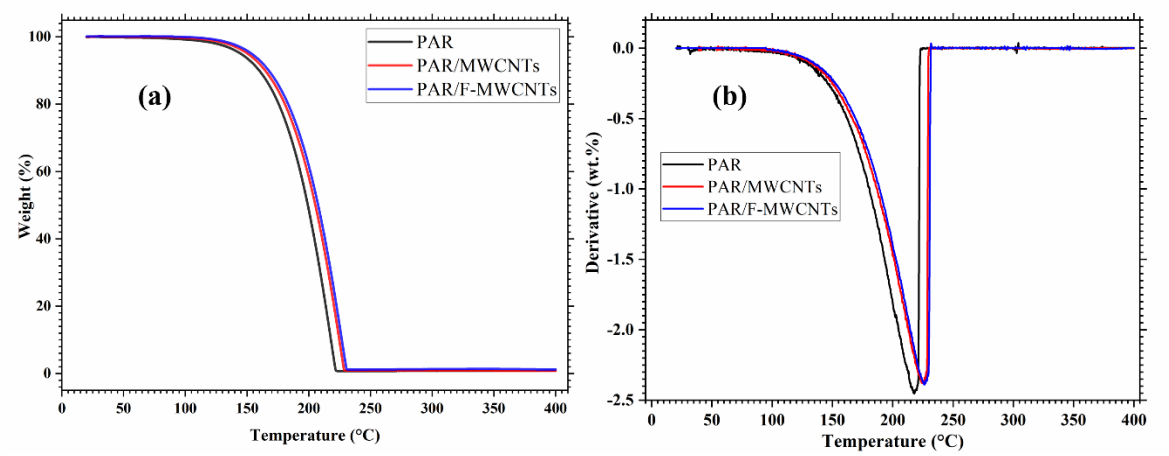

Figure 5.10 Analysis of thermal durability of pure PCM and nano-PAR (a) TGA curves, (b) DTG curves.

5.8 Thermal conductivity

Thermal conductivity is an important thermal property that influences the performance of nano-PCMs. The higher TC accelerates the heat transfer and improves the heating and cooling performance of the PCMs, while low TC slows the charging and discharging rates of the PCM, which results in the poor performance of the TES materials [6]. The TC of the pristine PCM, PCM/MWCNTs, and PCM/F-MWCNTs was measured for freshly prepared samples and on samples that had been stored in a thermal bath for 48 hours, to assess the reproducibility of the results. The tests were carried out in both liquid and solid states at temperatures varying from 5 °C to 55 °C, to provide a comprehensive understanding of the TC behaviour of these investigated materials.

As shown in Figure 5.11, at 5 °C, the TC value of the pure PAR was recorded as 0.195 W/m.K. However, freshly produced nano-PCM samples with untreated MWCNTs and treated MWCNTs demonstrated a 69.2% and 79.4% rise in TC, respectively. At 15°C, the TC remained relatively unchanged for all the freshly prepared samples as they were in a solid state and displayed their orderly microstructure. After being kept in a water bath for 48 hours, the TC of the PAR with untreated MWCNTs reduced significantly, with values of 0.233 W/m.K and 0.236 W/m.K at 5 °C and 15 °C, correspondingly, possibly due to their hydrophobicity. In contrast, the PAR with functionalised MWCNTs showed little to no change in their TC after the same period, as shown in Figure 5.11.

As can be seen in Figure 5.11, an abrupt increase of TC at 25 °C, occurred for all the samples apart from the measurement taken for the untreated MWCNTs after 48 hours. Such a sudden increase near the melting temperature of PCM was because near melting temperature the crystalline arrangement of the PAR became unstable, and a rise in temperature accelerated the molecular vibration in the lattice, so the TC values of pristine PAR and nano-PAR increased brusquely near the melting temperature (i.e., 25 °C). In the liquid state at 35 °C, 45 °C and 55 °C the TC values taken for all samples were below 0.2 W/m.K. This is because the organised microstructure present in the solids changes to a disorganized one in the liquids. Heat conduction in solids is primarily due to lattice vibrations, where molecules move within their lattice structures. Solids have a greater TC value compared with liquids as they possess greater free-electron motion and lattice vibrations. Overall, F-MWCNTs outperformed P-MWCNTs in terms of stability and TC. This is due to the -COOH groups adhesion to the surfaces of MWCNTs, which results in improved dispersion and bonding strength with the PCM matrix. Furthermore, functionalisation reduces surface resistance and improves the interaction between nanoparticles and PCM, hence increasing heat conductivity [70].

The thermal conductivity improvement after the addition of MWCNTs was also calculated and expressed as a percentage enhancement at various temperatures from 5 °C to 55 °C, as depicted in Figure 5.12. The TC enhancement ratio was determined using Equation 5.3.

$$\eta = \frac{K_{nano-PCM} - K_{PCM}}{K_{PCM}} * 100 \quad (5.3)$$

where, $K_{nano-PCM}$ and K_{PCM} are the thermal conductivities of nano-PCMs and pure PCM, correspondingly.

The percentage enhancement of the TC values of pristine MWCNTs was 69.23% at 5 °C and 70.85% at 15 °C, whereas the percentage enhancement of F-MWCNTs was 79.49% at 5°C and 79.90% at 15°C. The TC enhancement of the P-MWCNTs after 48 hours reduced

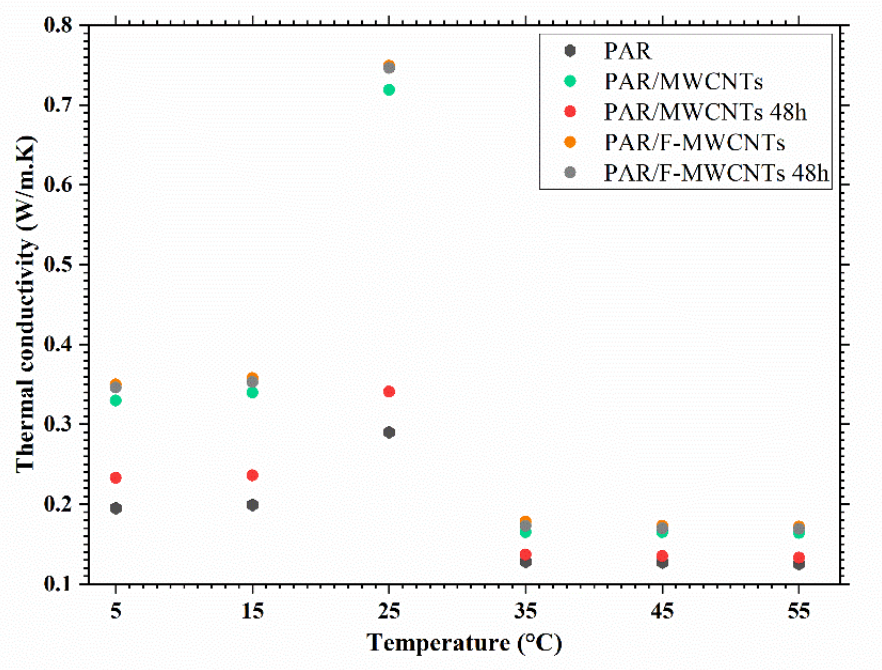

Figure 5.11 Thermal conductivity of fresh samples and samples after 48 hours.

significantly which demonstrates the poor stability of pristine MWCNTs. However, the functionalised MWCNTs maintain the TC level of the PCMs after 48 hours and no significant change was noticed, indicating a good stability of functionalised MWCNT PCM. The maximum enhancement of the TC was observed for functionalised MWCNTs at 25 °C with an enhancement factor of 158%.

At 35 °C, the thermal conductivity value of the pristine MWCNTs decreased by 28.9% compared to its original value. The functionalised MWCNTs, on the other hand, showed a 39.06% enhancement in thermal conductivity. At 45 °C and 55 °C, the improvement in TC for both pristine MWCNTs and functionalised MWCNTs showed a similar trend, with the functionalised MWCNTs exhibiting a higher thermal conductivity value compared to the pristine MWCNTs. Overall, the F-MWCNTs demonstrated greater enhancement since acid modification of MWCNTs lowed the surface resistance and increased the contact between PCM and nanofillers which improves the TC enhancement. In addition, the covalent connection formed by functionalised MWCNTs between nanoparticles and PCM is also an important factor in improving the TC [69]. This demonstrates how functionalised MWCNTs can improve PCMs thermal conductivity and preserve the TC level over time.

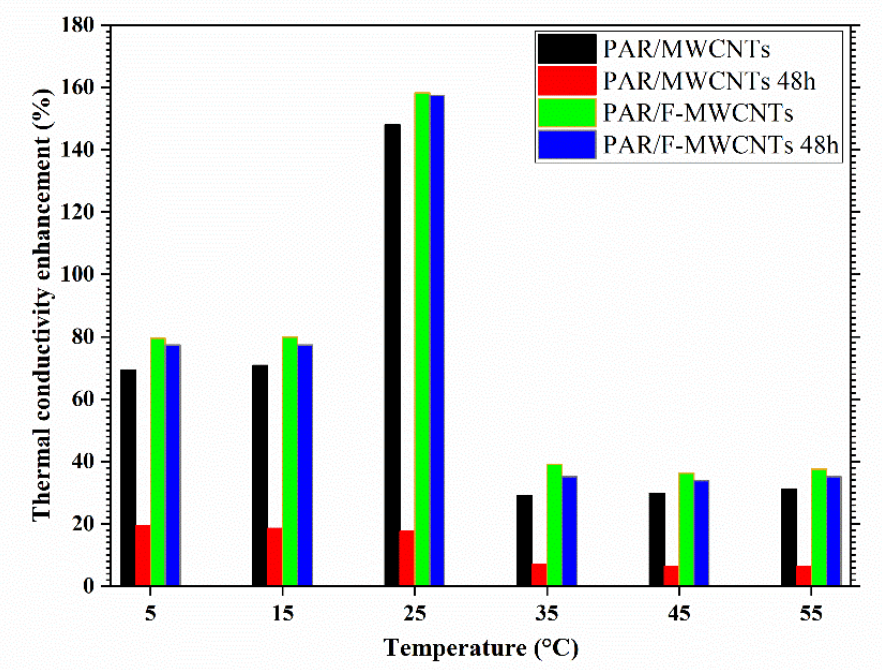

Figure 5.12 Thermal conductivity enhancement of fresh samples and after 48 hours.

Furthermore, the greater TC achieved with F-MWCNTs may be ascribed to physical changes in the MWCNTs during the functionalisation procedure. Since functionalization caused structural changes in the F-MWCNTs which may have resulted in reduced agglomeration and improved alignment. These modifications have led to uniform dispersion of MWCNTs within PCM, improved thermal channels within the PCM, lowering thermal resistance and increasing TC of nano-PCM.

5.9 Heat transfer analysis

The thermal performance of pure PCM and nano-PCMs was evaluated using infrared thermography (IRT). Typical IR thermal images of pure PCM and PCM incorporated with MWCNTs and F-MWCNTs are shown in Figure 5.13, which shows the temperature distribution during a melting process of samples at 5W for different time durations. The temperature of nano-PCMs was observed higher than that of pure PCM during the first 20 minutes, which shows that pure and functionalised MWCNTs improved the TC of composite PCMs. The pure paraffin fully melts after 80 minutes, and its temperature is substantially greater than the nano-PCMs, which are not fully melted. This is because the inclusion of MWCNTs improves viscosity while decreasing convective heat transfer. The

phase transition duration of nano-PCMs is substantially longer than that of pure PCM since the high thermal conductive MWCNTs reduced the convection heat transfer and the consistently lower temperature of nano-PCMs is advantageous for TES applications in buildings [252]. In the early phases of melting, when the temperature differential between the PCM and the heat source is most significant, conductive heat transfer is important. The significance of convective heat transfer, which gains prominence as the phase change proceeds, is not inherently diminished, but it does highlight the importance of thermal conductivity in the initial phases of melting.

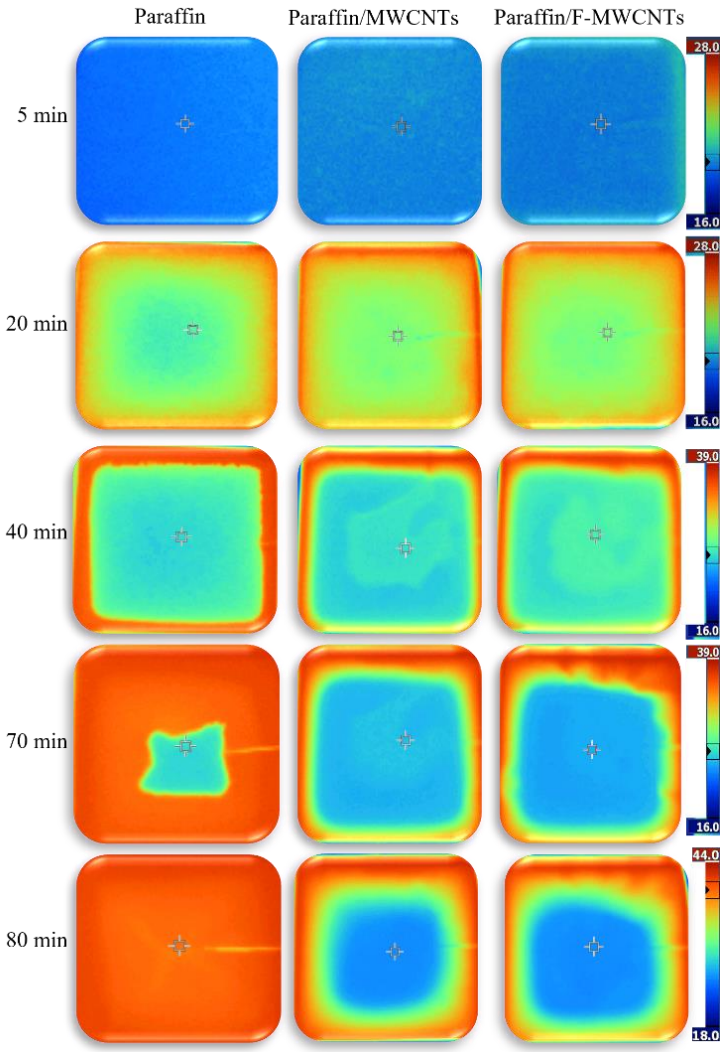

Figure 5.13 Images of infrared thermography during melting of pure PCM and nano-PCMs.

5.10 Summary

The impact of surface-functionalised and un-functionalised MWCNTs on PCM has been investigated, focusing on optimising MWCNT concentrations to balance enhanced thermal conductivity and minimal latent heat reduction. The findings indicated that surface functionalisation significantly enhances the dispersion and stability of MWCNTs within the PCM matrix. Functionalised MWCNTs (F-MWCNTs) at an optimal concentration of 1.0 wt.% improved thermal conductivity by up to 158% at 25 °C while maintaining a modest reduction in latent heat by 6.6%. Advanced characterisation techniques like TEM, XRD, and TGA reveal that functionalisation modifies the surfaces of MWCNTs, enhancing their dispersion within the PCM matrix, while preserving the core bulk structure. These findings highlight the potential of functionalised MWCNTs to significantly improve PCM performance, making them more effective for thermal energy storage applications in potential energy-efficient systems.

CHAPTER 6: HYBRID NANOPARTICLES OF FUNCTIONALISED MWCNTS T_iO_2 FOR ENHANCED NANO-PCMs

This chapter presents a comprehensive thermophysical analysis of the PCM-enhanced with functionalised MWCNTs and TiO_2-based hybrid nanoparticles. The selection of this hybrid combination was informed by the characterisation results from Chapters 4 and 5, particularly due to their enhanced stability. In addition, utilising them in a hybrid combination makes economically feasible, given the relatively high cost of MWCNTs compared to TiO_2 nanoparticles. The investigation primarily focused on examining the structures, thermal and chemical properties of the developed materials.

6.1 Micro-structure of MWCNTs

Transmission electron microscopy was employed to assess the sizes and structures of MWCNTs in their as-received state and after acid treatment. The original MWCNTs exhibited a thinner structure, with a thickness ranging from 6 to 10 nm, as depicted in Figure 6.1 (a). In contrast, acid treated MWCNTs displayed a ly greater thickness, approximately 12 to 18 nm, as shown in Figure 6.1 (b). This increase in thickness is indicative of the grafted carboxyl groups on the MWCNTs, a phenomenon consistent with prior observations made by other researchers [69,71]. Furthermore, the acid treated MWCNTs appeared to have straighter and smoother surfaces in comparison to the pristine CNTs, providing additional evidence of carboxyl group attachment to the MWCNT surfaces.

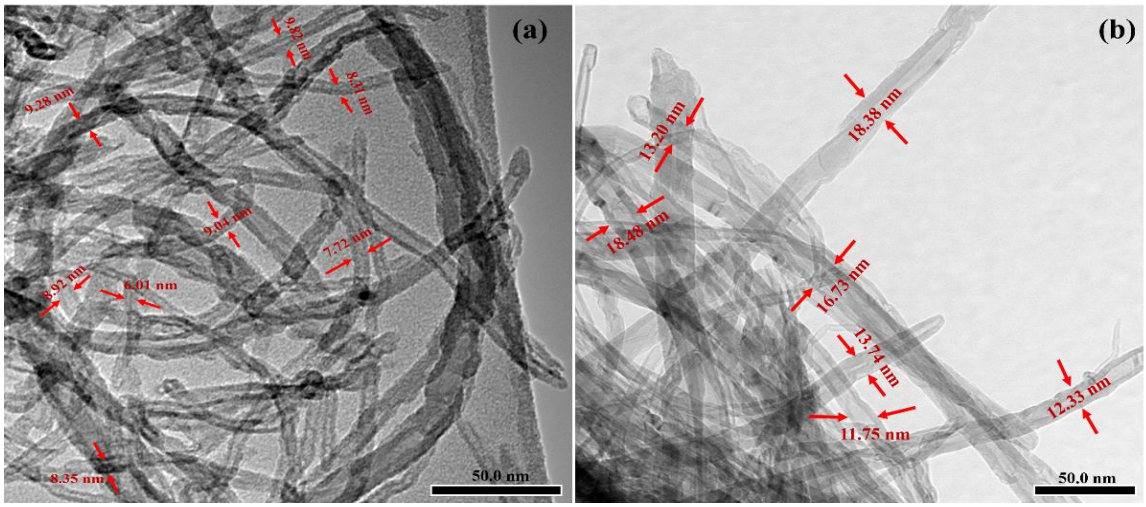

Figure 6.1 Typical TEM images of surface modified and untreated carbon nano tubes: (a) MWCNTs, (b) F-MWCNTs.

6.2 FT-IR Spectra Analysis

The chemical interactions and functional groups contained in the samples were investigated using FT-IR spectroscopy. The spectral transmittance was measured between 650 and 4000 cm^{-1} Figure 6.2 depicts the FT-IR bands for TiO_2, MWCNTs, F-MWCNTs, pure PAR, PAR/MWCNTs, PAR/F-MWWCNTs, and hybrid nanoparticle-based nano-PCMs. TiO_2 stretching vibrations are attributed to the spectral peaks at 635 and 643 cm^{-1}. Unmodified MWCNTs lack distinguishable functional groups, resulting in the absence of bending or stretching peaks [245]. Functionalised MWCNTs, on the other hand, show different characteristics: a broad hydroxyl (O-H) functional group at about 3400 cm^{-1}, a clear C=O stretching vibration peak at 1635 cm^{-1}, and a band at 1410 cm^{-1} indicating C-H bending [253]. These spectroscopic characteristics give solid evidence for the effective attachment of a carboxyl group, proving the effectiveness of MWCNT functionalisation. In the pure PAR sample, transmittance peaks within the range of 2800 to 3000 cm^{-1} signify the medium asymmetrical stretching vibrations of alkane groups, specifically $-CH_2$ and $-CH_3$. The spectral peak at approximately 1490 cm^{-1} indicates considerable C-H scissoring of these alkane groups. Furthermore, the 750 cm^{-1} peak corresponds to the rocking vibration of the C-H bonds within the long-chain methyl group [254]. In the functionalised and un-functionalised MWCNT-based single and hybrid nano-enhanced PCM composites, comparable spectrum peaks to those of pure PAR were observed. The absence of additional

spectral peaks implies that PAR experiences exclusively physical interactions with the nanofillers, without any chemical interactions. Notably, the functionalised MWCNT-based single and hybrid PCM composites do not exhibit carboxyl group peaks. This can be attributed to the minimal concentration of F-MWCNTs within the PAR matrix.

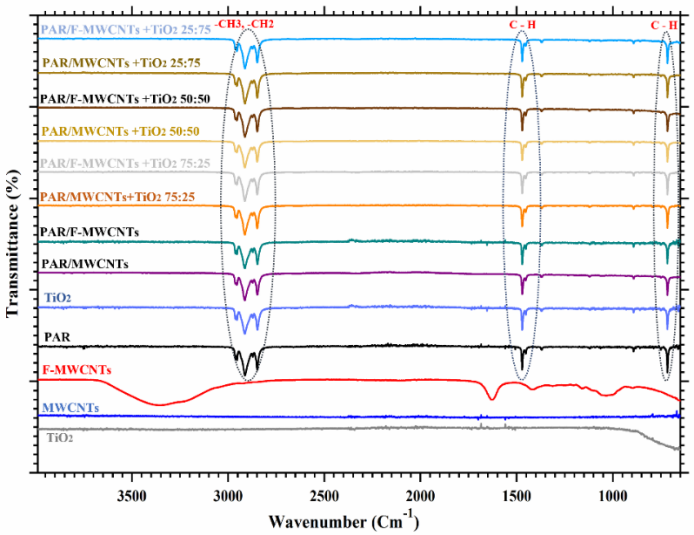

Figure 6.2 FT-IR spectra of nanoparticles and nano-enhanced PCMs.

6.3 Crystal structure Analysis

XRD analysis was conducted to examine the crystal structures of MWCNTs, acid-functionalized MWCNTs (F-MWCNTs), TiO_2, and their respective PCM composites. In Figure 6.3, the XRD profiles of nanoparticles, specifically TiO_2, MWCNTs, and acid-functionalised MWCNTs, are presented. Notably, both the pristine and oxidized MWCNT samples display a diffraction peak at 24.34° (002) and 41.12° (100), similar of the graphite crystal structure. This observation suggests that the functionalisation process does not induce changes in the bulk structures of the MWCNTs. However, the reduced peaks are evident for the (002) reflection at $2\theta = 25.58$ and 42.17° (100). This reduction in reflection between the pristine and functionalised MWCNT peaks signifies the removal of carbon-related impurities, indicating the successful functionalisation [248,249]. Moreover, the absence of impurity peaks further validates the achievement of acid functionalisation. Regarding TiO_2 nanoparticles, the peaks at $2\theta = 25°$, 37.4°, 47.3°, and 53.8° correspond to the (101), (004), (200), and (105) lattice planes, respectively, confirming the anatase form of TiO_2 nanofillers with PDF No. 03-065-5714.

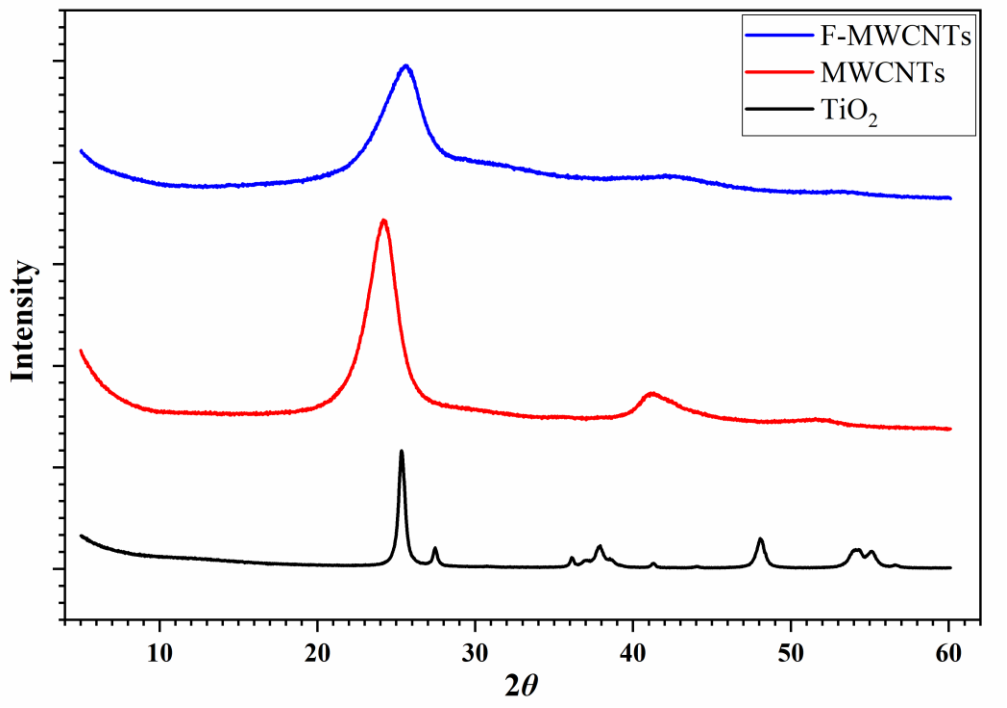

Figure 6.3 XRD curves of nanoparticles.

The XRD curves depicting PAR-based nanocomposites with pristine and acid-functionalised MWCNTs are presented in Figures 6.4 (a - b). Sharp spectrum peaks of PAR were observed at 7.92°, 11.7°, 15.5°, 19.4°, 19.8°, 22.19°, 23.4°, 24.64°, 27.1°, 31.0°, 34.08°, 39.4°, and 44.3° with Miller indices (002), (003), (004), (010), (011), (401), (102), (111), (007), (008), (009), (122), and (0010), corresponding to the crystal structure of n-octadecane as identified in the crystallography open database.

Given the limited presence of nanofillers in the PCM, minimal physical changes were observed. Despite the introduction of the nanoparticles within PAR particularly acid-functionalised MWCNTs as a singular and in combination with TiO_2 nanoparticles, no new peaks emerged. This indicates that the original crystal structure of pristine paraffin remained unaltered with the addition of nanofillers. Consequently, it is inferred that the crystal structure of paraffin remains unchanged, and the peaks of MWCNTs, acid-functionalized MWCNTs, and TiO_2 are retained in both single and hybrid nano-PCMs.

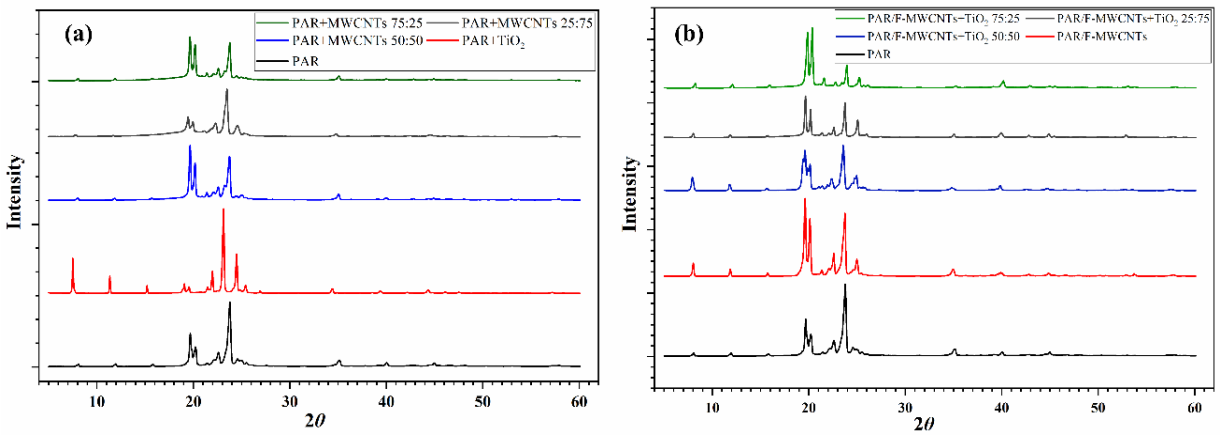

Figure 6.4 XRD patterns of (a) pristine MWCNTs based PAR, and (b) functionalised MWCNTs based PAR.

6.4 Stability of particle dispersion in PAR

Figures 6.5 and 6.6 present optical images of single and hybrid nano-enhanced PAR in their freshly prepared state and after 48 hours of observation. In Figure 6.5, it was observed that pristine MWCNTs tended to precipitate rapidly in the nano-PAR solution, primarily due to their hydrophobic nature, while the surface modified MWCNTs remained well-dispersed in the nano-PAR solution even after a 48-hour observation period.

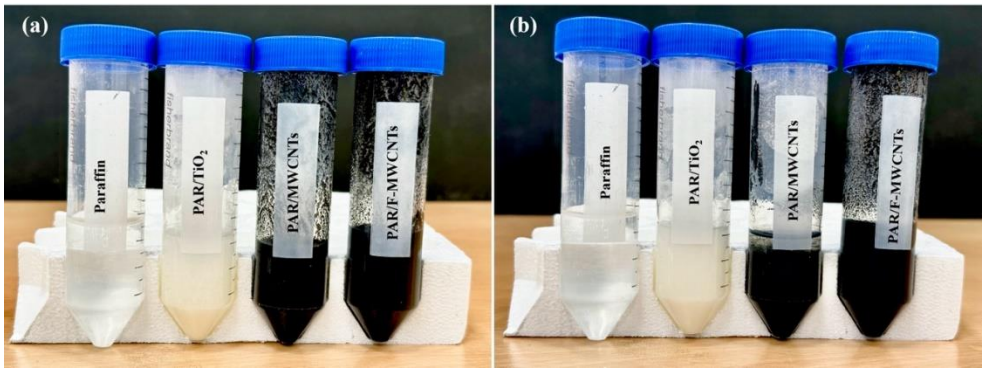

Figure 6.5 Physical behaviour of pure PAR and single-type nano-PAR samples with time (a) 0 hour, (b) 48 hours.

Likewise, in the hybrid particle-based nano-enhanced PAR, the untreated MWCNTs settled when used in higher concentrations alongside TiO_2 nanoparticles. However, functionalized MWCNTs exhibited a notable characteristic of remaining readily and stably dispersed within the PAR for all hybrid combinations, as evident in Figures 6.6 (a) – (d).

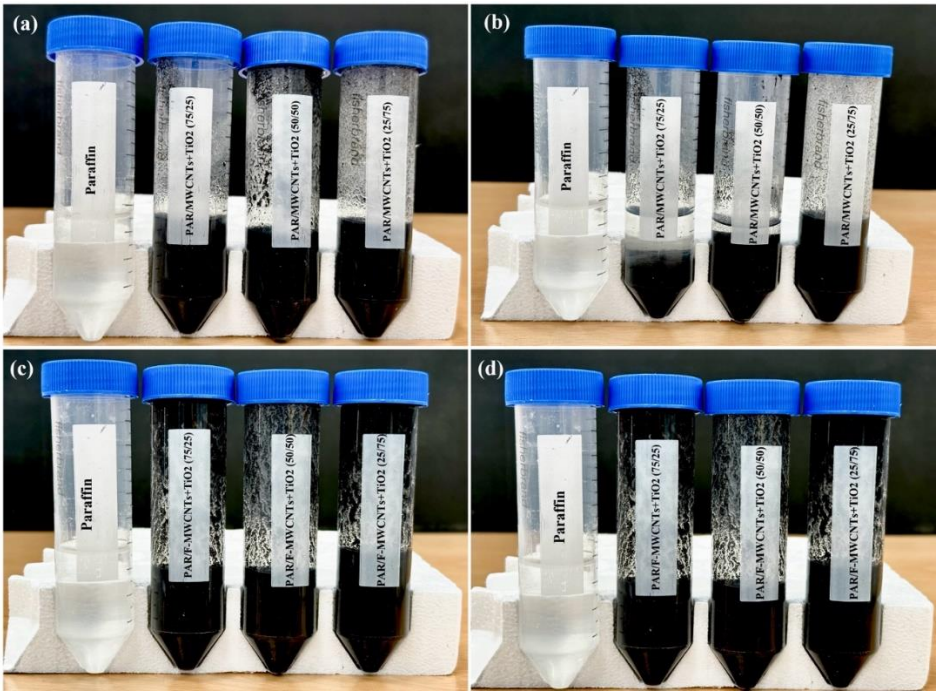

Figure 6.6 Physical behaviour of hybrid-type nano-PAR samples (a, c) 0 hours, (b, d) 48 hours.

This phenomenon was also observed in samples of both functionalized and unfunctionalized MWCNTs-based nano-PAR after they were left undisturbed for 48 hours in the thermal conductivity sample holder shown in Figure 6.7. Specifically, unfunctionalized MWCNTs tended to settle at the bottom of the container, while functionalized MWCNTs remained uniformly dispersed, as indicated in Figures 6.7 (a) – (d). The implications of these observations were further examined in the subsequent section 6.5, where changes in TC values resulting from the repeated TC experiments performed after 48 hours were discussed in detail.

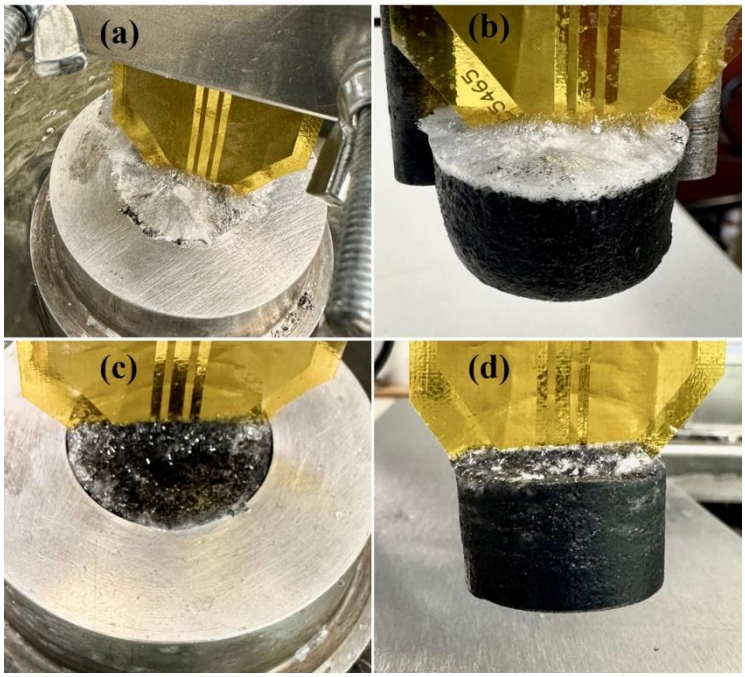

Figure 6.7 PAR/MWCNTs (a, b), and PAR/F-MWCNTs (c, d) composites in TC sample holder.

6.5 Thermal conductivity

Thermal conductivity (TC) is a significant indicator in determining the heating and cooling performance of phase change materials (PCMs). PCMs with low TC have slower charging and discharging rates, reducing the overall effectiveness of the system, and limiting their practical uses. PCMs with high TC, exhibit more efficient heat transfer capability [255]. The thermal conductivity of both functionalised and un-functionalised single and hybrid MWCNTs-based nano-PAR composites was measured. The measurements were taken using a Hot Disk Thermal Constant Analyzer at two ranges of temperature from 5°C to 25°C in a solid state and 35°C to 45°C in a liquid state, results shown in Figure 6.8.

The thermal conductivity of single-type nanoparticles within the nano-PAR remained constant at the range of temperatures of 5°C and 15°C, as shown in Figure 6.8(a). This range of temperature resulted in a completely solid state with a well-ordered microstructure in the PAR. The functionalised MWCNTs-based PAR had the highest TC values, measuring 0.355 W/m.k and 0.358 W/m.k, at 5°C and 15°C, respectively. Thermal conductivity values of pure PAR, PAR/MWCNTs, and PAR/TiO_2 were 0.1934 W/m.k,

0.339 W/m.k, and 0.259 W/m.k at 5°C, and 0.1982 W/m.k, 0.34 W/m.k, and 0.2558 W/m.k at 15°C, respectively.

To ensure result consistency and verify the stability of the nano-PCMs, the tests were repeated by leaving the samples in the holder. After 48 hours, it was clear that the thermal conductivity (TC) values of all samples remained mostly unchanged, apart from those containing un-functionalised MWCNTs. The TC value of PAR introduced with un-functionalised MWCNTs was significantly reduced at all ranges of temperature. This decrease can be attributable to the poor dispersion induced by the MWCNTs hydrophobic nature [256], as seen in Figure 6.8. In contrast, the TC value of functionalised MWCNTs exhibited no change, highlighting the impact of the -COOH functional group attached to their surfaces. This group promotes strong bonding and favourable dispersion properties, thus maintaining TC stability of the functionalised MWCNT PAR.

A sudden increase in the TC value was noticed at a temperature of 25°C. It has been reported that the proximity of the melting point (28°C) caused faster molecular mobility within the lattice, which caused the temperature to rise [232]. As a result, the PAR's crystalline structure became unstable, resulting in a substantial TC value increase at 25°C. At this temperature, the functionalised MWCNTs-based PAR had the greatest TC value, measuring 0.749 W/m.k. However, when this phase change material (PCM) was completely melted at 35°C and 45°C, a considerable drop in TC values was seen for both PAR and all nano-composites. This drop can be attributed to the change from a solid-state organised microstructure to a disordered structure during melting. Also, solids have greater free electron motion since in solids conduction heat is mainly due to lattice vibrations, where molecules move within their lattice structures that is the reason that a higher TC value was observed in solids [231]. For all single-type particles as shown in Figure 6.8 (a), functionalised MWCNTs depict better performance indicating that the attachment of the carboxyl group to their surfaces and also F-MWCNTs minimised the surface resistance and promoted the interaction with PAR molecules, resulting in improving TC. Furthermore, solids have greater electron mobility & flexibility because heat conduction in solids is predominantly caused by lattice vibrations involving molecule movement inside

their lattice structures [76]. This inherent property explains why solids have higher TC values.

To investigate an economically viable alternative to the expensive MWCNTs, a combination with low-cost nanoparticles, in particular TiO_2, was introduced in various ratios with MWCNTs. The goal was to develop an ideal composite with great TC, improved stability, and low cost. Figures 6.8 (b)-(d) depict the investigation of this unique hybrid nanoparticles-based PCMs. Figure 6.8 (b) shows PAR with a composition of 75wt.% MWCNTs and 25wt.% TiO_2 nanoparticles had the highest TC values: 0.3326 W/m.k, 0.3331 W/m.k, 0.58801 W/m.k, 0.166 W/m.k, and 0.168 W/m.k at the range of temperature of 5°C, 15°C, 25°C, 35°C, and 45°C, respectively. It can be seen that un-functionalised MWCNTs PAR had lower TC values over a 48-hour period at all temperatures, dropping from 0.55 W/m.k to 0.457 W/m.k at 25°C. Similarly, at a 50:50 wt.% hybrid particle ratio, the TC values of pure MWCNTs based nano-PAR fell down after 48 hours, but functionalised MWCNT based nano-PAR remained unchanged, as shown in Figures 6.8 (b) and (c). Meanwhile, using 75% TiO_2 particles ensured the stability of unfunctionalised MWCNT PAR. This could be ascribed to the low number of MWCNTs (25wt.%) mixed with a higher fraction of TiO_2 nanoparticles, both contribute to the improved stability of nano-PAR. Previous researchers have found that TiO_2 nanoparticles had improved stability due to favourable intermolecular interactions with PCM molecules [225,239].

Functionalised MWCNT PCM outperformed unfunctionalised MWCNT PCM in terms of overall performance. The greater cost of MWCNTs makes widespread application difficult. This study addresses this concern by combining low-cost hybrid particles with MWCNTs, with the goal of achieving great TC while remaining cost-effective. It can be suggested that these novel hybrid particles that developed have the potential to be used on a wider scale in thermal energy storage (TES) applications.

The percentage enhancement of TC with the inclusion of nanoparticles was also measured for the PAR with single type of and hybrid nano particles at the temperature range from

15°C to 45°C, as can be seen in Figures 6.9 (a) –(d). The enhancement ratio was calculated using Equation 6.1.

$$\eta = \frac{K_{nano-PAR} - K_{PAR}}{K_{PAR}} * 100 \quad (6.1)$$

where, $K_{nano-PAR}$ and K_{PAR} are the thermal conductivities of nano-PAR composites and pure paraffin, respectively.

The enhancement of 33.9%, 75.28%, 83.55% and 29.06%, 71.54%, and 80.62% in the nano-PAR TC values with TiO_2, MWCNTs, F-MWCNTs nanoparticles was observed at 15°C and 25°C respectively as shown in Figure 6.9 (a). The maximum TC value enhancement of nano-PAR with F-MWCNTs is 160.4%. Moreover, at 35°C and 45°C a small increase of TC values, 21.18%, 29%, 39.17% and 22.16%, 30.04% and 36.43%, was obtained for TiO_2, MWCNTs, and F-MWCNT PAR, correspondingly. After 48 hours, the TC value of un-modified MWCNTs based PAR were reduced to 43.12%, 40.16%, 33.51%, 23.53%, and 19.87% at 15°C, 25°C, 35°C and 45°C respectively.

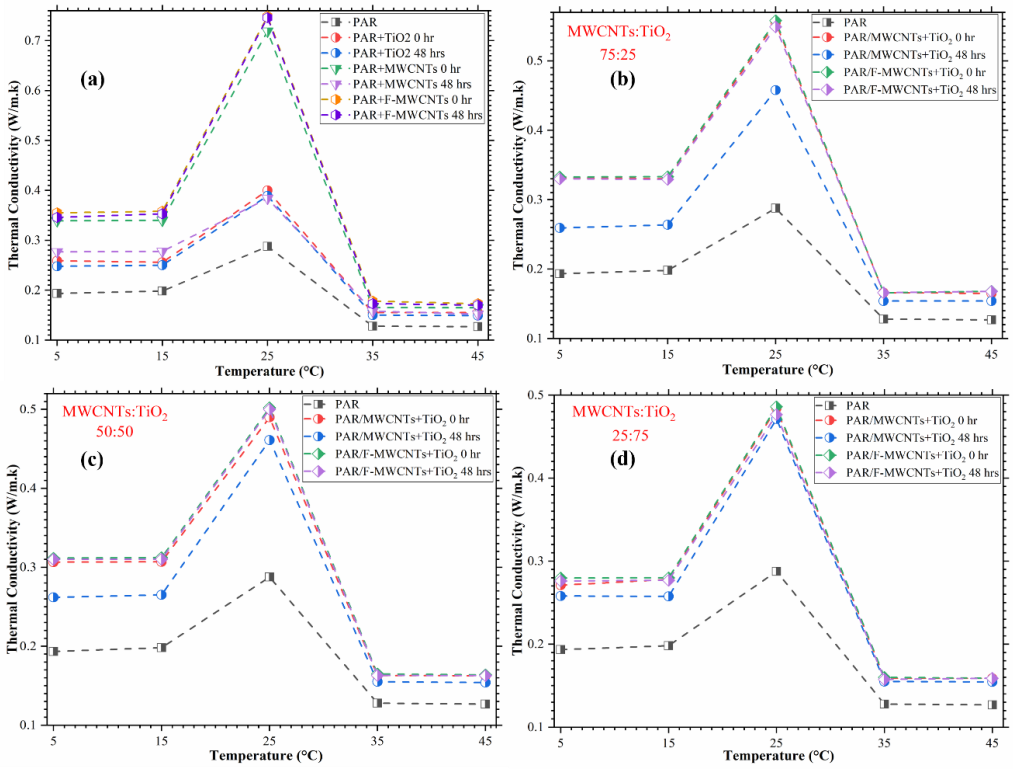

Figure 6.8 Thermal Conductivity of nano-PAR composites with single type of and hybrid nano particles.

It is evident that the single-type functionalised MWCNT PCM has showed greater TC enhancement compared to that with the TiO_2 and MWCNTs based hybrid particles. Since the TC value of CNTs is much higher than that of TiO_2 although they are not economical and sustainable without modification. However, the introduction of hybrid particles overcomes the economic challenges associated with unmodified MWCNT PCM while also improving TC significantly. It is also suggested that the hybridization process is an economically viable approach for improving thermal conductivity.

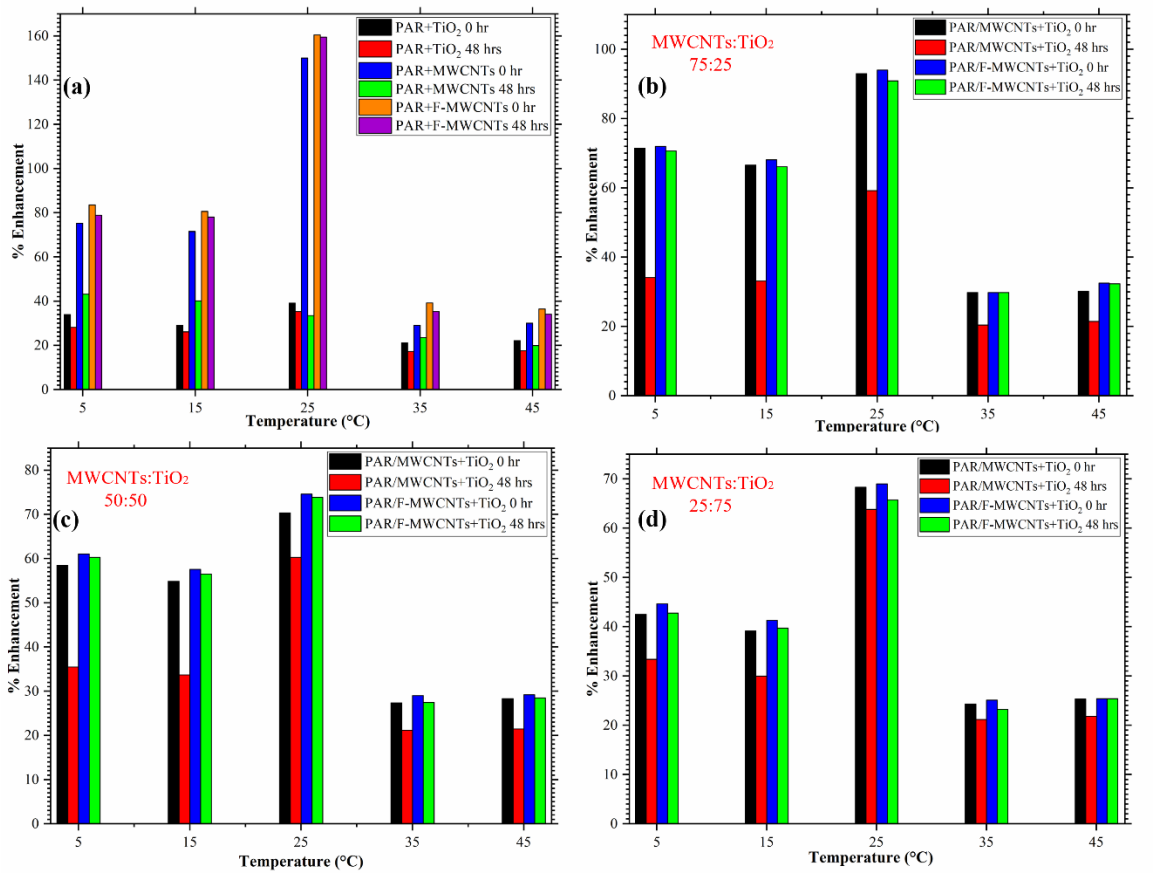

Figure 6.9 High performance in thermal conductivity nano-PAR composites with single and hybrid type of nano particles.

6.6 An analysis of material's phase changes

Figures 6.10 (a) – (d) and Table 6.1 show the DSC curves for nano-PAR composites with single type of and hybrid particles before and after 200 thermal cycles. Many studies have found that dispersing nanofillers in a PCM impacts the latent heat of fusion (ΔH) because there is less PCM per unit mass or volume and the dispersed particles can disturb the local

bonding environment of the PCM molecules [255]. In addition, numerous prior research articles have reported diverse outcomes regarding the impact of nanofiller dispersion on ΔH. Some studies have indicated a reduction in ΔH upon nanoparticle inclusion, whereas others have observed negligible alterations. For instance, Fan et al. [257] observed a decrease of up to 10% in ΔH upon introducing 1wt.% carbon-based nanofillers into paraffin wax. Conversely, Sami and Etesami [225] documented an increase in ΔH when incorporating up to 3wt.% TiO_2 nanoparticles into paraffin wax. In current investigation, the latent heat of all nano-PAR composites exhibited minimal variation compared to the values exhibited by pure paraffin.

For a single type nanofillers based PAR, a minimum decrement in ΔH for TiO_2 PAR was noticed compared to PAR with carbon based nanofillers. The decrement percentage in ΔH melting values for PAR/TiO_2, PAR/MWCNTs, and PAR/F-MWCNTs were -3.34%, -6.73%, and -7.66% respectively. Among the hybrid nanoparticle-based nano-PAR composites, wherein functionalized and un-functionalized MWCNT PARs were compared, the functionalized nano-PAR exhibited a more modest decrease in ΔH for melting and crystallization. Remarkably, the most significant reduction was -0.36% for F-MWCNTs+TiO2 (25:75) based PCM during melting, and -1.19% during crystallisation. The investigation revealed a notable pattern in the melting temperatures of several nano-composites, which primarily coincided with the melting point of the base PCM. Particularly, as compared to other nanocomposites, the PCM nanocomposite comprising hybrid nanoparticles of F-MWCNTs had a slightly higher melting temperature. This improvement is due to the increased stability of these hybrid particles-based PAR composites. The improved intermolecular interactions between the functionalized MWCNTs and PAR molecules can be responsible for the observed enhancement in melting and crystallisation behaviour [70]. Unlike the intermolecular forces that exist only between PAR molecules, the interactions involving these hybrid nanoparticles appear to have a higher propensity for heat absorption. As a result, a greater amount of energy is required for the hybrid nano-PAR composite to convert from its solid to liquid phase. Basically, the hybrid nano-PAR composite's distinctive characteristics, such as increased stability and improved intermolecular interactions, contribute to its elevated melting temperature and enhanced energy-absorbing properties during the phase transition process.The small

differences in melting/crystallisation enthalpies can be attributed to the different weights, structures, and sizes of the nanofillers used [258]. It can be suggested that the intermolecular interactions between F-MWCNTs+TiO_2 hybrid nanoparticles and the PAR PCM matrix contribute to a lesser reduction in latent heat when compared to other nano-PAR composites.

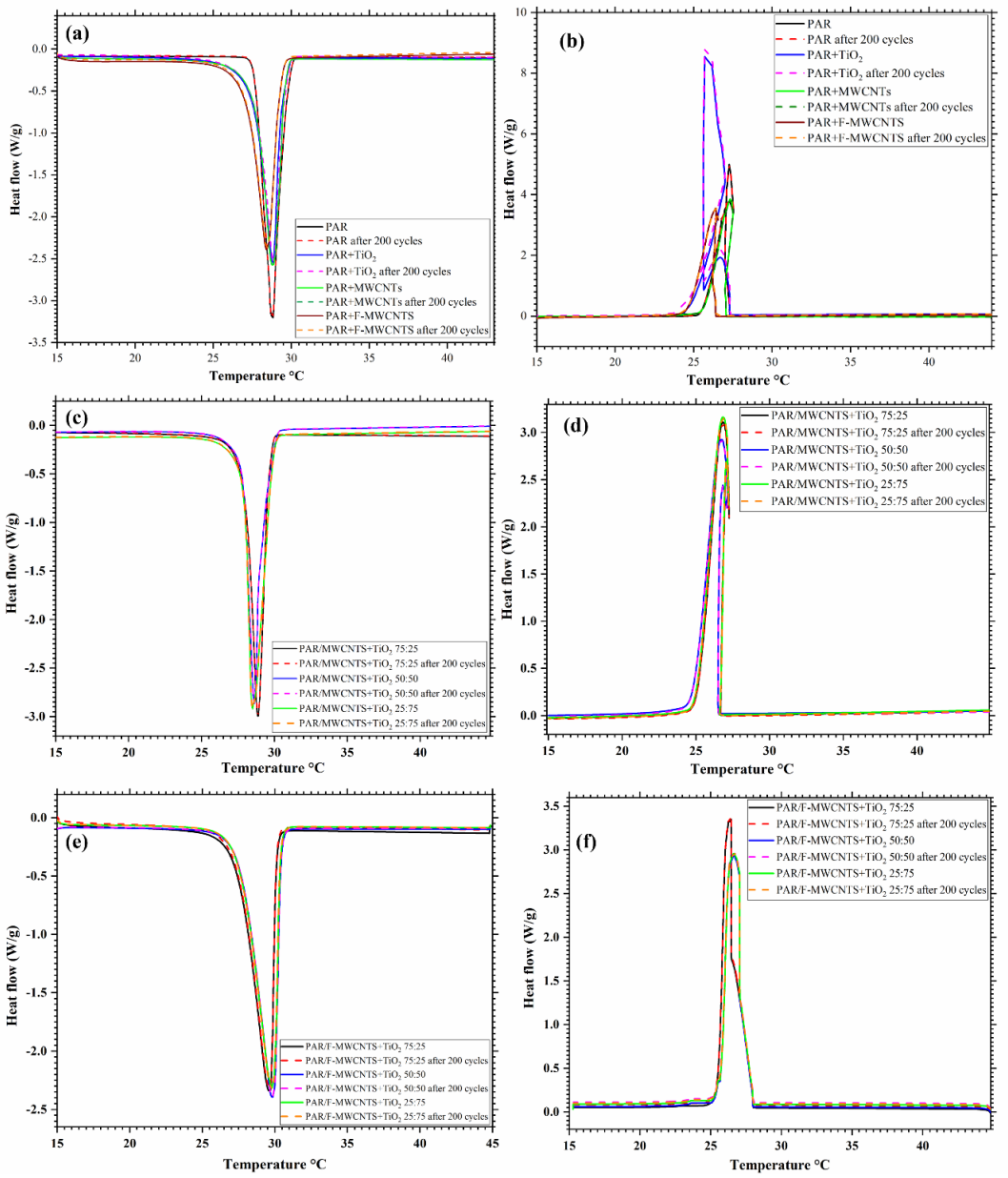

Figure 6.10 DSC heating and cooling curves of PAR nanocomposite with single type and hybrid nanoparticles.

6.7 Specific heat capacity (Cp) of the materials

The conventional MDSC technique was adopted to measure the specific heat capacity of pure PAR and nano-PAR samples. Notably, before conducting the calorimetric measurements, a sapphire disk was used to perform calibration, and an appropriate thermal cycle was designed. The measured Cp values of pure PAR and different nanocomposites as a function of temperature are depicted in Figures 6.11 (a) - (b).

In the solid phase (15°C to 25°C), a notable progressive increase in Cp was observed with rising temperature, as illustrated in Figure 6.11 (a). Notably, the incorporation of nanoparticles, as evidenced in the nano-PAR samples, resulted in a discernible enhancement of Cp for nano-PAR when compared to pure PAR. This phenomenon can be attributed to the inherently higher Cp values of the integrated nanoparticles, contributing to an overall augmentation. However, during the liquid phase (35°C to 45°C), Cp values exhibited notable stability, as demonstrated in Figure 6.11 (b). Similar trends were observed by [235,259]. In those studies, various nanofillers were introduced into the PCM. Particularly, carbon-based particles exhibited higher Cp values when compared to metal oxide particles. Furthermore, it was noted that the Cp values of these particles increased in the solid phase and remained constant in the liquid phase. These consistent findings align with the outcomes of our present investigation. The maximum Cp value of 3.5 J/g °C and 2.5 J/g °C was observed for F-MWCNTs based nano-PAR at 25°C and 45°C, correspondingly.

In a detailed analysis, it was observed that the inclusion of nanofillers in the PAR matrix led to a substantial improvement in Cp, both in the solid and liquid states. This improvement can be attributed to several key factors: (a) the heightened specific surface energy due to the nanoparticle's expansive surface areas per unit volume [260], (b) the presence of impurities [261], and (c) an increased level of anharmonicity resulting from atomic interactions, which are exacerbated as the nanofillers expand in volume. These findings underscore the positive impact of nanofillers on the heat capacity of the composite material, offering valuable insights for potential TES applications.

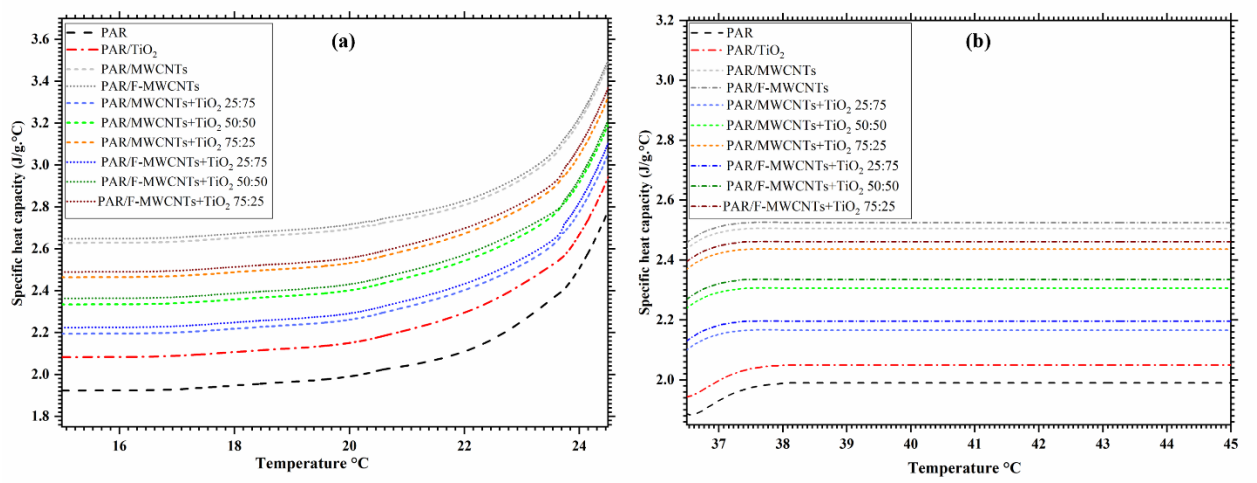

Figure 6.11 Specific heat capacity of two state PAR and nano-PAR samples: (a) solid, (b) liquids.

6.8 An analysis of thermal consistency

Thermogravimetric analysis (TGA) was used to evaluate the thermal stability of PAR-based nanocomposites, with weight loss percentages used as indicators of sample behaviour across a temperature range of 15°C to 400°C. The weight loss percentage profiles, illustrated in Figure 6.12, portray the thermal responses of both pure PAR and nano-PAR specimens. It was noticed that the pristine PAR and nano-PAR samples remained stable with no detectable weight loss up to approximately 130°C, as the temperature increased, the weight loss became more pronounced. The maximum degradation temperature of ~140°C was observed for F-MWCNTs+TiO_2 (25:75) hybrid nano-PAR composite. Overall, with the infusion of nanoparticles within PAR resulted in an increase in the degradation temperature compared to the pure PAR. The onset degradation temperature of all pure PCM and nano-PCM samples fell within a narrow range of ±10°C, which confirms that the developed nano-PAR composites are thermally stable and can be operated up to 130°C. The thermal stability claims are supported further by the derivative thermogravimetry (DTG) profiles shown in Figures 6.13 (a) – (b). The nano-PAR specimens revealed constant stability up to 130°C, with the hybrid F-MWCNTs+TiO_2 particle-infused PAR composite exhibiting the highest degradation temperature among the tested specimens. The thermal stability of the developed nano-PAR composites highlights their feasibility for applications requiring robust performance at temperatures up to 130°C.

Table 6.1 Phase transition properties of single and hybrid nano-PAR composites.

Sample	Melting			Crystallisation			
	T_{melt}	ΔHm_{exp}	Change in LH %	T_{crys}	ΔHm_{exp}	Change in LH %	ΔT
Paraffin (PAR)	28.90	248.4		27.26	251.6		1.64
Paraffin (PAR) 200 cycles	28.92	248.2	-0.08	27.24	251.1	-0.19	1.68
PAR/TiO_2	28.85	240.1	-3.34	26.66	241.3	-4.09	2.19
PAR/TiO_2 200 cycles	28.88	240.1	-3.35	26.68	241.3	-4.1	2.2
PAR/MWCNTs	28.94	231.7	-6.73	27.32	233.2	-7.31	1.62
PAR/MWCNTs 200 cycles	28.96	229.9	-7.45	27.30	232.1	-7.75	1.66
PAR/F-MWCNTs	28.46	229.4	-7.66	26.78	232.2	-7.71	1.68
PAR/F-MWCNTs 200 cycles	28.44	227.6	-8.38	26.73	231.3	-8.06	1.71
PAR/M+ T 75:25	28.88	233.0	-6.20	26.84	234.9	-6.63	2.04
PAR/M+T 75:25 200 cycles	28.82	232.3	-6.49	26.83	233.0	-7.39	1.99
PAR/ M+T 50:50	28.53	231.3	-6.89	26.77	231.3	-8.07	1.76
PAR/ M+T 50:50 200 cycles	28.51	230.2	-7.33	26.76	231.9	-7.82	1.75
PAR/ M+T 25:75	28.48	234.6	-5.56	26.85	235.3	-6.47	1.63
PAR/ M+T 25:75 200 cycles	28.82	233.3	-6.08	26.44	234.8	-6.67	2.38
PAR/ F-M+T 75:25	29.58	236.1	-4.95	26.71	238.5	-5.20	2.87
PAR/ F-M+T 75:25 200 cycles	29.57	234.2	-5.72	26.10	237.2	-5.72	3.47
PAR/ F-M+T 50:50	29.82	247.1	-0.52	26.44	248.5	-1.23	3.38
PAR/ F-M+T 50:50 200 cycles	29.80	245.3	-1.25	26.41	246.3	-2.10	3.39
PAR/ F-M+T 25:75	29.71	247.5	-0.36	26.69	248.6	-1.19	3.02
PAR/ F-M+T 25:75 200 cycles	29.69	246.0	-0.96	26.70	247.9	-1.47	2.99

T_{melt}: melting temperature (°C), **T_{crys}**: crystallisation temperature (°C), **ΔHm_{exp}**: Experimental enthalpy (J/g), **ΔT**: super–cooling temperature (°C), **M+T:** Pure MWCNTs+TiO_2, **F-M+T:** Functionalised-MWCNTs+TiO_2.

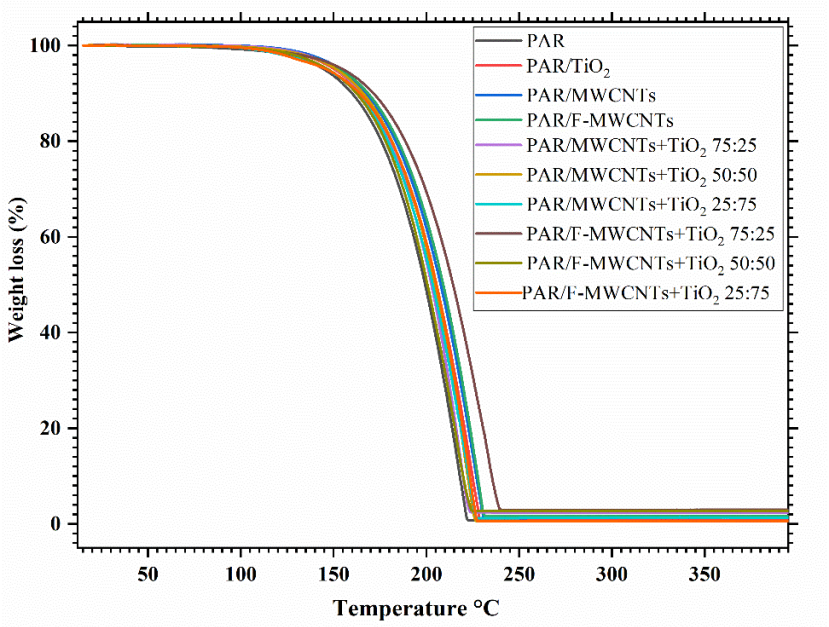

Figure 6.12 Thermogravimetric analysis curves of single and hybrid nano-PAR composites.

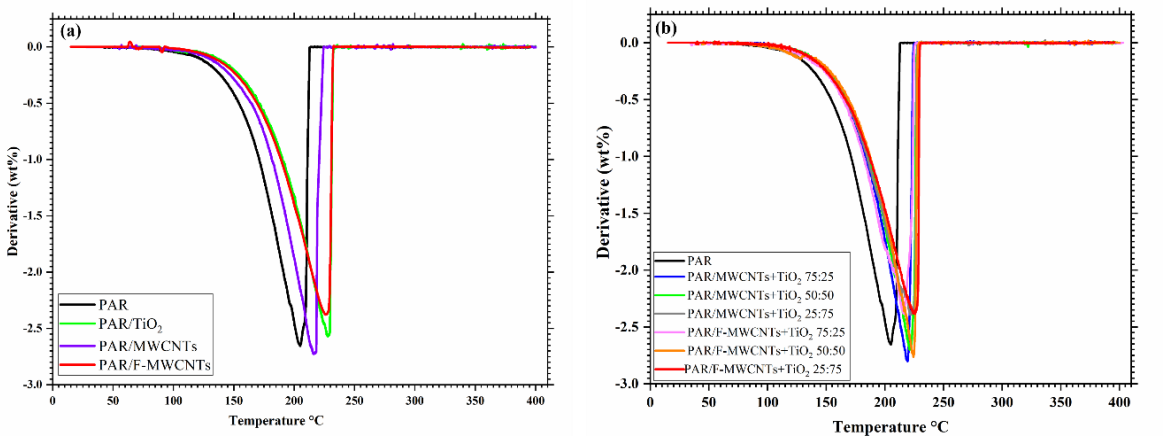

Figure 6.13 Derivative thermogravimetry (DTG) profiles of nano PCMs: (a) single, (b) hybrid nano-PAR samples.

6.9 Summary

A thorough analysis has been performed on hybrid nanoparticles (i.e., F-MWCNTs and TiO_2) enhanced nano-PCMs, highlighting the structures as well as both thermal and chemical properties of these materials. By incorporating functionalised MWCNTs with TiO_2, the thermal conductivity of the composites was improved by 80.62% without compromising their chemical stability. Despite these gains in thermal conductivity, the latent heat of fusion for the nano-PCM composed of functionalized MWCNTs and TiO_2 experienced a modest reduction of approximately 7.66%, illustrating the trade-offs associated with nanoparticle incorporation. By an effectively integration of the results with previous studies, it has been provided that a

comprehensive understanding of how nanoparticle-enhanced PCMs can be optimised for both performance and cost-effectiveness in thermal management applications.

CHAPTER7: DISCUSSION AND COMPARISON OF THERMOPHYSICAL CHARACTERISTICS OF NANO-PCMs

The findings in Chapters 2, 4, 5, and 6 have been assessed and summarised in this chapter, which focused on the incorporation of various nanofillers within PCM. MWCNTs, TiO_2, and GNP were selected for their unique features that could increase the thermal performance and stability of PCMs. How various nano-fillers, both single and hybrid type, affect the thermal characteristics, stability, and economic feasibility of PCMs in actual applications has been explained and discussed. By comparing the results across different nano-enhancements, this discussion seeks to highlight the optimal strategies for improving PCM formulations.

7.1 Foundations and potential of nano-enhanced PCMs

In chapter 2, the foundational concepts and initial potential of integrating nanoparticles with phase change materials are highlighted, providing critical insights into the enhanced properties and behaviours of these composites. Chapter 2 has provided a critical analysis of how nanoparticles enhance the thermal properties of phase change materials, and emphasised the significant impact of nanoparticles particularly carbon-based nanoparticles like graphene and carbon nanotubes (CNTs), renowned for their exceptionally high thermal conductivities, which range from 2000 to 6000 W/mK. These values are significantly superior to those of traditional PCMs and demonstrate how the incorporation of these nanoparticles can dramatically increase the overall thermal conductivity of the composite materials.

In contrast, metal and metal oxide nanoparticles such as Al_2O_3 and TiO_2 show more modest thermal conductivities, typically ranging from 8.4 to 40 W/mK. While these figures are lower than those of carbon-based nanoparticles, metal and metal oxide nanoparticles still contribute positively to the thermal management of PCMs. They enhance thermal stability and mitigate cycling degradation, which is vital for applications that undergo repetitive thermal cycling. This characteristic is crucial for ensuring the durability and structural integrity of PCMs across multiple melting and solidification cycles. The introduction of nanoparticles has been generally found to enhance the thermal conductivity, though at the potential cost of reducing latent heat capacity. This reduction is attributed to the displacement of PCM volume by non-phase changing nanoparticles, which could dilute the overall phase change effectiveness. The role of

nanoparticle concentration and size in modulating PCM properties is very critical. It was observed that while increasing the nanoparticle concentration boosts thermal conductivity, it may inversely impact the latent heat capacity due to the replacement of more PCM volume.

7.2 A comparative analysis of chemical compatibility and structural integrity

This section presents a lateral comparison of the chemical compatibility and structural integrity of nano-enhanced phase change materials investigated in Chapters 4, 5, and 6. The focus is on understanding how different nanoparticles and their configurations, including single, functionalised, and hybrid forms, interact chemically with paraffin and affect its crystalline structure.

7.2.1 FT-IR analysis

In all results from Chapters 4, 5, and 6, FT-IR spectroscopy was used to investigate the chemical interactions between paraffin and the added nanoparticles. Across all samples, no significant new peaks or shifts were observed, indicating that the interactions between paraffin and the nanoparticles are purely physical. This consistency in results was evident from Figure 4.2 for mono nanoparticles (GNP, MWCNTs, TiO_2) in Chapter 4, functionalised MWCNTs in Chapter 5, and hybrid nanoparticles in Chapter 6.

Specifically, the FT-IR spectra for functionalised MWCNTs shown in Figure 5.5 in Chapter 5 revealed characteristic peaks of carboxyl groups (O-H and C=O stretching), indicating successful functionalisation. However, these peaks were absent in the FT-IR spectra of the composite PCMs, likely due to the low concentration of functionalised MWCNTs within the paraffin matrix. This was also observed in the hybrid combinations showed in Figure 6.2 of Chapter 6, confirming the physical interaction in both single and hybrid forms. This finding is critical as it confirms that the incorporation of nanoparticles does not chemically alter the PCM, preserving its inherent properties.

7.2.2 XRD analysis

The results from XRD analyses across all chapters have showed that the addition of nanoparticles, whether single, functionalised, or hybrid, do not introduce new peaks or alter the crystallinity of paraffin, as shown in Figures 4.3, 4.4 (Chapter 4), 5.6, 5.7 (Chapter 5), and 6.3, 6.4 (Chapter 6). The diffraction peaks corresponding to the crystal structures of the

nanoparticles (GNP, MWCNTs, TiO_2) and the anatase form of TiO_2 were consistently observed.

In Chapter 4, the presence of GNP, MWCNTs, and TiO_2 in paraffin showed no new XRD peaks, indicating no structural change to the paraffin matrix. Chapter 5's XRD analysis of functionalised MWCNTs confirmed successful removal of impurities without altering the bulk structure of MWCNTs. Chapter 6 further reinforced these findings, showing that even with hybrid configurations of functionalised MWCNTs and TiO_2, the paraffin's crystalline structure remained unchanged. Whether the nanoparticles are used in single, functionalised, or hybrid forms, the paraffin's structural integrity remains intact, ensuring the stability of the PCM. The functionalisation of MWCNTs improves their dispersion and stability within the PCM without altering the core structure, as evidenced by both FT-IR and XRD analyses.

Overall, the lateral comparison of chemical compatibility and structural integrity across Chapters 4, 5, and 6 indicates that the integration of various forms of nanoparticles into paraffin-based PCMs results in physical interactions without chemical or structural alterations to the PCM. This consistency across different configurations highlights the robustness and compatibility of these nano-enhancements for advanced thermal energy storage applications.

7.3 Comparative thermal conductivity performance

Thermal conductivity is a critical property of materials used in thermal energy storage systems, such as PCMs. High thermal conductivity in these materials significantly enhances their energy efficiency by improving the rate at which they absorb, store, and release heat. This section presents a comprehensive comparison of the TC performance of various nano-enhanced phase change materials analysed across Chapters 4, 5, and 6. It is highlighted how different types and configurations of nanoparticles, including single, functionalised, and hybrid forms, influence the TC of paraffin-based PCMs. Tabel 7.1 shows the comparison of thermal conductivity of both single and hybrid nano-PCMs at 1 wt.% of nanoparticles.

7.3.1 Thermal Conductivity in Solid State (5°C to 25°C)

- **Nano-PCM with single nanoparticles:**

  The TC values of RT-28+TiO_2 at 1 wt.% increased from 0.1934 W/m·K (pure RT-28) to approximately 0.249 W/m·K at 5°C and 0.2558 W/m·K at 15°C. The enhancement continues at 25°C with a value of 0.4 W/m·K, showing moderate improvements due to the

relatively lower intrinsic thermal conductivity of TiO_2. The TC of RT-28+GNP at 1 wt.% has showed significant improvements, reaching 0.759 W/m·K at 25°C, which is a considerable enhancement from the pure RT-28 TC value. GNP provided a better enhancement due to its high intrinsic thermal conductivity. For RT-28+MWCNTs at 1 wt.%, the TC values were 0.33 W/m·K at 5°C and increased to 0.719 W/m·K at 25°C, indicating a substantial enhancement. Functionalisation of MWCNTs further improved TC, with values reaching 0.749 W/m·K at 25°C, highlighting the effectiveness of functionalisation in improving dispersion and bonding.

- **Nano-PCM withhybrid nanoparticles:**

  The hybrid of GNP and MWCNTs at 1 wt.% provided the highest TC values among the tested configurations. At 25°C, the TC was 0.785 W/m·K, reflecting a 170% enhancement. This significant improvement is attributed to the synergistic effects of combining two high thermal conductivity materials. The TC values for RT-28+TiO_2+MWCNTs at 1 wt.% were 0.484 W/m·K at 25°C, which is lower than the GNP+MWCNTs hybrid but still a notable improvement over single TiO_2 based PCM. The TC for RT-28+TiO_2+GNP at 1 wt.% reached 0.51 W/m·K at 25°C, indicating that while the enhancement is significant, it is not as high as the GNP+MWCNTs hybrid. The functionalised MWCNTs combined with TiO_2 at different ratios showed stable and high TC values. For instance, the F-MWCNTs/TiO_2 (75:25) hybrid reached 0.55801 W/m·K at 25°C, maintaining stability over time.

7.3.2 Thermal Conductivity in Liquid State (35°C to 55°C)

- **Nano-PCM with single nanoparticles:**

  As indicated in sections 4.7, 5.8, and 6.5 that in the liquid state, the TC values generally decreased due to the disorganised microstructure of the melted PCM, which reduces lattice vibrations and free-electron motion that contribute to heat conduction in solids. The TC values of RT-28+TiO_2 at 1 wt.% dropped to around 0.155 W/m·K at 35°C and further decreased to approximately 0.154 W/m·K at 55°C. RT-28+GNP at 1 wt.% showed a TC value of 0.364 W/m·K at 5°C, which dropped significantly in the liquid phase, with values around 0.1679 W/m·K at 45°C. The TC value for RT-28+MWCNTs at 1 wt.% decreased to 0.164 W/m·K at 55°C. It is evident that functionalised MWCNTs demonstrated better performance, maintaining higher TC values due to improved dispersion.

- **Nano-PCM with hybrid nanoparticles:**

  The TC values for RT-28+GNP+MWCNTs hybrid at 1 wt.% were higher than other configurations, with 0.785 W/m·K at 25°C, but reduced to around 0.173 W/m·K at 55°C. Despite the decrease, this hybrid still outperformed others in the liquid state. RT-28+TiO_2+MWCNTs at 1 wt.% showed a TC value of 0.484 W/m·K at 25°C, which decreased to 0.158 W/m·K at 55°C, maintaining a relatively higher TC compared to single TiO_2. The TC value for RT-28+TiO_2+GNP at 1 wt.% was 0.0.51 W/m·K at 25°C, dropping to around 0.159 W/m·K at 55°C.

  It can be seen that the functionalised hybrid of F-MWCNTs and TiO_2 (50:50) maintained a TC of 0.5021 W/m·K at 25°C, and despite a reduction in the liquid state, it remained higher than non-functionalised hybrids. It is suggested that the functionalisation significantly contributed to maintaining higher TC values across the temperature range.

  It has been observed, as shown in Figure 5.3 and Figure 5.11, that functionalisation of MWCNTs significantly improved the stability and thermal conductivity of the nano-PCMs, respectively. This improvement is due to better dispersion, reduced surface resistance, and enhanced interaction between the nanoparticles and PCM. It is evident that the use of functionalised and hybrid nanoparticles offers a cost-effective solution for enhancing the thermal properties of PCMs. These enhancements make nano-PCMs suitable for practical

Table 7.1 A comparative analysis of thermal conductivity results at 1 wt.% nanoparticle concentration for nano enhanced PCMs.

Samples	**5°C**	**15°C**	**25°C**	**35°C**	**45°C**
Paraffin (PAR)	0.195	0.199	0.290	0.128	0.127
PAR/TiO_2	0.249	0.255	0.400	0.155	0.154
PAR/MWCNTs	0.330	0.34	0.719	0.165	0.164
PAR/GNP	0.364	0.367	0.759	0.168	0.167
PAR/MWCNTs+GNP 25:75	0.393	0.394	0.785	0.174	0.173
PAR/MWCNTs+TiO_2 25:75	0.271	0.278	0.484	0.159	0.158
PAR/GNP+TiO_2 25:75	0.300	0.299	0.510	0.16	0.159
PAR/F-MWCNTs	0.350	0.358	0.749	0.178	0.173
PAR/M+ T 75:25	0.331	0.330	0.555	0.166	0.165
PAR/ M+T 50:50	0.306	0.306	0.489	0.162	0.162
PAR/ M+T 25:75	0.271	0.278	0.484	0.159	0.158
PAR/ F-M+T 75:25	0.332	0.333	0.558	0.166	0.168
PAR/ F-M+T 50:50	0.311	0.312	0.502	0.165	0.163
PAR/ F-M+T 25:75	0.279	0.280	0.486	0.160	0.159

*** M+T:** Pure MWCNTs+TiO_2, **F-M+T:** Functionalised-MWCNTs+TiO_2.

applications in thermal energy storage systems, contributing to improved energy efficiency and sustainability.

Overall, the lateral comparison of TC performance across various nanoparticle configurations highlights the significant improvements achievable with carbon-based and hybrid nanoparticles. Functionalised MWCNTs, particularly in hybrid forms, offer the best balance of performance and stability, making them ideal for advanced thermal energy storage applications.

7.4 Comparative analyses of latent heat and specific heat capacity

A comprehensive lateral comparison of the thermal properties is presented specifically focusing on the latent heat and specific heat capacity of various nano-enhanced phase change materials (PCMs) examined in Chapters 4, 5, and 6.

7.4.1 Latent heat of fusion and crystallisation

The latent heat of fusion and crystallisation is a critical parameter in evaluating the efficiency of PCMs in TES systems. It was observed in the studies that the inclusion of nanoparticles generally resulted in minor reductions in the latent heat values of the PCMs. As shown in Table 7.2, pure paraffin (RT-28) exhibited latent heats of melting and crystallisation of 248.4 J/g and 251.7 J/g, respectively. When single nanoparticles were introduced, TiO_2 demonstrated the smallest reduction, with a latent heat of melting at 239.2 J/g and crystallisation at 241.3 J/g at 1 wt%. This suggests that TiO_2-based PCMs maintain better stability and energy storage capacity compared to carbon-based nanoparticles. In contrast, GNP and MWCNTs exhibited more reductions in latent heat. For instance, GNP at 1 wt% reduced the latent heat of melting to 232.4 J/g and crystallisation to 233.5 J/g. Similarly, MWCNTs reduced the values to 231.3 J/g and 233.3 J/g, respectively. The reduction in latent heat for these carbon-based nanoparticles can be attributed to their higher thermal conductivity, which accelerates paraffin evaporation and affects heat storage capability [29].

As shown in table 7.2, functionalised MWCNTs showed improved stability, with latent heat values slightly lower than unfunctionalised MWCNTs. For example, F-MWCNTs at 1 wt% demonstrated latent heats of 229.7 J/g for melting and 232.2 J/g for crystallisation, indicating that surface modification enhances the thermal properties by reducing surface resistance and improving dispersion within the PCM matrix.

Hybrid nanoparticles presented a balanced performance, combining the benefits of individual nanoparticles. MWCNTs+TiO_2 and GNP+TiO_2 hybrids have showed reduced impacts on latent heat compared to single nanoparticles. Notably, F-MWCNTs+TiO_2 (75:25 wt%) have exhibited latent heats of 236.1 J/g and 238.5 J/g for melting and crystallisation, respectively. Moreover, PAR/F-MWCNTs+TiO_2 (25:75 wt%) have also showed latent heats of 247.5 J/g for melting and 248.6 J/g for crystallisation, demonstrating values very close to pure paraffin. This indicates that hybrid particles with a higher content of TiO_2 have a lesser effect on the latent heat of fusion and crystallisation, making them more stable and efficient for practical applications.

Table 7.2 A comparative analysis of latent heat results at 1 wt.% nanoparticle concentration for nano-enhanced PCMs from Chapters 4, 5, and 6.

Samples	**Melting**		**Crystallisation**	
	ΔHm_{exp} (J/g)	T_{peak} (°C)	ΔHm_{exp} (J/g)	T_{peak} (°C)
Paraffin (PAR)	248.4	28.92	251.7	27.26
PAR/TiO_2	239.2	28.83	241.32	26.67
PAR/MWCNTs	231.3	28.96	233.3	27.35
PAR/GNP	232.4	28.59	233.5	27.67
PAR/MWCNTs+GNP 25:75	230.9	28.96	234.1	27.19
PAR/MWCNTs+TiO_2 25:75	234.6	28.86	235.5	27.48
PAR/GNP+TiO_2 25:75	235.4	28.88	236.8	27.20
PAR/F-MWCNTs	229.7	28.46	232.2	26.78
PAR/M+ T 75:25	233.0	28.48	234.9	26.85
PAR/ M+T 50:50	231.3	28.53	231.9	26.77
PAR/ M+T 25:75	234.6	28.48	235.3	26.85
PAR/ F-M+T 75:25	236.1	29.58	238.5	26.71
PAR/ F-M+T 50:50	247.1	29.82	248.5	26.44
PAR/ F-M+T 25:75	247.5	29.96	248.6	26.69

T_{peak}: peak temperature (°C), **ΔHm_{exp}**: latent heat of melting experimental (J/g)

7.4.2 Specific Heat Capacity (Cp)

The Cp of the PCMs was evaluated in both solid and liquid states. Pure paraffin exhibited Cp values of 1.928 J/g°C in the solid state and 1.887 J/g°C in the liquid state. It was observed that the addition of nanoparticles generally increased the specific heat capacity, enhancing the PCM's ability to store thermal energy. Single nanoparticles showed various improvements in Cp. TiO_2-based PCMs demonstrated moderate increases, with Cp values of 3.112 J/g°C in the solid state and 2.315 J/g°C in the liquid state at 1 wt%. GNP and MWCNTs exhibited higher increases, with GNP showing Cp values of 3.948 J/g°C (solid) and 2.475 J/g°C (liquid), and MWCNTs showing 3.838 J/g°C (solid) and 2.505 J/g°C (liquid) at 1 wt%. Functionalised MWCNTs further improved the specific heat capacity compared to their unfunctionalised MWCNTs. F-MWCNTs demonstrated Cp values of 3.858 J/g°C in the solid state and 2.525 J/g°C in the liquid state at 1 wt%. This indicates that functionalisation significantly enhances the thermal properties by improving the interaction between the nanoparticles and the PCM molecules.

As shown in Figures 4.7 and 6.11, hybrid nanoparticles, MWCNTs+GNP and MWCNTs+TiO_2 have showed enhanced specific heat capacities, with MWCNTs+TiO_2 (1 wt%) exhibiting Cp values of 3.512 J/g°C in the solid state and 2.388 J/g°C in the liquid state. The F-MWCNTs+TiO_2 (75:25 wt%) hybrid has showed the highest improvement, with Cp values of 3.5 J/g°C in the solid state and 2.5 J/g°C in the liquid state, demonstrating that hybrid configurations can significantly enhance the thermal properties of PCMs. The small difference in Cp values for both functionalised and unfunctionalised MWCNTs with TiO_2 suggests that they effectively enhance thermal properties, with functionalisation providing slightly better dispersion and bonding within the PCM matrix.

7.5 Stability and long-term performance comparison

The stability and long-term performance of various nano-enhanced phase change materials were examined and have been presented across Chapters 4, 5, and 6. The focus of this section is on the dispersion stability of the nanoparticles, repeatability of thermal conductivity measurements, and the thermal and chemical stability of the PCMs over multiple heating and cooling cycles.

7.5.1 Dispersion Stability and Repeatability

It has been presented across all chapters that the dispersion stability of the PCMs varied significantly depending on the type of nanoparticles used and whether they were functionalised. Chapter 4 revealed that single MWCNT-based PCMs exhibited significant sedimentation due to the hydrophobic nature of MWCNTs, leading to poor dispersion stability. However, hybrid nano-PCMs, such as those combining MWCNTs with TiO_2 or GNP, showed uniform dispersion after 48 hours. This improved stability in hybrid formulations was attributed to the synergistic interactions between the different nanoparticles, which facilitated better dispersion. The presence of TiO_2 or GNP nanoparticles helps to disrupt the tendency of MWCNTs to aggregate, thereby improving their distribution within the PCM matrix. This effect can be attributed to the different surface properties and interactions at the molecular level. TiO_2 nanoparticles, for instance, have surface properties that can interact more effectively with the PCM, creating a more stable suspension. In contrast, the GNPs provide a planar structure that can enhance the overall network within the PCM, preventing sedimentation and ensuring a more uniform dispersion. These synergistic interactions enhance the overall stability and performance of the nano-PCMs, making them more effective for thermal energy storage applications. Chapter 5 reinforced these findings, showing that functionalised MWCNTs remained well-dispersed even after 48 hours in a thermal bath, unlike unfunctionalised MWCNTs. This indicates that surface modification of MWCNTs significantly enhances their dispersion stability, preventing agglomeration and sedimentation. Chapter 6 further supported the superior performance of functionalised MWCNTs, demonstrating that these remained stably dispersed within the PCM matrix over extended periods. This was evident in both single and hybrid configurations, with functionalised MWCNTs showing no significant settling, unlike unfunctionalised MWCNTs, which rapidly precipitated.

7.5.2 Long-Term Thermal and Chemical Stability

Long-term thermal stability was assessed by subjecting the nano-PCMs to multiple heating and cooling cycles. Chapter 4 demonstrated that the phase change properties of the PCMs were not significantly affected after 100 cycles, with variations in phase change temperatures and enthalpies being less than 1%. This indicated high stability, which was further confirmed after 200 cycles, where both pure PCM and hybrid nano-PCMs (e.g., GNP+MWCNTs) remained stable without notable changes, as shown in Figure 4.14. Chapter 5 similarly showed that functionalised MWCNT-based PCMs exhibited minimal changes in thermal properties after

200 cycles, with less than 1% variation, indicating excellent long-term stability, depicted in Figure 5.8. The functionalised PCMs outperformed unfunctionalised ones, which exhibited greater variability and instability. In Chapter 6, both functionalised and hybrid nano-PCMs maintained their thermal properties over 200 cycles, with functionalised MWCNTs showing superior stability compared to unfunctionalised ones, as highlighted in Figure 6.10 and table 6.1. The consistent performance of functionalised nano-PCMs suggests that the surface treatment of nanoparticles plays a crucial role in achieving long-term stability. This finding implies that future research and development should focus on optimising nanoparticle surface modifications to enhance the durability and effectiveness of nano-PCMs in practical applications. The ability of these materials to withstand numerous thermal cycles without significant degradation makes them viable candidates for sustainable and efficient thermal energy storage solutions.

7.6 Practical implications and cost-effectiveness

The findings from the comparative analysis of nano-PCMs have significant practical implications, particularly for their application in TES systems. The enhanced thermal properties, stability, and long-term performance of these materials offer several advantages for real-world applications, while considerations of cost-effectiveness ensure their viability for widespread use.

7.6.1 Enhanced Thermal Properties

The improved TC and Cp of nano-PCMs suggest that these materials can significantly enhance the efficiency of TES systems. The incorporation of nanoparticles, especially functionalised and hybrid nanoparticles, leads to better thermal management by increasing the rate of heat transfer and storage capacity. This is particularly important for applications requiring rapid charging and discharging cycles, such as in building energy management, where efficient thermal regulation can lead to substantial energy savings and improved indoor thermal comfort. For instance, hybrid nanoparticles combining functionalised MWCNTs (50%) with TiO_2 (50%) have demonstrated 73% increase in thermal conductivity and showed excellent stability. This combination not only maintained high thermal conductivity over time but also showed minimal reductions in latent heat, ensuring that the thermal storage capacity of the PCM remains effective even after a significant number of thermal cycles. This makes these materials ideal for applications where long-term reliability and efficiency are critical.

7.6.2 Cost-Effectiveness

While the incorporation of nanoparticles into PCMs enhances their thermal properties, the cost-effectiveness of these materials is a crucial factor for their commercial viability. MWCNTs, priced at £118 per gram, provide excellent thermal performance but are expensive. However, the hybridising with cost-effective TiO_2, which costs £2.46 per gram, offers a practical solution.

Hybrid nanoparticles, particularly those with a higher proportion of TiO_2, provide a cost-effective alternative without compromising on performance. For example, the F-MWCNTs+TiO_2 (25:75 wt.%) hybrid nano-PCM showed minute (0.36%) decrease in LH of fusion which is very close to pure paraffin and increase in TC by 67.5%, demonstrating that a higher TiO_2 content can achieve the desired thermal enhancements while keeping costs manageable. This approach not only reduces material costs but also leverages the superior stability and thermal properties of TiO_2, making it a potential viable option for large-scale applications. Moreover, the use of functionalised nanoparticles, which improve dispersion stability and reduce sedimentation, minimises the need for additional stabilising agents or complex processing techniques, further reducing costs. The scalability of these materials also enhances their cost-effectiveness, making them suitable for various TES applications, from residential heating systems to industrial thermal management.

7.7 Summary

Various comparative analyses have highlighted the superior stability and long-term performance of functionalised and hybrid nano-PCMs. Functionalised MWCNTs consistently demonstrated improved dispersion stability, maintained thermal conductivity, and exhibited minimal changes in thermal properties over extended thermal cycling. Hybrid nanoparticles, particularly those combining functionalised MWCNTs with TiO_2, offered balanced performance with enhanced stability and minimal impact on latent heat. Moreover, the hybrid nano-PCMs combine superior thermal properties with stability and cost-effectiveness, making them promising candidates for improving energy efficiency and sustainability in various thermal management sectors. These findings underscore the potential of functionalised and hybrid nano-PCMs for reliable and efficient thermal energy storage applications. The results collectively indicate that functionalisation and hybridisation are effective strategies for enhancing the stability and long-term performance of nano-PCMs.

CHAPTER: 8 CONCLUSIONS AND FUTURE WORK

This chapter provides a comprehensive conclusion to our research, which aimed to develop and critically evaluate the performance of nano-enhanced PCM for use in building energy storage systems. The study was structured around a series of precise objectives: beginning with an exhaustive literature review to identify existing knowledge gaps and to lay down a solid theoretical framework. Following this foundation, the investigation delved into the selection and testing of PCM combined with different nano-fillers, examining their impact on the thermal properties of the PCM. The research specifically focused on understanding the effects of nanofiller concentrations and explored the distinctions between mono and hybrid nanofillers. Furthermore, it assessed the influence of surface-modified nanoparticles on the thermophysical characteristics of the PCM. This final chapter summarises the significant insights gained from the study, evaluates how these findings meet the initial research objectives, and discusses potential directions for future research in this vital field of energy technology. Each research objective of the research is addressed below with the findings from the study.

8.1 Conclusions

8.1.1 Chemical Compatibility and Structural Stability:

- Chemical interaction analyses and crystal structures of nano PCMs with FT-IR and XRD confirmed that the addition of nanoparticles such as GNP, MWCNTs, and TiO_2, both in mono and hybrid types of particles, to paraffin, resulted only in physical interactions as evidenced by the absence of new chemical peaks.
- Moreover, the Chemical interaction analyses and crystal structures with FT-IR and XRD for functionalised MWCNTs and their hybrid combinations with TiO_2 revealed no significant chemical interaction, maintaining the structural stability and compatibility within the PCM matrix. This indicates their chemical compatibility with paraffin and underscores that the crystal structure of the paraffin remains unchanged, which is critical for maintaining the integrity of the nano-PCMs.

8.1.2 Thermal Properties and Conductivity Enhancements:

- Thermal analysis revealed minimal impact on the peak melting and solidification temperatures of nano-PCMs. Notable reductions in latent heat were observed,

particularly -7% for the hybrid GNP+MWCNTs nano-PCM and -3.7% for the paraffin/TiO_2. These reductions are balanced by substantial improvements up to 170% in thermal conductivity, especially pronounced in the GNP+MWCNTs hybrid nano-PCM, which showed the highest conductivity across all temperatures.

8.1.3 Peak Thermal Conductivity and Economic Viability:

- The highest thermal conductivity was observed at 1.0 wt.% of GNP+MWCNTs hybrid particles based PCM, showing a maximum enhancement of 170% at 25°C. This peak performance highlights not only the effectiveness of hybrid nano-PCMs in enhancing thermal energy transfer capabilities. Using hybrid combinations, particularly those involving GNP and MWCNTs, leverages the superior thermal properties of these materials while reducing overall costs by minimising the amount of expensive carbon-based nanoparticles needed. The inclusion of cheaper TiO_2 nanoparticles in other hybrid combinations further enhances stability and cost-effectiveness, making these solutions economically viable for large-scale applications.

8.1.4 Surface Modification and Enhanced Stability:

- Surface-modified MWCNTs demonstrated significant improvements in dispersion stability and thermal properties. Functionalised MWCNTs, especially when combined with TiO_2, enhanced the overall stability and performance of the nano-PCMs, showing minimal property degradation even after extensive thermal cycling and maintaining stability in long-term applications.

8.1.5 Superior Performance of Hybrid Particles:

- Hybrid nanoparticles, particularly combinations such as GNP+MWCNTs, demonstrated exceptional thermal conductivity (TC) improvements. For instance, GNP+MWCNTs at 1.0 wt.% concentration showed a TC enhancement of 170% at 25°C. Additionally, TiO_2+functionalised MWCNTs hybrids, at various ratios (25:75, 50:50, 75:25), exhibited significant TC enhancement and particle stability. These hybrids leverage the high thermal conductivity of carbon-based nanoparticles and the structural stability and cost-effectiveness of TiO_2. This synergy results in nano-PCMs that are not only more efficient in thermal energy transfer but also economically viable for large-scale applications.

8.1.6 Long-term Performance and Practical Implications:

- Extensive thermal cycling tests and stability evaluations up to 200 cycles illustrated that the hybrid nano-PCMs, particularly those involving functionalised MWCNTs and TiO_2, showed robust performance with minimal degradation, making them suitable for reliable and sustainable use in building energy storage systems.

8.2 Future Directions for the Development of Nano-PCMs

The continuous advancement of thermal management technologies, particularly in the context of energy-efficient building solutions and sustainable technologies, highlights the crucial need for ongoing research and development of nano-PCMs. Critical research directions could considerably improve the installation and performance of nano-PCMs in building energy systems. Firstly, an in-depth study of nanomaterial behavior is essential. Investigating the dynamics of nanomaterial agglomeration and sedimentation during the melting and solidification processes of PCMs will help enhance the stability and efficiency of Nano-PCMs within building energy systems.

Exploring inorganic PCMs and their composites with metallic, metallic-oxide, and carbon additives is another promising area. Inorganic PCMs often exhibit higher melting points and thermal conductivity, potentially offering enhanced performance for building applications. Additionally, studying how the shape and morphology of nanomaterials affect the thermophysical properties of nano-PCMs is crucial. Different nanoparticle shapes may influence heat transfer rates and energy storage capacities differently, impacting overall system efficiency.

Developing new thermal property correlations is also very important. Creating models that predict how changes in nanoparticle type, size, shape, and concentration affect the thermal properties of PCMs will aid in designing more effective nano-PCMs for building applications. Furthermore, developing leak-proof and stable nano-PCMs systems, potentially using biomimetic foams or encapsulation techniques, will ensure the PCM retains its properties over time without leakage.

Researching the integration of nano-PCMs with traditional building materials to create responsive building envelopes capable of actively managing heat transfer could significantly reduce HVAC energy needs in residential and commercial buildings. Additionally, focusing on the long-term durability and reliability of nano-PCMs in real-world applications is essential.

Research should aim to understand and enhance the longevity of these materials under continuous thermal cycling and varying environmental conditions.

Investigating cost-effective synthesis and manufacturing processes for nano-PCMs is another crucial area. Developing scalable and economical production methods will be key for their widespread adoption in the building industry. Future work should also address areas that were beyond the scope of the current study, such as the detailed analysis of multi-component hybrid nanoparticles and the long-term environmental impacts of nano-PCMs. Moreover, exploring advanced encapsulation techniques and their impact on thermal performance and material stability could provide valuable insights.

Due to limitations with our current SEM, which was unable to analyse volatile samples, we were unable to conduct microstructure analysis in this study. Future research could include such analyses to visualize how nanoparticles are dispersed within the paraffin matrix. This will offer a clearer understanding of the interactions and stability of the nanoparticles within the PCM.

These targeted research directions aim to enhance the practical application and effectiveness of nano-PCMs in thermal energy storage for buildings, aligning with the evolving needs of energy efficiency and sustainability. The economic benefits are clear: by improving thermal conductivity and stability through the use of hybrid nanoparticles, particularly those involving low-cost materials like TiO_2, and optimising production processes, we can reduce both initial and long-term costs. This makes nano-PCMs a viable and attractive solution for enhancing energy efficiency in buildings, leading to lower energy bills and reduced environmental impact.

REFERENCES

[1] Y. Li, Z. Ding, M. Shakerin, N. Zhang, A multi-objective optimal design method for thermal energy storage systems with PCM: A case study for outdoor swimming pool heating application, J Energy Storage 29 (2020) 101371.

[2] G. Wei, G. Wang, C. Xu, X. Ju, L. Xing, X. Du, Y. Yang, Selection principles and thermophysical properties of high temperature phase change materials for thermal energy storage: A review, Renewable and Sustainable Energy Reviews 81 (2018) 1771–1786.

[3] G. Alva, Y. Lin, G. Fang, An overview of thermal energy storage systems, Energy 144 (2018) 341–378.

[4] H.M. Ali, A. Saieed, W. Pao, M. Ali, Copper foam/PCMs based heat sinks: an experimental study for electronic cooling systems, Int J Heat Mass Transf 127 (2018) 381–393.

[5] H. Usman, H.M. Ali, A. Arshad, M.J. Ashraf, S. Khushnood, M.M. Janjua, S.N. Kazi, An experimental study of PCM based finned and un-finned heat sinks for passive cooling of electronics, Heat and Mass Transfer 54 (2018) 3587–3598.

[6] M.A. Hayat, H.M. Ali, M.M. Janjua, W. Pao, C. Li, M. Alizadeh, Phase change material/heat pipe and Copper foam-based heat sinks for thermal management of electronic systems, J Energy Storage 32 (2020) 101971.

[7] S.L. Tariq, H.M. Ali, M.A. Akram, M.M. Janjua, Experimental investigation on graphene based nanoparticles enhanced phase change materials (GbNePCMs) for thermal management of electronic equipment, J Energy Storage 30 (2020) 101497.

[8] B.M.S. Punniakodi, R. Senthil, Recent developments in nano-enhanced phase change materials for solar thermal storage, Solar Energy Materials and Solar Cells 238 (2022) 111629.

[9] P.B. Salunkhe, P.S. Shembekar, A review on effect of phase change material encapsulation on the thermal performance of a system, Renewable and Sustainable Energy Reviews 16 (2012) 5603–5616.

[10] J. Jeon, J.-H. Lee, J. Seo, S.-G. Jeong, S. Kim, Application of PCM thermal energy storage system to reduce building energy consumption, J Therm Anal Calorim 111 (2013) 279–288.

[11] K.; G. Dean, B.; Dulac, J.; Petrichenko, Global Status Report; Global Alliance for Buildings and Construction (GABC), 2016.

[12] N. Soares, J.J. Costa, A.R. Gaspar, P. Santos, Review of passive PCM latent heat thermal energy storage systems towards buildings' energy efficiency, Energy Build 59 (2013) 82–103.

[13] L.W. Davis, P.J. Gertler, Contribution of air conditioning adoption to future energy use under global warming, Proceedings of the National Academy of Sciences 112 (2015) 5962–5967.

[14] M. Alam, S.K.M. Yasin, M. Gain, S. Mondal, Renewable energy sources (res): an overview with Indian context, International Journal of Engineering and Computer Science 3 (2014).

[15] L. Liu, D. Su, Y. Tang, G. Fang, Thermal conductivity enhancement of phase change materials for thermal energy storage: a review, Renewable and Sustainable Energy Reviews 62 (2016) 305–317.

[16] Y. Lin, Y. Jia, G. Alva, G. Fang, Review on thermal conductivity enhancement, thermal properties and applications of phase change materials in thermal energy storage, Renewable and Sustainable Energy Reviews 82 (2018) 2730–2742.
[17] C.E. Dorgan, J.S. Elleson, ASHRAE's new design guide for cool thermal storage, ASHRAE Journal (American Society of Heating, Refrigerating and Air-Conditioning Engineers);(United States) 36 (1994).
[18] A.L.S. Chan, T.-T. Chow, S.K.F. Fong, J.Z. Lin, Performance evaluation of district cooling plant with ice storage, Energy 31 (2006) 2750–2762.
[19] S. Boonnasa, P. Namprakai, The chilled water storage analysis for a university building cooling system, Appl Therm Eng 30 (2010) 1396–1408.
[20] A. H Abedin, M. A Rosen, A critical review of thermochemical energy storage systems, The Open Renewable Energy Journal 4 (2011).
[21] S. Wu, C. Zhou, E. Doroodchi, R. Nellore, B. Moghtaderi, A review on high-temperature thermochemical energy storage based on metal oxides redox cycle, Energy Convers Manag 168 (2018) 421–453.
[22] H.P. Garg, S.C. Mullick, V.K. Bhargava, Solar thermal energy storage, Springer Science & Business Media, 2012.
[23] I. Dincer, M. Rosen, Thermal energy storage: systems and applications, John Wiley & Sons, 2002.
[24] D. Fernandes, F. Pitié, G. Cáceres, J. Baeyens, Thermal energy storage:"How previous findings determine current research priorities," Energy 39 (2012) 246–257.
[25] Y. Zhang, G. Zhou, K. Lin, Q. Zhang, H. Di, Application of latent heat thermal energy storage in buildings: State-of-the-art and outlook, Build Environ 42 (2007) 2197–2209.
[26] S. Jegadheeswaran, S.D. Pohekar, Performance enhancement in latent heat thermal storage system: a review, Renewable and Sustainable Energy Reviews 13 (2009) 2225–2244.
[27] S.A. Mohamed, F.A. Al-Sulaiman, N.I. Ibrahim, M.H. Zahir, A. Al-Ahmed, R. Saidur, B.S. Yılbaş, A.Z. Sahin, A review on current status and challenges of inorganic phase change materials for thermal energy storage systems, Renewable and Sustainable Energy Reviews 70 (2017) 1072–1089.
[28] R.R. Kumar, M. Samykano, A.K. Pandey, K. Kadirgama, V. V Tyagi, Phase change materials and nano-enhanced phase change materials for thermal energy storage in photovoltaic thermal systems: A futuristic approach and its technical challenges, Renewable and Sustainable Energy Reviews 133 (2020) 110341.
[29] M.A. Hayat, Y. Chen, M. Bevilacqua, L. Li, Y. Yang, Characteristics and potential applications of nano-enhanced phase change materials: A critical review on recent developments, Sustainable Energy Technologies and Assessments 50 (2022) 101799.
[30] R. Agromayor, D. Cabaleiro, A.A. Pardinas, J.P. Vallejo, J. Fernandez-Seara, L. Lugo, Heat transfer performance of functionalized graphene nanoplatelet aqueous nanofluids, Materials 9 (2016) 455.
[31] D.G. Papageorgiou, I.A. Kinloch, R.J. Young, Mechanical properties of graphene and graphene-based nanocomposites, Prog Mater Sci 90 (2017) 75–127.
[32] T. Zhang, Q. Xue, S. Zhang, M. Dong, Theoretical approaches to graphene and graphene-based materials, Nano Today 7 (2012) 180–200.
[33] S. Kim, L.T. Drzal, High latent heat storage and high thermal conductive phase change materials using exfoliated graphite nanoplatelets, Solar Energy Materials and Solar Cells 93 (2009) 136–142.
[34] J. Jeon, S.-G. Jeong, J.-H. Lee, J. Seo, S. Kim, High thermal performance composite PCMs loading xGnP for application to building using radiant floor heating system, Solar Energy Materials and Solar Cells 101 (2012) 51–56.

[35] G.-Q. Qi, C.-L. Liang, R.-Y. Bao, Z.-Y. Liu, W. Yang, B.-H. Xie, M.-B. Yang, Polyethylene glycol based shape-stabilized phase change material for thermal energy storage with ultra-low content of graphene oxide, Solar Energy Materials and Solar Cells 123 (2014) 171–177.
[36] G.-Q. Qi, J. Yang, R.-Y. Bao, Z.-Y. Liu, W. Yang, B.-H. Xie, M.-B. Yang, Enhanced comprehensive performance of polyethylene glycol based phase change material with hybrid graphene nanomaterials for thermal energy storage, Carbon N Y 88 (2015) 196–205.
[37] L. He, H. Wang, H. Zhu, Y. Gu, X. Li, X. Mao, Thermal properties of PEG/graphene nanoplatelets (GNPs) composite phase change materials with enhanced thermal conductivity and photo-thermal performance, Applied Sciences 8 (2018) 2613.
[38] N. Zhang, Y. Jing, Y. Song, Y. Du, Y. Yuan, Thermal properties and crystallization kinetics of pentaglycerine/graphene nanoplatelets composite phase change material for thermal energy storage, Int J Energy Res 44 (2020) 448–459.
[39] K. Cui, L. Liu, F. Ma, M. Jing, Z. Li, Y. Tong, M. Sun, S. Li, J. Zhang, Y. Zhang, Enhancement of thermal conductivity of Ba (OH) 2· 8H2O phase change material by graphene nanoplatelets, Mater Res Express 5 (2018) 65522.
[40] M. Amin, N. Putra, E.A. Kosasih, E. Prawiro, R.A. Luanto, T.M.I. Mahlia, Thermal properties of beeswax/graphene phase change material as energy storage for building applications, Appl Therm Eng 112 (2017) 273–280.
[41] A. Zabalegui, D. Lokapur, H. Lee, Nanofluid PCMs for thermal energy storage: Latent heat reduction mechanisms and a numerical study of effective thermal storage performance, Int J Heat Mass Transf 78 (2014) 1145–1154.
[42] F. Yavari, H.R. Fard, K. Pashayi, M.A. Rafiee, A. Zamiri, Z. Yu, R. Ozisik, T. Borca-Tasciuc, N. Koratkar, Enhanced thermal conductivity in a nanostructured phase change composite due to low concentration graphene additives, The Journal of Physical Chemistry C 115 (2011) 8753–8758.
[43] N. Putra, M. Amin, E.A. Kosasih, R.A. Luanto, N.A. Abdullah, Characterization of the thermal stability of RT 22 HC/graphene using a thermal cycle method based on thermoelectric methods, Appl Therm Eng 124 (2017) 62–70.
[44] J.-N. Shi, M.-D. Ger, Y.-M. Liu, Y.-C. Fan, N.-T. Wen, C.-K. Lin, N.-W. Pu, Improving the thermal conductivity and shape-stabilization of phase change materials using nanographite additives, Carbon N Y 51 (2013) 365–372.
[45] Y. Zhang, J. Wang, J. Qiu, X. Jin, M.M. Umair, R. Lu, S. Zhang, B. Tang, Ag-graphene/PEG composite phase change materials for enhancing solar-thermal energy conversion and storage capacity, Appl Energy 237 (2019) 83–90.
[46] J. Yang, L.-S. Tang, R.-Y. Bao, L. Bai, Z.-Y. Liu, W. Yang, B.-H. Xie, M.-B. Yang, Largely enhanced thermal conductivity of poly (ethylene glycol)/boron nitride composite phase change materials for solar-thermal-electric energy conversion and storage with very low content of graphene nanoplatelets, Chemical Engineering Journal 315 (2017) 481–490.
[47] L. Zhou, L.-S. Tang, X.-F. Tao, J. Yang, M.-B. Yang, W. Yang, Facile fabrication of shape-stabilized polyethylene glycol/cellulose nanocrystal phase change materials based on thiol-ene click chemistry and solvent exchange, Chemical Engineering Journal (2020) 125206.
[48] L.-W. Fan, X. Fang, X. Wang, Y. Zeng, Y.-Q. Xiao, Z.-T. Yu, X. Xu, Y.-C. Hu, K.-F. Cen, Effects of various carbon nanofillers on the thermal conductivity and energy storage properties of paraffin-based nanocomposite phase change materials, Appl Energy 110 (2013) 163–172.

[49] G. Zhang, Z. Yu, G. Cui, B. Dou, W. Lu, X. Yan, Fabrication of a novel nano phase change material emulsion with low supercooling and enhanced thermal conductivity, Renew Energy 151 (2020) 542–550.
[50] X. Meng, H. Zhang, L. Sun, F. Xu, Q. Jiao, Z. Zhao, J. Zhang, H. Zhou, Y. Sawada, Y. Liu, Preparation and thermal properties of fatty acids/CNTs composite as shape-stabilized phase change materials, J Therm Anal Calorim 111 (2013) 377–384.
[51] A. Avid, S.H. Jafari, H.A. Khonakdar, M. Ghaffari, B. Krause, P. Pötschke, Surface modification of MWCNT and its influence on properties of paraffin/MWCNT nanocomposites as phase change material, J Appl Polym Sci 137 (2020) 48428.
[52] S. Shaikh, K. Lafdi, K. Hallinan, Carbon nanoadditives to enhance latent energy storage of phase change materials, J Appl Phys 103 (2008) 94302.
[53] T. Qian, J. Li, X. Min, W. Guan, Y. Deng, L. Ning, Enhanced thermal conductivity of PEG/diatomite shape-stabilized phase change materials with Ag nanoparticles for thermal energy storage, J Mater Chem A Mater 3 (2015) 8526–8536.
[54] T. Qian, S. Zhu, H. Wang, A. Li, B. Fan, Comparative study of single-walled carbon nanotubes and graphene nanoplatelets for improving the thermal conductivity and solar-to-light conversion of PEG-infiltrated phase-change material composites, ACS Sustain Chem Eng 7 (2018) 2446–2458.
[55] Z.-T. Yu, X. Fang, L.-W. Fan, X. Wang, Y.-Q. Xiao, Y. Zeng, X. Xu, Y.-C. Hu, K.-F. Cen, Increased thermal conductivity of liquid paraffin-based suspensions in the presence of carbon nano-additives of various sizes and shapes, Carbon N Y 53 (2013) 277–285.
[56] A. Elgafy, K. Lafdi, Effect of carbon nanofiber additives on thermal behavior of phase change materials, Carbon N Y 43 (2005) 3067–3074.
[57] M.E. Darzi, S.I. Golestaneh, M. Kamali, G. Karimi, Thermal and electrical performance analysis of co-electrospun-electrosprayed PCM nanofiber composites in the presence of graphene and carbon fiber powder, Renew Energy 135 (2019) 719–728.
[58] V. Chinnasamy, H. Cho, Investigation on thermal properties enhancement of lauryl alcohol with multi-walled carbon nanotubes as phase change material for thermal energy storage, Case Studies in Thermal Engineering 31 (2022) 101826.
[59] M. He, L. Yang, W. Lin, J. Chen, X. Mao, Z. Ma, Preparation, thermal characterization and examination of phase change materials (PCMs) enhanced by carbon-based nanoparticles for solar thermal energy storage, J Energy Storage 25 (2019) 100874.
[60] R. Bharathiraja, T. Ramkumar, M. Selvakumar, Studies on the thermal characteristics of nano-enhanced paraffin wax phase change material (PCM) for thermal storage applications, J Energy Storage 73 (2023) 109216.
[61] U. Yogeswaran, S.-M. Chen, Separation and concentration effect of f-MWCNTs on electrocatalytic responses of ascorbic acid, dopamine and uric acid at f-MWCNTs incorporated with poly (neutral red) composite films, Electrochim Acta 52 (2007) 5985–5996.
[62] G.K. Amudhalapalli, J.K. Devanuri, Synthesis, characterization, thermophysical properties, stability and applications of nanoparticle enhanced phase change materials–A comprehensive review, Thermal Science and Engineering Progress 28 (2022) 101049.
[63] Z. Cao, L. Qiu, Y. Yang, Y. Chen, X. Liu, The surface modifications of multi-walled carbon nanotubes for multi-walled carbon nanotube/poly (ether ether ketone) composites, Appl Surf Sci 353 (2015) 873–881.
[64] A. Rahimpour, M. Jahanshahi, S. Khalili, A. Mollahosseini, A. Zirepour, B. Rajaeian, Novel functionalized carbon nanotubes for improving the surface properties and performance of polyethersulfone (PES) membrane, Desalination 286 (2012) 99–107.

[65] C.-C. Teng, C.-C.M. Ma, C.-H. Lu, S.-Y. Yang, S.-H. Lee, M.-C. Hsiao, M.-Y. Yen, K.-C. Chiou, T.-M. Lee, Thermal conductivity and structure of non-covalent functionalized graphene/epoxy composites, Carbon N Y 49 (2011) 5107–5116.
[66] S. Shen, S. Tan, S. Wu, C. Guo, J. Liang, Q. Yang, G. Xu, J. Deng, The effects of modified carbon nanotubes on the thermal properties of erythritol as phase change materials, Energy Convers Manag 157 (2018) 41–48.
[67] Q. Tang, J. Sun, S. Yu, G. Wang, Improving thermal conductivity and decreasing supercooling of paraffin phase change materials by n-octadecylamine-functionalized multi-walled carbon nanotubes, RSC Adv 4 (2014) 36584–36590.
[68] L. Han, X. Zhang, J. Ji, K. Ma, Research progress on the influence of nano-additives on phase change materials, J Energy Storage 55 (2022) 105807.
[69] R. Kumar, A.K. Pandey, M. Samykano, Y.N. Mishra, R. V Mohan, K. Sharma, V. V Tyagi, Effect of surfactant on functionalized multi-walled carbon nano tubes enhanced salt hydrate phase change material, J Energy Storage 55 (2022) 105654.
[70] R. Kumar, M. Samykano, A.K. Pandey, K. Kadirgama, V. V Tyagi, A comparative study on thermophysical properties of functionalized and non-functionalized Multi-Walled Carbon Nano Tubes (MWCNTs) enhanced salt hydrate phase change material, Solar Energy Materials and Solar Cells 240 (2022) 111697.
[71] M.A. Fikri, A.K. Pandey, M. Samykano, K. Kadirgama, M. George, R. Saidur, J. Selvaraj, N. Abd Rahim, K. Sharma, V. V Tyagi, Thermal conductivity, reliability, and stability assessment of phase change material (PCM) doped with functionalized multi-wall carbon nanotubes (FMWCNTs), J Energy Storage 50 (2022) 104676.
[72] H. Babar, H.M. Ali, Towards hybrid nanofluids: preparation, thermophysical properties, applications, and challenges, J Mol Liq 281 (2019) 598–633.
[73] H.M. Ali, H. Babar, T.R. Shah, M.U. Sajid, M.A. Qasim, S. Javed, Preparation techniques of TiO2 nanofluids and challenges: a review, Applied Sciences 8 (2018) 587.
[74] M.U. Sajid, H.M. Ali, Thermal conductivity of hybrid nanofluids: a critical review, Int J Heat Mass Transf 126 (2018) 211–234.
[75] M.A. Kibria, M.R. Anisur, M.H. Mahfuz, R. Saidur, I. Metselaar, A review on thermophysical properties of nanoparticle dispersed phase change materials, Energy Convers Manag 95 (2015) 69–89.
[76] P. Ji, H. Sun, Y. Zhong, W. Feng, Improvement of the thermal conductivity of a phase change material by the functionalized carbon nanotubes, Chem Eng Sci 81 (2012) 140–145.
[77] J. Wang, H. Xie, Z. Xin, Y. Li, Increasing the thermal conductivity of palmitic acid by the addition of carbon nanotubes, Carbon N Y 48 (2010) 3979–3986.
[78] T.-P. Teng, C.-M. Cheng, C.-P. Cheng, Performance assessment of heat storage by phase change materials containing MWCNTs and graphite, Appl Therm Eng 50 (2013) 637–644.
[79] J. Wang, H. Xie, Z. Guo, L. Guan, Y. Li, Improved thermal properties of paraffin wax by the addition of TiO2 nanoparticles, Appl Therm Eng 73 (2014) 1541–1547.
[80] T.-P. Teng, C.-C. Yu, Characteristics of phase-change materials containing oxide nano-additives for thermal storage, Nanoscale Res Lett 7 (2012) 611.
[81] S. Sami, N. Etesami, Improving thermal characteristics and stability of phase change material containing TiO2 nanoparticles after thermal cycles for energy storage, Appl Therm Eng 124 (2017) 346–352.
[82] A. Haghighi, A. Babapoor, M. Azizi, Z. Javanshir, H. Ghasemzade, Optimization of the thermal performance of PCM nanocomposites, Journal of Energy Management and Technology 4 (2020) 14–19.

[83] S. Harikrishnan, S. Magesh, S. Kalaiselvam, Preparation and thermal energy storage behaviour of stearic acid–TiO2 nanofluids as a phase change material for solar heating systems, Thermochim Acta 565 (2013) 137–145.
[84] R.K. Sharma, P. Ganesan, V. V Tyagi, H.S.C. Metselaar, S.C. Sandaran, Thermal properties and heat storage analysis of palmitic acid-TiO2 composite as nano-enhanced organic phase change material (NEOPCM), Appl Therm Eng 99 (2016) 1254–1262.
[85] Y. Liu, K. Yu, Y. Yang, M. Jia, F. Sun, Size effects of nano-rutile TiO2 on latent heat recovered of binary eutectic hydrate salt phase change material, Thermochim Acta 684 (2020) 178492.
[86] N.H. Mohamed, F.S. Soliman, H. El Maghraby, Y.M. Moustfa, Thermal conductivity enhancement of treated petroleum waxes, as phase change material, by α nano alumina: Energy storage, Renewable and Sustainable Energy Reviews 70 (2017) 1052–1058.
[87] A. Babapoor, G. Karimi, Thermal properties measurement and heat storage analysis of paraffinnanoparticles composites phase change material: Comparison and optimization, Appl Therm Eng 90 (2015) 945–951.
[88] L. Colla, L. Fedele, S. Mancin, L. Danza, O. Manca, Nano-PCMs for enhanced energy storage and passive cooling applications, Appl Therm Eng 110 (2017) 584–589.
[89] C.J. Ho, J.Y. Gao, Preparation and thermophysical properties of nanoparticle-in-paraffin emulsion as phase change material, International Communications in Heat and Mass Transfer 36 (2009) 467–470.
[90] Y. Liu, Y. Yang, Use of nano-α-Al2O3 to improve binary eutectic hydrated salt as phase change material, Solar Energy Materials and Solar Cells 160 (2017) 18–25.
[91] B. Akhmetov, M.E. Navarro, A. Seitov, A. Kaltayev, Z. Bakenov, Y. Ding, Numerical study of integrated latent heat thermal energy storage devices using nanoparticle-enhanced phase change materials, Solar Energy 194 (2019) 724–741.
[92] M. Bayat, M.R. Faridzadeh, D. Toghraie, Investigation of finned heat sink performance with nano enhanced phase change material (NePCM), Thermal Science and Engineering Progress 5 (2018) 50–59.
[93] A.V. Arasu, A.S. Mujumdar, Numerical study on melting of paraffin wax with Al2O3 in a square enclosure, International Communications in Heat and Mass Transfer 39 (2012) 8–16.
[94] H. Chen, S. Li, P. Wei, Y. Gong, P. Nie, X. Chen, C. Wang, Experimental study on characteristics of a nano-enhanced phase change material slurry for low temperature solar energy collection, Solar Energy Materials and Solar Cells 212 (2020) 110513.
[95] A.A. Valan, A.P. Sasmito, A.S. Mujumdar, Numerical performance study of paraffin wax dispersed with alumina in a concentric pipe latent heat storage system, Thermal Science 17 (2013) 419–430.
[96] C. Ma, Y. Zhang, X. Chen, X. Song, K. Tang, Experimental Study of an Enhanced Phase Change Material of Paraffin/Expanded Graphite/Nano-Metal Particles for a Personal Cooling System, Materials 13 (2020) 980.
[97] W. Cui, Y. Yuan, L. Sun, X. Cao, X. Yang, Experimental studies on the supercooling and melting/freezing characteristics of nano-copper/sodium acetate trihydrate composite phase change materials, Renew Energy 99 (2016) 1029–1037.
[98] N. Gupta, A. Kumar, S.K. Dhawan, H. Dhasmana, A. Kumar, V. Kumar, A. Verma, V.K. Jain, Metal nanoparticles enhanced thermophysical properties of phase change material for thermal energy storage, Mater Today Proc (2020).
[99] S. Sharma, L. Micheli, W. Chang, A.A. Tahir, K.S. Reddy, T.K. Mallick, Nano-enhanced Phase Change Material for thermal management of BICPV, Appl Energy 208 (2017) 719–733.

[100] M. George, A.K. Pandey, N. Abd Rahim, V. V Tyagi, S. Shahabuddin, R. Saidur, A novel polyaniline (PANI)/paraffin wax nano composite phase change material: Superior transition heat storage capacity, thermal conductivity and thermal reliability, Solar Energy 204 (2020) 448–458.
[101] A. Ebrahimi, A. Dadvand, Simulation of melting of a nano-enhanced phase change material (NePCM) in a square cavity with two heat source–sink pairs, Alexandria Engineering Journal 54 (2015) 1003–1017.
[102] R.P. Singh, S.C. Kaushik, D. Rakshit, Melting phenomenon in a finned thermal storage system with graphene nano-plates for medium temperature applications, Energy Convers Manag 163 (2018) 86–99.
[103] S. Ebadi, S.H. Tasnim, A.A. Aliabadi, S. Mahmud, Geometry and nanoparticle loading effects on the bio-based nano-PCM filled cylindrical thermal energy storage system, Appl Therm Eng 141 (2018) 724–740.
[104] A. Farzanehnia, M. Khatibi, M. Sardarabadi, M. Passandideh-Fard, Experimental investigation of multiwall carbon nanotube/paraffin based heat sink for electronic device thermal management, Energy Convers Manag 179 (2019) 314–325.
[105] A.M. Abdulateef, J. Abdulateef, A.A. Al-Abidi, K. Sopian, S. Mat, M.S. Mahdi, A combination of fins-nanoparticle for enhancing the discharging of phase-change material used for liquid desiccant air conditioning unite, J Energy Storage 24 (2019) 100784.
[106] Z. Khan, Z.A. Khan, Experimental and numerical investigations of nano-additives enhanced paraffin in a shell-and-tube heat exchanger: a comparative study, Appl Therm Eng 143 (2018) 777–790.
[107] S. Kalaiselvam, R. Parameshwaran, S. Harikrishnan, Analytical and experimental investigations of nanoparticles embedded phase change materials for cooling application in modern buildings, Renew Energy 39 (2012) 375–387.
[108] Z. Ma, W. Lin, M.I. Sohel, Nano-enhanced phase change materials for improved building performance, Renewable and Sustainable Energy Reviews 58 (2016) 1256–1268.
[109] X. Xiao, P. Zhang, M. Li, Experimental and numerical study of heat transfer performance of nitrate/expanded graphite composite PCM for solar energy storage, Energy Convers Manag 105 (2015) 272–284.
[110] N. Sahan, H.O. Paksoy, Thermal enhancement of paraffin as a phase change material with nanomagnetite, Solar Energy Materials and Solar Cells 126 (2014) 56–61.
[111] N. Şahan, M. Fois, H. Paksoy, Improving thermal conductivity phase change materials—A study of paraffin nanomagnetite composites, Solar Energy Materials and Solar Cells 137 (2015) 61–67.
[112] S.G. Ranjbar, G. Roudini, F. Barahuie, Fabrication and characterization of phase change material-SiO2 nanocomposite for thermal energy storage in buildings, J Energy Storage 27 (2020) 101168.
[113] X. Zhang, C. Zhu, G. Fang, Preparation and thermal properties of n-eicosane/nano-SiO2/expanded graphite composite phase-change material for thermal energy storage, Mater Chem Phys 240 (2020) 122178.
[114] M.A. Tony, S.A. Mansour, Sunlight-driven organic phase change material-embedded nanofiller for latent heat solar energy storage, International Journal of Environmental Science and Technology 17 (2020) 709–720.
[115] X. Fang, L.-W. Fan, Q. Ding, X.-L. Yao, Y.-Y. Wu, J.-F. Hou, X. Wang, Z.-T. Yu, G.-H. Cheng, Y.-C. Hu, Thermal energy storage performance of paraffin-based composite phase change materials filled with hexagonal boron nitride nanosheets, Energy Convers Manag 80 (2014) 103–109.

[116] J. Huang, B. Zhang, M. He, X. Huang, G. Wu, G. Yin, Y. Cui, Preparation of anisotropic reduced graphene oxide/BN/paraffin composite phase change materials and investigation of their thermal properties, J Mater Sci (2020) 1–14.
[117] N. Aslfattahi, R. Saidur, A. Arifutzzaman, R. Sadri, N. Bimbo, M.F.M. Sabri, P.A. Maughan, L. Bouscarrat, R.J. Dawson, S.M. Said, Experimental investigation of energy storage properties and thermal conductivity of a novel organic phase change material/MXene as A new class of nanocomposites, J Energy Storage 27 (2020) 101115.
[118] Y. Krishna, R. Saidur, N. Aslfattahi, M. Faizal, K.C. Ng, Enhancing the thermal properties of organic phase change material (palmitic acid) by doping MXene nanoflakes, in: AIP Conf Proc, AIP Publishing LLC, 2020: p. 20013.
[119] Z.H. Rao, S.H. Wang, Y.L. Zhang, G.Q. Zhang, J.Y. Zhang, Thermal properties of paraffin/nano-AlN phase change energy storage materials, Energy Sources, Part A: Recovery, Utilization, and Environmental Effects 36 (2014) 2281–2286.
[120] V. Selvaraj, B. Morri, L.M. Nair, H. Krishnan, Experimental investigation on the thermophysical properties of beryllium oxide-based nanofluid and nano-enhanced phase change material, J Therm Anal Calorim 137 (2019) 1527–1536.
[121] L. Wu, Q. Liu, X. Wang, S. Cao, N. Tang, Q. Wang, G. Lv, L. Liao, Preparation of two-dimensional nano motmorillonite/stearic acid energy storage composites with excellent stability and heat storage property, Appl Clay Sci 191 (2020) 105614.
[122] X. Liu, Z. Rao, Experimental study on the thermal performance of graphene and exfoliated graphite sheet for thermal energy storage phase change material, Thermochim Acta 647 (2017) 15–21.
[123] X. Fang, L.-W. Fan, Q. Ding, X. Wang, X.-L. Yao, J.-F. Hou, Z.-T. Yu, G.-H. Cheng, Y.-C. Hu, K.-F. Cen, Increased thermal conductivity of eicosane-based composite phase change materials in the presence of graphene nanoplatelets, Energy & Fuels 27 (2013) 4041–4047.
[124] D. Yang, F. Peng, H. Zhang, H. Guo, L. Xiong, C. Wang, S. Shi, X. Chen, Preparation of palygorskite paraffin nanocomposite suitable for thermal energy storage, Appl Clay Sci 126 (2016) 190–196.
[125] L. Liu, K. Zheng, Y. Yan, Z. Cai, S. Lin, X. Hu, Graphene Aerogels Enhanced Phase Change Materials prepared by one-pot method with high thermal conductivity and large latent energy storage, Solar Energy Materials and Solar Cells 185 (2018) 487–493.
[126] J. Yang, G.-Q. Qi, Y. Liu, R.-Y. Bao, Z.-Y. Liu, W. Yang, B.-H. Xie, M.-B. Yang, Hybrid graphene aerogels/phase change material composites: thermal conductivity, shape-stabilization and light-to-thermal energy storage, Carbon N Y 100 (2016) 693–702.
[127] N. Putra, M. Amin, E.A. Kosasih, R.A. Luanto, N.A. Abdullah, Characterization of the thermal stability of RT 22 HC/graphene using a thermal cycle method based on thermoelectric methods, Appl Therm Eng 124 (2017) 62–70.
[128] L. He, H. Wang, H. Zhu, Y. Gu, X. Li, X. Mao, Thermal properties of PEG/graphene nanoplatelets (GNPs) composite phase change materials with enhanced thermal conductivity and photo-thermal performance, Applied Sciences 8 (2018) 2613.
[129] U.N. Temel, K. Somek, M. Parlak, K. Yapici, Transient thermal response of phase change material embedded with graphene nanoplatelets in an energy storage unit, J Therm Anal Calorim 133 (2018) 907–918.
[130] S. Wi, S.-G. Jeong, S.J. Chang, J. Lee, S. Kim, Evaluation of energy efficient hybrid hollow plaster panel using phase change material/xGnP composites, Appl Energy 205 (2017) 1548–1559.

[131] J. Jeon, S.-G. Jeong, J.-H. Lee, J. Seo, S. Kim, High thermal performance composite PCMs loading xGnP for application to building using radiant floor heating system, Solar Energy Materials and Solar Cells 101 (2012) 51–56.
[132] Y. Liu, Y. Yang, S. Li, Graphene oxide modified hydrate salt hydrogels: form-stable phase change materials for smart thermal management, J Mater Chem A Mater 4 (2016) 18134–18143.
[133] G. Zhang, Z. Yu, G. Cui, B. Dou, W. Lu, X. Yan, Fabrication of a novel nano phase change material emulsion with low supercooling and enhanced thermal conductivity, Renew Energy 151 (2020) 542–550.
[134] T.-P. Teng, C.-C. Yu, Characteristics of phase-change materials containing oxide nano-additives for thermal storage, Nanoscale Res Lett 7 (2012) 611.
[135] N. Şahan, M. Fois, H. Paksoy, Improving thermal conductivity phase change materials—A study of paraffin nanomagnetite composites, Solar Energy Materials and Solar Cells 137 (2015) 61–67.
[136] N.H. Mohamed, F.S. Soliman, H. El Maghraby, Y.M. Moustfa, Thermal conductivity enhancement of treated petroleum waxes, as phase change material, by α nano alumina: Energy storage, Renewable and Sustainable Energy Reviews 70 (2017) 1052–1058.
[137] C.J. Ho, J.Y. Gao, Preparation and thermophysical properties of nanoparticle-in-paraffin emulsion as phase change material, International Communications in Heat and Mass Transfer 36 (2009) 467–470.
[138] W. Cui, Y. Yuan, L. Sun, X. Cao, X. Yang, Experimental studies on the supercooling and melting/freezing characteristics of nano-copper/sodium acetate trihydrate composite phase change materials, Renew Energy 99 (2016) 1029–1037.
[139] M. George, A.K. Pandey, N. Abd Rahim, V. V Tyagi, S. Shahabuddin, R. Saidur, A novel polyaniline (PANI)/paraffin wax nano composite phase change material: Superior transition heat storage capacity, thermal conductivity and thermal reliability, Solar Energy 204 (2020) 448–458.
[140] G.-Q. Qi, C.-L. Liang, R.-Y. Bao, Z.-Y. Liu, W. Yang, B.-H. Xie, M.-B. Yang, Polyethylene glycol based shape-stabilized phase change material for thermal energy storage with ultra-low content of graphene oxide, Solar Energy Materials and Solar Cells 123 (2014) 171–177.
[141] A.S. Manirathnam, M.K.D. Manikandan, R.H. Prakash, B.K. Kumar, M.D. Amarnath, Experimental analysis on solar water heater integrated with Nano composite phase change material (SCi and CuO), Mater Today Proc 37 (2021) 232–240.
[142] A. Arshad, M. Jabbal, Y. Yan, Preparation and characteristics evaluation of mono and hybrid nano-enhanced phase change materials (NePCMs) for thermal management of microelectronics, Energy Convers Manag 205 (2020) 112444.
[143] M. Zhang, Q. Xiao, C. Chen, L. Li, W. Yuan, Developing a heat-insulating composite phase change material with light-to-thermal conversion performance from graphene oxide/silica hybrid aerogel, Appl Therm Eng (2020) 115303.
[144] M. Zhang, Q. Xiao, C. Chen, L. Li, W. Yuan, Developing a heat-insulating composite phase change material with light-to-thermal conversion performance from graphene oxide/silica hybrid aerogel, Appl Therm Eng (2020) 115303.
[145] A. Arshad, M. Jabbal, Y. Yan, Preparation and characteristics evaluation of mono and hybrid nano-enhanced phase change materials (NePCMs) for thermal management of microelectronics, Energy Convers Manag 205 (2020) 112444.
[146] A.S. Manirathnam, M.K.D. Manikandan, R.H. Prakash, B.K. Kumar, M.D. Amarnath, Experimental analysis on solar water heater integrated with Nano composite phase change material (SCi and CuO), Mater Today Proc (2020).

[147] R. Parameshwaran, G.N. Kumar, V.V. Ram, Experimental analysis of hybrid nanocomposite-phase change material embedded cement mortar for thermal energy storage, Journal of Building Engineering (2020) 101297.
[148] H.M. Ali, H. Babar, T.R. Shah, M.U. Sajid, M.A. Qasim, S. Javed, Preparation techniques of TiO2 nanofluids and challenges: a review, Applied Sciences 8 (2018) 587.
[149] S.L. Tariq, H.M. Ali, M.A. Akram, M.M. Janjua, M. Ahmadlouydarab, Nanoparticles enhanced Phase Change Materials (NePCMs)-A Recent Review, Appl Therm Eng (2020) 115305.
[150] M. Eltaweel, A.A. Abdel-Rehim, Energy and exergy analysis for stationary solar collectors using nanofluids: A review, Int J Energy Res (n.d.).
[151] Y. Hwang, J.K. Lee, C.H. Lee, Y.M. Jung, S.I. Cheong, C.G. Lee, B.C. Ku, S.P. Jang, Stability and thermal conductivity characteristics of nanofluids, Thermochim Acta 455 (2007) 70–74.
[152] S.T. Latibari, M. Mehrali, M. Mehrali, T.M.I. Mahlia, H.S.C. Metselaar, Synthesis, characterization and thermal properties of nanoencapsulated phase change materials via sol–gel method, Energy 61 (2013) 664–672.
[153] A. Sari, A. Karaipekli, K. Kaygusuz, Fatty acid/expanded graphite composites as phase change material for latent heat thermal energy storage, Energy Sources, Part A: Recovery, Utilization, and Environmental Effects 30 (2008) 464–474.
[154] S. Wi, S. Jeong, S.J. Chang, J. Lee, S. Kim, Energy-Efficient Heat Storage using Gypsum Board with Fatty Acid Ester as Layered Phase Change Material, Energy Technology 5 (2017) 1392–1398.
[155] S. Wi, S.-G. Jeong, S.J. Chang, J. Lee, S. Kim, Evaluation of energy efficient hybrid hollow plaster panel using phase change material/xGnP composites, Appl Energy 205 (2017) 1548–1559.
[156] J.-L. Zeng, J. Gan, F.-R. Zhu, S.-B. Yu, Z.-L. Xiao, W.-P. Yan, L. Zhu, Z.-Q. Liu, L.-X. Sun, Z. Cao, Tetradecanol/expanded graphite composite form-stable phase change material for thermal energy storage, Solar Energy Materials and Solar Cells 127 (2014) 122–128.
[157] G. Chen, T. Shi, X. Zhang, F. Cheng, X. Wu, G. Leng, Y. Liu, M. Fang, X. Min, Z. Huang, Polyacrylonitrile/polyethylene glycol phase-change material fibres prepared with hybrid polymer blends and nano-SiC fillers via centrifugal spinning, Polymer (Guildf) 186 (2020) 122012.
[158] A.E. Kabeel, R. Sathyamurthy, A.M. Manokar, S.W. Sharshir, F.A. Essa, A.H. Elshiekh, Experimental study on tubular solar still using Graphene Oxide Nano particles in Phase Change Material (NPCM's) for fresh water production, J Energy Storage 28 (2020) 101204.
[159] Q. He, S. Wang, M. Tong, Y. Liu, Experimental study on thermophysical properties of nanofluids as phase-change material (PCM) in low temperature cool storage, Energy Convers Manag 64 (2012) 199–205.
[160] Y.B. Tao, C.H. Lin, Y.L. He, Effect of surface active agent on thermal properties of carbonate salt/carbon nanomaterial composite phase change material, Appl Energy 156 (2015) 478–489.
[161] M. Silakhori, H. Fauzi, M.R. Mahmoudian, H.S.C. Metselaar, T.M.I. Mahlia, H.M. Khanlou, Preparation and thermal properties of form-stable phase change materials composed of palmitic acid/polypyrrole/graphene nanoplatelets, Energy Build 99 (2015) 189–195.
[162] Z. Mingzheng, X. Guodong, L. Jian, C. Lei, Z. Lijun, Analysis of factors influencing thermal conductivity and viscosity in different kinds of surfactant solutions, Exp Therm Fluid Sci 36 (2012) 22–29.

[163] M. Nourani, N. Hamdami, J. Keramat, A. Moheb, M. Shahedi, Thermal behavior of paraffin-nano-Al2O3 stabilized by sodium stearoyl lactylate as a stable phase change material with high thermal conductivity, Renew Energy 88 (2016) 474–482.
[164] J.L. Zeng, Z. Cao, D.W. Yang, F. Xu, L.X. Sun, X.F. Zhang, L. Zhang, Effects of MWNTs on phase change enthalpy and thermal conductivity of a solid-liquid organic PCM, J Therm Anal Calorim 95 (2009) 507–512.
[165] A. Asadi, M. Asadi, M. Siahmargoi, T. Asadi, M.G. Andarati, The effect of surfactant and sonication time on the stability and thermal conductivity of water-based nanofluid containing Mg (OH) 2 nanoparticles: An experimental investigation, Int J Heat Mass Transf 108 (2017) 191–198.
[166] S. Wu, D. Zhu, X. Zhang, J. Huang, Preparation and melting/freezing characteristics of Cu/paraffin nanofluid as phase-change material (PCM), Energy & Fuels 24 (2010) 1894–1898.
[167] S. Harish, D. Orejon, Y. Takata, M. Kohno, Thermal conductivity enhancement of lauric acid phase change nanocomposite with graphene nanoplatelets, Appl Therm Eng 80 (2015) 205–211.
[168] S. Shenogin, L. Xue, R. Ozisik, P. Keblinski, D.G. Cahill, Role of thermal boundary resistance on the heat flow in carbon-nanotube composites, J Appl Phys 95 (2004) 8136–8144.
[169] S.T. Huxtable, D.G. Cahill, S. Shenogin, L. Xue, R. Ozisik, P. Barone, M. Usrey, M.S. Strano, G. Siddons, M. Shim, Interfacial heat flow in carbon nanotube suspensions, Nat Mater 2 (2003) 731–734.
[170] S. Harikrishnan, S.I. Hussain, A. Devaraju, P. Sivasamy, S. Kalaiselvam, Improved performance of a newly prepared nano-enhanced phase change material for solar energy storage, Journal of Mechanical Science and Technology 31 (2017) 4903–4910.
[171] D.D.W. Rufuss, L. Suganthi, S. Iniyan, P.A. Davies, Effects of nanoparticle-enhanced phase change material (NPCM) on solar still productivity, J Clean Prod 192 (2018) 9–29.
[172] R. Parameshwaran, R. Jayavel, S. Kalaiselvam, Study on thermal properties of organic ester phase-change material embedded with silver nanoparticles, J Therm Anal Calorim 114 (2013) 845–858.
[173] F. Bahiraei, A. Fartaj, G.-A. Nazri, Experimental and numerical investigation on the performance of carbon-based nanoenhanced phase change materials for thermal management applications, Energy Convers Manag 153 (2017) 115–128.
[174] J. Wang, H. Xie, Z. Xin, Y. Li, C. Yin, Investigation on thermal properties of heat storage composites containing carbon fibers, J Appl Phys 110 (2011) 94302.
[175] A. Avid, S.H. Jafari, H.A. Khonakdar, M. Ghaffari, B. Krause, P. Pötschke, Surface modification of MWCNT and its influence on properties of paraffin/MWCNT nanocomposites as phase change material, J Appl Polym Sci 137 (2020) 48428.
[176] L. He, H. Wang, H. Zhu, Y. Gu, X. Li, X. Mao, Thermal properties of PEG/graphene nanoplatelets (GNPs) composite phase change materials with enhanced thermal conductivity and photo-thermal performance, Applied Sciences 8 (2018) 2613.
[177] M. Afrand, Experimental study on thermal conductivity of ethylene glycol containing hybrid nano-additives and development of a new correlation, Appl Therm Eng 110 (2017) 1111–1119.
[178] S. Salyan, S. Suresh, Study of thermo-physical properties and cycling stability of D-Mannitol-copper oxide nanocomposites as phase change materials, J Energy Storage 15 (2018) 245–255.

[179] S. Motahar, A.A. Alemrajabi, R. Khodabandeh, Experimental study on solidification process of a phase change material containing TiO2 nanoparticles for thermal energy storage, Energy Convers Manag 138 (2017) 162–170.
[180] J.A.R. Babu, K.K. Kumar, S.S. Rao, State-of-art review on hybrid nanofluids, Renewable and Sustainable Energy Reviews 77 (2017) 551–565.
[181] M.H. Esfe, S. Saedodin, S. Wongwises, D. Toghraie, An experimental study on the effect of diameter on thermal conductivity and dynamic viscosity of Fe/water nanofluids, J Therm Anal Calorim 119 (2015) 1817–1824.
[182] P.B. Maheshwary, C.C. Handa, K.R. Nemade, A comprehensive study of effect of concentration, particle size and particle shape on thermal conductivity of titania/water based nanofluid, Appl Therm Eng 119 (2017) 79–88.
[183] S. Suresh, K.P. Venkitaraj, P. Selvakumar, Synthesis, Characterisation of Al2O3-Cu Nano composite powder and water based nanofluids, in: Adv Mat Res, Trans Tech Publ, 2011: pp. 1560–1567.
[184] W. Xian-Ju, L. Xin-Fang, Influence of pH on nanofluids' viscosity and thermal conductivity, Chinese Physics Letters 26 (2009) 56601.
[185] P. Van Trinh, N.N. Anh, N.T. Hong, P.N. Hong, P.N. Minh, B.H. Thang, Experimental study on the thermal conductivity of ethylene glycol-based nanofluid containing Gr-CNT hybrid material, J Mol Liq 269 (2018) 344–353.
[186] A. Akhgar, D. Toghraie, An experimental study on the stability and thermal conductivity of water-ethylene glycol/TiO2-MWCNTs hybrid nanofluid: developing a new correlation, Powder Technol 338 (2018) 806–818.
[187] S. Askari, H. Koolivand, M. Pourkhalil, R. Lotfi, A. Rashidi, Investigation of Fe3O4/Graphene nanohybrid heat transfer properties: Experimental approach, International Communications in Heat and Mass Transfer 87 (2017) 30–39.
[188] S.H. Qing, W. Rashmi, M. Khalid, T. Gupta, M. Nabipoor, M.T. Hajibeigy, Thermal conductivity and electrical properties of hybrid SiO2-graphene naphthenic mineral oil nanofluid as potential transformer oil, Mater Res Express 4 (2017) 15504.
[189] G. Fang, F. Tang, L. Cao, Preparation, thermal properties and applications of shape-stabilized thermal energy storage materials, Renewable and Sustainable Energy Reviews 40 (2014) 237–259.
[190] Y. Konuklu, M. Ostry, H.O. Paksoy, P. Charvat, Review on using microencapsulated phase change materials (PCM) in building applications, Energy Build 106 (2015) 134–155.
[191] R. Parameshwaran, S. Kalaiselvam, Energy conservative air conditioning system using silver nano-based PCM thermal storage for modern buildings, Energy Build 69 (2014) 202–212.
[192] H. Ke, Y. Li, J. Wang, B. Peng, Y. Cai, Q. Wei, Ag-coated polyurethane fibers membranes absorbed with quinary fatty acid eutectics solid-liquid phase change materials for storage and retrieval of thermal energy, Renew Energy 99 (2016) 1–9.
[193] S.I. Hussain, R. Dinesh, A.A. Roseline, S. Dhivya, S. Kalaiselvam, Enhanced thermal performance and study the influence of sub cooling on activated carbon dispersed eutectic PCM for cold storage applications, Energy Build 143 (2017) 17–24.
[194] M. Sayyar, R.R. Weerasiri, P. Soroushian, J. Lu, Experimental and numerical study of shape-stable phase-change nanocomposite toward energy-efficient building constructions, Energy Build 75 (2014) 249–255.
[195] S. Zhang, J.-Y. Wu, C.-T. Tse, J. Niu, Effective dispersion of multi-wall carbon nano-tubes in hexadecane through physiochemical modification and decrease of supercooling, Solar Energy Materials and Solar Cells 96 (2012) 124–130.

[196] S.L. Tariq, H.M. Ali, M.A. Akram, M.M. Janjua, Experimental investigation on graphene based nanoparticles enhanced phase change materials (GbNePCMs) for thermal management of electronic equipment, J Energy Storage 30 (2020) 101497.
[197] L.-W. Fan, Z.-Q. Zhu, Y. Zeng, Y.-Q. Xiao, X.-L. Liu, Y.-Y. Wu, Q. Ding, Z.-T. Yu, K.-F. Cen, Transient performance of a PCM-based heat sink with high aspect-ratio carbon nanofillers, Appl Therm Eng 75 (2015) 532–540.
[198] K.R.S. Kumar, R. Dinesh, A.A. Roseline, S. Kalaiselvam, Performance analysis of heat pipe aided NEPCM heat sink for transient electronic cooling, Microelectronics Reliability 73 (2017) 1–13.
[199] W.G. Alshaer, E. Palomo del Barrio, M.A. Rady, O.E. Adellatif, S.A. Nada, Analysis of the anomalous thermal properties of phase change materials based on paraffin wax and multi walls carbon nanotubes, Int. J. on Heat and Mass Transfer, Theory and Applications 1 (2013) 297–307.
[200] M. Alimohammadi, Y. Aghli, E.S. Alavi, M. Sardarabadi, M. Passandideh-Fard, Experimental investigation of the effects of using nano/phase change materials (NPCM) as coolant of electronic chipsets, under free and forced convection, Appl Therm Eng 111 (2017) 271–279.
[201] Y. Wang, X. Gao, P. Chen, Z. Huang, T. Xu, Y. Fang, Z. Zhang, Preparation and thermal performance of paraffin/Nano-SiO2 nanocomposite for passive thermal protection of electronic devices, Appl Therm Eng 96 (2016) 699–707.
[202] L. Colla, L. Fedele, S. Mancin, B. Buonomo, D. Ercole, O. Manca, Nano-PCMs for passive electronic cooling applications, in: J Phys Conf Ser, IOP Publishing, 2015: p. 12030.
[203] G. Nelson, Application of microencapsulation in textiles, Int J Pharm 242 (2002) 55–62.
[204] N. Sarier, E. Onder, The manufacture of microencapsulated phase change materials suitable for the design of thermally enhanced fabrics, Thermochim Acta 452 (2007) 149–160.
[205] V. Ilić, Z. Šaponjić, V. Vodnik, R. Molina, S. Dimitrijević, P. Jovančić, J. Nedeljković, M. Radetić, Antifungal efficiency of corona pretreated polyester and polyamide fabrics loaded with Ag nanoparticles, J Mater Sci 44 (2009) 3983–3990.
[206] P. Potiyaraj, P. Kumlangdudsana, S.T. Dubas, Synthesis of silver chloride nanocrystal on silk fibers, Mater Lett 61 (2007) 2464–2466.
[207] A. Hebeish, M.E. El-Naggar, M.M.G. Fouda, M.A. Ramadan, S.S. Al-Deyab, M.H. El-Rafie, Highly effective antibacterial textiles containing green synthesized silver nanoparticles, Carbohydr Polym 86 (2011) 936–940.
[208] Q. Li, S. Chen, W. Jiang, Durability of nano ZnO antibacterial cotton fabric to sweat, J Appl Polym Sci 103 (2007) 412–416.
[209] R. Dastjerdi, M. Montazer, S. Shahsavan, A novel technique for producing durable multifunctional textiles using nanocomposite coating, Colloids Surf B Biointerfaces 81 (2010) 32–41.
[210] D.M. Tobaldi, C. Piccirillo, R.C. Pullar, A.F. Gualtieri, M.P. Seabra, P.M.L. Castro, J.A. Labrincha, Silver-modified nano-titania as an antibacterial agent and photocatalyst, The Journal of Physical Chemistry C 118 (2014) 4751–4766.
[211] A.R. Hirst, B. Escuder, J.F. Miravet, D.K. Smith, High-tech applications of self-assembling supramolecular nanostructured gel-phase materials: from regenerative medicine to electronic devices, Angewandte Chemie International Edition 47 (2008) 8002–8018.

[212] M.A. Seo, H.R. Park, S.M. Koo, D.J. Park, J.H. Kang, O.K. Suwal, S.S. Choi, P.C.M. Planken, G.S. Park, N.K. Park, Terahertz field enhancement by a metallic nano slit operating beyond the skin-depth limit, Nat Photonics 3 (2009) 152–156.
[213] N. Xie, J. Niu, T. Wu, X. Gao, Y. Fang, Z. Zhang, Fabrication and characterization of CaCl2· 6H2O composite phase change material in the presence of CsxWO3 nanoparticles, Solar Energy Materials and Solar Cells 200 (2019) 110034.
[214] M. Zhao, X. Zhang, X. Kong, Preparation and characterization of a novel composite phase change material with double phase change points based on nanocapsules, Renew Energy 147 (2020) 374–383.
[215] D. Li, Y. Wu, C. Liu, G. Zhang, M. Arıcı, Energy investigation of glazed windows containing Nano-PCM in different seasons, Energy Convers Manag 172 (2018) 119–128.
[216] K.P. Venkitaraj, S. Suresh, B. Praveen, S.C. Nair, Experimental heat transfer analysis of macro packed neopentylglycol with CuO nano additives for building cooling applications, J Energy Storage 17 (2018) 1–10.
[217] K. Biswas, J. Lu, P. Soroushian, S. Shrestha, Combined experimental and numerical evaluation of a prototype nano-PCM enhanced wallboard, Appl Energy 131 (2014) 517–529.
[218] Y. Huang, X. She, C. Li, Y. Li, Y. Ding, Evaluation of thermal performance in cold storage applications using EG-water based nano-composite PCMs, Energy Procedia 158 (2019) 4840–4845.
[219] D.D.W. Rufuss, S. Arulvel, S. Iniyan, L. Suganthi, Numerical study of titanium oxide nanoparticle enhanced energy storage material in solar desalination, Mater Today Proc (2020).
[220] P.K. Namburu, D.P. Kulkarni, D. Misra, D.K. Das, Viscosity of copper oxide nanoparticles dispersed in ethylene glycol and water mixture, Exp Therm Fluid Sci 32 (2007) 397–402.
[221] S. Jegadheeswaran, S.D. Pohekar, Performance enhancement in latent heat thermal storage system: a review, Renewable and Sustainable Energy Reviews 13 (2009) 2225–2244.
[222] Rubitherm, (n.d.). https://www.rubitherm.eu/media/products/datasheets/Techdata_-RT28HC_EN_09102020.PDF.
[223] S. Manikandan, K.S. Rajan, New hybrid nanofluid containing encapsulated paraffin wax and sand nanoparticles in propylene glycol-water mixture: Potential heat transfer fluid for energy management, Energy Convers Manag 137 (2017) 74–85.
[224] L. Zhichao, Z. Qiang, W. Gaohui, Preparation and enhanced heat capacity of nano-titania doped erythritol as phase change material, Int J Heat Mass Transf 80 (2015) 653–659.
[225] S. Sami, N. Etesami, Improving thermal characteristics and stability of phase change material containing TiO2 nanoparticles after thermal cycles for energy storage, Appl Therm Eng 124 (2017) 346–352.
[226] R.K. Sharma, P. Ganesan, V. V Tyagi, H.S.C. Metselaar, S.C. Sandaran, Thermal properties and heat storage analysis of palmitic acid-TiO2 composite as nano-enhanced organic phase change material (NEOPCM), Appl Therm Eng 99 (2016) 1254–1262.
[227] H. Babar, H.M. Ali, Airfoil shaped pin-fin heat sink: potential evaluation of ferric oxide and titania nanofluids, Energy Convers Manag 202 (2019) 112194.
[228] J.H. Lehman, M. Terrones, E. Mansfield, K.E. Hurst, V. Meunier, Evaluating the characteristics of multiwall carbon nanotubes, Carbon N Y 49 (2011) 2581–2602.
[229] A. Arshad, M. Jabbal, Y. Yan, J. Darkwa, The micro-/nano-PCMs for thermal energy storage systems: A state of art review, Int J Energy Res 43 (2019) 5572–5620.

[230] TA Instruments, (n.d.). https://www.tainstruments.com/.
[231] M.A. Hayat, Y. Yang, L. Li, M. Bevilacqua, Y.K. Chen, Preparation and thermophysical characterisation analysis of potential nano-phase transition materials for thermal energy storage applications, J Mol Liq (2023) 121464.
[232] A. Arshad, M. Jabbal, L. Shi, J. Darkwa, N.J. Weston, Y. Yan, Development of TiO2/RT–35HC based nanocomposite phase change materials (NCPCMs) for thermal management applications, Sustainable Energy Technologies and Assessments 43 (2021) 100865.
[233] X. Zhang, C. Zhu, G. Fang, Preparation and thermal properties of n-eicosane/nano-SiO2/expanded graphite composite phase-change material for thermal energy storage, Mater Chem Phys 240 (2020) 122178.
[234] T.M. Keller, S.B. Qadri, C.A. Little, Carbon nanotube formation in situ during carbonization in shaped bulk solid cobalt nanoparticle compositions, J Mater Chem 14 (2004) 3063–3070.
[235] A. Arshad, M. Jabbal, Y. Yan, Thermophysical characteristics and application of metallic-oxide based mono and hybrid nanocomposite phase change materials for thermal management systems, Appl Therm Eng 181 (2020) 115999.
[236] A.M. Taggart, F. Voogt, G. Clydesdale, K.J. Roberts, An examination of the nucleation kinetics of n-alkanes in the homologous series C13H28 to C32H66, and their relationship to structural type, associated with crystallization from stagnant melts, Langmuir 12 (1996) 5722–5728.
[237] M.J. Oliver, P.D. Calvert, Homogeneous nucleation of n-alkanes measured by differential scanning calorimetry, J Cryst Growth 30 (1975) 343–351.
[238] I. Shamseddine, F. Pennec, P. Biwole, F. Fardoun, Supercooling of phase change materials: A review, Renewable and Sustainable Energy Reviews 158 (2022) 112172.
[239] S. Harikrishnan, S. Magesh, S. Kalaiselvam, Preparation and thermal energy storage behaviour of stearic acid–TiO2 nanofluids as a phase change material for solar heating systems, Thermochim Acta 565 (2013) 137–145.
[240] H. Tian, W. Wang, J. Ding, X. Wei, M. Song, J. Yang, Thermal conductivities and characteristics of ternary eutectic chloride/expanded graphite thermal energy storage composites, Appl Energy 148 (2015) 87–92.
[241] S. Wu, D. Zhu, X. Zhang, J. Huang, Preparation and melting/freezing characteristics of Cu/paraffin nanofluid as phase-change material (PCM), Energy & Fuels 24 (2010) 1894–1898.
[242] M. Chieruzzi, A. Miliozzi, T. Crescenzi, L. Torre, J.M. Kenny, A new phase change material based on potassium nitrate with silica and alumina nanoparticles for thermal energy storage, Nanoscale Res Lett 10 (2015) 1–10.
[243] B. Dudda, D. Shin, Effect of nanoparticle dispersion on specific heat capacity of a binary nitrate salt eutectic for concentrated solar power applications, International Journal of Thermal Sciences 69 (2013) 37–42.
[244] T. Kozlowski, Modulated Differential Scanning Calorimetry (MDSC) studies on low-temperature freezing of water adsorbed on clays, apparent specific heat of soil water and specific heat of dry soil, Cold Reg Sci Technol 78 (2012) 89–96.
[245] J. Wang, H. Xie, Z. Xin, Y. Li, L. Chen, Enhancing thermal conductivity of palmitic acid based phase change materials with carbon nanotubes as fillers, Solar Energy 84 (2010) 339–344.
[246] X. Chen, P. Cheng, Z. Tang, X. Xu, H. Gao, G. Wang, Carbon-based composite phase change materials for thermal energy storage, transfer, and conversion, Advanced Science 8 (2021) 2001274.

[247] M.A. Hayat, Y. Chen, Y. Yang, L. Li, M. Bevilacqua, Enhancing Thermal Energy Storage in Buildings with Novel Functionalised MWCNTs-Enhanced Phase Change Materials: Towards Efficient and Stable Solutions, Thermal Science and Engineering Progress (2023) 102313.
[248] I. Mazov, V.L. Kuznetsov, I.A. Simonova, A.I. Stadnichenko, A. V Ishchenko, A.I. Romanenko, E.N. Tkachev, O.B. Anikeeva, Oxidation behavior of multiwall carbon nanotubes with different diameters and morphology, Appl Surf Sci 258 (2012) 6272–6280.
[249] H. Khani, O. Moradi, Influence of surface oxidation on the morphological and crystallographic structure of multi-walled carbon nanotubes via different oxidants, J Nanostructure Chem 3 (2013) 1–8.
[250] X. Liu, Z. Rao, Experimental study on the thermal performance of graphene and exfoliated graphite sheet for thermal energy storage phase change material, Thermochim Acta 647 (2017) 15–21.
[251] W. Aftab, J. Shi, M. Qin, Z. Liang, F. Xiong, A. Usman, S. Han, R. Zou, Molecularly elongated phase change materials for mid-temperature solar-thermal energy storage and electric conversion, Energy Storage Mater 52 (2022) 284–290.
[252] K.W. Shah, P.J. Ong, M.H. Chua, S.H.G. Toh, J.J.C. Lee, X.Y.D. Soo, Z.M. Png, R. Ji, J. Xu, Q. Zhu, Application of phase change materials in building components and the use of nanotechnology for its improvement, Energy Build 262 (2022) 112018.
[253] L.Y. Jun, N.M. Mubarak, L.S. Yon, C.H. Bing, M. Khalid, E.C. Abdullah, Comparative study of acid functionalization of carbon nanotube via ultrasonic and reflux mechanism, J Environ Chem Eng 6 (2018) 5889–5896.
[254] B. Xu, Z. Li, Paraffin/diatomite/multi-wall carbon nanotubes composite phase change material tailor-made for thermal energy storage cement-based composites, Energy 72 (2014) 371–380.
[255] H. Ji, D.P. Sellan, M.T. Pettes, X. Kong, J. Ji, L. Shi, R.S. Ruoff, Enhanced thermal conductivity of phase change materials with ultrathin-graphite foams for thermal energy storage, Energy Environ Sci 7 (2014) 1185–1192.
[256] F. Avilés, J. V Cauich-Rodríguez, L. Moo-Tah, A. May-Pat, R. Vargas-Coronado, Evaluation of mild acid oxidation treatments for MWCNT functionalization, Carbon N Y 47 (2009) 2970–2975.
[257] L.-W. Fan, X. Fang, X. Wang, Y. Zeng, Y.-Q. Xiao, Z.-T. Yu, X. Xu, Y.-C. Hu, K.-F. Cen, Effects of various carbon nanofillers on the thermal conductivity and energy storage properties of paraffin-based nanocomposite phase change materials, Appl Energy 110 (2013) 163–172.
[258] S. Harikrishnan, S.I. Hussain, A. Devaraju, P. Sivasamy, S. Kalaiselvam, Improved performance of a newly prepared nano-enhanced phase change material for solar energy storage, Journal of Mechanical Science and Technology 31 (2017) 4903–4910.
[259] A. Arshad, M. Jabbal, L. Shi, Y. Yan, Thermophysical characteristics and enhancement analysis of carbon-additives phase change mono and hybrid materials for thermal management of electronic devices, J Energy Storage 34 (2021) 102231. https://doi.org/10.1016/j.est.2020.102231.
[260] L. Wang, Z. Tan, S. Meng, D. Liang, G. Li, Enhancement of molar heat capacity of nanostructured Al2O3, Journal of Nanoparticle Research 3 (2001) 483–487.
[261] E. Hellstern, H.J. Fecht, Z. Fu, W.L. Johnson, Structural and thermodynamic properties of heavily mechanically deformed Ru and AlRu, J Appl Phys 65 (1989) 305–310.

Appendix A

List of Symbols

Ø	Diameter
K	Thermal conductivity
$\mathbf{T_m}$	Melting temperature
$\mathbf{T_c}$	Crystallization temperature
wt. %	Mass fraction of nanoparticles
RE	Relative error
$\mathbf{T_{peak}}$	Peak melting temperature
ΔH	Latent heat
ΔT	Degree of super cooling
L	Length
W	Width
T	Thickness

Appendix B: Abstracts of Published Journal Papers

B.1 Review Paper

Sustainable Energy Technologies and Assessments 50 (2022) 101799

Contents lists available at ScienceDirect

Sustainable Energy Technologies and Assessments

journal homepage: www.elsevier.com/locate/seta

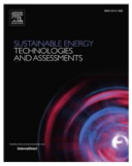

Review article

Characteristics and potential applications of nano-enhanced phase change materials: A critical review on recent developments

Muhammad Aamer Hayat [a], Yong Chen [a,*], Mose Bevilacqua [a], Liang Li [a], Yongzhen Yang [b]

[a] School of Physics, Engineering and Computer Science, University of Hertfordshire, Hatfield, AL10 9AB, United Kingdom
[b] Key Laboratory of Interface Science and Engineering in Advanced Materials, Ministry of Education, Taiyuan University of Technology, Taiyuan, Shanxi, China

ARTICLE INFO

Keywords:
Nanofillers
Phase change materials
Latent heat
Thermal conductivity
Energy storage

ABSTRACT

Owing to incessant proliferation of challenges pertaining to energy storage systems to attain optimum design and efficient performance, massive research is underway on the development of optimal storage medium (used to overcome the low thermal storage capacity of most of the thermal transport fluids). Phase change materials (PCMs) are of the high energy storage capacity and extensively used in various applications for thermal energy storage purposes. However, the poor thermal conductivity of PCMs limits their potential in different applications. Substantial research is being conducted on the dispersion of thermally conductive nanoparticles to tackle the low thermal conductivity of PCMs. This article reviews the recent numerical and experimental studies on the nano-enhanced PCMs (nano-PCMs) to analyse the effects of nanofillers on the thermophysical properties (latent heat and thermal conductivity) of the nano-PCMs. Comprehensive details of stability enhancement techniques such as dispersant addition, sonication, and surface treatment as well as concomitant challenges along with stability measurement techniques have also been presented in this paper. Furthermore, various applications, preparation, and characterization methods of nano-PCMs are also discussed. Lastly, this review article suggests the potential research directions of nano-enhanced PCMs for the storage of thermal energy.

Appendix B: Abstracts of Published Journal Papers

B.2 Original Research Article

Journal of Molecular Liquids 376 (2023) 121464

Contents lists available at ScienceDirect

Journal of Molecular Liquids

journal homepage: www.elsevier.com/locate/molliq

Preparation and thermophysical characterisation analysis of potential nano-phase transition materials for thermal energy storage applications

Muhammad Aamer Hayat [a,*], Yongzhen Yang [b], Liang Li [a], Mose Bevilacqua [a], Yongkang Chen [a,*]

[a] School of Physics, Engineering and Computer Science, University of Hertfordshire, Hatfield, Herts, AL10 9AB, United Kingdom
[b] Key Laboratory of Interface Science and Engineering in Advanced Materials, Ministry of Education, Taiyuan University of Technology, Taiyuan, Shanxi, China

ARTICLE INFO

Article history:
Received 17 November 2022
Revised 3 February 2023
Accepted 11 February 2023
Available online 14 February 2023

Keywords:
Nano phase change material
Nanofiller
Thermal conductivity
Latent heat
Energy storage

ABSTRACT

The efficacious use of phase change materials (PCMs) is mainly confined by their poor thermal conductivity (TC). In this study, multiwalled carbon nanotubes (MWCNTs), graphene nanoplatelets (GNP) and titanium oxide (TiO_2) based single, and novel hybrid nano additives were incorporated into paraffin, a typical PCM, to find the optimal composite which could not only enhance the thermal conductivity but also limit the latent heat. Both unitary and hybrid nanoparticles at five different concentrations (0.2, 0.4, 0.6, 0.8 & 1.0 wt%) were investigated using various characterisation techniques, including FT-IR, XRD, DSC, TGA, and TC apparatus. The results depicted good intermolecular interactions between the PCM and the nanoparticles and showed that the dispersion of nanoparticles within the PCM did not affect the chemical structure of pristine paraffin but enhanced its thermal and chemical stability. Novel hybrid nanocomposites were found to be more stable and exhibit better thermal performance than single nanocomposites. The highest value of thermal conductivity was observed at 1.0 wt% of GNP + MWCNTs hybrid particles based PCM with a maximum enhancement of 170% at 25 °C. However, compared with single and hybrid carbon-based nanofillers, TiO_2 based mono and hybrid nano-PCM showed a minimum reduction in the latent heat with a maximum decrease of −3.7%, −5.2%, and −5.5% at 1 wt% of TiO_2, TiO_2 + GNP and TiO_2 + MWCNTs, respectively. The significant improvement in the thermal properties of PCMs with the inclusion of these nanofillers indicates that they have the potential to be employed in thermal energy storage applications.

Appendix B: Abstracts of Published Journal Papers

B.3 Original Research Article

Thermal Science and Engineering Progress 47 (2024) 102313

Contents lists available at ScienceDirect

Thermal Science and Engineering Progress

journal homepage: www.sciencedirect.com/journal/thermal-science-and-engineering-progress

Enhancing thermal energy storage in buildings with novel functionalised MWCNTs-enhanced phase change materials: Towards efficient and stable solutions

Muhammad Aamer Hayat [a,*], Yongkang Chen [a,*], Yongzhen Yang [b], Liang Li [c], Mose Bevilacqua [a]

[a] School of Physics, Engineering and Computer Science, University of Hertfordshire, Hatfield AL10 9AB, United Kingdom
[b] Key Laboratory of Interface Science and Engineering in Advanced Materials, Ministry of Education, Taiyuan University of Technology, Taiyuan, Shanxi, China
[c] College of Engineering Design and Physical Sciences, Brunel University London, Uxbridge, UB8 3PH, United Kingdom

ARTICLE INFO

Keywords:
Functionalised MWCNTs
Phase change material
Thermal energy storage
Latent heat
Buildings
Nanocomposites

ABSTRACT

Phase change materials (PCMs) are a promising panacea to tackle the intermittency of renewable energy sources, but their thermal performance is limited by low thermal conductivity (TC). This pioneering work investigates the potential of organic PCM-enriched surface-modified and un-modified multi-walled carbon nanotubes (MWCNTs) for low-temperature thermal energy storage (TES) applications. The functionalised and un-functionalised MWCNTs enhanced PCM have demonstrated a TC enhancement of 158 % and 147 %, respectively, at 25 °C. However, the TC value of the unmodified MWCNTs-based PCM dropped by 52.5 % after 48 h at 25 °C, while that of the functionalised MWCNTs-based PCM remained stable. A DSC analysis of up to 200 thermal cycles confirmed that the surface-modified and un-modified MWCNTs had no major effect on the peak melting and cooling temperatures of the nano-enhanced PCMs although a minor decrease of 7.5 % and 7.7 % in the melting and crystallisation enthalpies, respectively, was noticed with the inclusion of functionalised MWCNTs. Moreover, functionalised MWCNTs incorporated PCMs have led to increases in specific heat capacity by 23 % with an optimal melting enthalpy value of 229.7 J/g. In addition, no super-cooling, no phase segregation, and a small phase change temperature were noticed with these nano-enhanced PCMs. Finally, no chemical interaction from nano-PCMs was seen in the FT-IR spectra with the incorporation of both functionalised and un-treated MWCNTs. It is evident that the functionalised MWCNT-based PCM has better thermal stability and it offers a promising alternative for improving thermal storage and management capabilities in buildings, contributing to a sustainable and energy-efficient building design.

Appendix B: Abstracts of Published Journal Papers

B.4 Original Research Article

Journal of Thermal Analysis and Calorimetry (2024) 149:2549–2560
https://doi.org/10.1007/s10973-023-12859-x

An experimental study on thermophysical properties of nano-TiO_2-enhanced phase change materials for cold climate applications

Lucrezia Ravasio[1] · Muhammad Aamer Hayat[2] · Rajnish Kaur Calay[1] · Raymond Riise[1] · Yong Chen[2]

Received: 9 July 2023 / Accepted: 14 December 2023 / Published online: 30 January 2024

Abstract
In high-energy-demand regions, such as the Arctic, the building sector is focused on reducing the carbon footprint and mitigating environmental impact. To achieve this, phase change materials (PCMs) are being investigated for thermal energy storage due to their high latent heat of fusion. However, their limited applications arise from poor thermal conductivity. In addressing this issue, the research delves into the preparation and characterization of nano-PCMs. These materials, synthesized in a laboratory setting, exhibit enhanced thermal performance compared to pure PCMs, attributed to the incorporation of nanoparticles in the material composition. Therefore, in the study, three paraffins with different melting temperatures (10, 15 and 18 °C) are modified by incorporating titanium oxide at various concentrations (0.05, 0.1, 0.2 and 0.5 mass%). Thermal conductivity and latent heat capacity measurements were undertaken using a thermal conductivity measuring apparatus and differential scanning calorimetry, respectively. The aim was to evaluate the enhanced performance of the modified PCMs in comparison with pure PCMs and to assess their suitability for cold climate regions. Results showed that nanoparticle incorporation increased thermal conductivity by up to 37%, albeit with a slight reduction in latent heat capacity of up to 12%. Among the samples, RT18 exhibited the most significant improvement in thermal conductivity, while RT10 experienced a minor decrease in enthalpy values. Ultimately, RT10 was identified as the optimal PCM option for cold climates, as its phase change temperature range aligns with the outdoor temperatures in the Arctic.

Keywords PCMs · Nanoparticles · Energy · Sustainability · Building

Appendix B: Abstracts of Published Journal Papers

B.5 Original Research Article

Case Studies in Thermal Engineering 49 (2023) 103262

Contents lists available at ScienceDirect

Case Studies in Thermal Engineering

journal homepage: www.elsevier.com/locate/csite

Experimental optimization of various heat sinks using passive thermal management system

Imran Zahid [a], Adnan Qamar [b], Muhammad Farooq [b,*], Fahid Riaz [c,**], Muhammad Salman Habib [b], Muhammad Farhan [b,***], Muhammad Sultan [d], Ateekh Ur Rehman [e], Muhammad Aamer Hayat [f]

[a] Department of Mechanical Engineering and Technology, Government College University Faisalabad, Pakistan
[b] Faculty of Mechanical Engineering, University of Engineering and Technology, Lahore, Pakistan
[c] Department of Mechanical Engineering, Abu Dhabi University, P.O. Box 59911, United Arab Emirates
[d] Dept. of Agricultural Engg., Bahauddin Zakariya University (BZU), Multan 60800 Pakistan
[e] Department of Industrial Engineering, College of Engineering, King Saud University, Riyadh, 11421, Saudi Arabia
[f] School of Physics, Engineering and Computer Science, University of Hertfordshire, Hatfield, Herts, AL10 9AB, United Kingdom

ARTICLE INFO

Handling Editor: Huihe Qiu

Keywords:
Unfinned heat sink
Circular pin-fin heat sink
Metallic foam
Phase change materials
Safe functional time

ABSTRACT

Organic phase change materials are extensively researched for passive cooling of electronic components due to the high heat of fusion, however, owing to the issue of thermal conductivity, it is difficult to improve the thermal performance of electronic components. However, the effective thermal performance of modern electronic devices is becoming popular due to thermal constraints of the circuit's non-uniform temperature distribution and high heating power generation. Thus, nanomaterials incorporated into phase change materials (PCMs) to improve thermal conductivity, which aids in heat removal and sustains significant heat sink operational performance for extended periods of time. In current research work, at heating powers of (10–30 W), the thermal performance outcome of three heat sink -configurations such as unfinned heat sink, circular pin-finned heat sink and metallic foam integrated heat sink were investigated with several alumina nanomaterials mass concentrations (0.15, 0.20 and 0.25 wt%) incorporated in phase change materials (for example RT-70HC). All three heat sinks revealed lower base temperature with the addition of alumina NePCM (αRT-70HC) phase change materials in their internal cavity compared to the empty unfinned heat sink. The findings showed good performance of metallic foam integrated heat sink in lowering the temperature & increasing safe functional time at two distinct temperatures. The largest decrease in temperature was found to be 35.76% and the largest growth in maximum functional time was 400% for metallic foam integrated heat sink. Therefore, using alumina nanomaterials in phase change material is recommended to optimize the thermal performance of the passive cooling techniques.